

WISSENSCHAFTLICH-TECHNISCHE BERICHTE

FZR-249

Januar 1999

ISSN 1437-322X

Archiv-Ex.:

Preprint

**2nd Workshop
on Kaon Production**

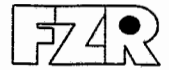
Editors:

Eckart Grosse, Burkhard Kämpfer

Herausgeber:
FORSCHUNGSZENTRUM ROSSENDORF
Postfach 51 01 19
D-01314 Dresden
Telefon +49 351 26 00
Telefax +49 351 2 69 04 61
<http://www.fz-rossendorf.de/>

Als Manuskript gedruckt
Alle Rechte beim Herausgeber

FORSCHUNGSZENTRUM ROSSENDORF



WISSENSCHAFTLICH-TECHNISCHE BERICHTE

FZR-249

Januar 1999

Preprint

**2nd Workshop
on Kaon Production**

Transparencies of the Kaon Workshop
Forschungszentrum Rossendorf, December 10-11, 1998

Editors:

Eckart Grosse, Burkhard Kämpfer

2nd Workshop on Kaon Production

During the fall of 1996 an internal mini-workshop on kaon production was organized at Rossendorf (cf. FZR-150 [September 1996]). The aim of this first workshop was to give a survey on the experimental and theoretical status of kaon production in elementary hadron reactions and in heavy-ion collisions. Since then the Department of Hadron Physics in the Institute of Nuclear and Hadron Physics of the FZR focused in its research activities on near-threshold strangeness production in colliding hadron systems and on activities devoted to studies with electromagnetic probes.

Since 1996 a considerable progress has been achieved in the field. New results from COSY (COSY-11, ToF, COSY-13 and first runs at ANKE) as well as SIS (KaoS and FOPI) allow to determine various elementary cross sections in hadron reactions and kaon yields from heavy-ion collisions. These new results led us to organize a second workshop bringing together the experts of these experiments and various theoreticians. An important purpose of the workshop was to enforce the mutual information and to demonstrate the close interrelation of COSY physics and the heavy-ion programme at SIS.

Highlights in the field are (i) the consolidation of the need of strong in-medium modifications to describe the K^- production in heavy-ion reactions and (ii) refined measurements of various elementary strangeness channels near threshold. For the latter the role of final state interactions must be clarified to arrive at a unique input to transport-model calculations for heavy-ion reactions.

Many experimental aspects included in the programme have been proposed by P. Senger (GSI), whereas the composition of its theoretical part benefitted a lot from the support by J. Aichelin (Nantes).

E. Grosse, B. Kämpfer
(local organizers)

Kaon Workshop

Forschungszentrum Rossendorf near Dresden

December 10-11, 1998

The workshop is devoted to kaon production near threshold, with emphasis put on heavy-ion collisions. Embedded in the workshop is a meeting of the KaoS collaboration. In parallel the representants of theory groups are going to compare in detail the results of their transport codes relevant for the experiments.

Programme

December 9: Arrival

December 10 (Tandemseminarraum):

- 9.00 - 9.30 E. Grosse: Opening (chairman: E. Grosse)
W. Cassing/E. Bratkovskaya (Giessen):
RBUU approach, the implemented kaon production and optical potentials,
Discussion of my benchmark tests
- 9.30 - 9.50 Gy. Wolf (Budapest):
Differences between RBUU of Giessen and my approach,
Discussion of my benchmark tests
- 9:50 - 10.20 C.-H. Lee (Stony Brook):
Differences between RBUU of Giessen and my approach,
Discussion of my benchmark tests
- 10.20 - 10.50 **Coffee break**
- 10.50 - 11.20 J. Aichelin (Nantes): (chairman: W. Cassing)
QMD: What is important for the kaon production,
discussion of my benchmark tests for HQMD
- 11.20 - 11.40 C. Hartnack (Nantes):
IQMD - Differences to HQMD as far as of importance for the
kaon production, discussion of my benchmark tests for IQMD
- 11.40 - 12.05 C. Fuchs (Tübingen):
Differences as compared to HQMD,
discussion of my benchmark tests with Tübingen kaon production
- 12:05 - 12.35 S. Soff (Frankfurt):
Kaon production around 1 GeV/N in URQMD - Differences to QMD,
discussion of my benchmark tests for UrQMD
- 12.35 - 13.00 A. Sibirtsev (Giessen):
News from elementary kaon production reactions
- 13.00 - 14.00 **Break**
- 14.00 - 14.20 F. Laue (GSI): (chairman: W. Oelert)
Recent results from KaoS (1): K^+/K^- ratios
- 14.20 - 14.40 Y. Shin (Frankfurt):
Results from KaoS (2): azimuthal anisotropy of K^+
- 14.40 - 15.00 C. Sturm (Darmstadt):
Recent results from KaoS (3): K production and nuclear EoS
- 15.00 - 15.30 P. Crochet (C-Ferrand):
Results from FOPI (1)
- 15.30 - 16.00 C. Plettner (Rossendorf):
Results from FOPI (2)
- 16.00 - 16.30 **Coffee break**
- 16.30 - 17.00 A. Metzger (Erlangen): (chairman: N. Herrmann)
Results from COSY-TOF
- 17.00 - 17.30 T. Lister / S. Sewerin:

Results from COSY-11

- 17.30 - 18.00 M. Debowski (Rossendorf):
Prospects of ANKE
- 18.00 - 18.20 A. Gillitzer (München):
Strangeness programme at FRS
- 18.20 - 18.40 P. Kulessa (Crakow):
A nuclei
- 18.40 - 18.55 W. Scheinast (Rossendorf):
pA runs at KaoS
- 19.00 - ∞ **Buffet**

December 11:

Parallel sessions 9.00 - 12.00:

1. KaoS collaboration meeting (Seminarraum Flachbau, organizer: P. Senger)
2. Theory session (Tandemseminarraum, organizer: J. Aichelin)

Afternoon session (Auditorium):

- 13.00 - 13.20 K. Schubert (Dresden): (chairman: B. Kamys)
Recent results on symmetry breaking in K systems
- 13.20 - 13.45 E. Kolomeitsev (GSI):
In-medium kaonic excitations
- 13.45 - 14.10 J. Knoll (GSI):
Transport kinetics of broad resonances
- 14.10 - 14.40 B. Kämpfer (Rossendorf):
Comparison of the benchmark tests
- 14.40 - 15.00 **Coffee break**
- 15.00 - 16.00 Round table discussion about the different models (chairman: P. Senger)
Conclusions & perspectives for our kaon physics

Departure

(e.g. 17.27 p.m. Dresden-Neustadt --> Frankfurt/Main)

Kaon Workshop Participants

Who	From	Where	When
Aichelin, J.	Nantes	Gästehaus	9. - 12.
Böttcher, I.	Uni Marburg	Zu d.Linden	9. - 13.
Bratkovskaya, E.	Giessen	Schänkhübel	9. - 11.
Büscher, M.	Jülich	Zu den Linden	9. - 11.
Cassing, W.	Giessen	Schänkhübel	9. - 11.
Crochet, P.	C-Ferrand	Arcade	9. - 11.
Förster, A.	TU Darmsdtadt	Arcade	9. - 13.
Fuchs, C.	Tübingen	Arcade	9. - 13.
Gillitzer, A.	München	Arcade	9. - 11.
Nantes	Arcade	10. - 11.	
Khoukaz	Münster	Arcade	9. - 11.
Herrmann, N.	GSI	Gästehaus	9. - 11.
Kamys, B.	Krakau	Gästehaus	10. - 11.
Knoll, J.	GSI	Gästehaus	9. - 11.
Koczon, P.	GSI	Arcade	9. - 12.
Kohlmeier, B.	Uni Marburg	Gästehaus	9. - 11.
Kolomeitsev, E.	GSI	privat	
Krusche, R.		Arcade	9. - 11.
Laue, F.	GSI	Arcade	9. - 11.
Lee, C.-H.	Stony Brook	Arcade	9. - 13.
Lister, Th.	Münster	Arcade	9. - 11.
Menzel, M.	Marburg	Arcade	9. - 11.
Metzger, A.	Erlangen	Gästehaus	9. - 11.
Moscal, P.	Crakow	Arcade	9. - 11.
Oelert, W.	Jülich	Zu d. Linden	9. - 12.
Oeschler, H.	TU Darmstadt	Zu d. Linden	9. - 11.

Quentmeier, Ch.	Münster	Arcade	9. - 11.
Reisdorf, W.	GSI	Zu d.Linden	9. - 11.
Scheinast, W.	FZR	Arcade	9. - 11.
Schepers, G.	Jülich	Arcade	9. - 12.
Senger, P.	GSI	privat	
Sewerin, S.	Jülich	Arcade	9. - 12.
Shin, Y.	Uni Frankfurt	Arcade	9. - 13.
Sibirtsev, A.	Giessen	Schänkhübel	9. - 11.
Sistemich, K.	Jülich	Zu d. Linden	9. - 11.
Soff, S.	Frankfurt	Arcade	9. - 11.
Sturm, C.	TU Darmstadt	Arcade	9. - 11.
Uhlig, F.	TU Darmstadt	Arcade	9. - 11.
Walus, W.	Cracow	Zu d. Linden	9. - 11.
Wolf, Gy.	Budapest	Wohnunterk.	
Wisniewski, C.	GSI	Gästehaus	9. - 11.
Grosse, E.	FZR		9. - 11.
Kämpfer, B.	FZR		9. - 11.
Müller, H.	FZR		9. - 11.
Debowski, M.	FZR		9. - 11.
Schneider, C.	FZR		9. - 11.
Naumann, L.	FZR		9. - 11.
Barz, H.W.	FZR		9. - 11.
Kotte, R.	FZR		9. - 11.
Plettner, C.	FZR		9. - 11.
Wohlfarth, D.	FZR		9. - 11.
Dohrmann, F.	FZR		9. - 11.

Back to the parent document

Transparencies of the Kaon Workshop

1. Experimental Part

T. Lister:
 $pp \rightarrow ppK^+Y$ near the $f_0(980)$

A. Metzger:
Strangeness production -- results from COSY-TOF

M. Debowski:
Prospects of ANKE

P. Kulessa:
Determination of Λ lifetime in heavy hypernuclei

A. Gülitzer:
 K^- production at the GSI fragment separator

P. Crochet:
Results from FOPI (1)

C. Plettner:
Results from FOPI (2):
Investigation of charged K mesons at low p_T and around midrapidity

Y. Shin:
Azimuthally anisotropic emission of K^+ mesons in Au + Au collisions at 2 AGeV

F. Laue:
Kaons and anti-kaons in hot and dense nuclear matter

C. Sturm:
 K^+ production in heavy-ion reactions as a probe for the nuclear equation of state

K.R. Schubert:
Recent results on symmetry breaking in the K^0 system

2. Theoretical part

W. Cassing & E. Braukovskaya:
The RBUU (IISD) approach to strangeness production

C.-H. Lee:
Benchmark test of the RVUU model

J. Aichelin:
QMD

S. Soff:
Kaon production at SIS energies in the UrQMD approach

Gy. Wolf:
Kaon production -- benchmark test

C. Fuchs:
 K^+ production with Tübingen QMD

B. Kämpfer:
Comparison of benchmark tests

E.E. Kolomeitsev:
Kaonic excitation in HICs

A. Sibirtsev:
Theoretical news on strangeness production in p + p collisions

J. Knoll:
Transport kinetics of broad resonances

Experimental Part

T. Lister:

pp \rightarrow *ppK*⁺*X* near the *f*₀(980)

I. Lister

pp → ppκ⁺X near the f₀(980)

inner structure of the f₀(980):???

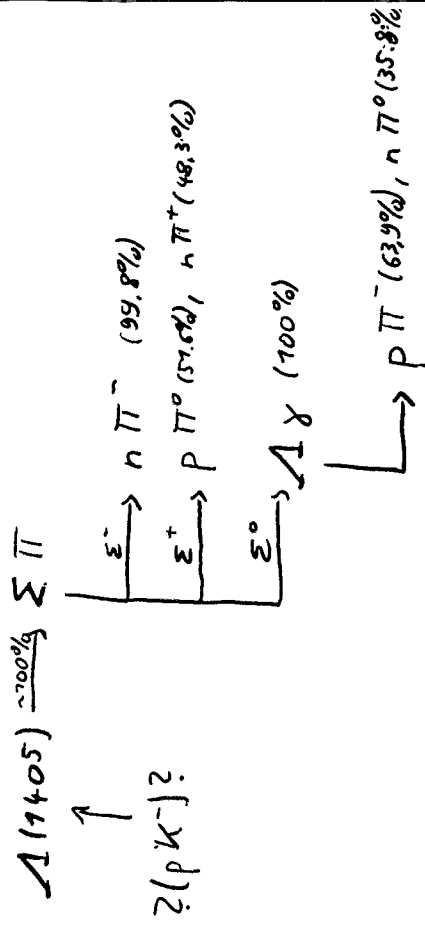


- modified q \bar{q} - meson
- glueball
- q $q\bar{q}\bar{q}$ - state
- κ $\bar{\kappa}$ - molecule?



pp → pp(κ⁺κ⁻)

other channels in pp → pκ⁺(pX):

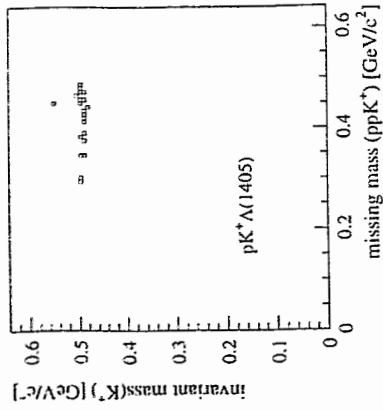
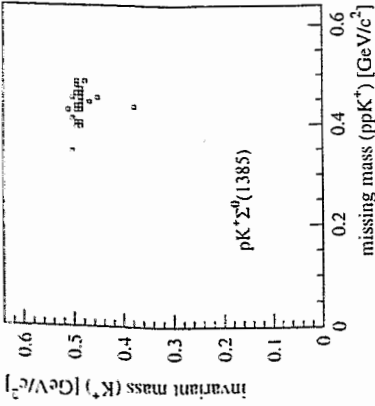
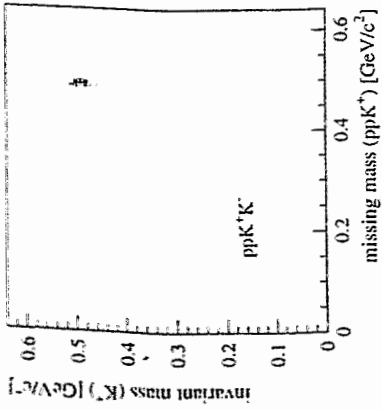


$\Sigma^0(17385) \rightarrow \Delta\pi(88\%), \Sigma\pi(12\%)$



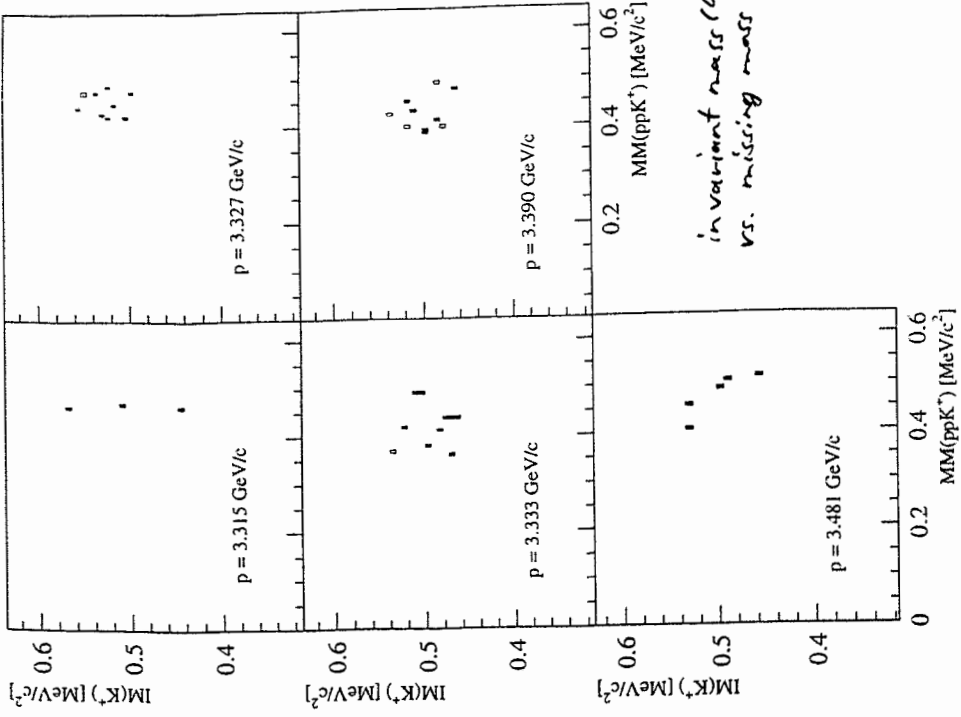
(pκ⁺p) + X

MC - simulations



→ similar invariant masses, differing missing mass distributions

experimental data



detection efficiencies

beam momentum	$\epsilon_{ppK^+K^-}$	$\epsilon_{pA+\Sigma^0(1385)}$	$\epsilon_{pK^+A(1405)}$
3.315 GeV/c	$3.44 \cdot 10^{-2} \cdot (1^{+43.8\%}_{-16.8\%})$	$7.5 \cdot 10^{-5} \cdot (1 \pm 11.5\%)$	$1.3 \cdot 10^{-4} \cdot (1 \pm 6.7\%)$
3.327 GeV/c	$1.65 \cdot 10^{-2} \cdot (1^{+20.7\%}_{-16.8\%})$	$7.5 \cdot 10^{-5} \cdot (1 \pm 11.5\%)$	$2.2 \cdot 10^{-4} \cdot (1 \pm 6.8\%)$
3.333 GeV/c	$1.20 \cdot 10^{-2} \cdot (1^{+16.7\%}_{-11.9\%})$	$6.1 \cdot 10^{-5} \cdot (1 \pm 12.8\%)$	$1.2 \cdot 10^{-4} \cdot (1 \pm 9.2\%)$
3.390 GeV/c	$2.54 \cdot 10^{-3} \cdot (1^{+8.1\%}_{-6.9\%})$	$6.0 \cdot 10^{-5} \cdot (1 \pm 12.9\%)$	$6.6 \cdot 10^{-5} \cdot (1 \pm 12.3\%)$
3.481 GeV/c	$1.07 \cdot 10^{-4} \cdot (1^{+12.2\%}_{-12.0\%})$	$1.8 \cdot 10^{-6} \cdot (1 \pm 23.6\%)$	$6.3 \cdot 10^{-6} \cdot (1 \pm 20.0\%)$

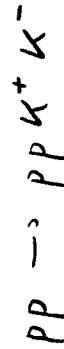
number of events

beam momentum	no. N of (ppK ⁺) events		no. n of possible (ppK ⁺ K ⁻)-events		η_0 (K ⁺ K ⁻)	N_0 ($\Sigma^0(1385)$) $\sqrt{\Lambda(1405)}$	CL=95% CL=95%
	events		(ppK ⁺ K ⁻)-events				
3.315 GeV/c	3		0		3.00	7.75	
3.321 GeV/c	2		0		3.00	6.30	
3.327 GeV/c	10		0		3.00	16.96	
3.333 GeV/c	10		2		6.30	16.96	
3.390 GeV/c	10		1		1.71	16.96	
3.481 GeV/c	5		1		1.71	10.51	

allowed detection in missing mass: 6 MeV/c²

beam momentum	η_0	ϵ_{ppA^+}	integrated luminosity	cross section
3.315 GeV/c	3.00	$3.44 \cdot 10^{-2} \cdot (1^{+43.8\%}_{-16.8\%})$	$5.17 \cdot 10^{35} \cdot \frac{1}{\text{cm}^2}$ $\cdot (1 \pm 10.78\%)$	$< 260 \text{ pb}$, CL = 95%
3.321 GeV/c	3.00	$5.15 \cdot 10^{-2} \cdot (1^{+10.6\%}_{-27.2\%})$	$7.90 \cdot 10^{35} \cdot \frac{1}{\text{cm}^2}$ $\cdot (1 \pm 3.3\%)$	$< 1.1 \text{ nb}$, CL = 95%
3.327 GeV/c	3.00	$1.65 \cdot 10^{-2} \cdot (1^{+20.7\%}_{-16.8\%})$	$3.52 \cdot 10^{35} \cdot \frac{1}{\text{cm}^2}$ $\cdot (1 \pm 11.25\%)$	$< 680 \text{ pb}$, CL = 95%
3.333 GeV/c	6.30	$1.20 \cdot 10^{-2} \cdot (1^{+16.7\%}_{-11.9\%})$	$4.64 \cdot 10^{35} \cdot \frac{1}{\text{cm}^2}$ $\cdot (1 \pm 11.55\%)$	$< 1.4 \text{ nb}$, CL = 95%
3.390 GeV/c	4.74	$2.54 \cdot 10^{-3} \cdot (1^{+8.1\%}_{-6.9\%})$	$7.52 \cdot 10^{35} \cdot \frac{1}{\text{cm}^2}$ $\cdot (1 \pm 11.62\%)$	$< 3.0 \text{ nb}$, CL = 95%
3.481 GeV/c	4.74	$1.07 \cdot 10^{-4} \cdot (1^{+12.2\%}_{-12.0\%})$	$1.38 \cdot 10^{35} \cdot \frac{1}{\text{cm}^2}$ $\cdot (1 \pm 12.63\%)$	$< 400 \text{ nb}$, CL = 95%

upper limits of



upper limits

$pp \rightarrow k^+ k^-$

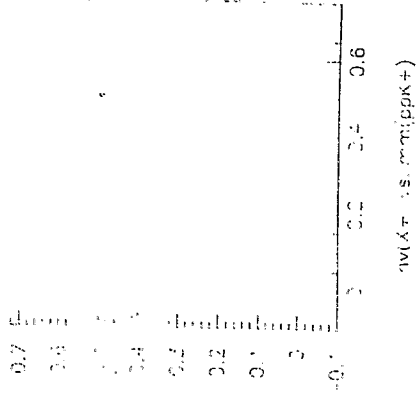
beam momentum	N_0	\mathcal{L}_{ppk^+}	integrated luminosity	cross section
3.315 GeV/c	7.75	$7.5 \cdot 10^{-5}$ ($1 \pm 11.5\%$)	$5.17 \cdot 10^{35} \cdot \frac{1}{\text{cm}^2}$ ($1 \pm 10.78\%$)	< 245 nb, CL = 95%
3.327 GeV/c	16.69	$7.5 \cdot 10^{-5}$ ($1 \pm 11.5\%$)	$3.52 \cdot 10^{35} \cdot \frac{1}{\text{cm}^2}$ ($1 \pm 11.25\%$)	< 775 nb, CL = 95%
3.333 GeV/c	16.69	$6.1 \cdot 10^{-5}$ ($1 \pm 12.8\%$)	$4.64 \cdot 10^{35} \cdot \frac{1}{\text{cm}^2}$ ($1 \pm 11.55\%$)	< 735 nb, CL = 95%
3.390 GeV/c	16.69	$6.0 \cdot 10^{-5}$ ($1 \pm 12.9\%$)	$7.52 \cdot 10^{35} \cdot \frac{1}{\text{cm}^2}$ ($1 \pm 11.62\%$)	< 460 nb, CL = 95%
3.481 GeV/c	10.51	$1.8 \cdot 10^{-6}$ ($1 \pm 23.6\%$)	$1.38 \cdot 10^{35} \cdot \frac{1}{\text{cm}^2}$ ($1 \pm 12.63\%$)	< 57.6 μb , CL = 95%

$pp \rightarrow p k^+ \Delta(17385)$

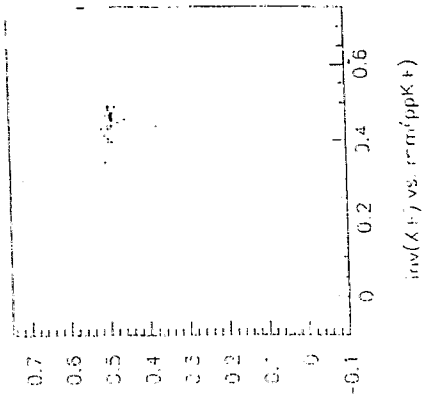
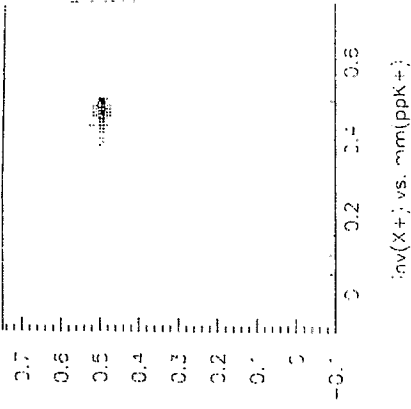
upper limits

beam momentum	N_0	\mathcal{L}_{ppk^+}	integrated luminosity	cross section
3.315 GeV/c	7.75	$1.31 \cdot 10^{-4}$ ($1 \pm 6.7\%$)	$5.17 \cdot 10^{35} \cdot \frac{1}{\text{cm}^2}$ ($1 \pm 10.78\%$)	< 135 nb, CL = 95%
3.327 GeV/c	16.69	$2.19 \cdot 10^{-4}$ ($1 \pm 6.8\%$)	$3.52 \cdot 10^{35} \cdot \frac{1}{\text{cm}^2}$ ($1 \pm 11.25\%$)	< 255 nb, CL = 95%
3.333 GeV/c	16.69	$1.17 \cdot 10^{-4}$ ($1 \pm 9.2\%$)	$4.64 \cdot 10^{35} \cdot \frac{1}{\text{cm}^2}$ ($1 \pm 11.55\%$)	< 370 nb, CL = 95%
3.390 GeV/c	16.69	$6.60 \cdot 10^{-5}$ ($1 \pm 12.3\%$)	$7.52 \cdot 10^{35} \cdot \frac{1}{\text{cm}^2}$ ($1 \pm 11.62\%$)	< 420 nb, CL = 95%
3.481 GeV/c	10.51	$6.25 \cdot 10^{-6}$ ($1 \pm 20.0\%$)	$1.38 \cdot 10^{35} \cdot \frac{1}{\text{cm}^2}$ ($1 \pm 12.63\%$)	< 1.6 μb , CL = 95%

$pp \rightarrow p k^+ \Delta(17405)$



$\mathcal{L} = p k^+ \Delta(1405)$



$\mathcal{L} = p k^+ \Delta(17385)$

conclusions.

• pp \rightarrow pp \bar{K}^+K^- events are seen

• upper limits of the cross sections of

pp \rightarrow pp \bar{K}^+K^-

pp \bar{K}^+K^- (1.385)

pp \bar{K}^+K^- (1.405)

are calculated

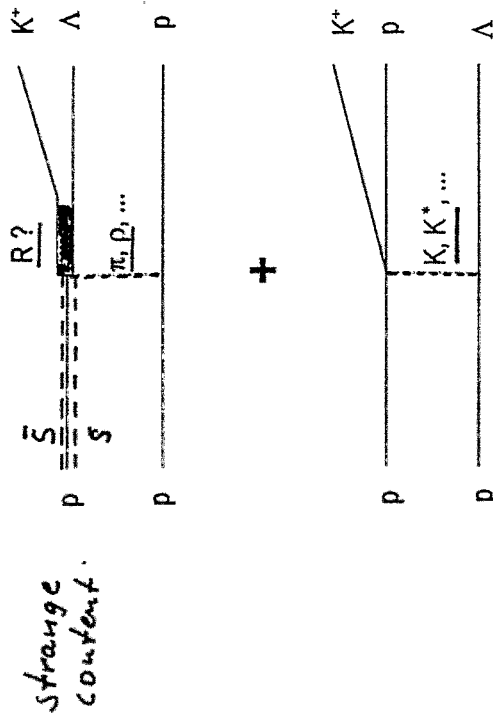
• further data, especially
below \bar{K}^+K^- -threshold
and with higher statistics
have to be taken

A. Metzger:

Strangeness production – results from COSY-TOF

Meson Exchange Model

One boson exchange



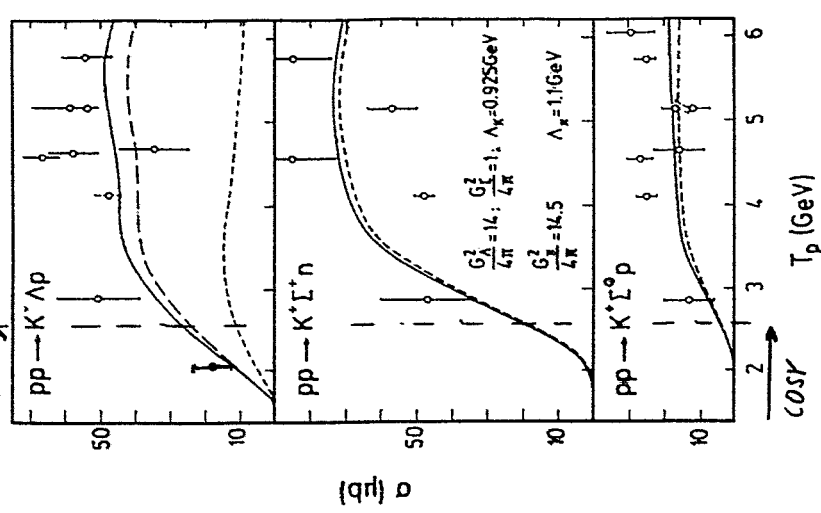
strange content.

initial + final state interaction
coupled channels effects

- Cassing, Sibirsev et al.
- Dillig, Kleeefeld
- Faldt, Wilkin
- Haidenbauer, Hanhart et al.
- Laget
- Li, Ko et al.
- and others

$pp \rightarrow KYN$

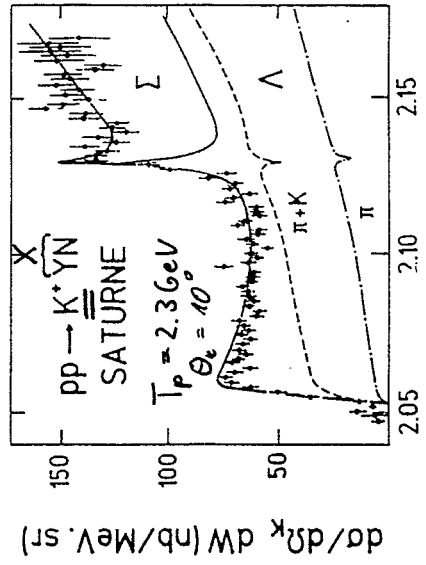
COSY



calculations:
Laget et al.

--- $\bar{u} + K$
--- \bar{u}

data:
CERN-HERA comp.
(1975)



+ FSJ

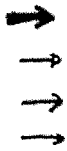
data
Siebert et al.
N.P. A 567 (1994)

W (GeV)

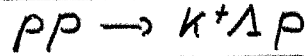
Experimental Constraints

Threshold momenta :

Reaction	\sqrt{s} GeV	Momentum GeV/c	kin. Energy GeV
$pp \rightarrow K^+ \Lambda p$	2.548	2.339	1.582
$pp \rightarrow K^+ \Sigma^+ n$	2.622	2.560	1.789
$pp \rightarrow K^+ \Sigma^0 p$	2.624	2.566	1.793
$pp \rightarrow K^0 \Sigma^+ p$	2.625	2.569	1.796
$pp \rightarrow K_s K_s pp$	2.875	3.327	2.518
$pd \rightarrow K^+ \Lambda d$	3.485	1.839	1.127
$p^4 He \rightarrow K^+ \Lambda^4 He$	5.338	1.581	0.900
$p^{12} C \rightarrow K^+ \Lambda X$		1.400	0.747

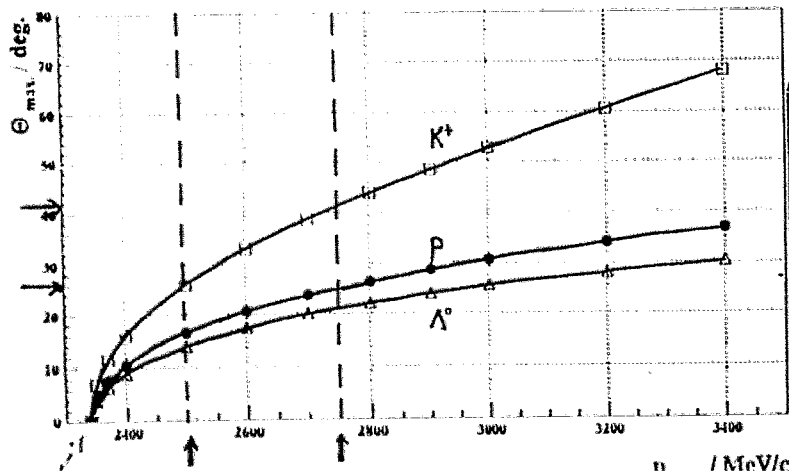


Signature :



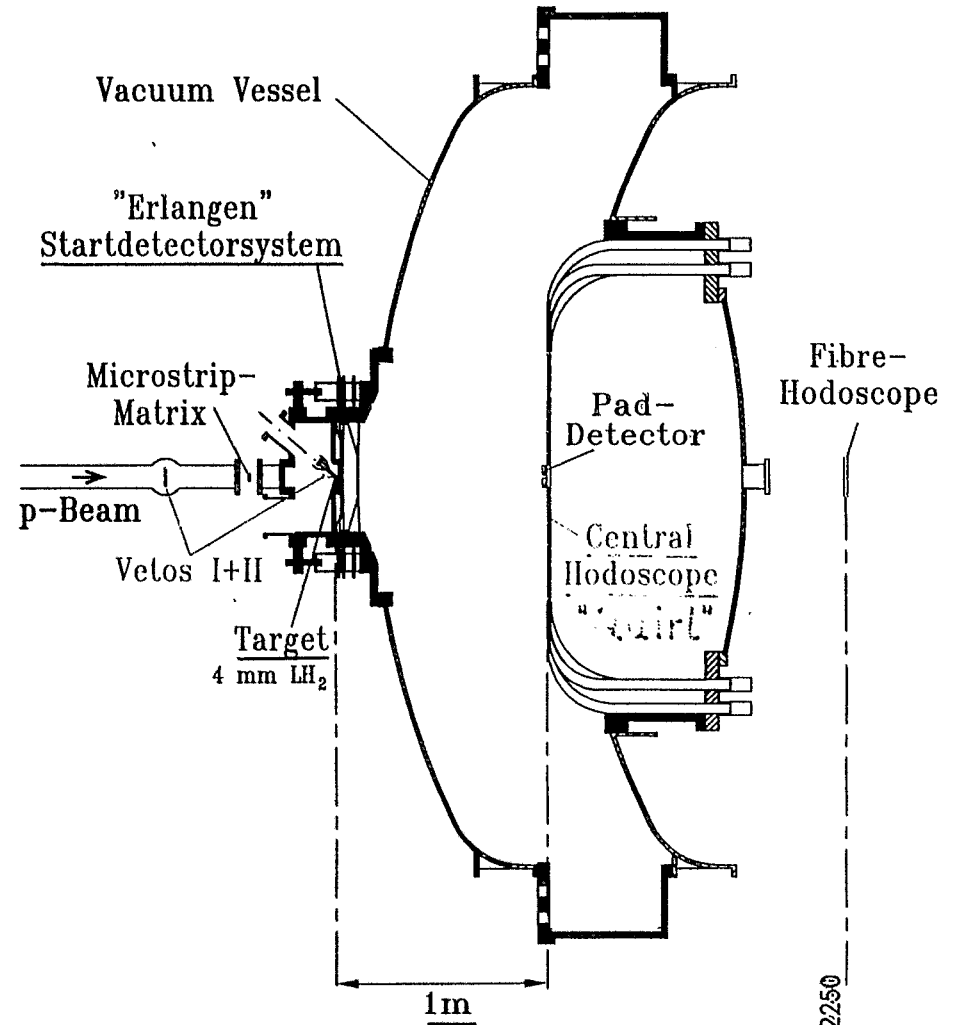
delayed decay $\Lambda \rightarrow \pi^- p$ ($c\tau_\Lambda = 7.9 \text{ cm}$) $\epsilon \approx 7\%$
 increase of charged multiplicity $2 \rightarrow 4$: Trigger!

Reaction angles :



forward detector
 $\Delta \approx 4\pi$

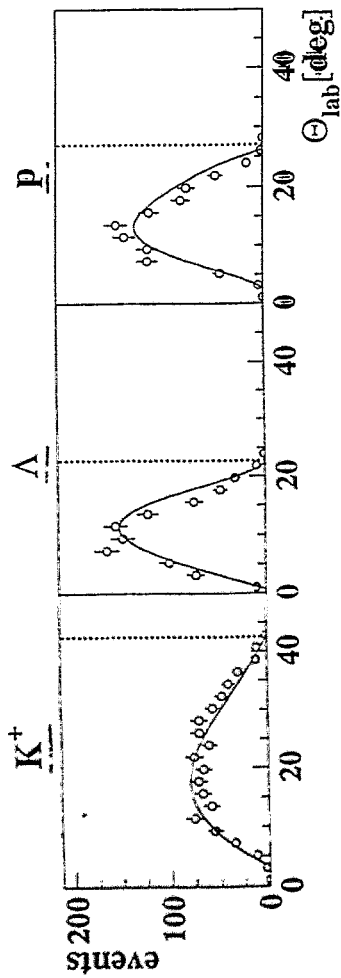
TOF-Setup '95/'96



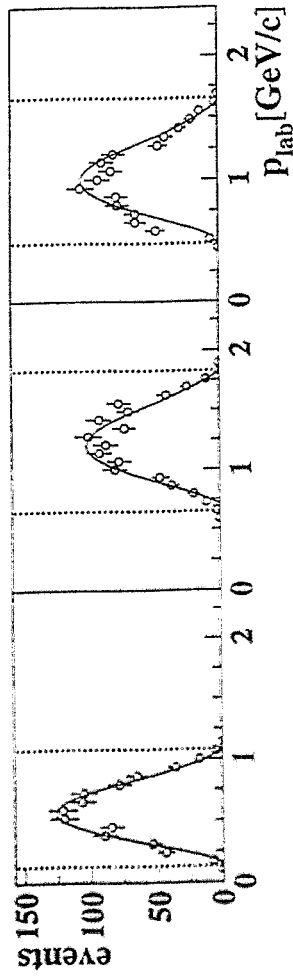
TOF

$pp \rightarrow K^+ \Lambda p$ at $p_{\text{beam}} = 2.75 \text{ GeV/c}$

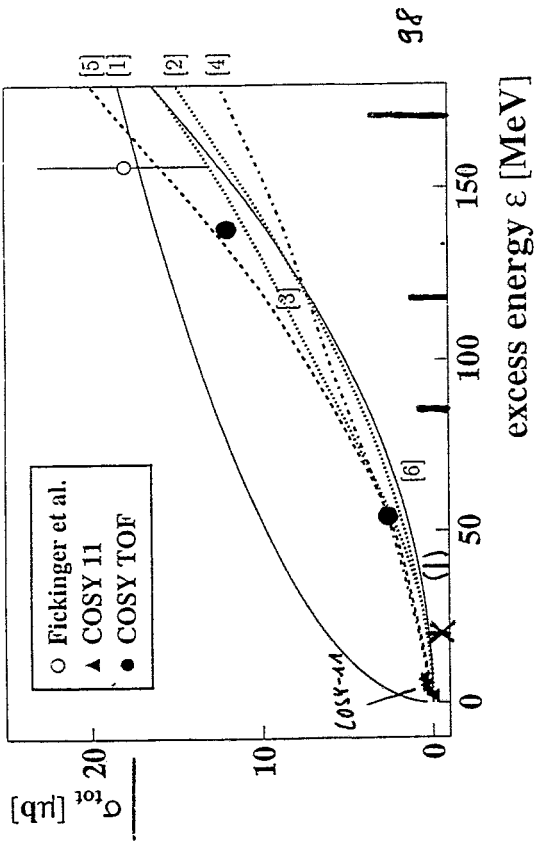
angular distributions.



momentum distributions.



$pp \rightarrow K^+ \Lambda p$



[1] J. Randrup and C.M. Ko, Nucl. Phys. A343 (1980) 519

[2] A. Sibiritev, Phys. Rev. Lett. B359 (1995) 29;

[3] K. Tsushima, A. Sibiritev, A.W. Thomas, Internal Rep. ADP-96-29/T228 (1996)

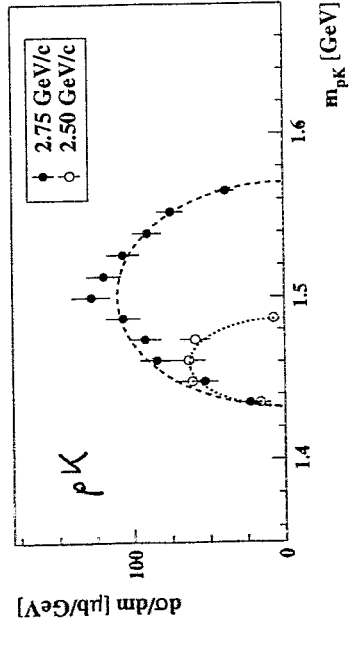
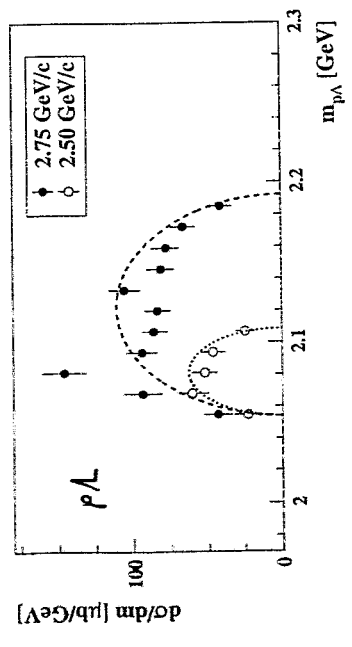
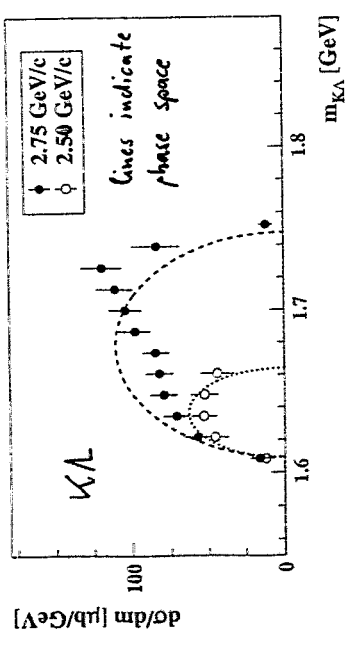
[4] J.M. Laget, Phys. Lett. B259 (1991) 24

[5] F. Kleefeld, M. Dillig, F. Pilotto, Acta Phys. Pol. B27 (1996)

[6] B. Schürmann and W. Zwermann, Mod. Phys. Lett. A3 (1988) 251

Differential X-Sections

invariant masses

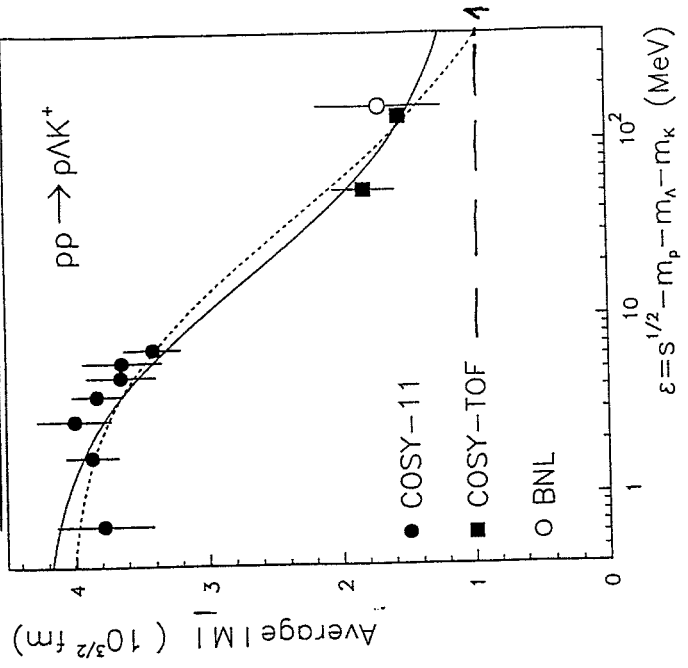


Influence of final-state-interaction (FSI)

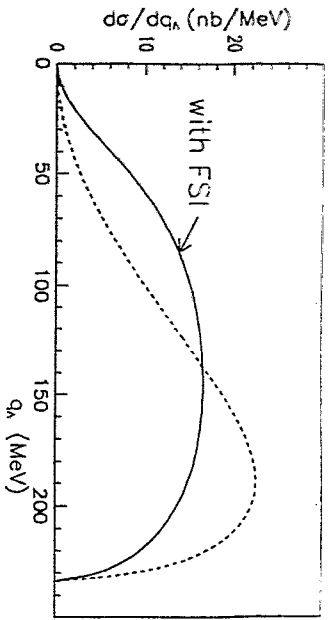
$$|M|^2 = \frac{\sigma_{tot}}{\sigma_{phase+pic}}$$

Reaction amplitude

Sibirtsev + Cassing (nucl-th 9802025)

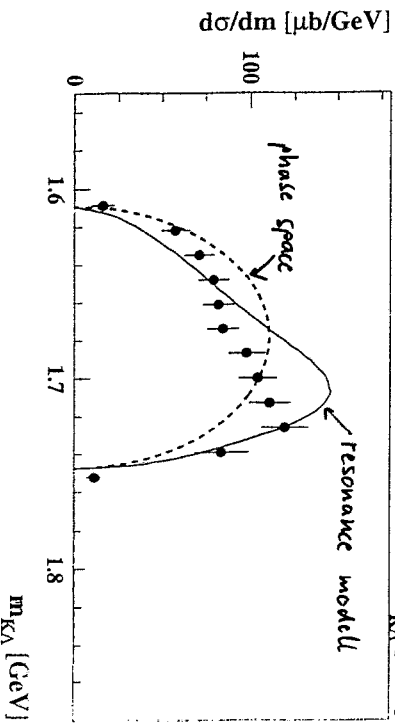
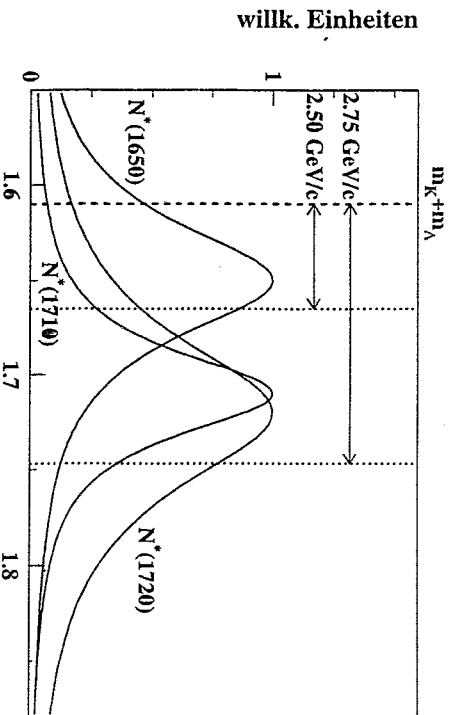
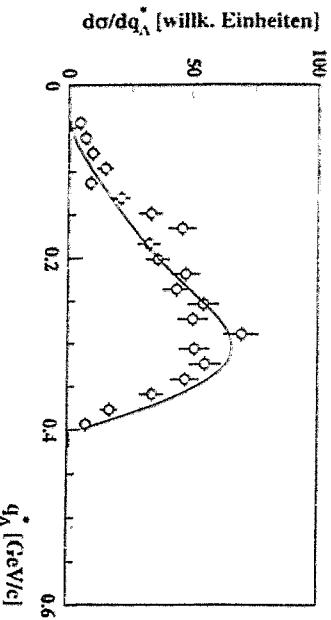
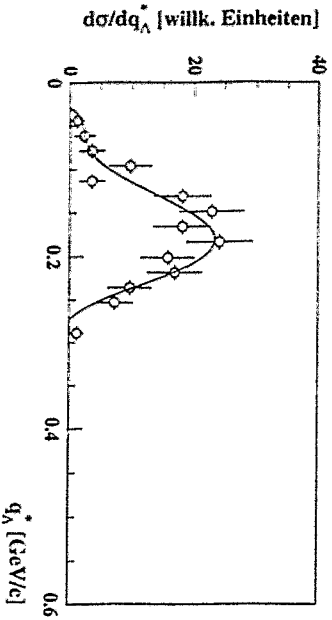


Resonance-Modell



A. Sibirtsev und W. Cassing, Preprint nucl-th/9802025 (1998).

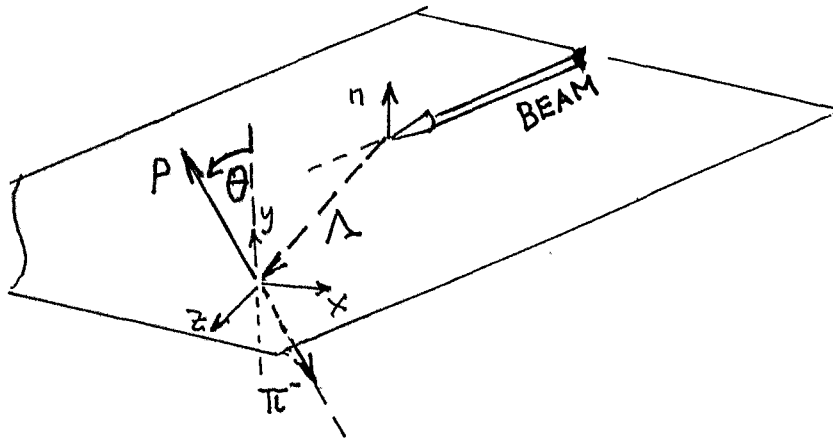
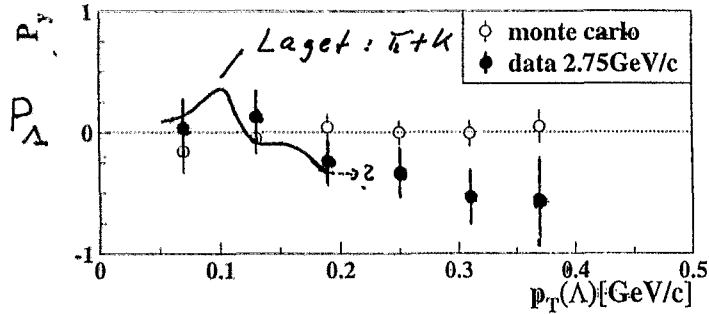
- Λ -momentum-distribution in the $p\Lambda$ -system
- FSI from elastic $p\Lambda$ -scattering



- K. Tsushima, S.W. Huang, A. Faessler, J. Phys. G21 (1995) 33.
- K. Tsushima, A. Sibirtsev, A.W. Thomas, Internal Report ADP-96-29/T228 (1996).

Λ-Polarisation

pp → K⁺Λp @ 2.75 GeV/c



$$dN/d\cos\theta = 1/2(1 + \alpha P_y \cos\theta)$$

$\alpha = 0.64$

Detector upgrade:

- start detector system ✓
 - double sided micro strip + additional fibre hodoscope
- stop detector
 - barrel detector ✓ + ring detector (✓)
- neutron detector ✓
- energy detector

Run April 98: pp → K⁺Λp („high statistics“)

pp → K⁺Σ⁺n , K⁰Σ⁺p (Search for Z⁺)

pd → KY... and pα → KY...

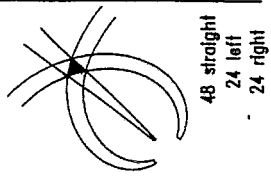
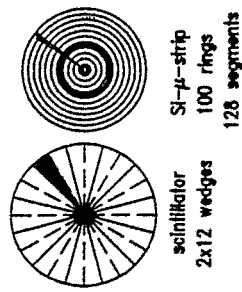
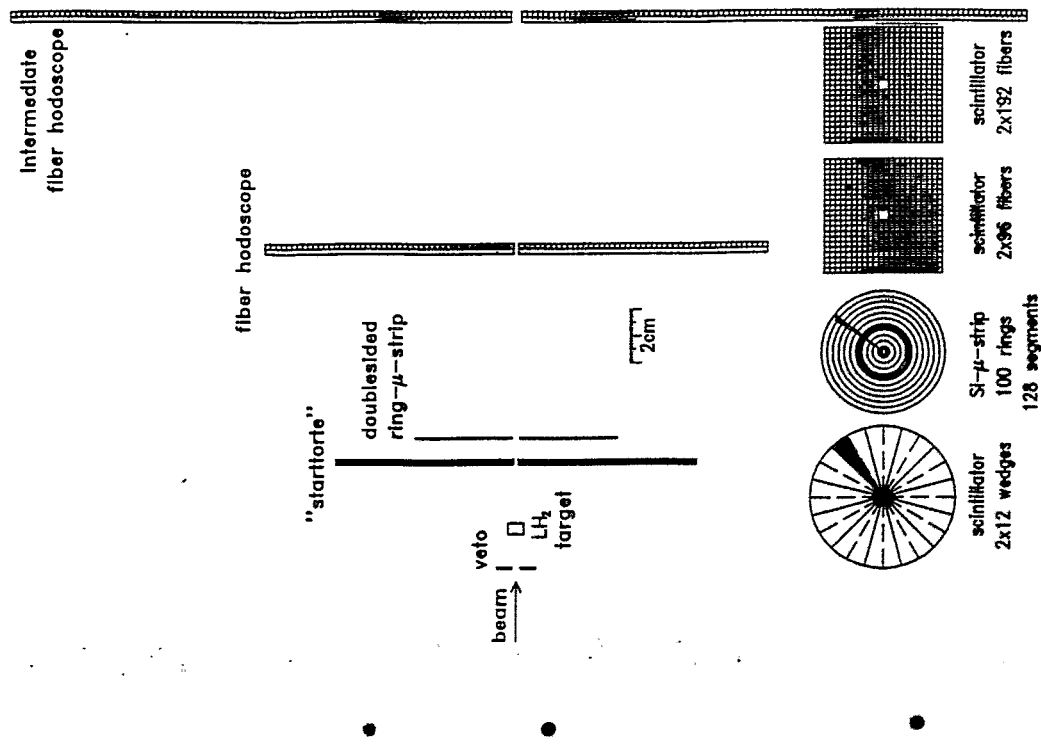
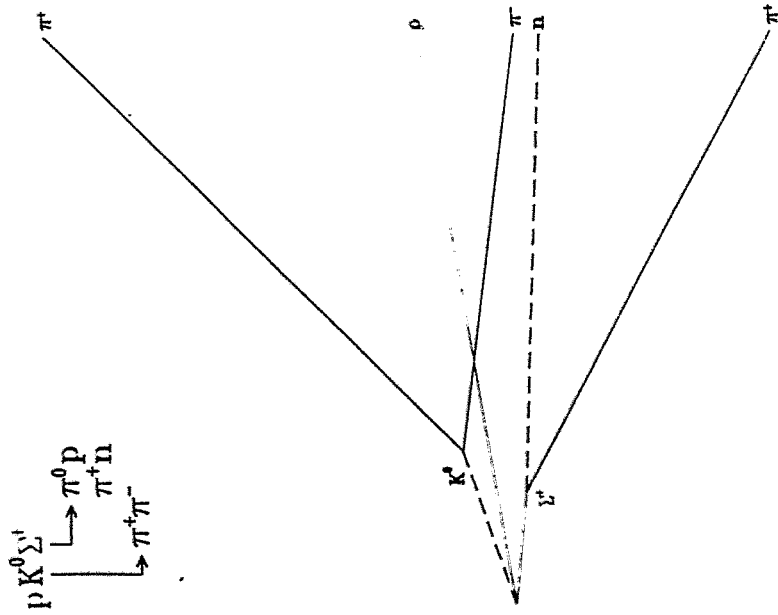
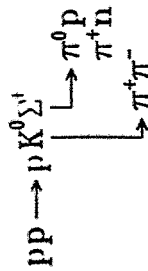
Polarized beam + Polarized target

Large Angle μ-Strip Detector +

Magnetic field and intermediate tracker:

- p ⁴He → α_{recoil} (N⁺ → KΛ)
 - scalar structure of the nucleon
- pp → ppKK

Erlangen Startdetector '98

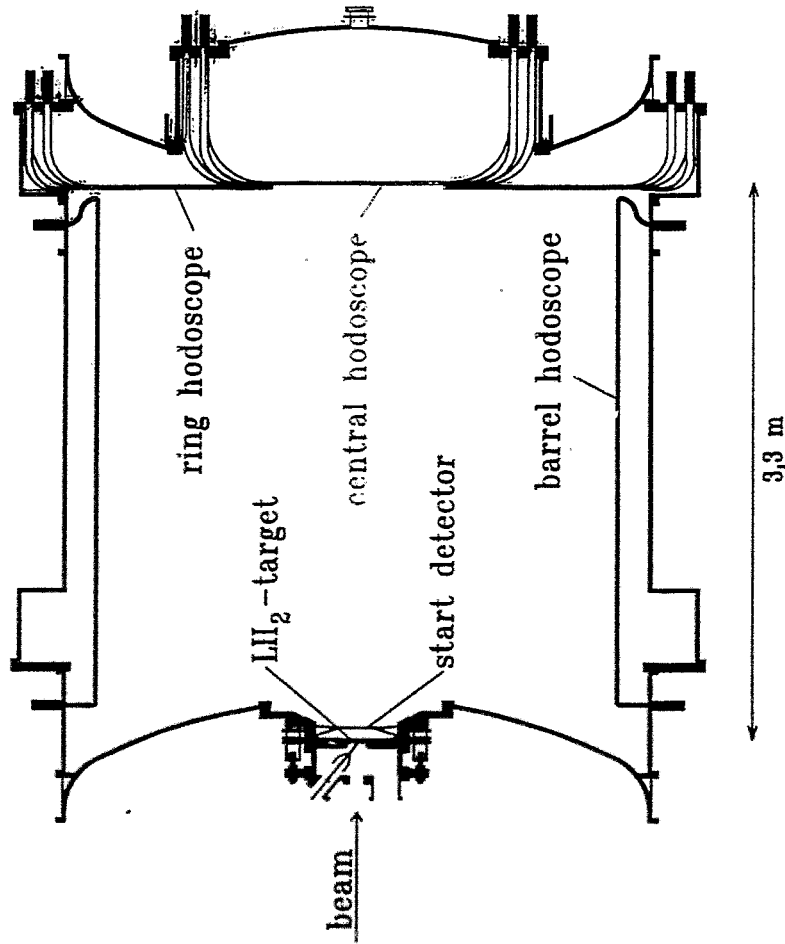


flight path

"quirl"

COSY-TOF

Bochum - Bonn - Dresden - Erlangen - Indiana - Jülich -
 Rossendorf - Tübingen - Turin



large angle spectrometer
 modular vacuum vessel
 miniaturized target
 startdetector system(s)
 stopdetector system

COSY-TOF - Kollaboration

R. BILGER⁷, A. BÖHM³, K.-Th. BRINKMANN³, H. CLEMENT⁷, H. DENNER⁴, S. DSHEMUCHADSE⁶, H. DUTZ², W. EYRICH⁴, D. FILGES⁵, H. FRIESELBEN³, M. FRITSCH⁴, R. GEYER⁶, A. HASSAN⁹, J. HAUFFE⁴, P. HERMANN¹, D. HESSELBAUTH⁵, B. HÜBNER³, P. JAHN⁵, K. KILIAN⁵, H. KOCH¹, J. KRESS⁷, J. KRUG¹, E. KÜHLMANN³, S. MARWINSKI⁵, A. METZGER⁴, W. MEYER¹, P. MICHEL⁶, K. MÖLLER⁶, H. P. MORSCH⁵, H. NANN⁶, B. NAUMANN⁶, L. NAUMANN⁶, K. NÜNIGHOFF⁵, E. RODERBURG⁵, M. ROGGE⁵, A. SCHAMLOTT⁶, P. SCHÖNMEIER³, W. SCHROEDER⁴, M. SCHULTE-WISSERMANN³, M. STEINKE¹, F. STINZING⁴, G.-Y. SUN³, J. WÄCHTER⁴, G.-J. WAGNER⁷, M. WAGNER⁴, S. WIRTH⁴, and U. ZIELINSKI¹

¹Institut für Experimentalphysik I, Ruhr-Universität Bochum, D-44780 Bochum

²Physikalisches Institut, Universität Bonn, D-53115 Bonn

³Institut für Kern- und Teilchenphysik, Technische Universität Dresden, D-01062 Dresden

⁴Physikalisches Institut, Universität Erlangen-Nürnberg, D-91058 Erlangen

⁵Institut für Kernphysik, Forschungszentrum Jülich, D-52425 Jülich D-01314 Dresden

⁶Institut für Kern- und Hadronenphysik, Forschungszentrum Rossendorf, D-01314 Dresden

⁷Physikalisches Institut, Universität Tübingen, D-72076 Tübingen

⁸IUCF Bloomington, Indiana 47408, USA

⁹Atomic Energy Authority NRC, Kairo, Egypt

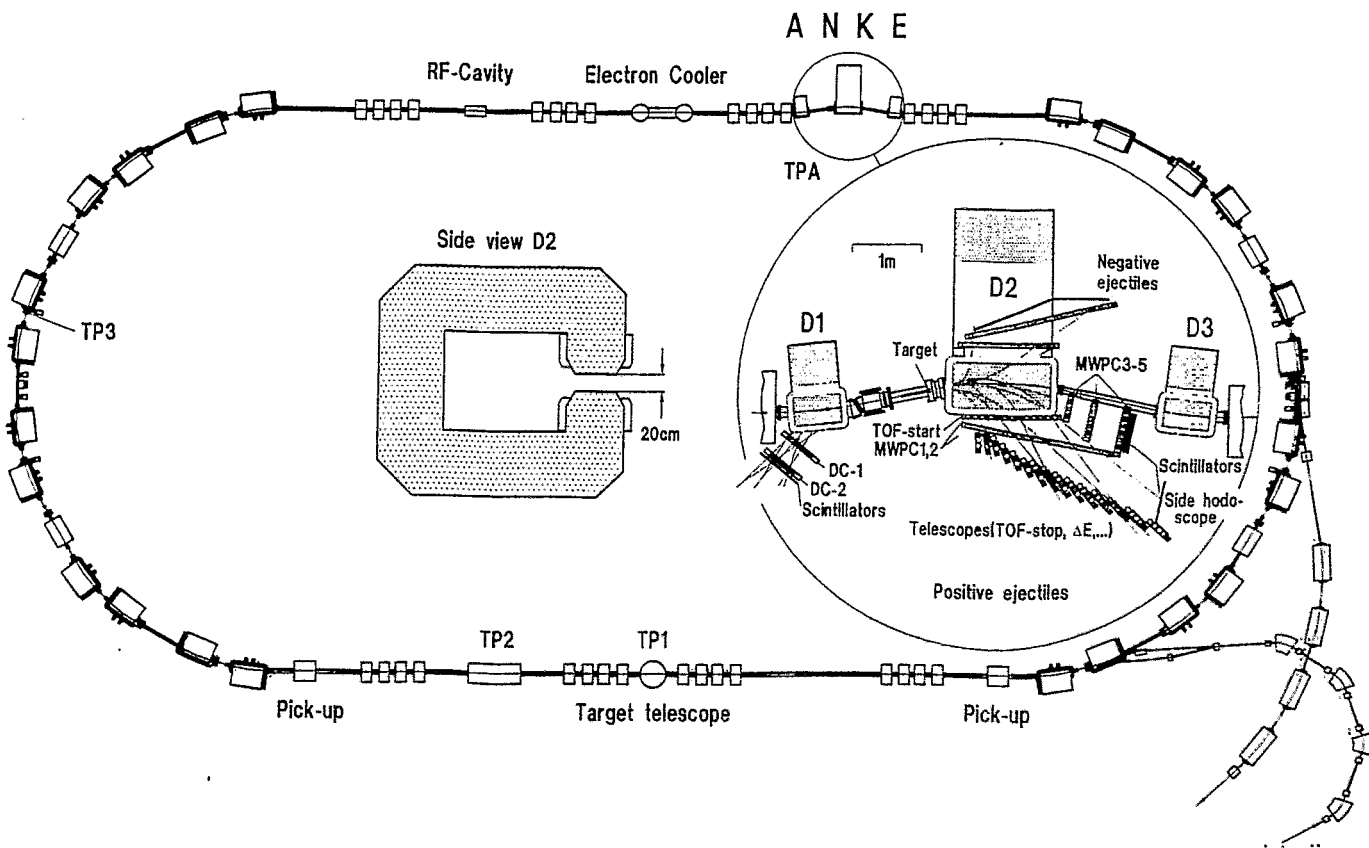
M. Debowski:

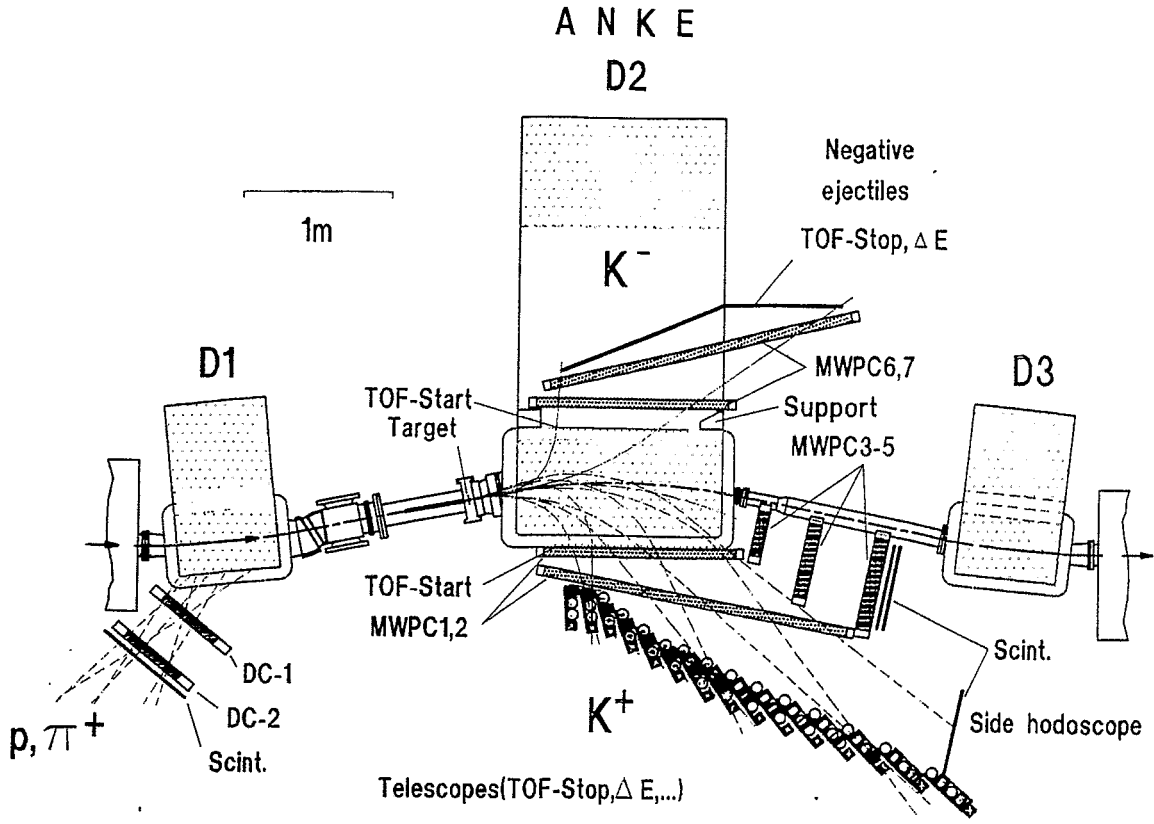
Prospects of ANKE

Prospects of Anke

M. Debowski

Fz Rossendorf



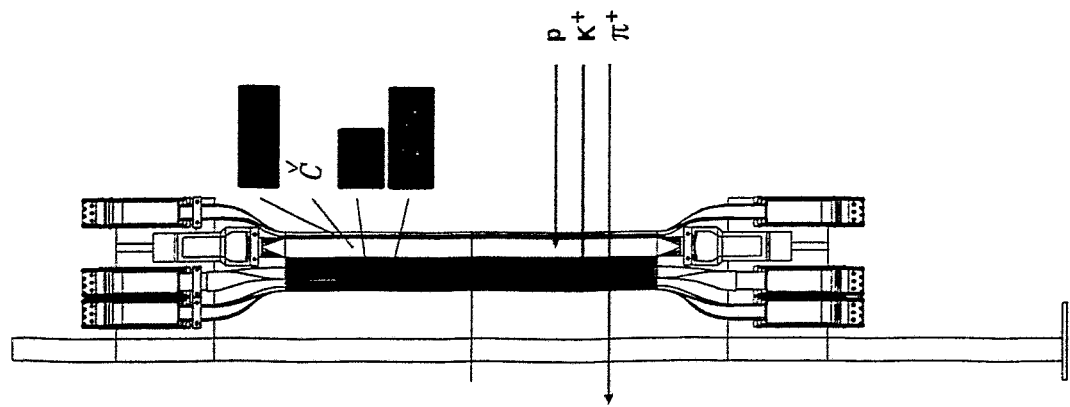


Telescopes for K^+ Detection

- Width = 10 cm
- Height = 52 ... 100 cm
- 13 Telescopes @ 1.3 T
- 15 Telescopes @ 1.6 T

- BC 408
- GS 233
- XP 2020
- GS 218
- XP2312

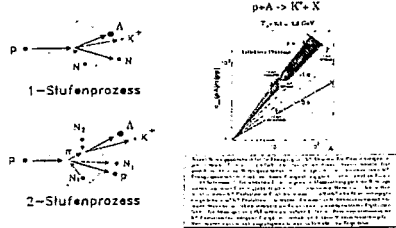
π^+ and p suppression
 $\geq 10^6$
 (tested)



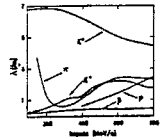
Geplante Experimente an ANKE

K⁺Mesonen-Produktion in Proton-Kern Stößen unterhalb der Nukleon-Nukleon-Schwelle (COSY-Proposal #18; K.Sistemich)

Information über den K⁺-Produktionsmechanismus.

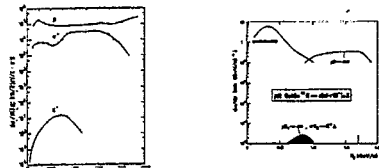


K⁺-Mesonen sind ideal geeignet zur Erforschung des Kerninneren.



Das Bild zeigt die mittleren freien Weglänge verschiedener Hadronen in Kernmaterie. Man sieht, daß K⁺ Mesonen unter allen geladenen Hadronen die größte freie Weglänge besitzen, da sie aufgrund ihres Aufzögerens Verhalten nur sehr schwach mit dem Zielkern wechselwirken. Daher sind K⁺-Mesonen sehr gut zur Erforschung des Kerninneren geeignet.

PROBLEM: Extrem kleine K⁺-Produktionsquerschnitte



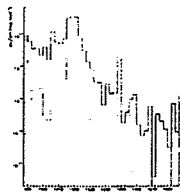
K⁺K⁻Mesonen-Produktion in Proton-Kern-Stößen unterhalb der Nukleon-Nukleon-Schwelle (COSY-LOI #21; H.Mueller, FZ Rossendorf)

Mögliche Reaktionsmechanismen

- Direkte Produktion: $pN \rightarrow N\bar{N}K^+K^-$
- Produktion über mesonische Resonanzen: $pN \rightarrow N\pi N\bar{N}K^+K^-$
 - $\rho(1020)$, $\Gamma = 1.2 \text{ MeV}$
 - $\omega(780)$, $\Gamma = 175 \text{ MeV}$
 - $f_0(980)$, $\Gamma = 220 \text{ MeV}$
- Produktion über die Δ_{33} Resonanz ($\Gamma = 115 \text{ MeV}$): $pN \rightarrow \Delta_{33}N\bar{N}K^+K^-$

ZIEL: Erforschung der Kernstruktur und der Reaktionsmechanismen.

- Hochimpulskomponenten der nuklearen Wellenfunktion
- Clusterbildung von mehreren Nukleonen im Kern
- Einfluß der Kernmaterie auf Hadronen und deren Produktion
- Bestimmung von s-Komponenten zur Grundzustandswellenfunktion des Nukleons
- Endzustandswechselwirkung von K⁻-Mesonen im Kern



Die meisten Spektren der verschiedenen Messen der K⁺K⁻ Paare zur Reaktion p¹²C → K⁺K⁻ + n, n₂ = 12 MeV und Energieauswertete die ρ^0 (Schichtgrenze kurz). Zur Identifizierung wurde die Elementarreaktion $p + n \rightarrow K^+ + K^- + p + n$ für $\sqrt{s} = 1020 \text{ MeV}$ in auf die Teilung von ϕ Mesonen in Teilchenpaare untersucht. Die ersten, getriebenen Verhältnisse zeigen sich mit einer Simulation des Experimentes am ANKE am Nationalen K⁺ Ring in der entsprechenden Darstellung. Die ϕ Mesonen im nach hier speziell zu verstehen und sollen sich mit der Eigenheit des K⁺ Paars in der entsprechenden Darstellung. Die ϕ Mesonen im nach hier speziell zu verstehen und sollen sich mit der Eigenheit des K⁺ Paars in der entsprechenden Darstellung. Die ϕ Mesonen im nach hier speziell zu verstehen und sollen sich mit der Eigenheit des K⁺ Paars in der entsprechenden Darstellung.

Exklusive Messung des Deuteronenaufbruchs mit einem polarisierten Protonenstrahl und einem polarisierten Deuteronentarge (COSY-Proposal #20; V.Komarov, JINR Dubna)

- $\sqrt{s} = 1020 \text{ MeV}$ in Nachweis der vorwärts und rückwärts emittierten Protonen
- Projektionenge $L = 1000 - 2500 \text{ MeV}$
- Exklusive Messung der Vektor- und Tensoranalytischen sowie der Spinokorrelative Asymmetrie

Messung der ϕ -Mesonen-Produktion mit polarisierten Protonenstrahlen und targets (COSY-LOI #35; M.Sapozhnikov, Dubna)

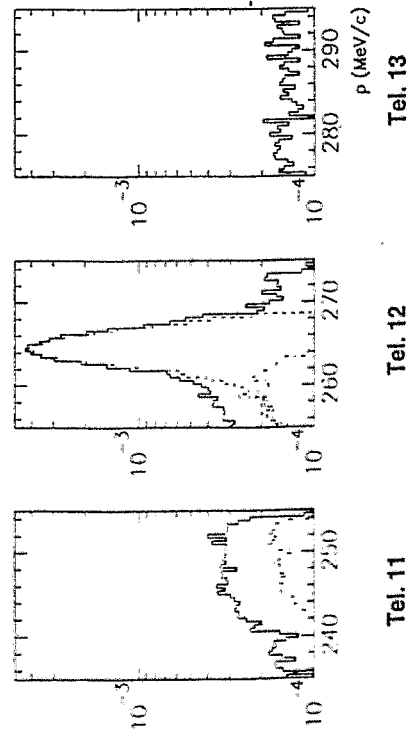
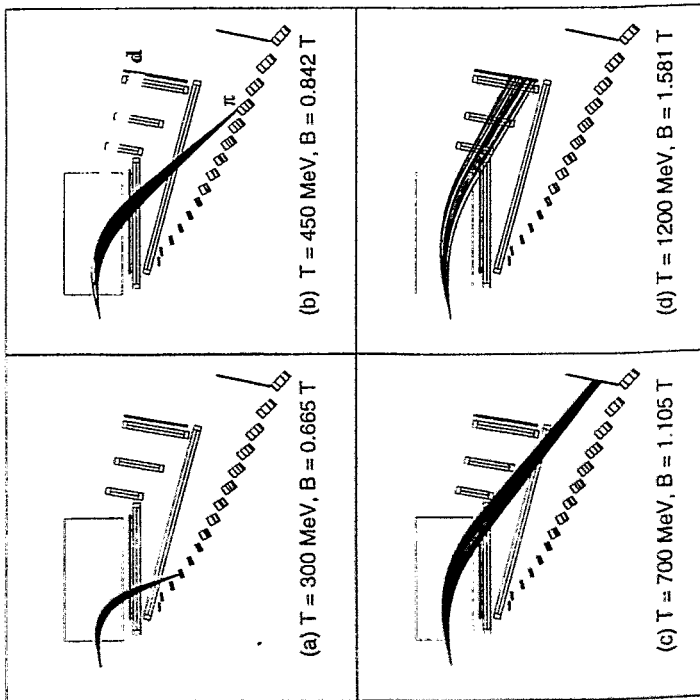
- $\sqrt{s} = 1020 \text{ MeV}$
- Nachweis aller von Teilchen im Ausgange aufgeführt der großen Winkelablenkung ANKE möglich
- Messung in Schwerionenebene bei einer Projektionenge von $L = 2000 \text{ MeV}$
- Information über die Polarisation der intensiven Nukleonen-Ströme

Untersuchung der η -Mesonen-Produktion in Proton-Kern-Stößen (COSY-Proposal #23; H.Seyfarth)

Weitere Experimentvorschläge:

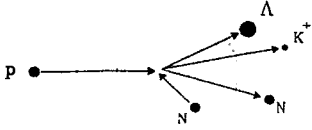
- Messung der ρ^0 Polarisationseigenfunktion in Reaktionen $p+p \rightarrow p+p+\pi^0$ im Energiebereich $L = 300 - 1000 \text{ MeV}$ (I. Kupke, FNPI Gatchina)
- Messung der ρ^0 π^0 Anregungsfunktion bei kleinen Winkeln (E.Hilbert, U. Hama)
- Studium des ρ^0 und π^0 Wechselwirkung in einem Systemzustand (S.L.Helms, FNPI Gatchina)
- Messung der π^+ Produktion unter Vorwärtswinkel in $p^12\text{C}$ Reaktionen bei $L = 1 \text{ GeV}$ (I. Kupke, FNPI Gatchina)
- Untersuchung der Produktion schneller Deuteronen in $p^12\text{C}$ Reaktionen bei $L = 1 \text{ GeV}$ (I. Kupke, FNPI Gatchina)
- Produktion leichter Isotopene und So bis nach abendlichen Hyperon-Nukleon-Zuständen (I. Kupke, FNPI Gatchina)
- Untersuchung des Einflusses der Kernmaterie auf die Massen und Breiten hadronischer Resonanzen (I. Kupke, FNPI Gatchina)
- Studium des "1 odd Asymmetry" in elastischer ρ^0 Rückstreuung (I.M.Sitok, JINR Dubna)

Kalibrierung des ANKE-Detektionssystems



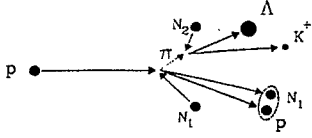
Reaction mechanism

1 step:



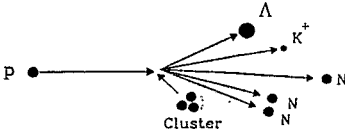
$$\sigma_{pA}^{K^+} = N_1 \int d^3q \rho(q) \sigma_{pN}^{K^+}(\sqrt{s})$$

2 step :



$$\sigma_{pA}^{K^+} = N_1 \int \int d^3q d^3p_\pi \rho(q) F(p_\pi) W(p_\pi, A) \sigma_{\pi N}^{K^+}(\sqrt{s})$$

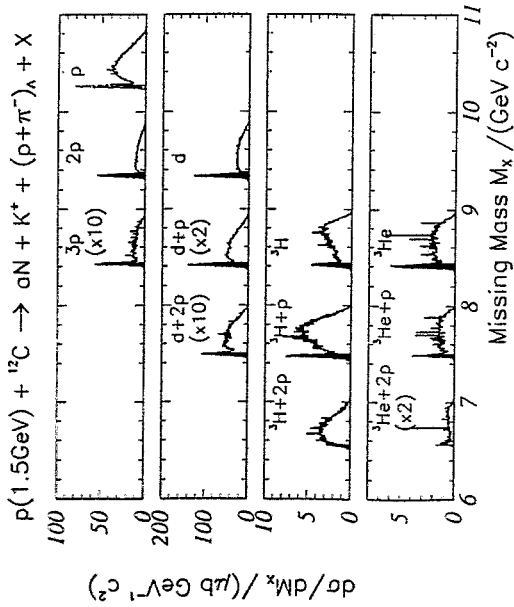
clusters:



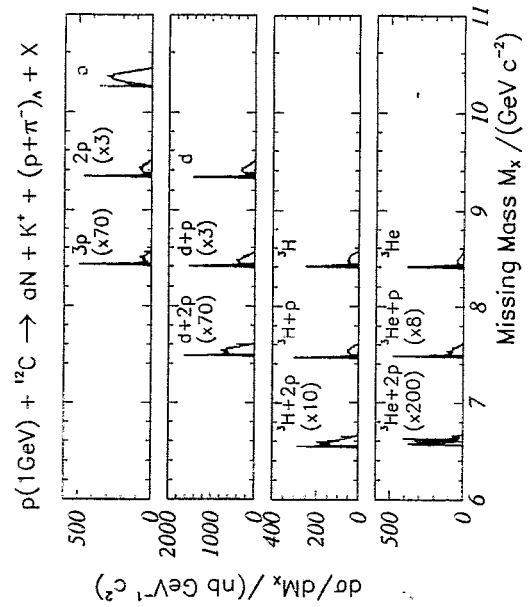
$$d\sigma(s) = \sum_a \sum_z \sigma_{az} \sum_{\alpha_{az}} dW_{az}(s, \alpha_{az})$$

Missing mass peaks

1.5 GeV

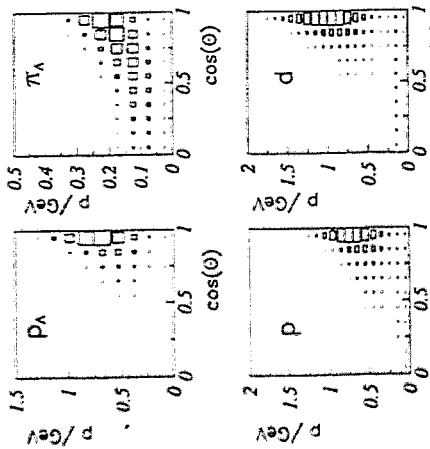


1.0 GeV

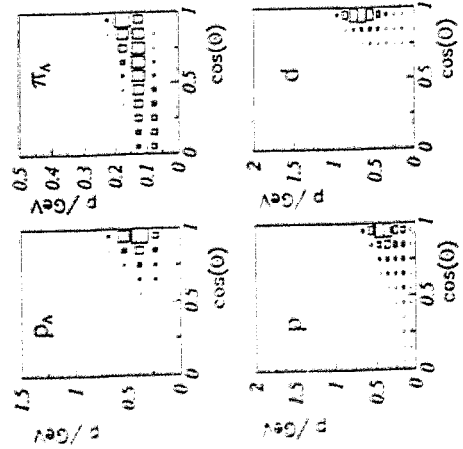


Winkel-Impuls-Korrelationen

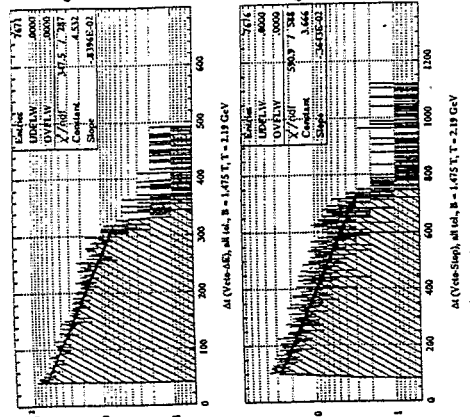
Projektilenergie 1,5 GeV



Projektilenergie 1,0 GeV



Resolving spectra



$\Delta t(Ve-4E)$
11.7 ns

$\Delta t(Ve-5D)$
12.1 ns

PAU fits a function $f(t) = \exp(a+bt)$. From 6 core can calculate

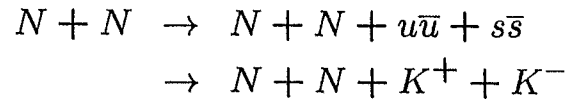
T [GeV]	spectrum	b [GeV]	$\tau = -1/b$ [ns]
212	Veto-Stop Veto-4E	$-3.64 \cdot 10^{-3}$ $-8.40 \cdot 10^{-3}$	274.7 119.0
213	Veto-Stop Veto-4E	$-3.65 \cdot 10^{-3}$ $-8.63 \cdot 10^{-3}$	274.0 115.9

The average value is $\tau_{kt} = 11.9 ns$

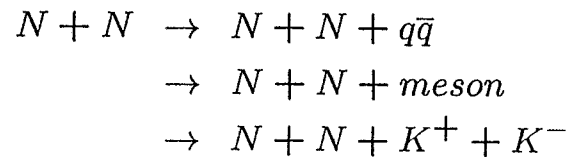
Why not 12.4 ns?
→ time calibration ok?

K^- production

1. direct



2. via mesonic resonances



- well established:

$$\phi(1020) \quad \Gamma = 4.2 \text{ MeV}$$

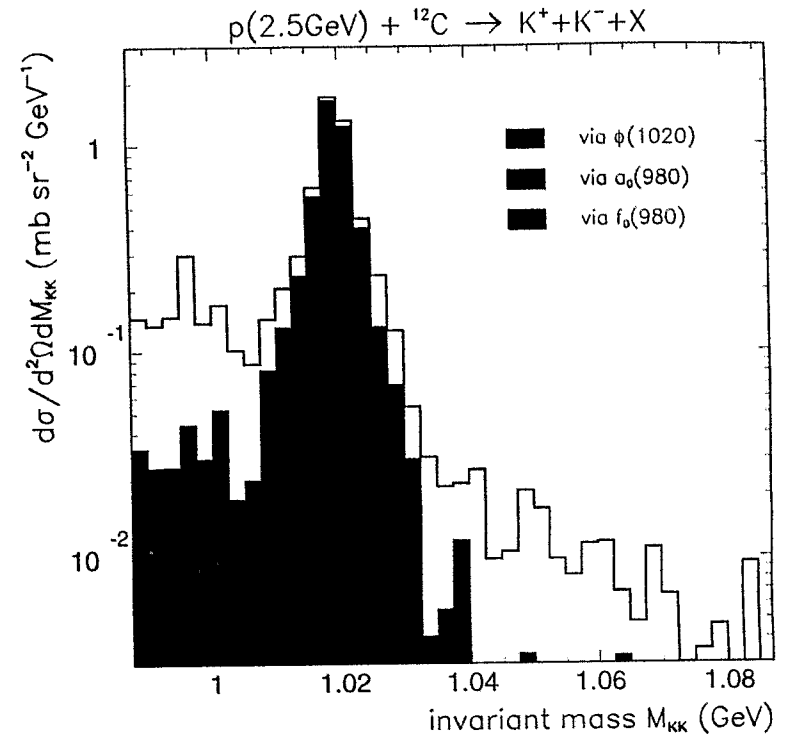
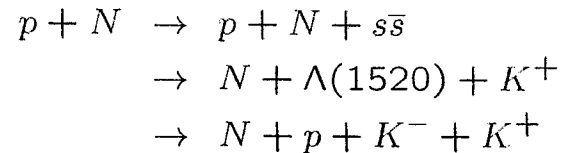
- structure under discussion:

$$a_0(980) \quad \Gamma = 50 \dots 300 \text{ MeV}$$

$$f_0(980) \quad \Gamma = 40 \dots 400 \text{ MeV}$$

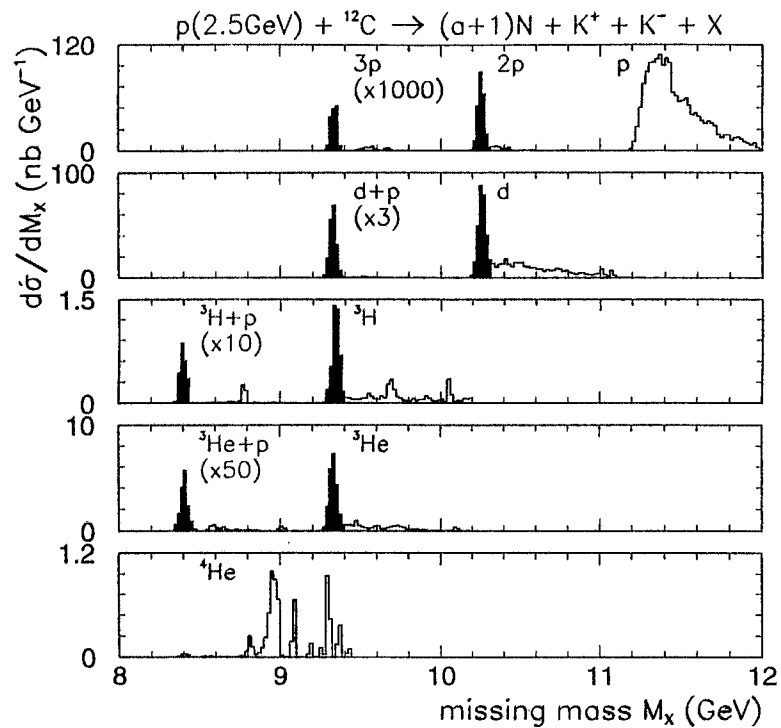
3. via baryonic $\Lambda(1520)$ resonance

$$\Gamma = 15.6 \text{ MeV}$$

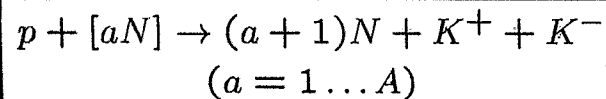


Calculated K^+K^- invariant-mass spectrum for emission angles $\theta \leq 10^\circ$

- strength of $\phi(1020)$ production
- propagation of $\phi(1020)$, K^+ and K^- through nuclear matter



Calculated missing mass spectra from $p^{12}\text{C}$ interactions at 2.5 GeV for the production of K^+/K^- pairs accompanied by $(a+1)$ nucleons with a being the number of participants according to



- ANKE Zero Degree Facility

$\text{K}^+ \text{K}^-$ spectrometer
subthreshold particle production

- $|\theta| < 10^\circ$
- momentum resolution $< 1.5\%$
- time resolution $< 500 \text{ ps}$
- trigger TOF & "telescope"
- PID TOF, ΔE , \check{C}

- K^+

- inclusive K^+ spectra
- different beam energies and targets
- "coincidence measurement"
- number of participating nucleons

- K^-

- inclusive spectra - enhancement?
- low $p_T \text{K}^-$

- $\text{K}^+ \text{K}^-$ pairs

- K^- production mechanism
- ϕ production and propagation in the nuclear medium
- "coincidence measurement"

ANKE - Kollaboration

K. ABRAHAMS¹², V. ABAZOV¹⁶, N. AMAGLOBELI²¹, V. ARTEMOV¹⁶, S. BARSOV¹⁸, U. BECHSTEDT¹, S. BELOSTOTSKI¹⁸, N. BONGERS¹, G. BORCHERT¹, W. BORGS¹, W. BRÄUTIGAM¹, M. BÜSCHER¹, W. CASSING⁸, V. CHERNETSKY¹⁹, B. CHILADZE²¹, M. CHUMAKOV¹⁹, J. DIETRICH¹, M. DROCHNER², S. DYMOV¹⁶, J. ERNST⁶, W. ERVEN², R. ESSER⁹, A. GERASIMOV¹⁹, YE.S. GOLUBEVA²⁰, O. GORCHAKOV¹⁶, D. GOTTA¹, O. GREBENYUK¹⁸, H. GRUPPELAAR¹², D. GRZONKA¹, M. HARTMANN¹, L. JARCZYK¹⁴, H. JUNGHANS¹, A. KACHARAVA¹⁶, N. KADAGIDZE¹⁶, B. KAMYS¹⁴, M. KARNADI¹, A. KHOUKAZ¹⁰, ST. KISTRYN¹⁴, F. KLEHR³, W. KLEIN¹, H.R. KOCH¹, N. KOCH⁷, M. KÖHLER², V.I. KOMAROV¹⁶, L. KONDRATYUK¹⁹, V. KOPTEV¹⁸, P. KRAVCHENKO¹⁸, V. KRUGLOV¹⁶, P. KULESSA¹⁴, A. KULIKOV¹⁶, A. KURBATOV¹⁶, H. LABUS¹, N. LANGENHAGEN⁵, S. LEMAÎTRE⁹, A. LEPGES¹, TH. LISTER¹⁰, H. LOEVENICH², G. MACHARASHVILI¹⁶, R. MAIER¹, S. MARTIN¹, Z. MENTESHASHVILI²¹, S. MIKIRTICHYANTS¹⁸, H. MÜLLER⁵, R. NELLEN¹, V. NELYUBIN¹⁸, M. NIORADZE²¹, W. OELERT¹, H. OHM¹, A. PETRUS¹⁶, H. POHL², D. PRASUHN¹, B. PRIETZSCH⁵, H.J. PROBST¹, C. QUENTMEIER¹⁰, F. RATHMANN⁷, B. RIMARZIG⁵, K. RITH⁷, Z. RUDY¹⁴, R. SANTO¹⁰, M. SAPOZHNIKOV¹⁶, H. PAETZ GEN.SCHIECK⁹, R. SCHLEICHERT¹, A. SCHNEIDER¹, CHR. SCHNEIDER⁵, H. SCHNEIDER¹, CHR. SCHNEIDERREIT⁵, G. SCHUG¹, O.W.B. SCHULT¹, U. SCHWARZ¹¹, H. SEYFARTH¹, A. SIBIRTSEV^{8,19}, U. SIELING², K. SISTEMICH¹, J. SMYRSKI¹⁴, H. STECHEMESSER³, E. STEFFENS⁷, H.J. STEIN¹, J. STENGER¹, A. STEPANOV¹⁹, H. STRÖHER¹, A. STRZALKOWSKI¹⁴, V. TCHERNYSHEV¹⁹, W. TENTEN², C. THOMAS⁷, S. TRUSOV¹⁷, YU. UZIKOV¹⁶, A. VASSHIEV¹⁸, A. VOLKOV¹⁶, K.-H. WATZLAWIK¹, C. WILKIN¹³, P. WÜSTNER², S. YASCHENKO¹⁶, V. YAZKOV¹⁷, B. ZALIKHANOV¹⁶, N. ZHURAVLEV¹⁶, K. ZWOLL² und I. ZYCHOR¹⁵

¹Institut für Kernphysik, Forschungszentrum Jülich, D-52425 Jülich

²Zentrallabor für Elektronik, Forschungszentrum Jülich, D-52425 Jülich

³Zentralabteilung Technologie, Forschungszentrum Jülich, D-52425 Jülich

⁴Institut für Schicht- und Ionentechnik, Forschungszentrum Jülich, D-52425 Jülich

⁵Institut für Hadronen- und Kernphysik, Forschungszentrum Rossendorf, D-01474 Dresden

⁶Institut für Strahlen- und Kernphysik, Universität Bonn, Nußallee 14, D-53115 Bonn

⁷Physikalisches Institut II, Universität Erlangen-Nürnberg, Erwin-Rommel-Str. 1, D-91058 Erlangen

⁸Institut für Theoretische Physik, Universität Gießen, H.-Buff-Ring 16, D-35392 Gießen

⁹Institut für Kernphysik, Universität Köln, Zùlpicher Str. 77, D-50937 Köln

¹⁰Institut für Kernphysik, Universität Münster, W.-Klemm-Str. 9, D-48149 Münster

¹¹Universität GH Paderborn, Abt. Soest, FB Elektrische Energietechnik, Steingraben 21, D-59494 Soest

¹²ECN-Nuclear Energy, P.O. Box 1, 1755 ZG Petten, The Netherlands

¹³Physics Department, University College London, Gower Street, London WC1 6BT, England

¹⁴Institute of Physics, Jagellonian University, Reymonta 4, PL-30059 Cracow, Poland

¹⁵Soltan Institute for Nuclear Studies, PL-05400 Swierk, Poland

¹⁶Laboratory of Nuclear Problems, Joint Institute for Nuclear Research, Dubna, 141980 Dubna Moscow Region, Russia

¹⁷Dubna Branch, Moscow State University, 141980 Dubna Moscow Region, Russia

¹⁸High Energy Physics Department, Petersburg Nuclear Physics Institute, 188350 Gatchina, Russia

¹⁹Institute for Theoretical and Experimental Physics, Cheremushkinskaya 25, 117259 Moscow, Russia

²⁰Institute for Nuclear Research, Russian Academy of Sciences, Moscow 117312, Russia

²¹High Energy Physics Institute, Tbilisi State University, University Str. 9, 380086 Tbilisi, Georgia

P. Kulessa:

Determination of Λ lifetime in heavy hypernuclei

Determination of the Λ lifetime in heavy hypernuclei

COSY-13

W. Borgs^(a), W. Cassing^(b), M. Hartmann^(a), L. Jarczyk^(c), B. Kamys^(c),
H.R. Koch^(a), P. Kulesza^(a,c), R. Maier^(a), M. Matoba^(d), H. Ohm^(a),
D. Prasuhn^(a), K. Pysz^(e), Z. Rudy^(e), O. Schult^(a), H. J. Stein^(a),
H. Ströher^(a), A. Strzałkowski^(c), Y. Uozumi^(d) and I. Zychor^(f)

^(a) Institut für Kernphysik, Forschungszentrum Jülich,
D-52425 Jülich, Germany

^(b) Institut für Theoretische Physik, Universität Giessen,
D-35392 Giessen, Germany

^(c) M. Smoluchowski Institute of Physics, Jagellonian University,
PL-30059 Cracow, Poland,

^(d) Department of Nuclear Engineering, Kyushu University,
Fukuoka 812, Japan

^(e) H. Niewodniczański Institute of Nuclear Physics,
PL-31342 Cracow, Poland

^(f) The Andrzej Soltan Institute for Nuclear Studies,
PL-05400 Świerk, Poland

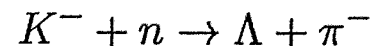
Supported by:

The Polish Committee for Scientific Research (Grant No.2 PO3B 065 12),
International Bureau of the BMBF, Bonn DLR

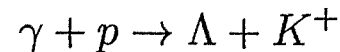
Λ production

• Reactions

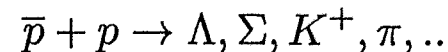
– Strangeness exchange



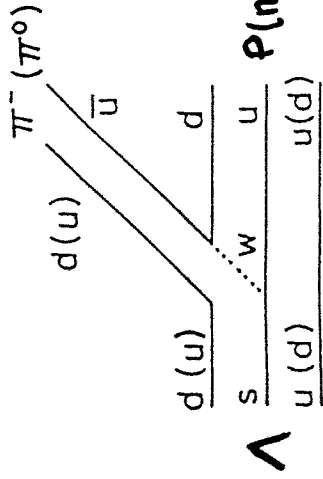
– Associated production



– Antiproton annihilation



The weak decay of the Λ particle



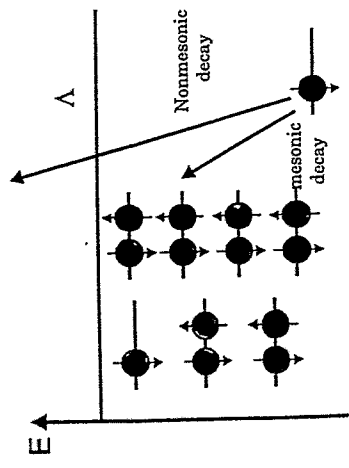
Mesonic decay

$$\Lambda \rightarrow p + \pi^- + 37.8 \text{ MeV}$$

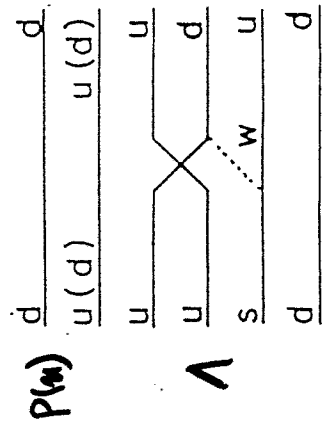
$$\Lambda \rightarrow n + \pi^0 + 41.1 \text{ MeV}$$

$$\tau_\Lambda = 263 \text{ ps}$$

Pauli blocking of the mesonic decay



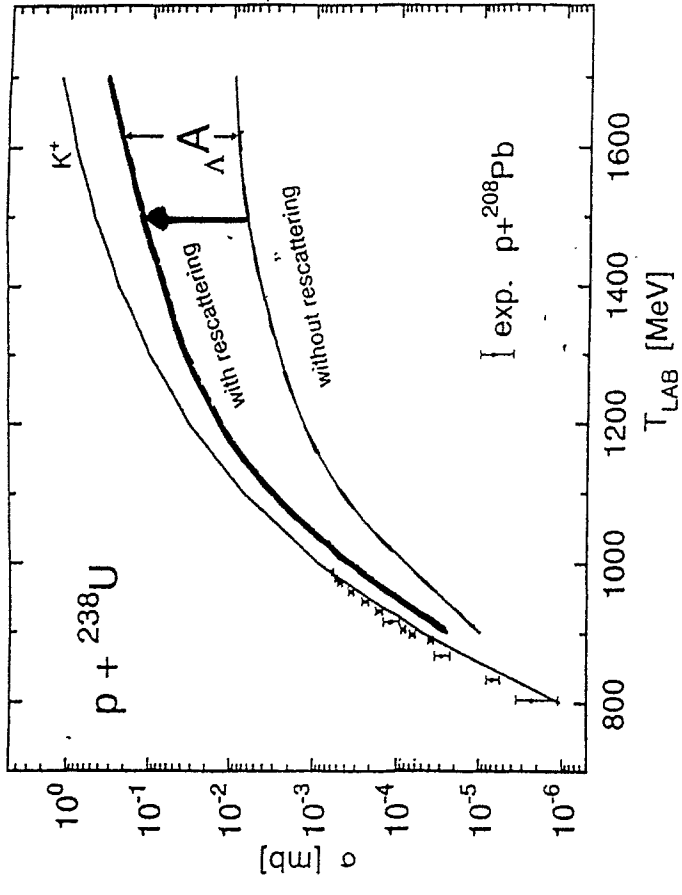
$P(n)$ Nonmesonic decay



$$\Lambda + N \rightarrow p + N + 176 \text{ MeV}$$

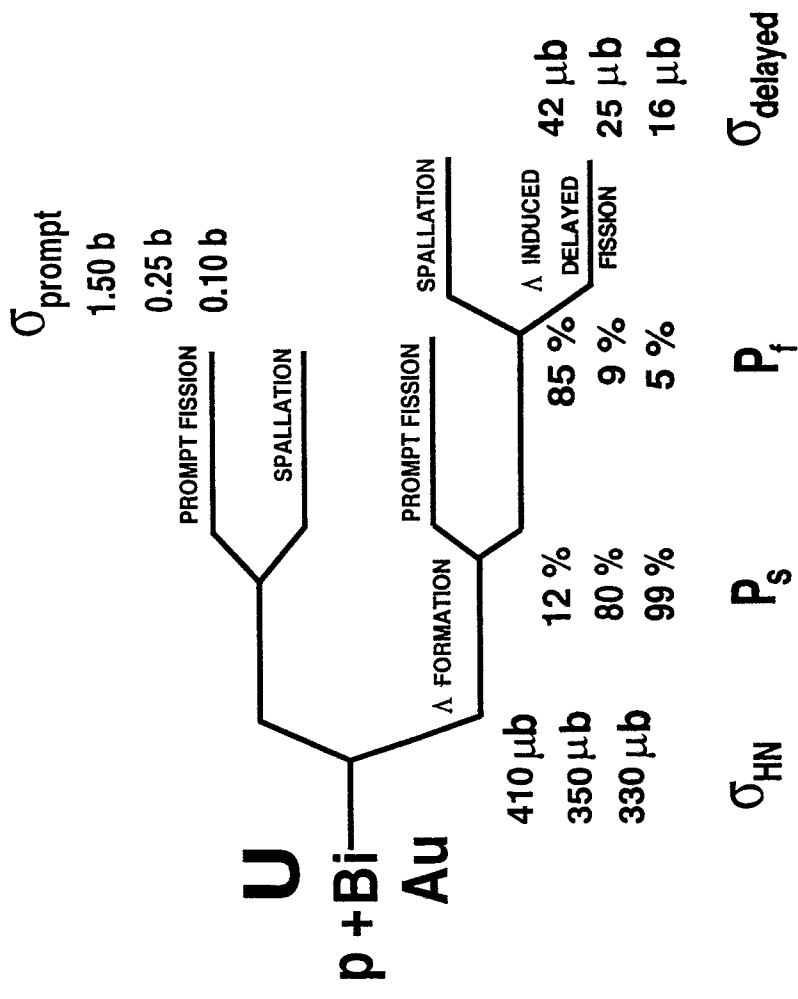
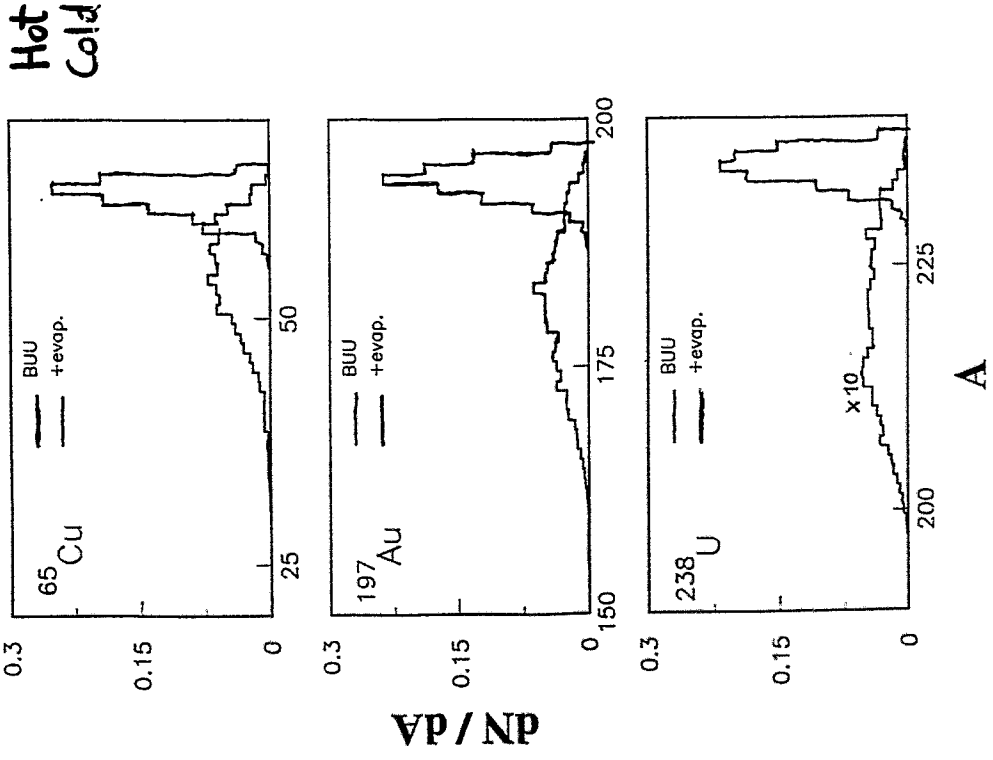
happens only in nuclei
medium effects!

(p, K) - production of heavy Hypernuclei



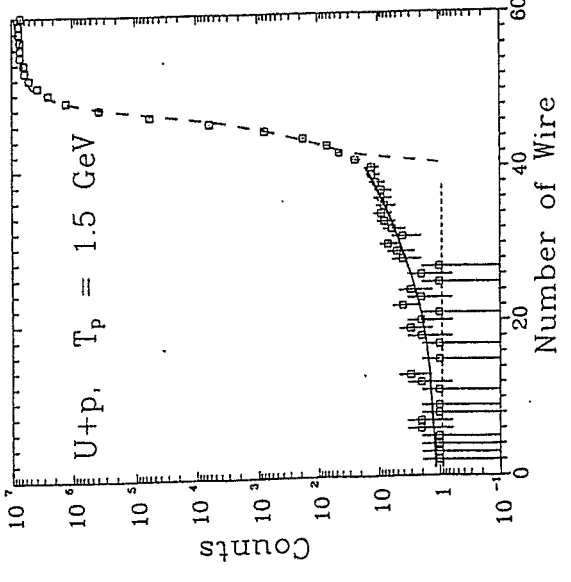
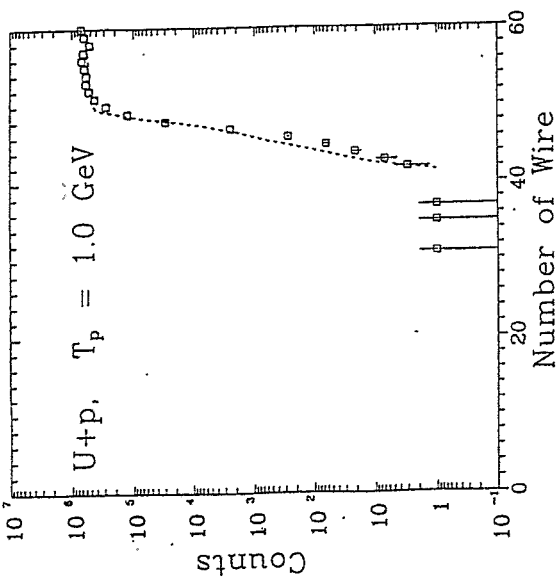
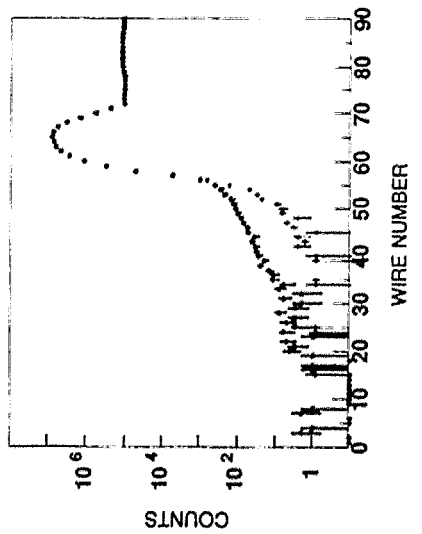
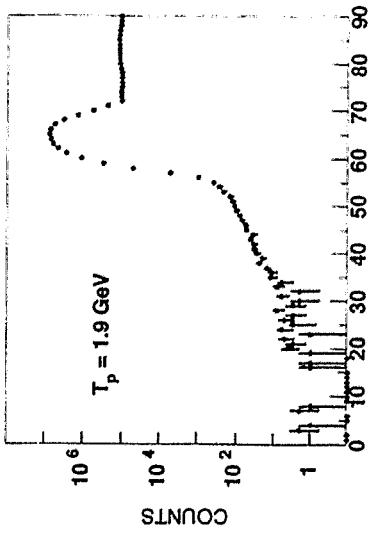
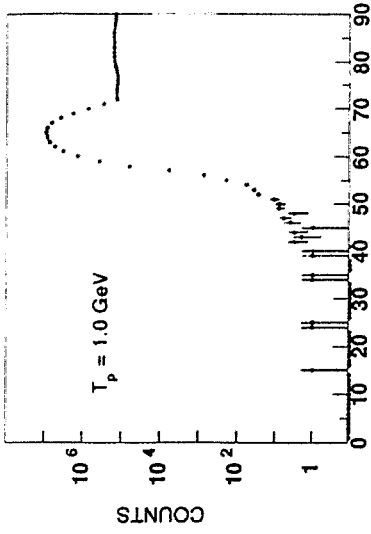
Mass distribution

08.12.98 pavol

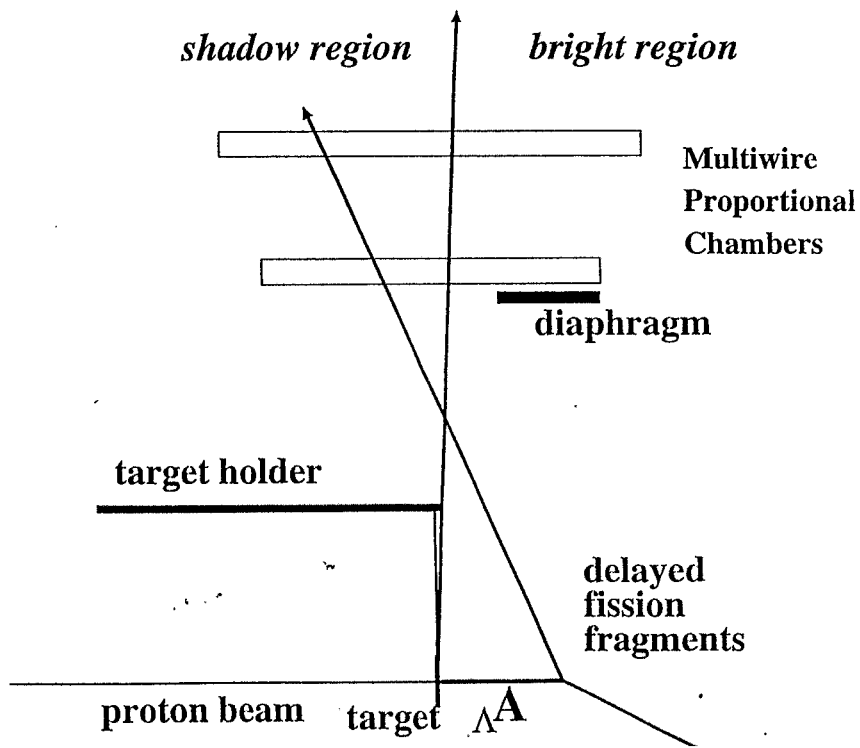
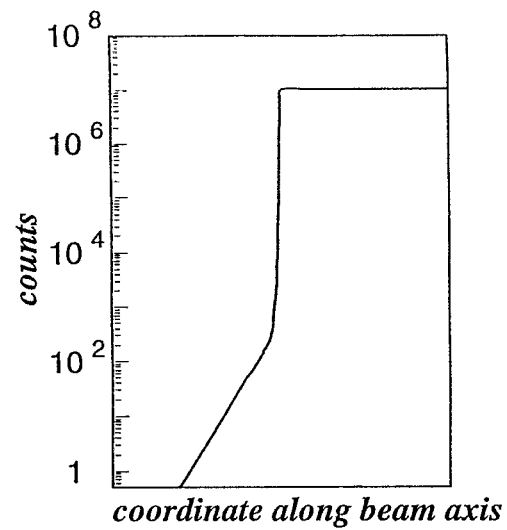
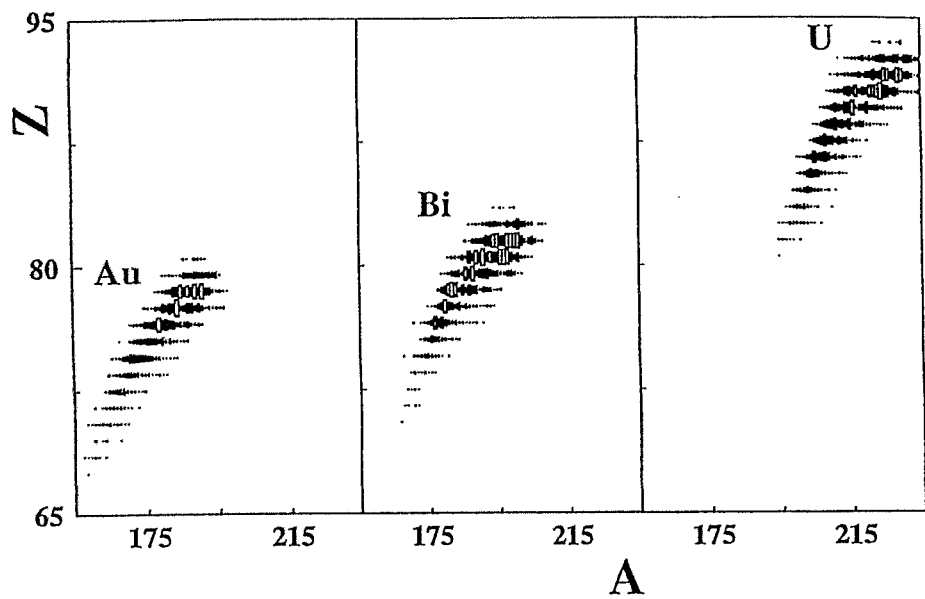


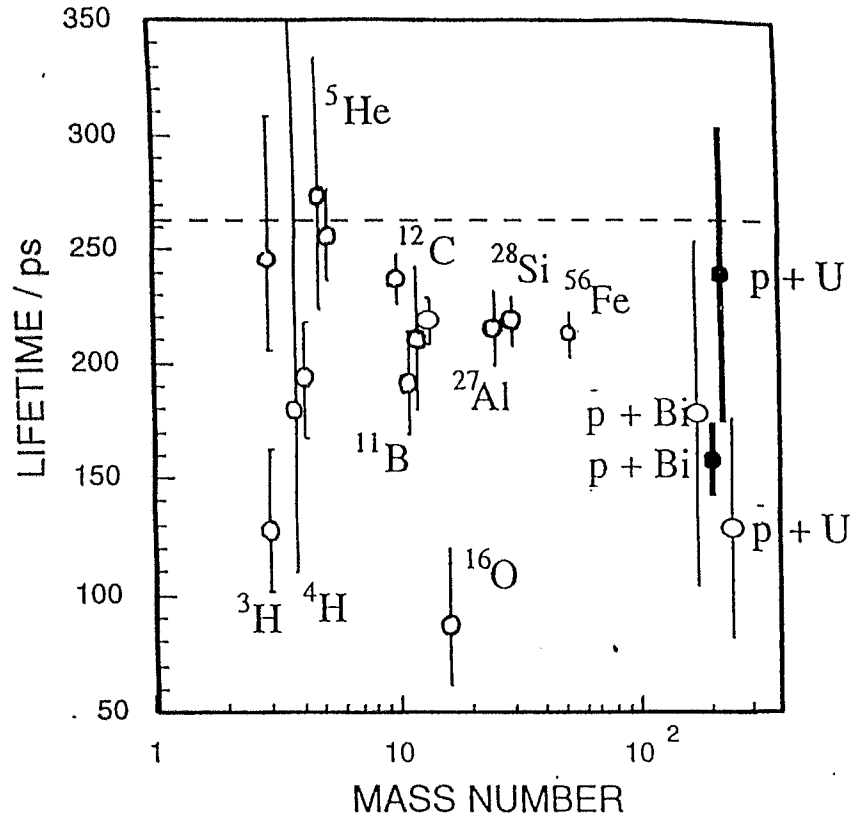
$$T_p = 156 \text{ eV}$$

P + 209 Bi



Number of Wire





Topics

- Decay of free and bound Λ
 - mesonic and nonmesonic decay
 - medium effect, Pauli blocking
- Production of heavy hypernuclei
 - Λ production
 - Hypernuclei production in the (p,K) reaction
- The hypernucleus experiment at COSY
 - principle, setup
 - results
- Summary

U $(240 \pm 60) \text{ ps}$

Bi $[161 \pm 7(\text{stat.}) \pm 14(\text{syst.})] \text{ ps}$

Cross Section

	Theory (hot)	Experiment (hot)
P + U (1.56eV)	110 μ b	150 \pm 150 μ b
P + Bi (1.96eV)	330 μ b	350 \pm 180 μ b

$$\sigma_{P+Bi} < 80 \text{ nb}$$

(P + Bi at 1.96eV)

CONCLUSIONS

1. production of heavy hypernuclei (cross sections \sim hundreds μ b) and investigation of the Λ hyperon lifetime can be performed using protons as projectiles and the recoil shadow method with a very thin heavy target placed in the beam circulating in an accelerator.
2. with the supercycle at COSY it was possible to carry out the background measurement and hypernucleus production at higher energies under identical target conditions \Rightarrow excitation functions.

PERSPECTIVES

continuation of measurements with Au and U targets to obtain precise lifetimes of Λ in hypernuclei.

A. Gillitzer:

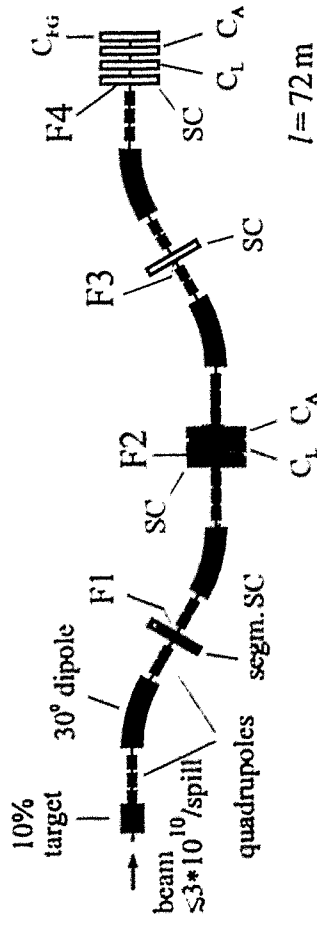
K⁻ production at the GSI fragment separator

K⁻ production at the Fragment Separator

1. K⁻ production in Ne and Ni induced collisions
 - method
 - results
2. ideas for future experiments
 - detection of K⁻ with low em momenta
 - K⁻ production in A + p collisions

subthreshold production of π^- , K^- and \bar{p} at the GSI Fragment Separator (FRS)

problem: $\sigma_\pi : \sigma_K : \sigma_{\bar{p}} \approx 10^7 : 3 \cdot 10^3 : 1$
 \Rightarrow requires high luminosity and good particle identification !



special ion optics: $\Omega = 3 \text{ msr}$, $\Delta p/p = \pm 3 \%$

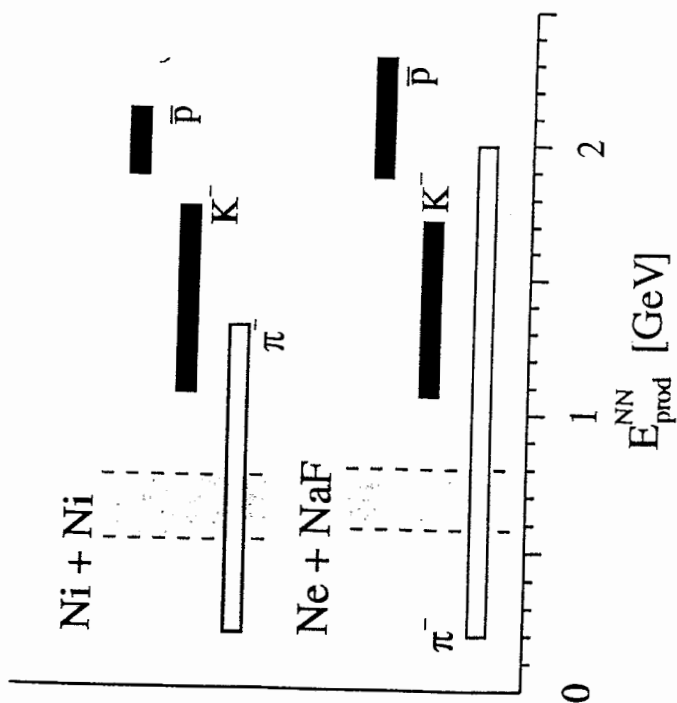
- SC: scintillation detector $\rightarrow 3 \times$ time of flight
- C_1 : lucite Cerenkov detector $\rightarrow \beta > 0.90$
- C_A : aerogel Cerenkov detector $\rightarrow \beta > 0.96, 0.98$
- C_{10} : glas/freon Cerenkov detector $\rightarrow \beta > 0.98$
- Cerenkov detectors used as veto counters

projectiles: ^{20}Ne ^{58}Ni targets: NaF , Cu , Sn , Bi
 Ni

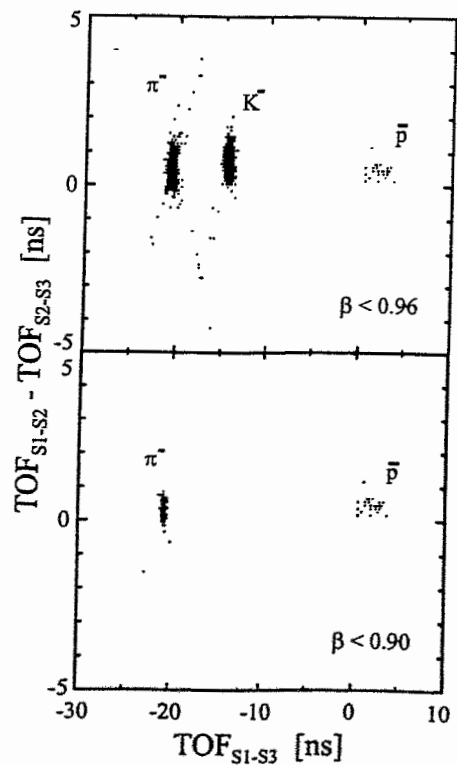
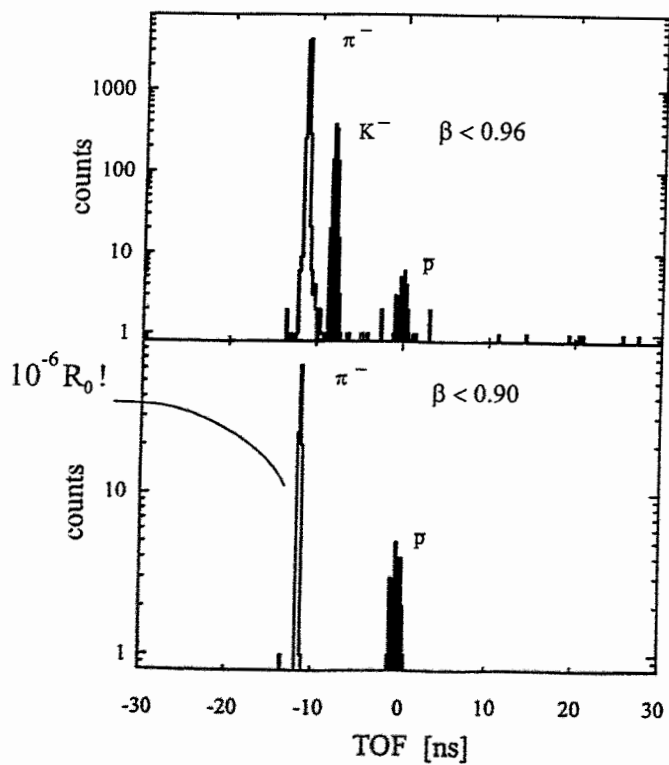
$E = 1.3 \dots 2.0 \text{ AGeV}$ ($-0.06 \dots -0.08$) AGeV

Teilchenerzeugung weit unter der Schwelle

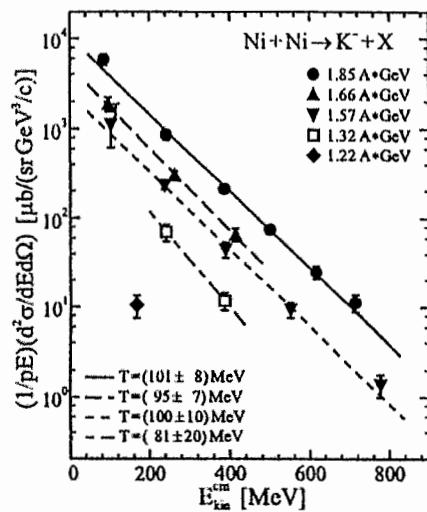
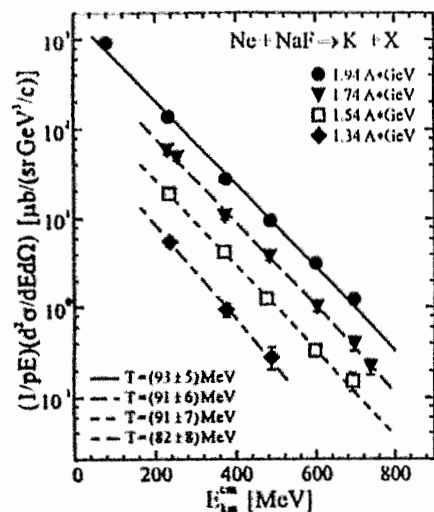
verfügbare Energie/NN: ca. 0.55 - 0.8 GeV
 aufzuwendende Energie: ca. 0.2 - 2.0 GeV (π^-)
 ca. 1.1 - 1.8 GeV (K^-)
 ca. 1.9 - 2.3 GeV (\bar{p})
 → fehlende Energie im NN System bis ca. 1.6 GeV



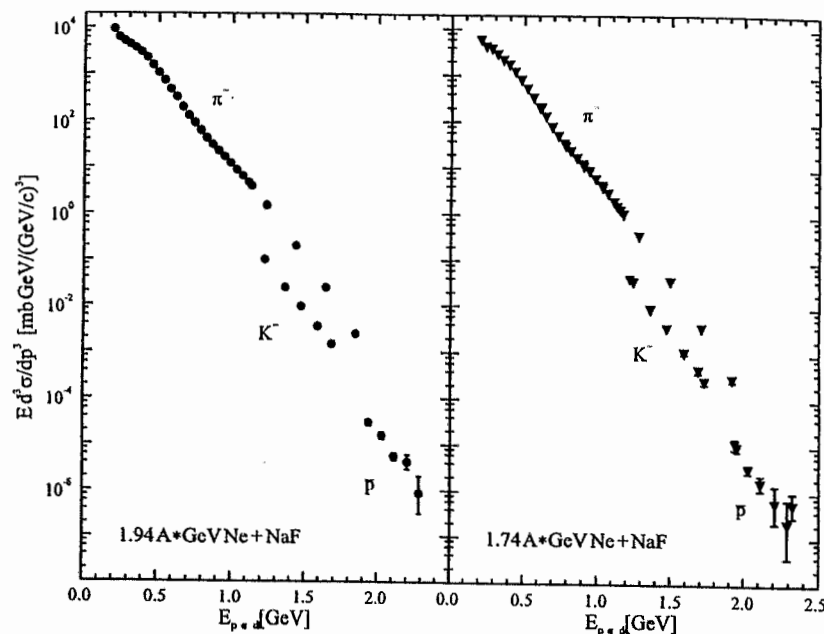
particle identification (1.94 A GeV $^{20}\text{Ne} + \text{Sn}$, $p_{\text{lab}} = 1.5 \text{ GeV}/c$)



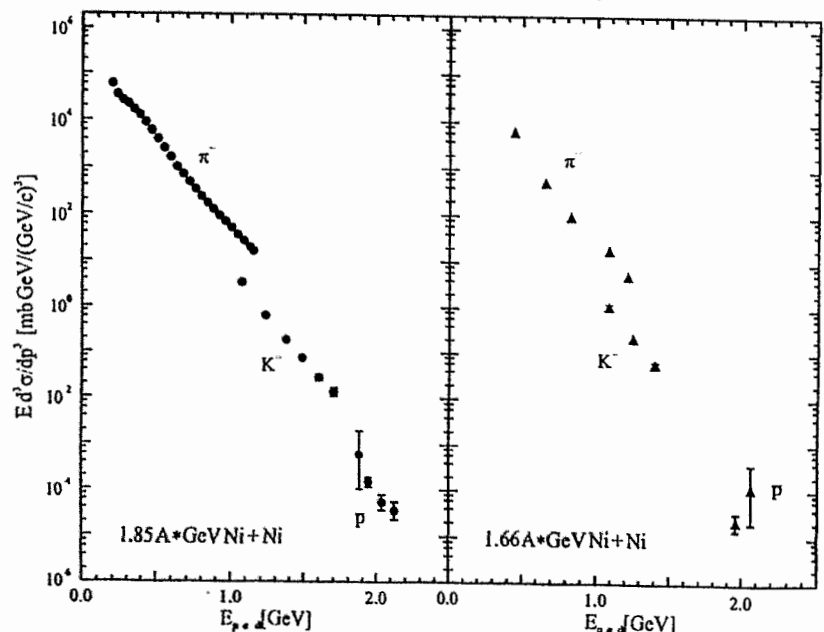
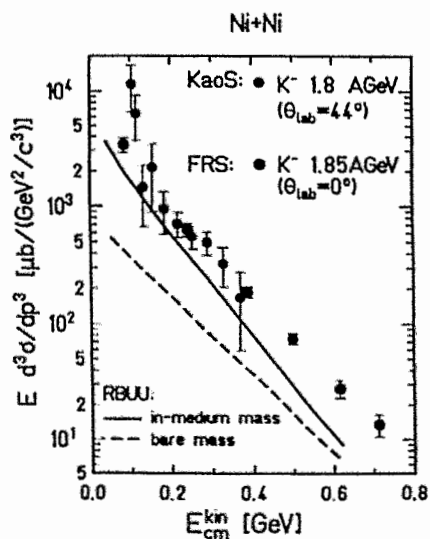
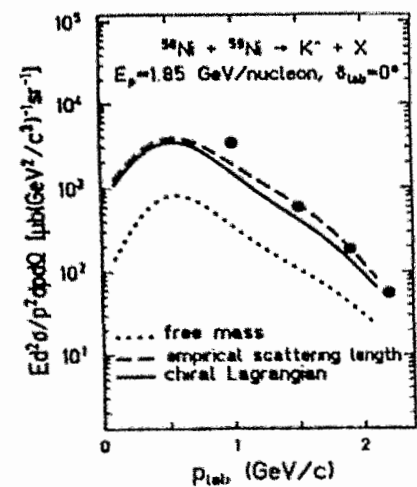
K^- production:



scaling of production cross section with required energy



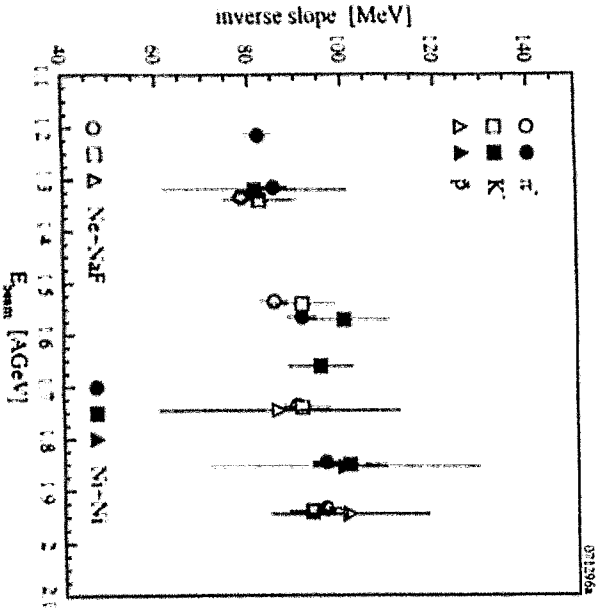
transport codes:



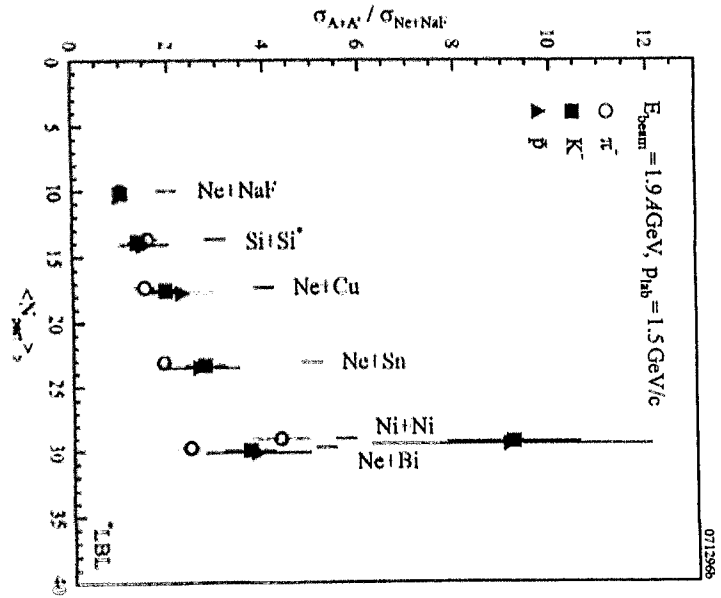
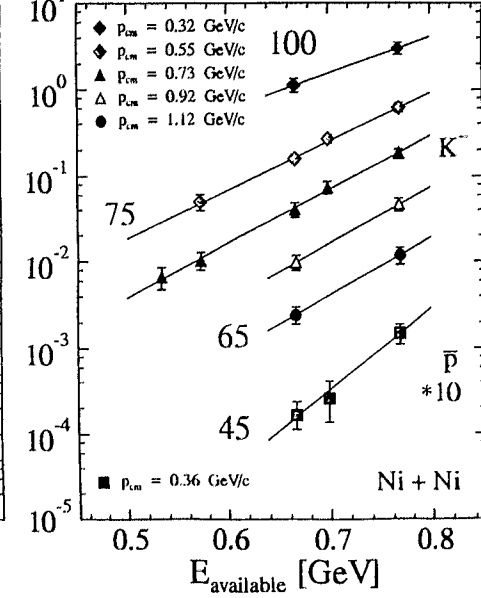
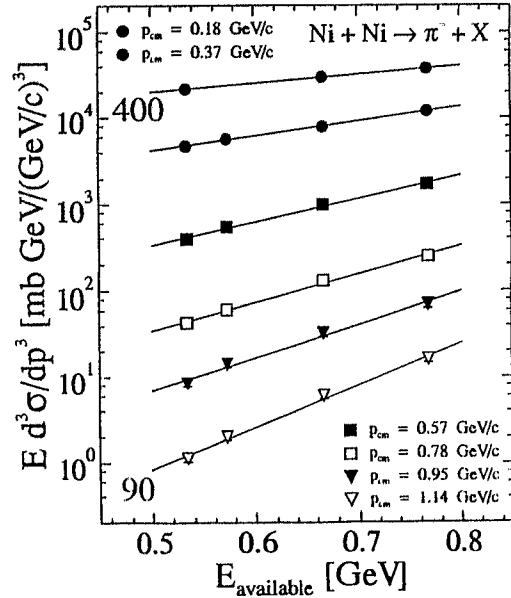
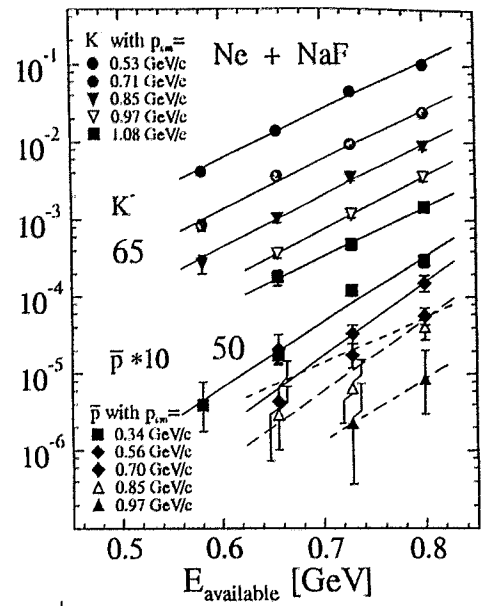
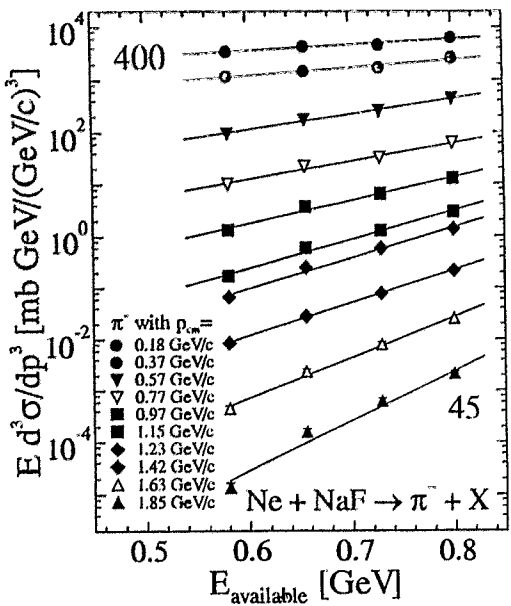
(G. Li *et al.*, Phys. Lett. B329(94)149)

KaoS: R. Barth *et al.*, PRL78(97)4007
 RBUU: W. Cassing *et al.*, NPA614(97)415

• observed K^- yields are not reproduced with the bare K^- mass



energy dependence of slope constants

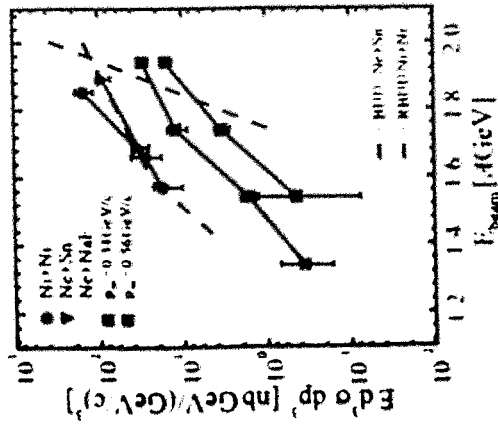


system size dependence of cross sections

Anregungsfunktion: $\sigma_{inv} \propto \exp(-E_{avail}/E_0) \rightarrow E_0$ in MeV

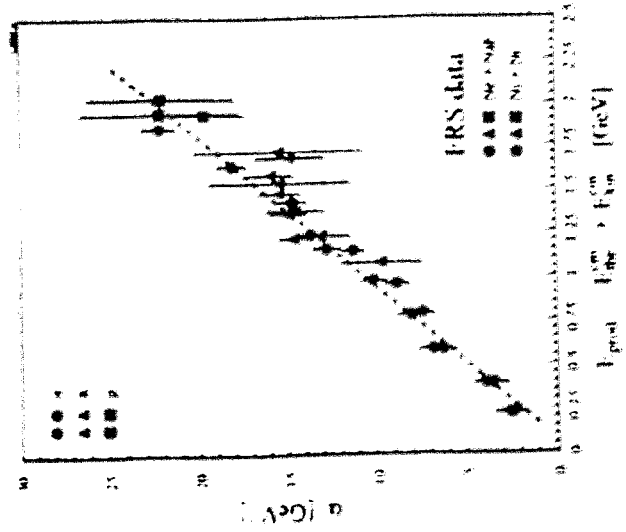
excitation function of \bar{p} and K^- production:

- slope of excitation function not affected by reabsorption
- sensitivity to medium modifications?



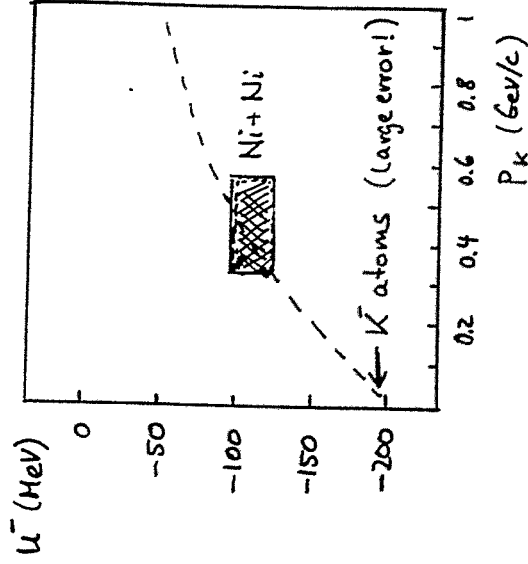
RBUU calculations with attractive \bar{p} mass shift reproduce slope of measured \bar{p} excitation function

RBUU W Cassing, S. Iets, Phys Comm
RBUU S Iets et al, Phys Rev C 50 (1994) 388



- for given particle species and cm momentum: production cross section increases exponentially with the available NN energy: $\sigma_{pp} \propto \exp(\alpha E_{available})$
- common dependence of the slope parameter α for $\pi, K^-,$ and \bar{p} with the required energy is observed: $\alpha \propto E_{prod} (E_{prod} = E_{lab}^* + E_{cm}^*)$
- no obvious indication for \bar{p} and K^- medium mass shifts (within exp. uncertainty)

Momentum dependence of K^- potential



see
A. Sibirtsev,
W. Cassing
nucl-th/9805021

⇒ model with reabsorption: $p_L \rightarrow 0$

→ detect K^- with low in-medium momenta! → $p_L \approx 0$



$$\beta_{K^-} \approx \beta_{cm} \rightarrow p_K^{lab} \sim 0.5 \text{ GeV}/c$$

$$p \sim (2-3) p_0$$

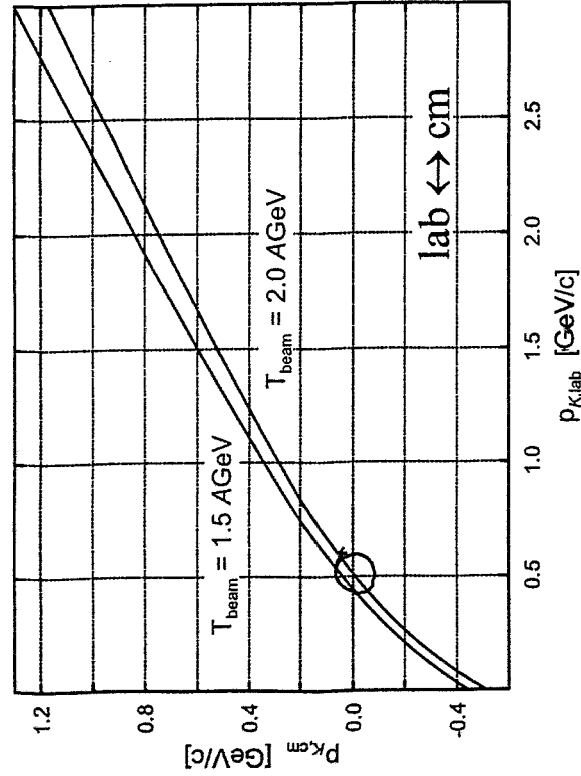


$$\beta_{K^-} \approx \beta_{proj} \rightarrow p_K^{lab} \sim 1.5 \text{ GeV}/c$$

$$p \sim p_0$$

K^- with low in-medium momenta

How to detect low momentum K^- ?



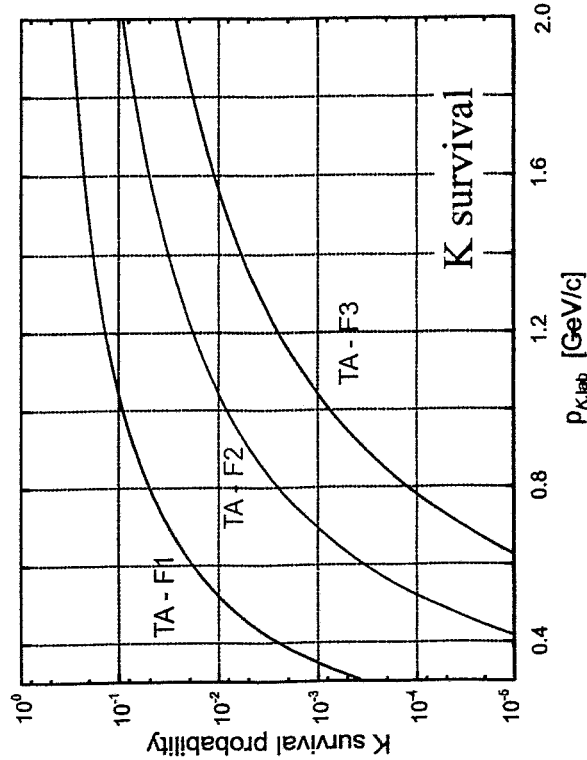
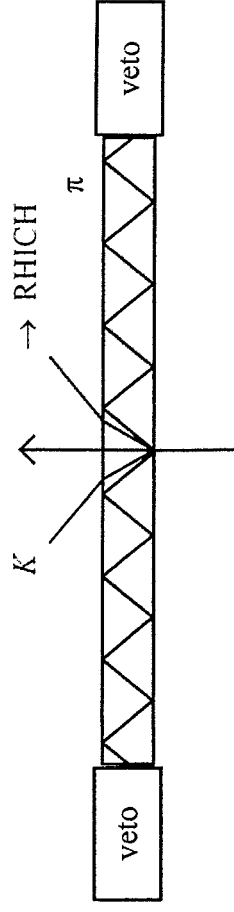
requirements:

- identify K^-
- suppress π^-

$p_{lab} = 0.50$ GeV/c \rightarrow $\beta_\pi = 0.963$ $\beta_K = 0.712$

possible concept:

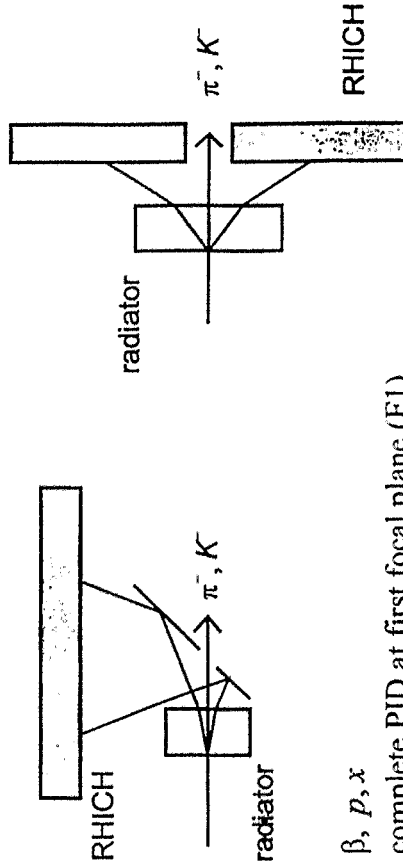
- threshold Cerenkov using total reflection combined with RHICH



total reflection:

$\beta_{krit} = \frac{1}{\sqrt{n^2 - 1}}$

- lucite: $n = 1.49 \rightarrow \beta_{krit} = 0.905$
- Pyrex glass: $n = 1.474 \rightarrow \beta_{krit} = 0.923$
- Quartz glass: $n = 1.458 \rightarrow \beta_{krit} = 0.942$



$\rightarrow \beta, p, x$
complete PID at first focal plane (F1)

$A + p \rightarrow K^- + X$ inverse kinematics ?

Estimate of observable K^- rate

Projectile : 2 GeV/u ^{40}Ca

Cross section estimate based on prediction by

A. Sibirtsev, W. Cassing, nucl-th/9805021

2.5 GeV $p + ^{12}\text{C}$ } $E \frac{d^3\sigma}{dp^3} \sim 2 \mu\text{b GeV}^{-2} \text{sr}^{-1}$
 $p_K \rightarrow 0$ } abs., no med.

2.5 GeV $p + ^{208}\text{Pb}$ } $E \frac{d^3\sigma}{dp^3} \sim 25 \mu\text{b GeV}^{-2} \text{sr}^{-1}$
 $p_e \rightarrow 0$ } abs., no med.

$\rightarrow \sigma_{inv} \propto A \rightarrow$ extrapolate to ^{40}Ca

extrapolation to $T_{beam} = 2.0 \text{ GeV}$:

using energy dependence of total K^- prod. cross sect.

in $p + ^{12}\text{C} \rightarrow K^- + X$

$\rightarrow \sigma_{inv} (2.0 \text{ GeV}) \sim 0.1 \cdot \sigma_{inv} (2.5 \text{ GeV})$

\Rightarrow for 2.0 GeV/u $^{40}\text{Ca} + p \rightarrow K^- + X$

$E \frac{d^3\sigma}{dp^3} \sim 0.7 \mu\text{b} / \text{GeV}^2 / \text{sr}$

attractive K^- potential

\rightarrow enhancement $\times 45$ for ^{12}C

$\times 20$ for ^{208}Pb

$R_{K^-} = E \frac{d^3\sigma}{dp^3} \frac{p^2}{E} \Delta\Omega \Delta p \int_{decay} I_0 \cdot n_H$

$\sigma_{inv} = 0.7 \mu\text{b GeV}^{-2} \text{sr}^{-1}$

$p_K = 1.5 \text{ GeV}/c$

$\Delta\Omega = 3 \text{ msv}$

$AP/p = \pm 3\%$

$f_{decay} = 0.041$ (TA \rightarrow S2 = 36 m)

$I_0 = 5 \times 10^9 / \text{spill} \sim 10^9 / \text{s}$

$n_H = 4.3 \times 10^{23} / \text{cm}^2$ (10 cm LH₂)

$\rightarrow R_{K^-} \sim 17 / \text{h}$ no medium effects

$\sim 500 / \text{h}$ with attractive K^- pot.

use shorter flight path:

- RICH instead of TOF and/or
- Pion (HADES) beamline instead of PLS

with $s = 18 \text{ m} \rightarrow f_{decay} = 0.20 \rightarrow$ factor 5

$\rightarrow R_{K^-} \sim 85 / \text{h}$ no medium effects

$\sim 2500 / \text{h}$ with K^- potential

SUMMARY

- Subthreshold K^- production yield indicates attractive K^- potential
- Problem: absorption in nuclear medium not well known
- slope parameter of excitation function for all particles (π^- , K^- , \bar{p}) increases linearly with energy required for the process
- Interesting to detect K^- with low in-medium momenta
- Such experiments seem to be feasible both for $A+A$ and $A+p$

P. Crochet:

Results from FOPI (1)

Results from FOPI (1)

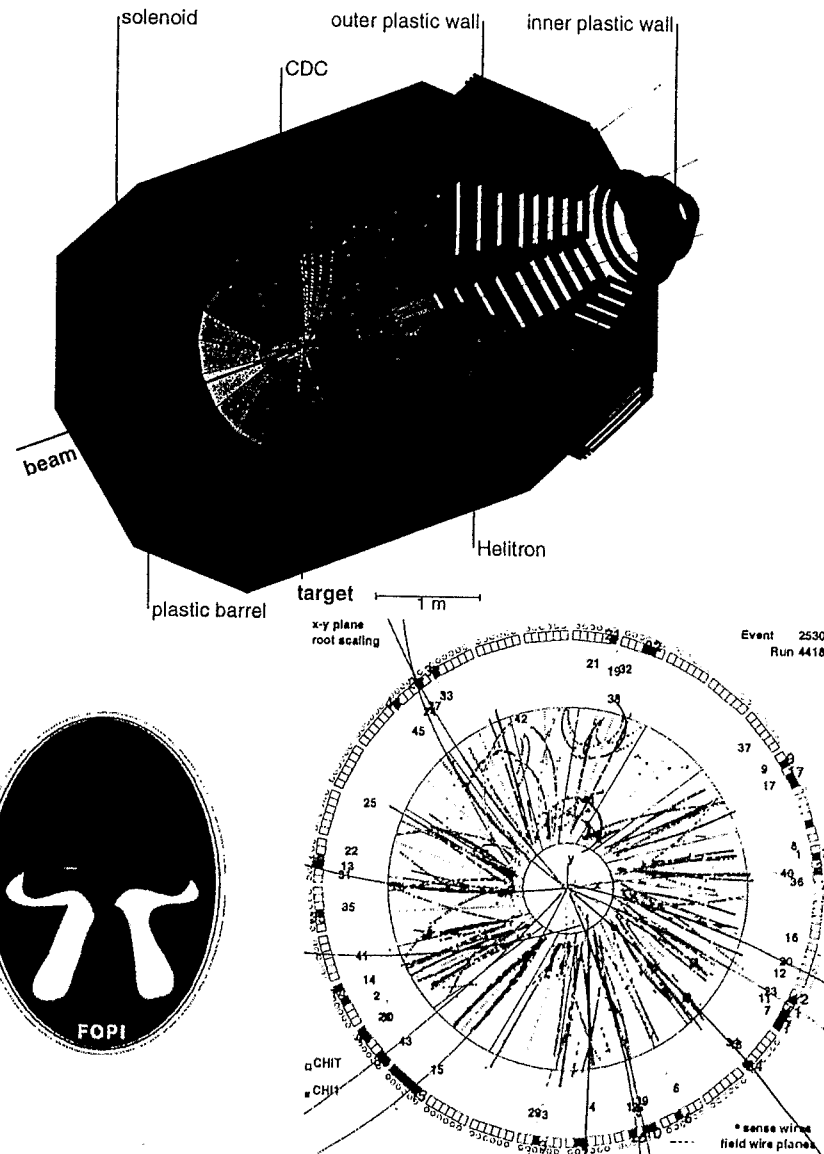
J.P. Alard, A. Andronic, R. Averbeck, Z. Basrak, N. Bastid, I. Belyaev, A. Bendarag, G. Berek, D. Best, R. Čaplar, N. Cindro, P. Crochet, A. D'Amico, P. Dabjeux, M. Dželalija, M. Eskef, Z. Fodor, L. Fraysse, A. Genoux-Lubain, A. Gobbi, Y. Gorbenko, W. Herrmann, K.D. Hildenbrand, B. Hong, J. Kecskemeti, Y.J. Kim, M. Kireczky, M. Kollia, R. Kotte, M. Kowalczyk, T. Kress, R. Kutsche, A. Lebedev, K.S. Lee, Y. Leifels, V. Manko, H. Maritz, S. Mohren, D. Moisa, W. Neubert, A. Nianine, D. Pelte, M. Petrovici, C. Plettner, F. Ram, W. Riel, J. B. de Schauenburg, D. Schüll, Z. Seres, B. Sikora, K.S. Sim, V. Simon, K. Simek, W. Sliwa, A. Somov, M. Stockmeier, G. Stoicea, M. Vasiliev, P. Wagner, G.S. Wang, K. Winiel, D. Wohlhuth, J.T. Yang, I. Yushmanov, A. Zhilin

IPNE Bucharest, Romania
 ITEP Moscow, Russia
 GRIP/KEK/Budapest, Hungary
 Kurchatov Institute, Moscow, Russia
 LPC Clermont, France
 Korea University, Seoul, Korea
 GSI Darmstadt, Germany
 IReS Strasbourg, France
 FZ Rossendorf/Dresden, Germany
 Univ. of Warsaw, Poland
 Univ. of Heidelberg, Germany
 RBI Zagreb, Croatia

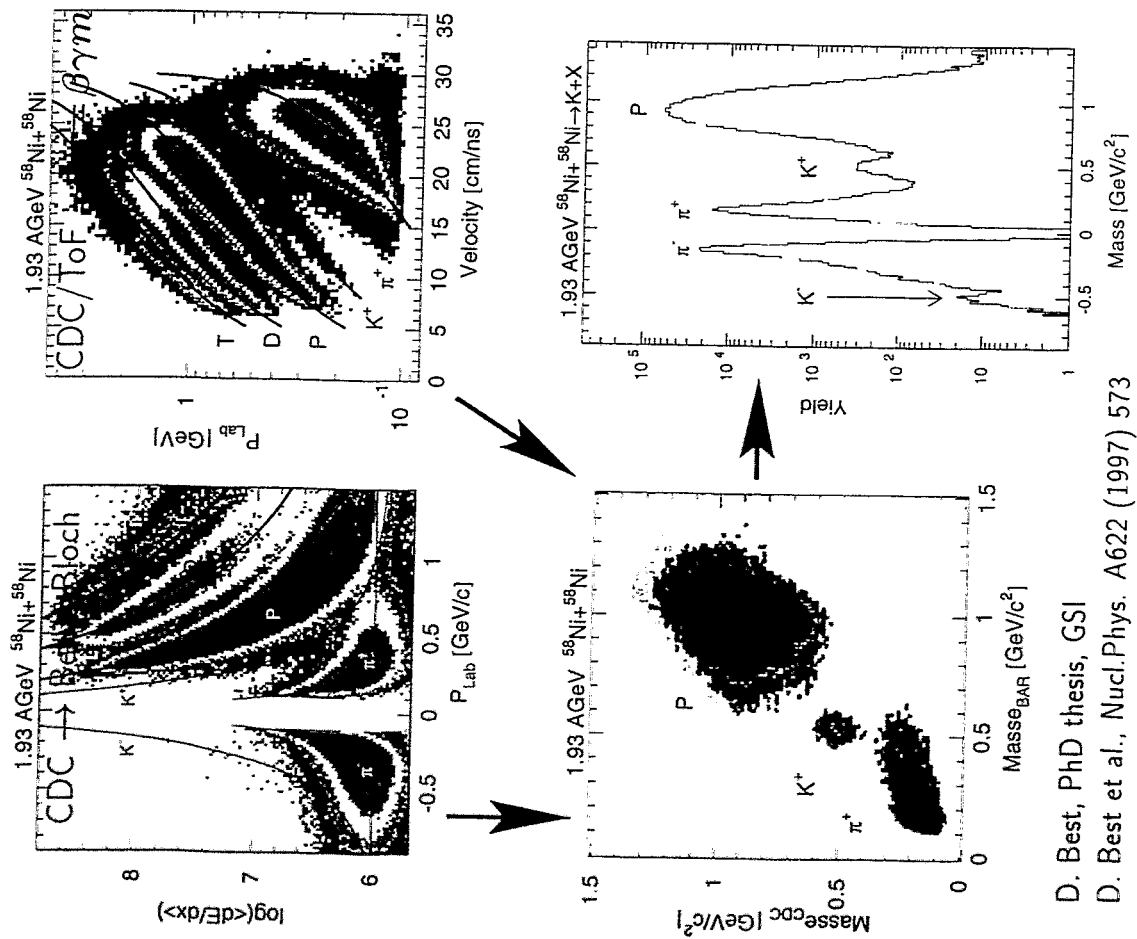
- 1] K^\pm Id. with FOPI
- 2] K^-/K^+ ratio
- 3] K^+ sideward flow
- 4] Comparison with model predictions

Ni+Ni @ 1.93 AGeV & Ru+Ru @ 1.69 AGeV

FOPI detector @ GSI

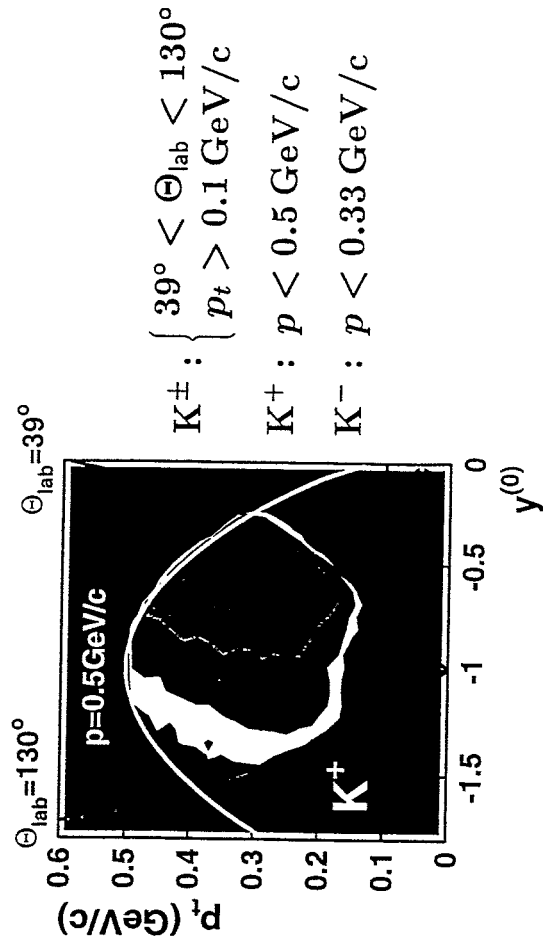


Charged Particle Identification



D. Best, PhD thesis, GSI
 D. Best et al., Nucl.Phys. A622 (1997) 573

K± Acceptance & Statistics



K^\pm : $\begin{cases} 39^\circ < \Theta_{lab} < 130^\circ \\ p_t > 0.1 \text{ GeV}/c \end{cases}$
 K^+ : $p < 0.5 \text{ GeV}/c$
 K^- : $p < 0.33 \text{ GeV}/c$

Year	System	Beam Energy	N events	K ⁺	K ⁻
1994	Ni+Ni	1.06 AGeV	2.8 · 10 ⁶	30	
		1.45 AGeV	1.8 · 10 ⁶	300	
		1.96 AGeV	2.9 · 10 ⁶	3000	50
1995	Ni+Ni	1.96 AGeV	4.7 · 10 ⁶	30000	220
1996	Ru+Ru/Zr	1.69 AGeV	7.7 · 10 ⁶	30000	240
1997	Ca+Ca	1.96 AGeV	5 · 10 ⁵	-	-
	Au+Au	1.49 AGeV	5 · 10 ⁵	-	-

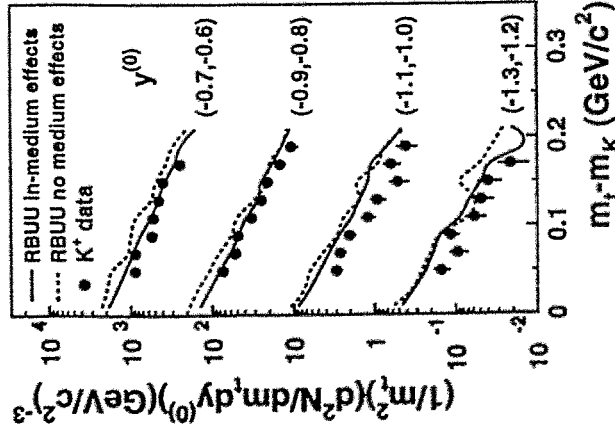
T_B & dN/dy in Ru+Ru @ 1.69 AGeV

$$\frac{1}{m_t^2} \frac{d^2N}{dm_t dy^{(0)}} = A \exp \left[- \frac{(m_t - m_0)}{T_B} \right]$$

$$m_t = \sqrt{p_t^2 + m_0^2}$$

$$T_B = T / \cosh(y - y_{cm})$$

RBUU : E.L. Bratkovskaya and W. Cassing



With in-medium effects :

- higher T_B ($\sim 20\%$ at $y^{(0)} = 0$)
- lower yield ($\sim 40\%$ at $y^{(0)} = 0$)

Low sensitivity to IME in the explored $y^{(0)}$ range
Slight better agreement with data if IME

K. Wiśniewski

K^-/K^+ Ratio : Model Predictions

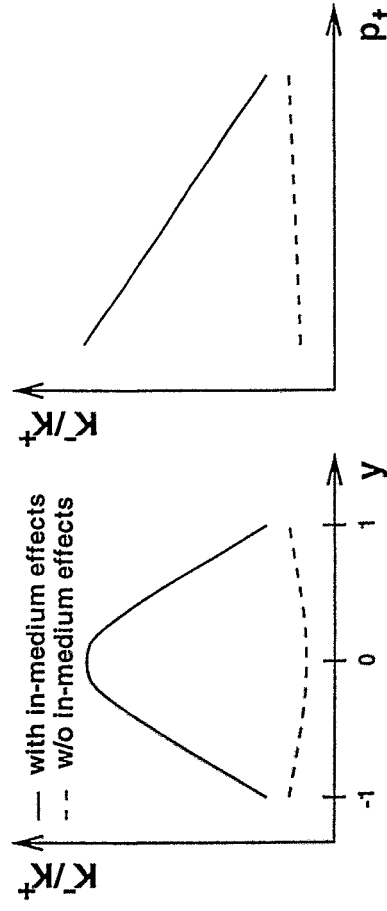
with in-medium effects

characteristic	mass	potential
K^-	decreased	attractive
K^+	increased	repulsive

observable	yield	momentum
K^-	increased	decreased
K^+	decreased	increased

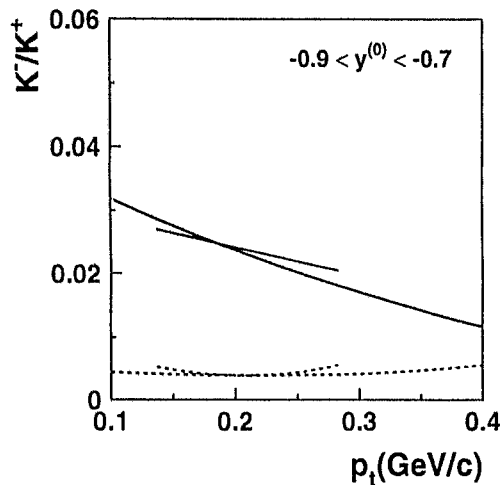
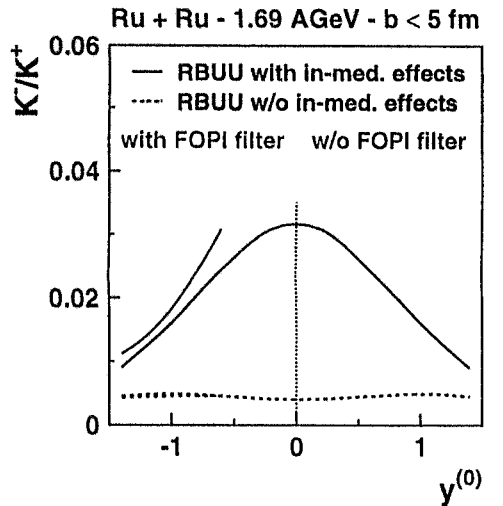
In-medium effects act oppositely on K^- and K^+
 \Rightarrow relevant observable : K^-/K^+ ratio

expected trends :



K^-/K^+ Ratio as Seen by FOPI

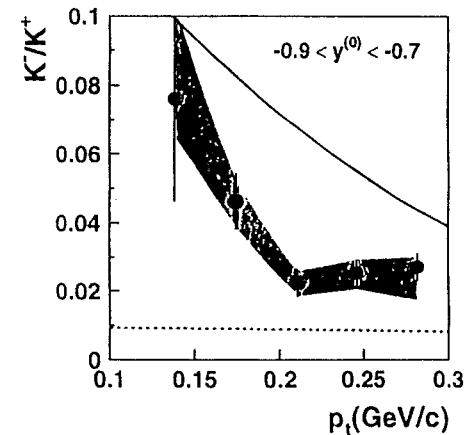
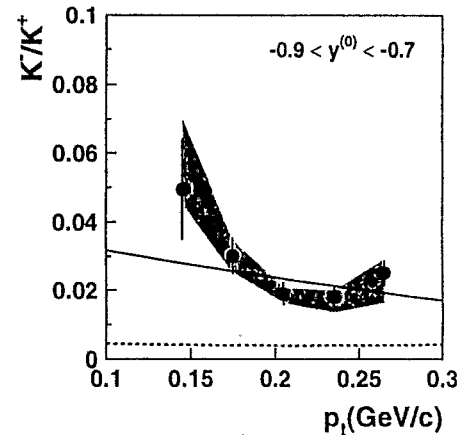
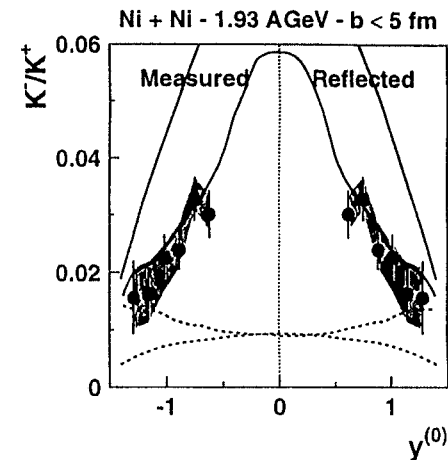
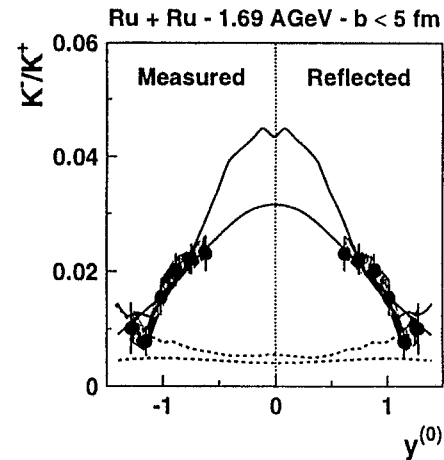
RBUU : E.L. Bratkovskaya and W. Cassing



K^-/K^+ Ratio versus $y^{(0)}$ and p_t

- DATA ■ Syst. errors
- RBUU in-medium effects
- - RBUU no medium effects

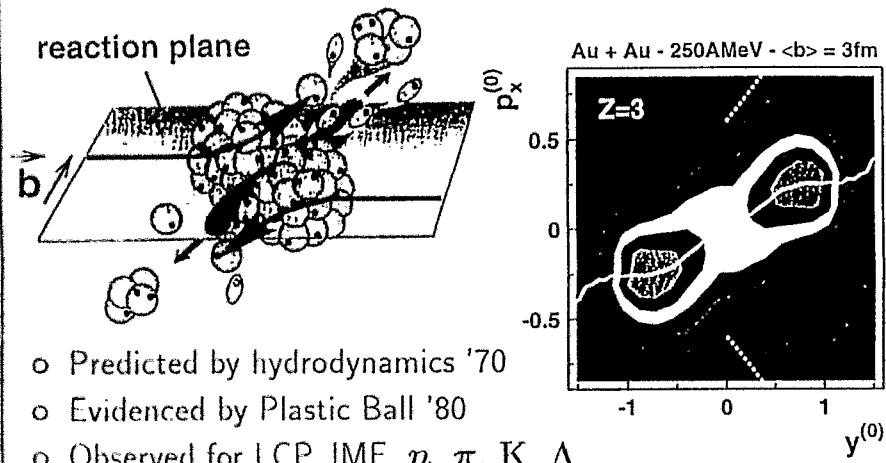
E.L. Bratkovskaya and W. Cassing
 G.Q. Li and G.E. Brown, PRC58(1998)1698



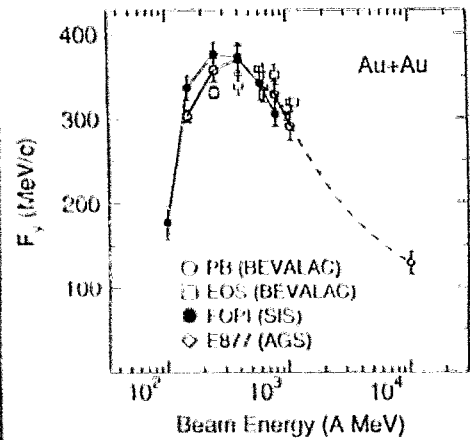
Data favour in-medium effects

K. Wiśniewski et al., GSI-report (1997), submitted to Phys. Rev. Lett.

Sideward Flow



- o Predicted by hydrodynamics '70
- o Evidenced by Plastic Ball '80
- o Observed for LCP, IMF, n , π , K , Λ
- o Studied from GANIL/MSU to SPS

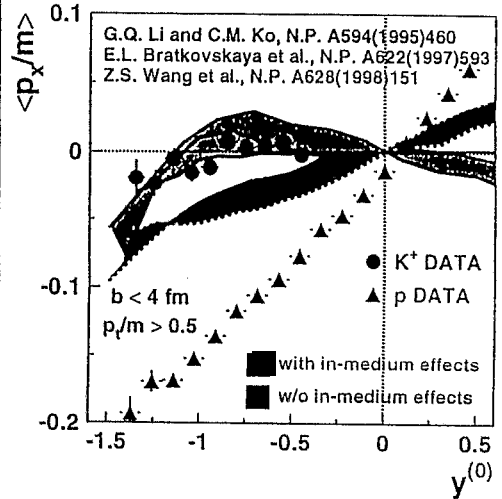


Excitation function :
maximum at SIS energie:

$$F_y = \frac{d \langle p_x \rangle}{dy} \Big|_{y=0}$$

W Reisdorf and H.G. Ritter, Annu.Rev.Nucl.Part.Sci. 47 (1997)

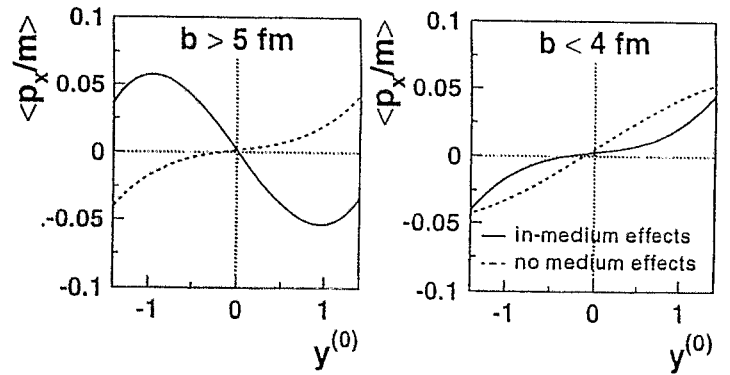
K⁺ Flow in Ni+Ni @ 1.93 AGeV



3 \neq models favour
in-medium potential for K⁺
BUT influence of:
production channels :
C. David et al., nucl-th/9805017
momentum dependent potential :
C. Fuchs et al., P.L. B 434 (98) 24!

K⁺ Flow in Ru+Ru @ 1.69 AGeV

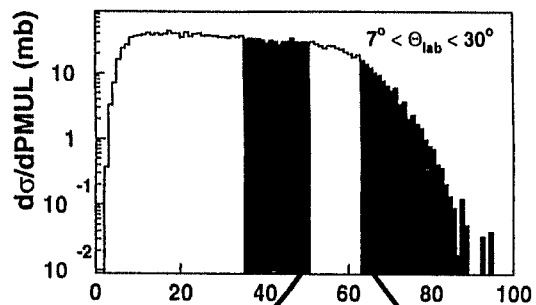
RBUU : E.L. Bratkovskaya and W. Cassing



Large sensitivity expected in non-central collisions
from NME to IME \Rightarrow flow to antiflow

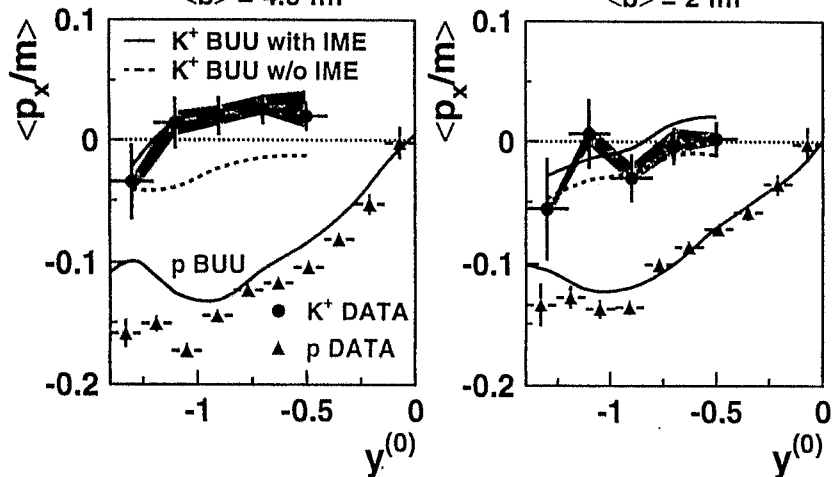
K⁺ Flow in Ru+Ru @ 1.69 AGeV

Centrality selection : charged particle multiplicity PMUL



40 < PMUL < 50
 = 4.5 fm

PMUL > 63
 = 2 fm



- K⁺ anti-flow in non-central reactions
- BUU reproduces K⁺ data if IME on
- BUU reproduces proton data

BUU : E.L. Bratkovskaya and W. Cassing

p_t Dependence of K⁺ Flow

Fourier expansion of azimuthal distributions

$$\frac{d^3N}{dy p_t dp_t d\Phi} = \frac{d^2N}{dy p_t dp_t} \frac{1}{2\pi} (1 + 2v_1 \cos(\Phi) + 2v_2 \cos(2\Phi) + \dots)$$

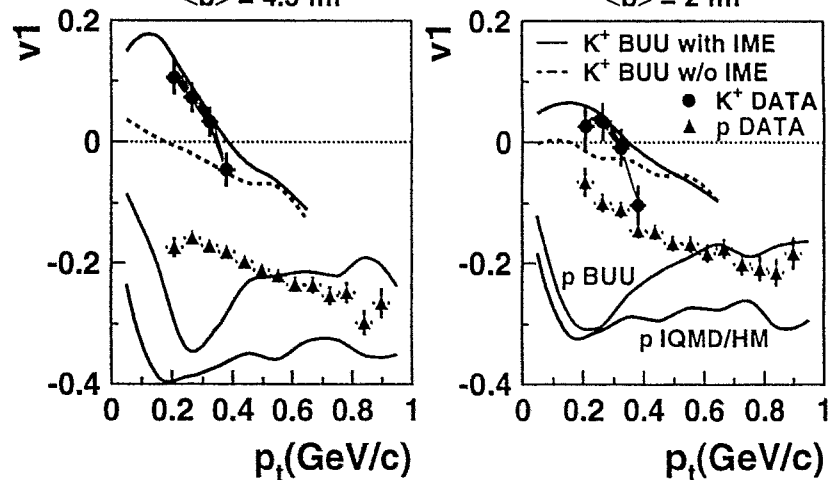
$$\Phi = \phi - \phi_{rp}$$

Fourier coefficients : $v_n = \langle \cos(n(\Phi)) \rangle$

In-plane flow : $v_1 = \langle p_x/p_t \rangle$

S. Voloshin and Y. Zhang, Z. Phys. C70 (1996) 665
J.Y. Ollitrault, Nucl. Phys. A 638 (1998) 195c

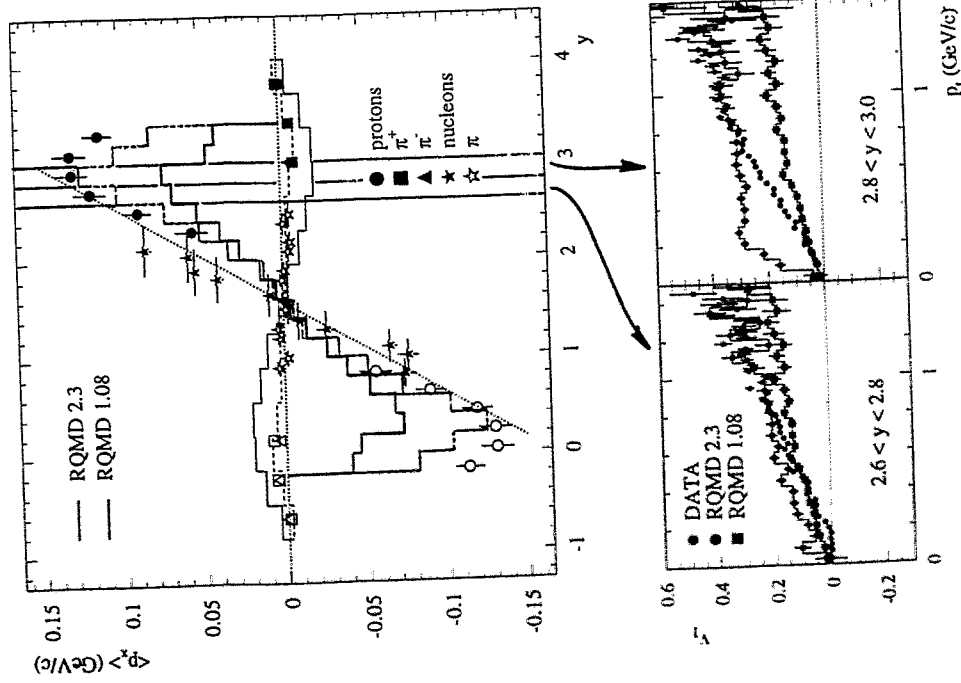
Ru + Ru @ 1.69 AGeV - 1.2 $y^{(0)}$ < -0.5
$\langle b \rangle = 4.5$ fm $\langle b \rangle = 2$ fm



Sensitivity to in-medium effects at low p_t
Neither BUU nor IQMD reproduces proton flow

BUU : E.L. Bratkovskaya and W. Cassing, IQMD/HM : C. Hartnack

Au+Au @ 11 AGeV



SUMMARY

FOPI Results (1)

Experimental data on

K^-/K^+ ratio and K^+ sideward flow

in Ni+Ni @ 1.93 AGeV and Ru+Ru @ 1.69 AGeV
 need in-medium modification of kaon properties
 to be satisfactory reproduced by transport models

Open questions and problems :

Theory : { alternative explanations for kaon data
 description of baryon data ($v_1 \%$ p_t)

Experiment : { systematical errors
 limited statistic

Future : K^- flow, Φ

Larger sensitivity to in-medium effects

FOPI ToF upgrade : { more precise measurements
 better statistic

C. Plettner:

Results from FOPI (2):

**Investigation of charged K mesons at low p_{\perp} and
around midrapidity**

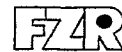
Investigation of charged K-mesons at low p_T and around midrapidity

- Presentation of the FOPI detector at GSI, Darmstadt
- (Anti)Kaon identification at low p_T and around midrapidity with FOPI

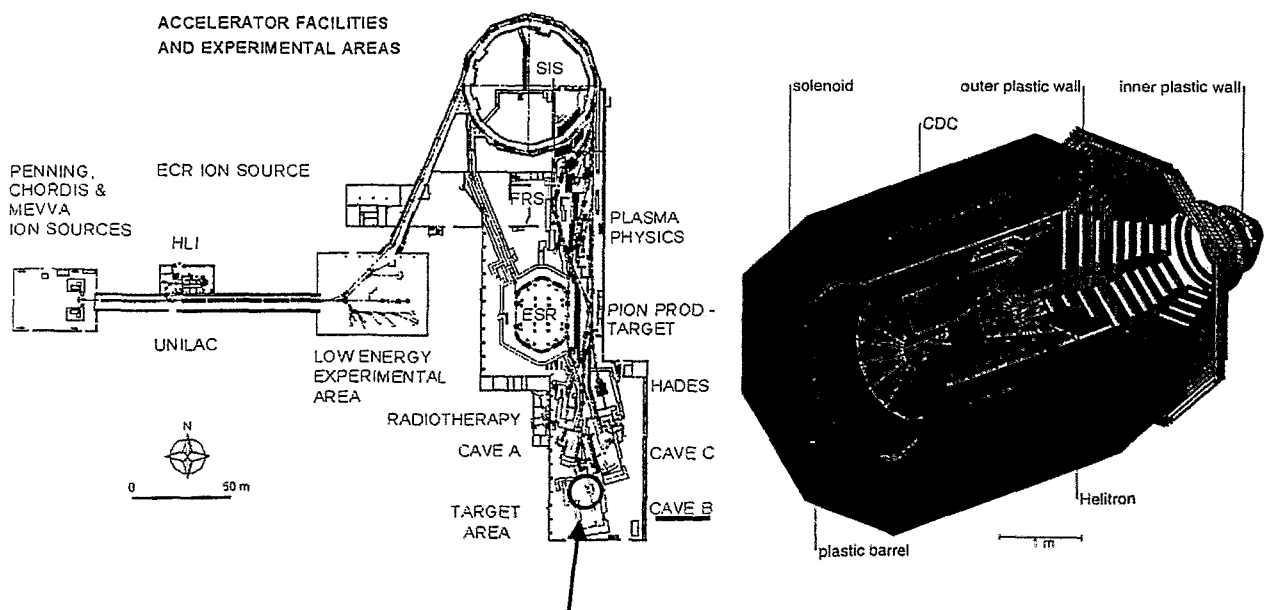
analysed system: $^{96}\text{Ru} + ^{96}\text{Ru}$ @ 1.7 AGeV

- Preliminary K^-/K^+ ratio, comparison with model prediction
- Preliminary momentum dependence of Kaon squeeze-out signal

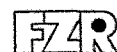
C. Plettner
Institut für Kern- und Hadronenphysik



The 4π Detektor FOPI

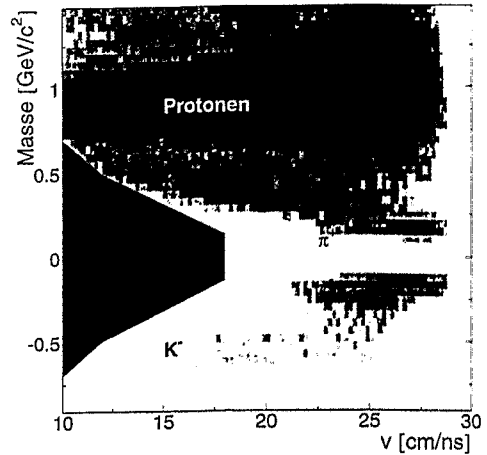
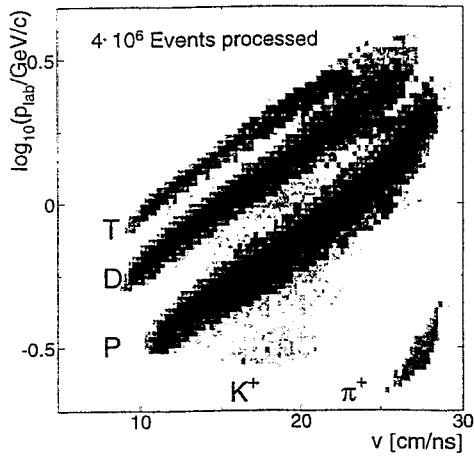


C. Plettner
Institut für Kern- und Hadronenphysik



Particle Identification ($Z=\pm 1$)

$^{96}\text{Ru}+^{96}\text{Ru}$ @ 1.69 AGeV, $b_{\text{geo}} < 4.2$ fm



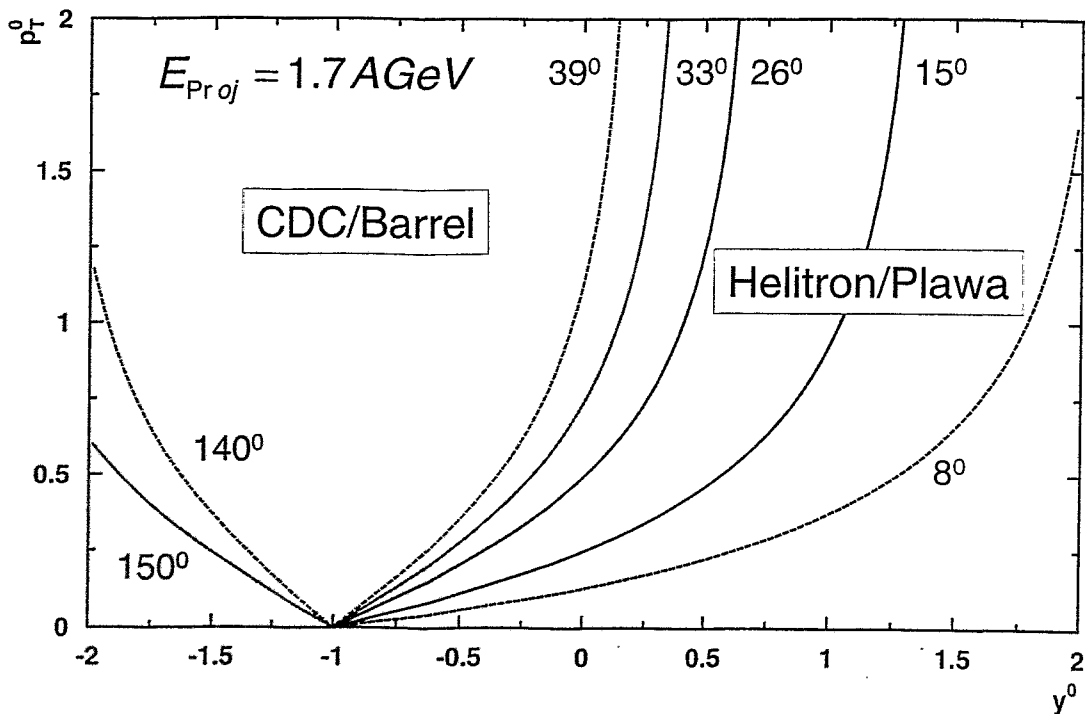
$$\text{Mass} = \frac{P}{\beta\gamma} + \text{corrections}$$

Rel. Resolution:
 $\Delta m/m = 6\%$ (Protons)

C. Plettner
Institut für Kern- und Hadronenphysik

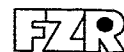


FOPi phase space

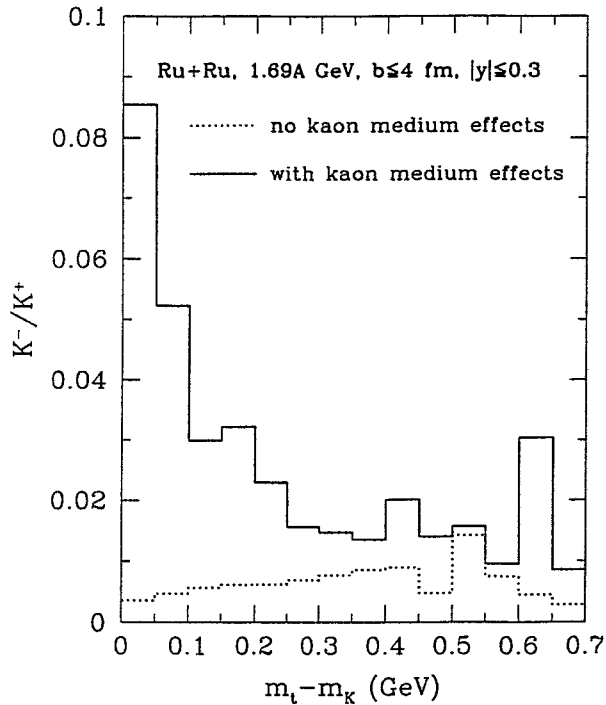


Symmetric system: $Y^0 = (Y_{\text{lab}} - Y_{\text{cm}}) / Y_{\text{cm}}$

C. Plettner
Institut für Kern- und Hadronenphysik



Comparison with RBUU predictions



G.Q. Li and G.E. Brown, Phys. Rev. C58 (1998), 1698

Analysis of Helitron data

$^{96}\text{Ru} + ^{96}\text{Ru}$ @ 1.69 AGeV, $b_{\text{Geo}} < 4.2$ fm

accessible transverse momenta range

$$p_t = (100 - 250) \text{ MeV}/c$$

transformation into transverse mass

$$m_t = \sqrt{(p_t/c)^2 + m_K^2} = (10 - 50) \text{ MeV}/c^2 + m_K$$

rapidity range

$$|y^0| \leq 0.3$$

K^-/K^+ ratio

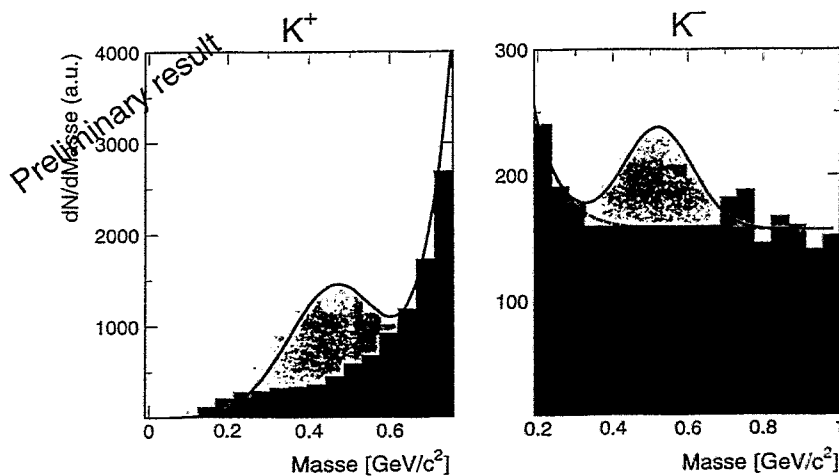
$$(7.5 \pm 3.5)\%$$

\Rightarrow compatible with in-medium modification of (Anti)Kaon mass

C. Plettner
 Institut für Kern- und Hadronenphysik



Identification of charged K-Mesons



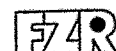
Velocity [cm/ns]
 $16 < v < 23$
 Center of Mass velocity.
 ≈ 21 cm/ns
 Momenta [MeV/c]
 $310 < p_{\text{lab}} < 590$

$$\sum_{K^+} = 4904 \pm 2000$$

$$\sum_{K^-} = 368 \pm 50$$

$$\Rightarrow K^-/K^+ = (7.5 \pm 3.5)\%$$

C. Plettner
 Institut für Kern- und Hadronenphysik



Squeeze-Out

Parametrization of azimuthal distributions

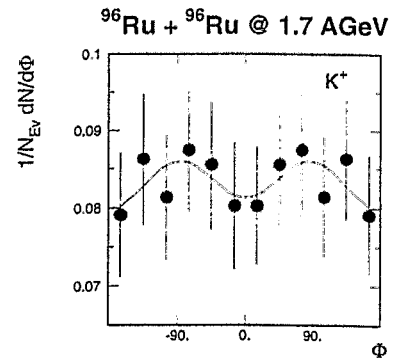
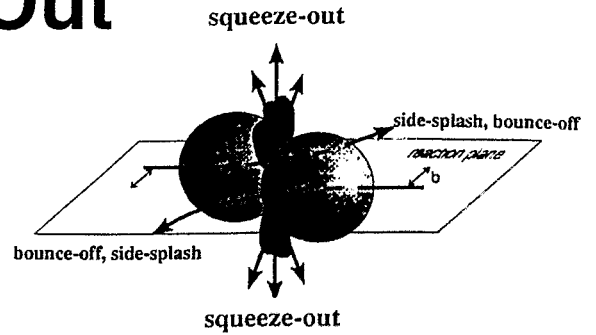
$$\frac{dN}{d\phi} = a'_0 (1 + a'_1 \cos \phi + a'_2 \cos 2\phi)$$

Out-of plane emission ratio

$$R'_N = \frac{1 - a'_2}{1 + a'_2}$$

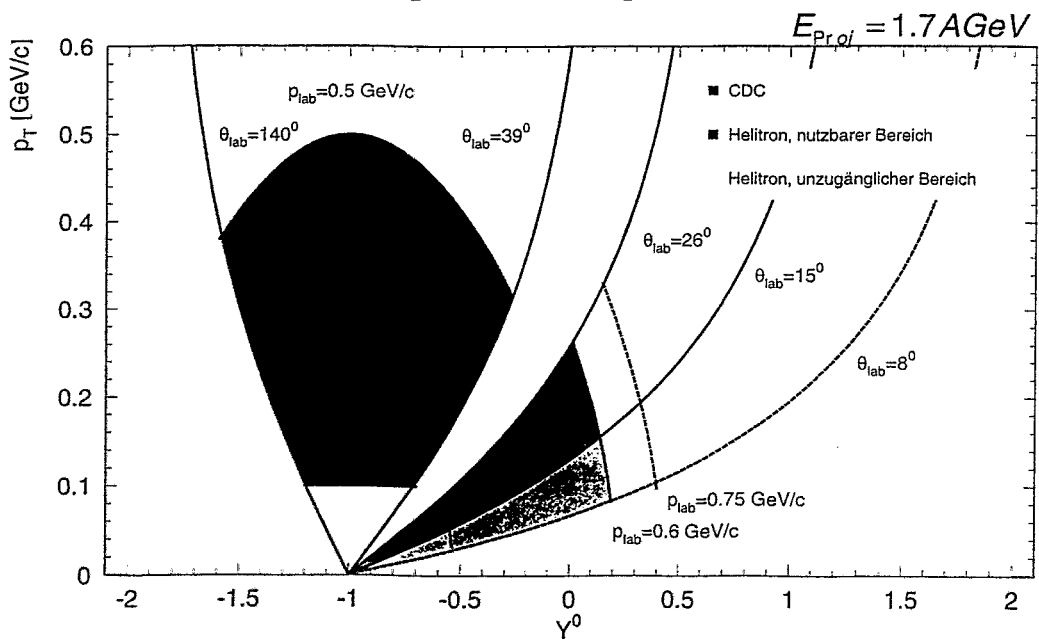
Correction

$$R'_N \Rightarrow R_N$$



Symmetrised azimuthal distributions of K⁺

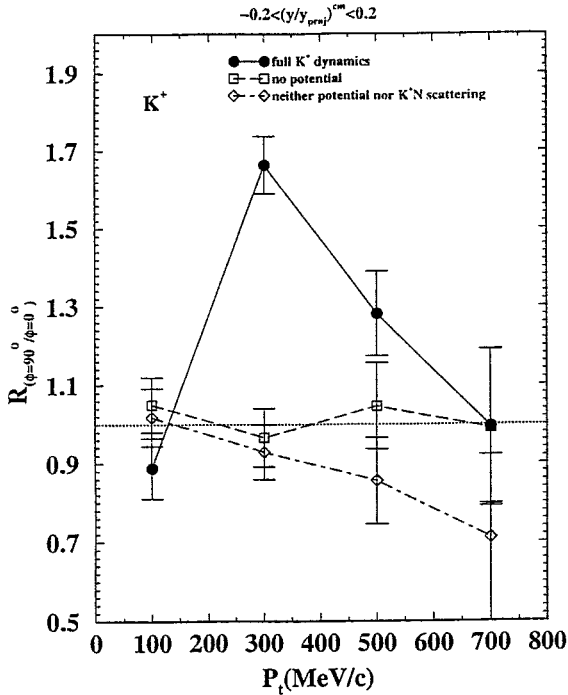
K⁺ phase space



Symmetric system $Y^0 = (Y_{lab} - Y_{cm}) / Y_{cm}$

Comparison with QMD

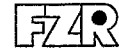
Au + Au 1 GeV/nucleon $b = 6\text{fm}$



- in system $Au + Au @ 1.0\text{ AGeV}$ prediction of a momenta dependent squeeze-out signal in case of a KN potential
- without a KN potential model predicts within error bars that $R_N \leq 1$
- analysis of momentum dependence of Kaon squeeze out signal in the system $Ru + Ru @ 1.7\text{ AGeV}$ shows within error bars $R_N \geq 1$

⇒ Hint for existence of an in-medium potential?

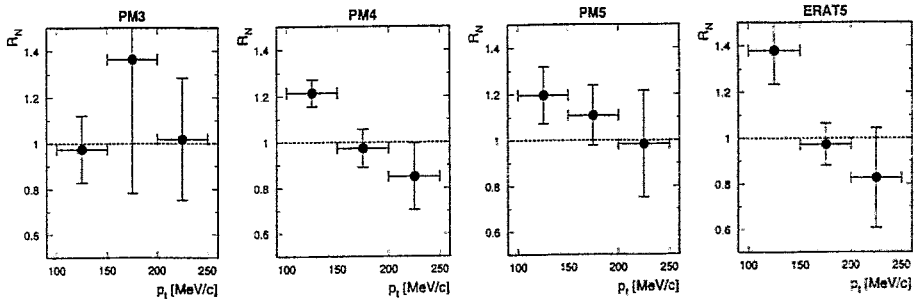
Z.S. Wang et al., Phys. Rev. C57 (1998), 3284



C. Plettner
Institut für Kern- und Hadronenphysik

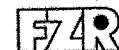
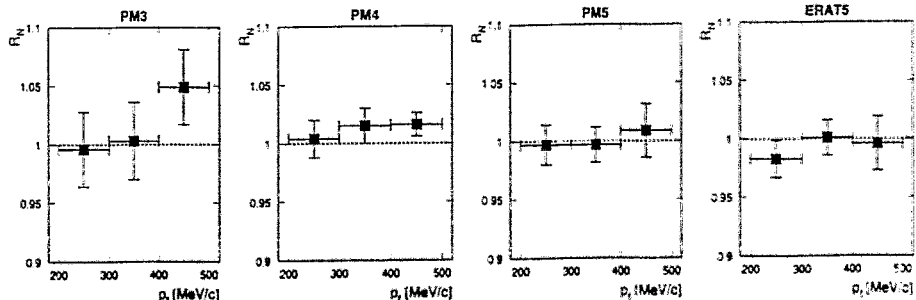
Momentum dependence of Squeeze-Out signal

Kaons, background corrected



centrality →

Protons



C. Plettner
Institut für Kern- und Hadronenphysik

Summary

- With detector combination Helitron/Plastic Wall (Anti)Kaons can be identified at midrapidity for low transverse momenta
- Measured K^-/K^+ ratio compatible with in-medium modification of (Anti)Kaon mass
- Measured p_T dependence of Kaon squeeze-out signal gives hint to existence of KN potential
On our wish list: calculations for $^{96}\text{Ru} + ^{96}\text{Ru}$ @ 1.7 AGeV

Y. Shin:

Azimuthally anisotropic emission of K^+ mesons in

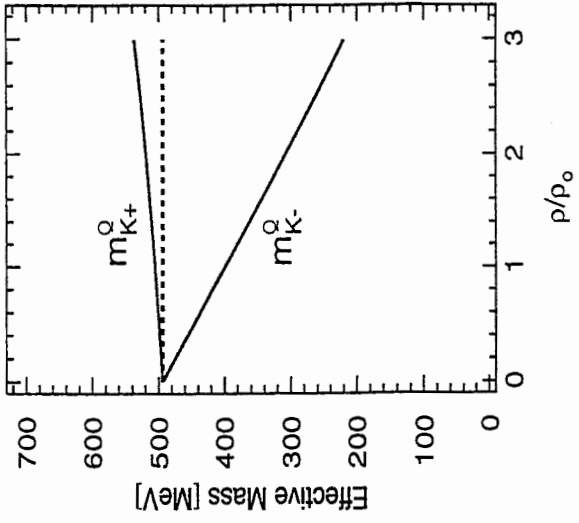
Au + Au collisions at 2 AGeV

Azimuthal Anisotrop Emission of K^+ Mesons in Au + Au Collisions at 1 AGeV

Y. Shin (Univ. Frankfurt)
for the KaoS Collaboration

1. Motivation
2. Experiment Setup
3. Analysis
4. Results
 - Spectral Distribution
 - Azimuthal Distribution
5. Summary

• Properties of Hadrons in Nuclear Medium



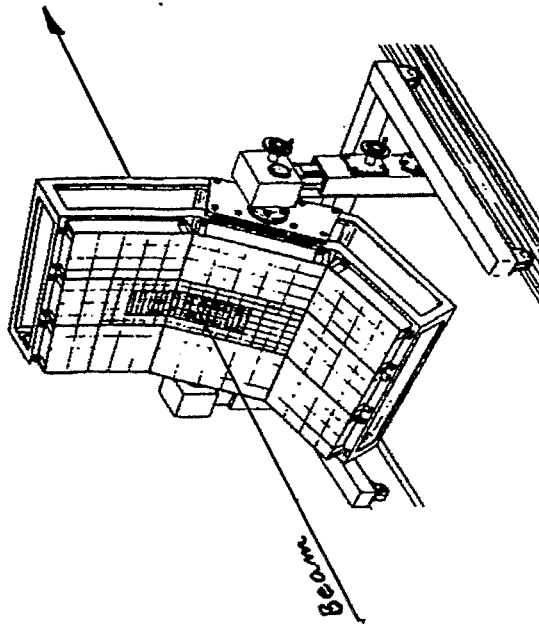
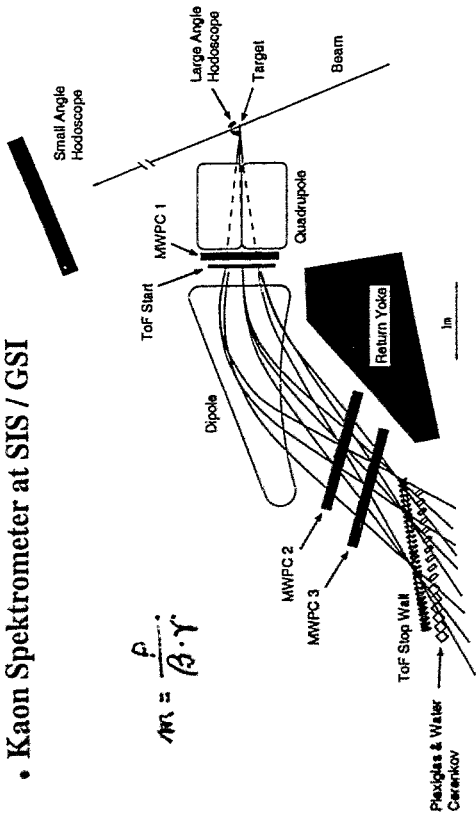
$$\begin{aligned}
 m_{K,\bar{K}}^* &\approx m_K \left[1 - \frac{\Sigma_{KN}}{f_K^2 m_K^2} \rho_s + \left(\frac{3}{8} \frac{1}{f_K^2 m_K} \rho_N \right)^{2/2} \right]^{1/2} \pm \frac{3 \rho_N}{8 f_K^2} \\
 &= \sqrt{m_K^2 + p^2 + U_s + U_v}
 \end{aligned}$$

RBUU : C. Ko and G. Li, JPG, V. 22(1996)

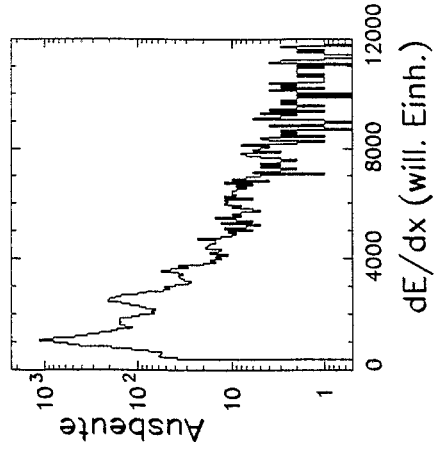
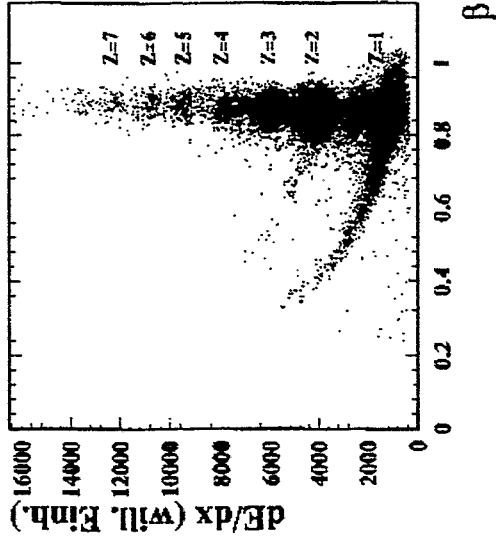
⇒ Repulsive KN Potential for K^+ Mesons

• Kaon Spektrometer at SIS / GSI

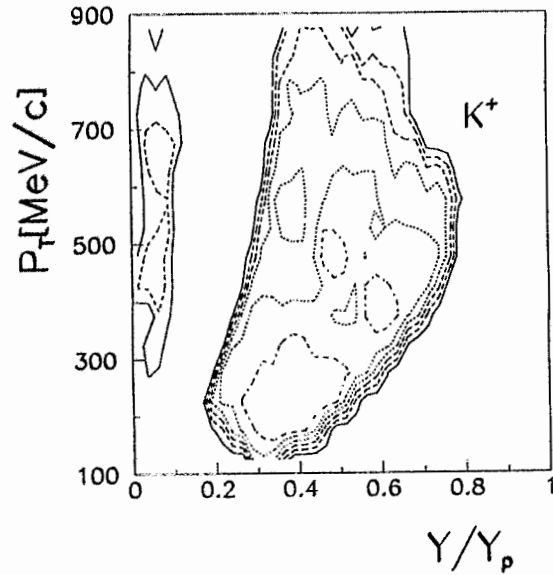
$$m = \frac{p}{\beta \cdot \gamma}$$



• Identifikation der Teilchen im Kleinwinkel Hodoskop

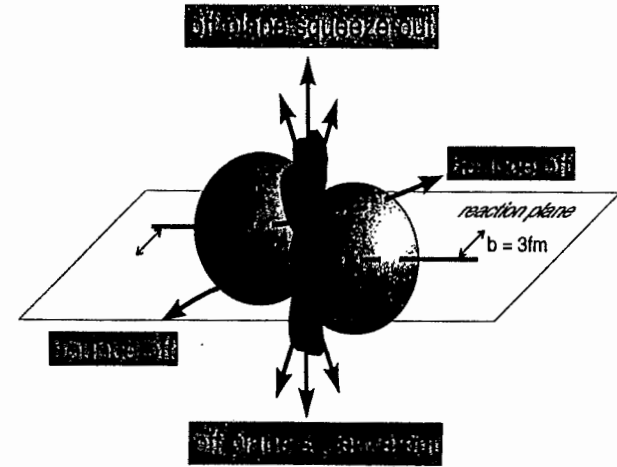


• K^+ Acceptance at 1 AGeV



- $\Theta_{Lab} = 34^\circ, 44^\circ, 54^\circ, 84^\circ$
($N_{K^+} = 8600, 9700, 5000, 250$)
- $B_{Dipol} = 0.6, 0.9, 1.4, 1.9T$
($270MeV/c \leq p_{Lab} \leq 1500MeV/c$)

1. Collective Flow of Nuclear Matter



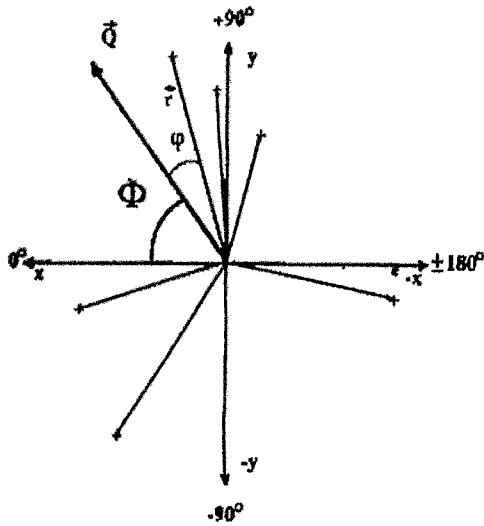
$$\vec{Q} = \sum_{\nu} \omega_{\nu} \vec{p}_i(\nu)$$

P. Danielewicz : Phys.Lett. 157B(1985)

2. K^+ as Probe for the hot and dense Phase

- (a) Subthreshold Production : $E_{th} = 1.58 \text{ GeV}$ ($NN \rightarrow N\Lambda K^+$)
- (b) Large Mean Free Path : $\lambda_{K^+} \approx 5 \text{ fm}$ ($\sigma_{Kp} \approx 12 \text{ mb}$)

• Determination of the Reaction Plane



$$\vec{Q} = \sum_v \omega_v \cdot \vec{p}_i(v)$$

⇒ for Particles with $\beta > 0.7$

⇒ $\omega_v = 1$ or $\omega_v = Z_v$

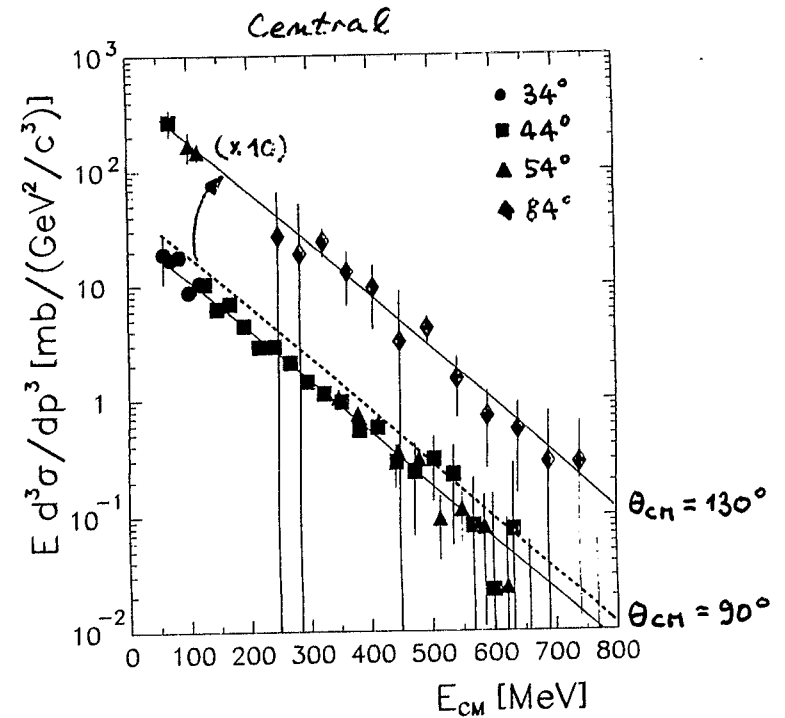
• Resolution of the Reaction Plane

Impactparameter	$\langle \Delta\phi_{12}^2 \rangle^{1/2}$	$\langle \Delta\phi^2 \rangle^{1/2}$	$\langle \cos(\Delta\phi) \rangle$	$\langle \cos(2\Delta\phi) \rangle$
MUL 1	91.2°	54.9°	0.66 (0.71)	0.30 (0.16)
MUL 2	77.5°	40.0°	0.81 (0.78)	0.50 (0.36)
MUL 3	73.1°	36.4°	0.84 (0.79)	0.55 (0.38)
MUL 4	89.0°	55.9°	0.65 (0.71)	0.31 (0.17)
MUL 5	101.1°	80.5°	0.35 (0.66)	0.08 (0.05)

• Spectral Distribution of K^+ Mesons

$$\sigma_{inv} = E \cdot \frac{d^3\sigma}{dp^3} = A \cdot E \cdot \exp(-E/T)$$

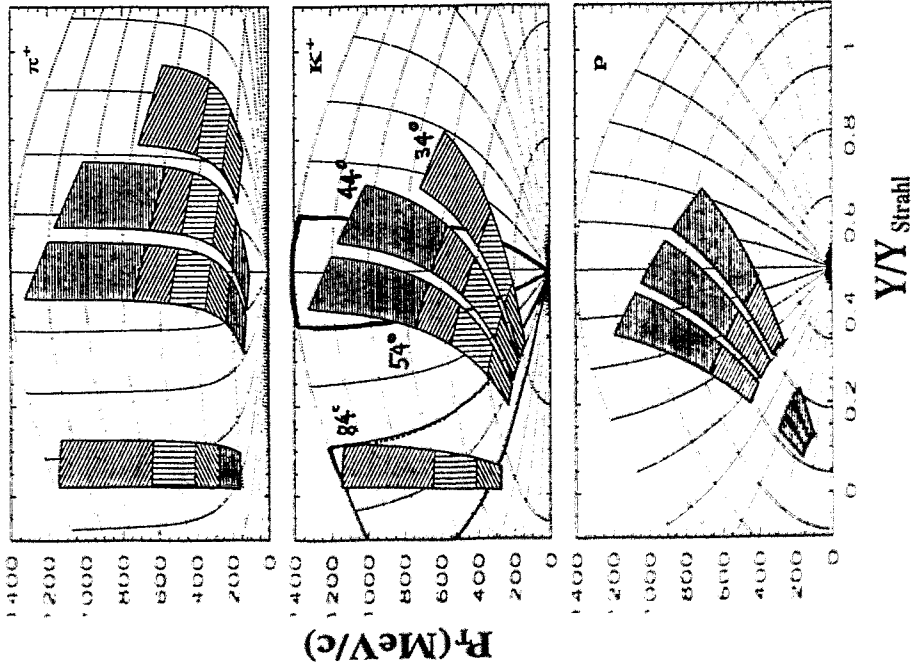
$$\Rightarrow T \approx 87 \text{ MeV}$$



⇒ Polar Anisotropy

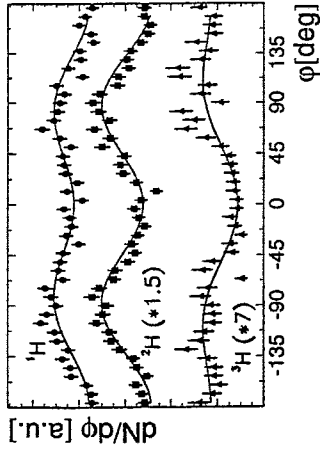
⇒ C. Sturm : Next Talk

• Experiment Au + Au at 1 AGeV



• Squeeze - Out of Nucleons and light Fragments
Bi+Bi at 0.4, 0.7, 1.0 AGeV

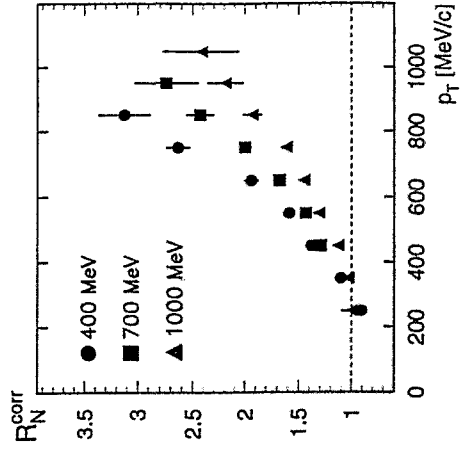
0.4 AGeV, Semicentral



$$\frac{dN}{d\varphi} \sim 1 + a_1 \cos\varphi + a_2 \cos 2\varphi$$

D. Brill et al., Z.Phys.A 355(1996)

Beam Energy Dependency, Semicentral



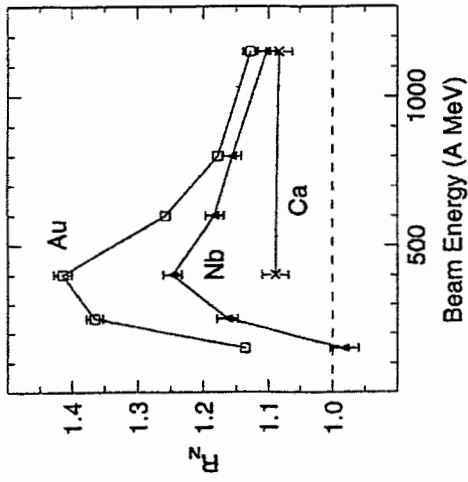
$$R = \frac{N(90^\circ) + N(-90^\circ)}{N(0^\circ) + N(180^\circ)} = \frac{1 - a_2}{1 + a_2}$$

$$a_1^{corr} = \frac{a_1}{\cos(\varphi)} >$$

$$a_2^{corr} = \frac{a_2}{\cos(2\varphi)} >$$

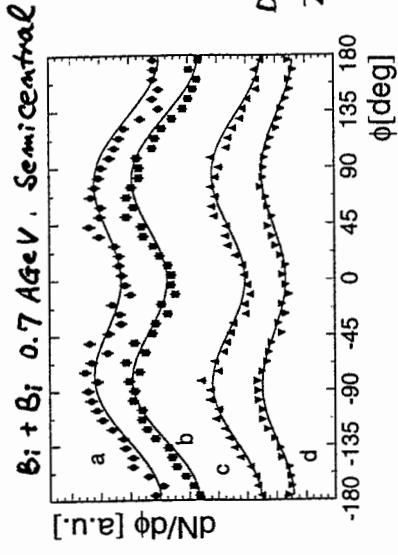
M. Demoulin et al.,
Phys.Lett. B241, 476(1990)

• Elliptic Flow of π Mesonen

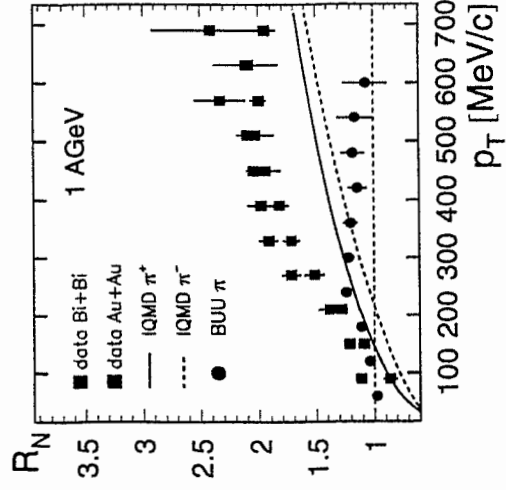


H. Gutbrod et al., PRC 42(1990)

⇒ Hydrodynamic Squeeze Out.



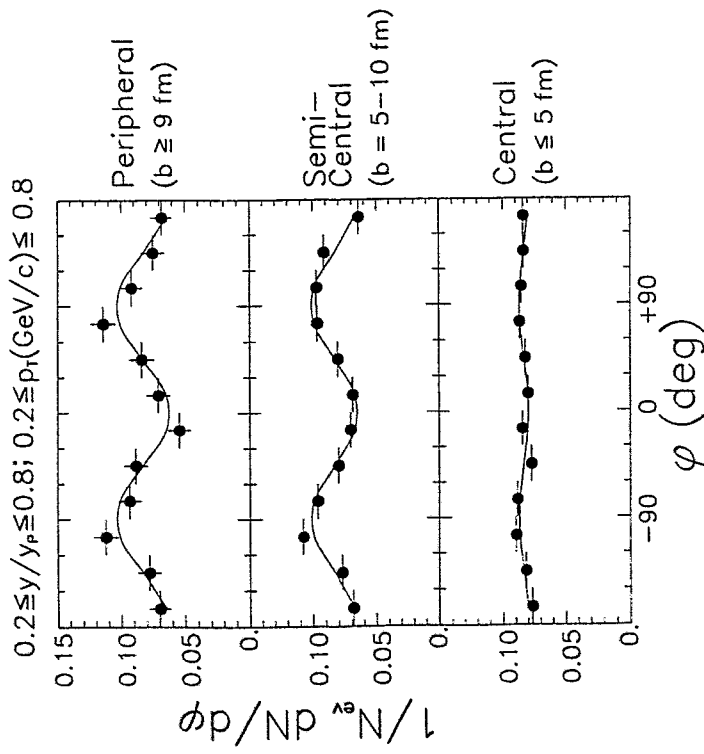
D. Brill et al.,
Z.Phys. A 357 (1997)



IQMD : S.A. Bass et al., Phys.Rev. C51, 3343(1995)
BUU : B.A. Li et al., Nucl.Phys. A570, 797(1994)

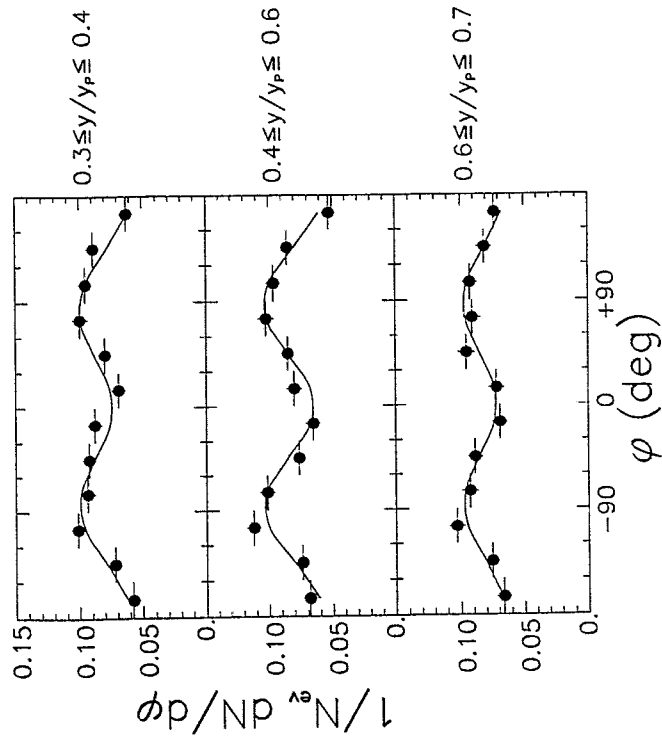
• Elliptic Flow of K^+ Mesons

Impact Parameter Dependence



• Elliptic Flow of K^+ Mesons
Rapidity Dependence

200 MeV/c $\leq p_T \leq 800$ MeV/c, Semicentral

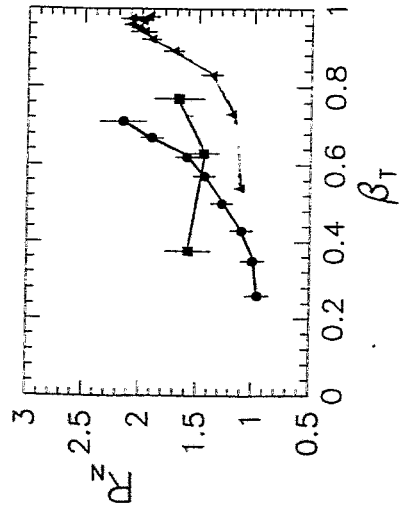
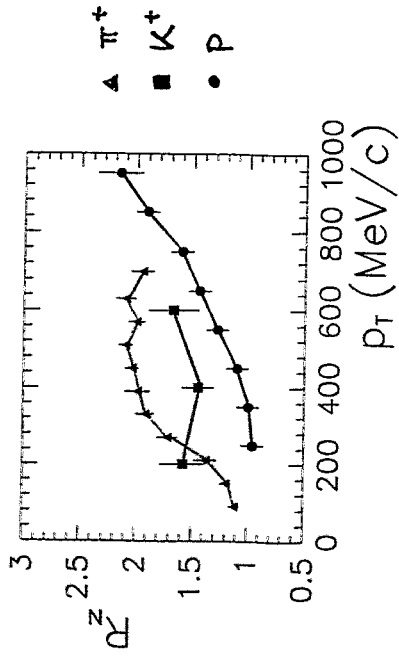


Y. Shin, PRL 81(1998)

⇒ No Flow Component into the Reaction Plane!

• Elliptic Flow of π^+ , K^+ and Nucleons

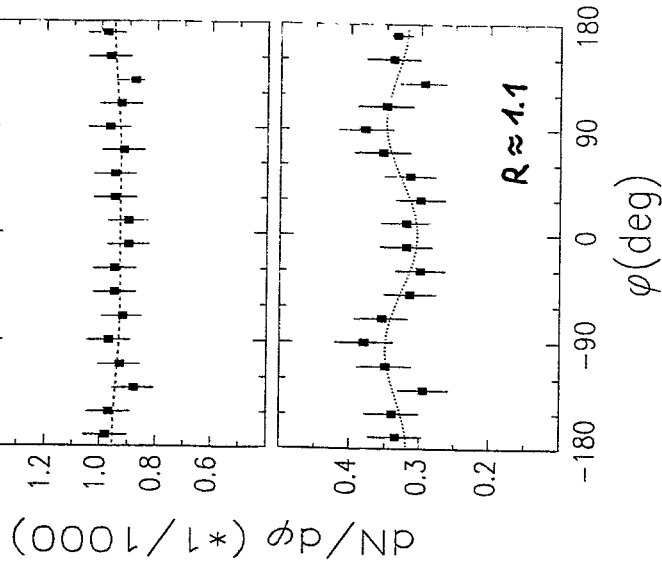
p_T Dependence, Semicentral Collisions



• UrQMD Model Calculation

S. Soff (Univ. Frankfurt, priv. Communication)

Au + Au 1.5 AGeV, UrQMD (Cascade)

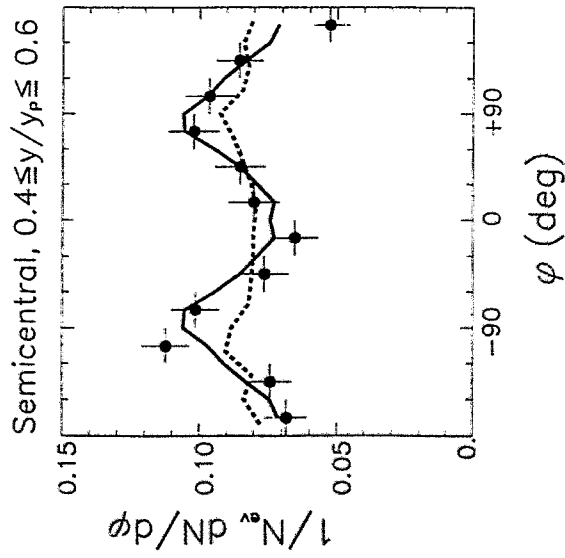


No Final Interaction

With Rescattering

• Comparison with RBUU Model Calculation

Exp. Data : Au + Au at 1 AGeV, Semicentral



— With KN Potential

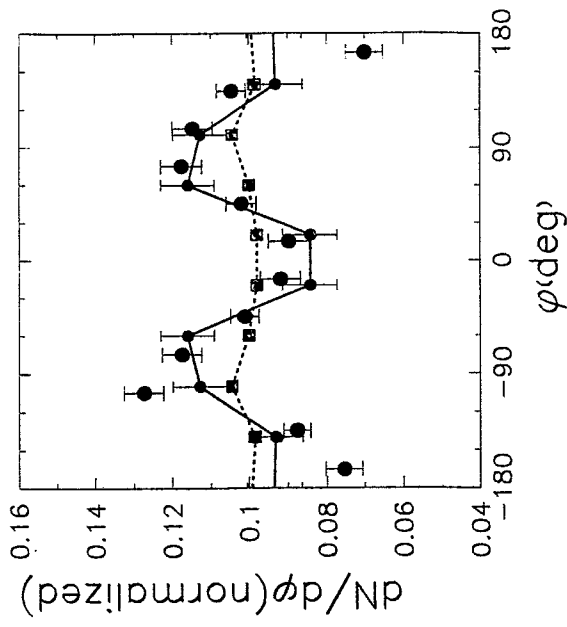
- - - Coulomb + Rescattering

G.Q. Li : priv. Communication(1997)

⇒ repulsive KN Potential in the Medium!

• Comparison with RQMD Model Calculation

Exp. Data : Au + Au at 1 AGeV, Semicentral



● With KN Potential

■ Coulomb + Rescattering

Z. Wang et al. : nucl-th/9809043

⇒ repulsive KN Potential in the Medium!

Summary

1. Spectral Distribution of K^+ Mesons

- Slope Parameter $T \approx 87$ MeV in Central Collisions.
- At $\Theta_{CM} \approx 120^\circ$ nearly 2 times more Yield than at $\Theta_{CM} \approx 90^\circ$.

\implies Polar Anisotropy

2. Azimuthal Distribution of K^+ Mesons

- Preferential Emission *perpendicular* to the Reaction Plane. The Effect increases with the increasing Impact Parameter. No p_T -Dependence. Decreases slightly in Forward- and Backward Hemisphere.
- No Flow Component *into* the Reaction Plane.

\implies According to Transport Models,

an Indication for the KN-Potential in the Nuclear Medium?

3. Outlook

- K^+ Sideward Flow at Target Rapidity in Au + Au 1 AGeV.
- K^- Elliptic and Sideward Flow in Au + Au 1.5 AGeV and Ni + Ni 1.93 AGeV.

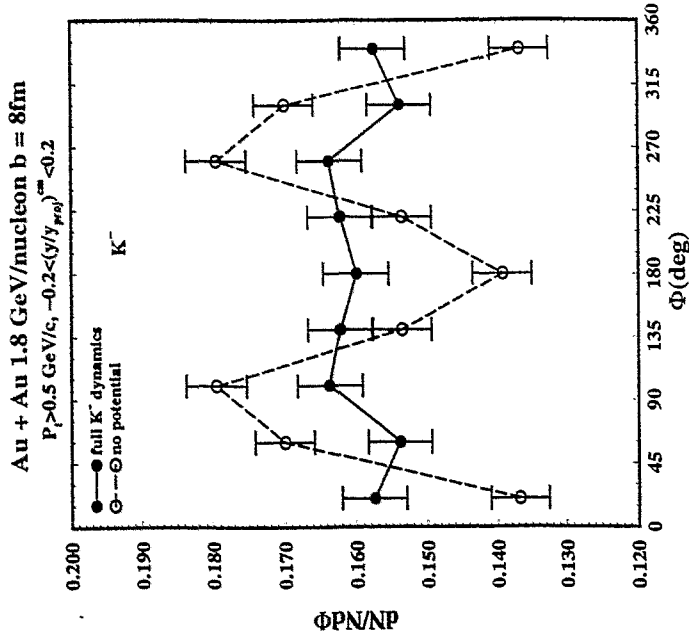


Fig. 1

KaoS Collaboration

D. Brill, Y. Shin, R. Stock, H. Ströbele

Johann Wolfgang Goethe Universität, D-60054 Frankfurt

R. Barth, M. Cieślak, M. Dębowski, E. Grosse[†], W. Henning[†],
P. Koczon, F. Laue, M. Mang, D. Miśkowiec, E. Schwab, P. Senger

Gesellschaft für Schwerionenforschung, D-64220 Darmstadt

P. Baltes, C. Müntz, H. Oeschler, C. Sturm, A. Wagner*

Technische Hochschule Darmstadt, D-64289 Darmstadt

W. Prokopowicz, W. Waluś

Uniwersytet Jagielloński, PL-30-059 Kraków

B. Kohlmeier, F. Pühlhofer, J. Speer, K. Völkel

Phillips-Universität Marburg, D-35037 Marburg/Lahn

[†] Forschungszentrum Rossendorf

[‡] Argonne National Laboratory

* Michigan State University

F. Laue:

**Kaons and anti-kaons in hot and dense nuclear
matter**

Kaons and Antikaons in Hot and Dense Nuclear Matter

F. Laue
for the

KaOS Collaboration

R. Barth^a, I. Böttcher^d, M. Dębowski^a, F. Dohrmann^f
A. Förster^b, E. Grosse^{f,g}, P. Koczoń^a, B. Kohlmeier^d,
F. Laue^a, M. Menzel^d, L. Naumann^f H. Oeschler^b,
F. Pühlhofer^d, E. Schwab^a, P. Senger^a, Y. Shin^c,
J. Speer^d, W. Scheinast^f, H. Ströbele^c, Ch. Sturm^b,
G. Surowka^c, F. Uhlir^b, A. Wagner^h, W. Waluś^e

^a GSI Darmstadt, ^b TU Darmstadt, ^c Univ. Frankfurt,
^d Univ. Marburg, ^e Univ. Kraków, ^f PZ Rossendorf,
^g TU Dresden, ^h Michigan State University, USA

Outline

- Introduction
- Setup
- Experimental Data C+C (Ni+Ni)
- Comparison with RBUU C+C (Ni+Ni)
- Summary
- Outlook (The C+Au System)

K⁺ and K⁻-Production at SIS (0.6 A GeV < E_{Beam} < 2 A GeV)

Production thresholds:

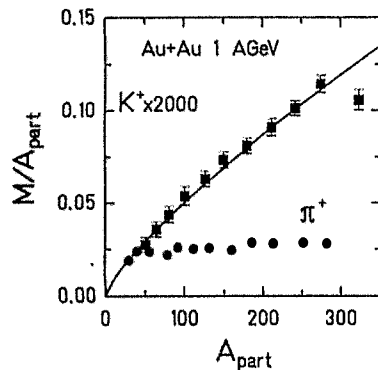
$$NN \rightarrow N\Lambda K^+ \quad E_{th}^{Lab} = 1.58 GeV$$

$$NN \rightarrow NNK^+K^- \quad E_{th}^{Lab} = 2.5 GeV$$

Subthreshold K[±]-production via multiple collisions

Experiment:

Transport models:



$$NN \rightarrow \Delta N$$

$$\Delta N \rightarrow NK^+Y$$

$$\Delta\Delta \rightarrow NK^+Y$$

$$NN \rightarrow NN\pi$$

$$\pi N \rightarrow K^+Y$$

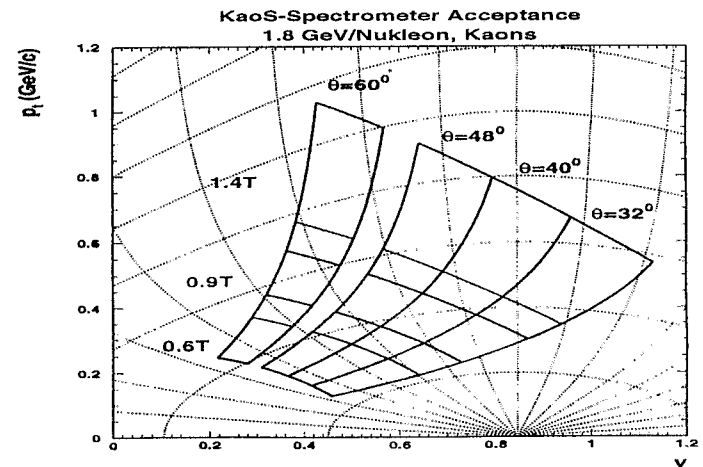
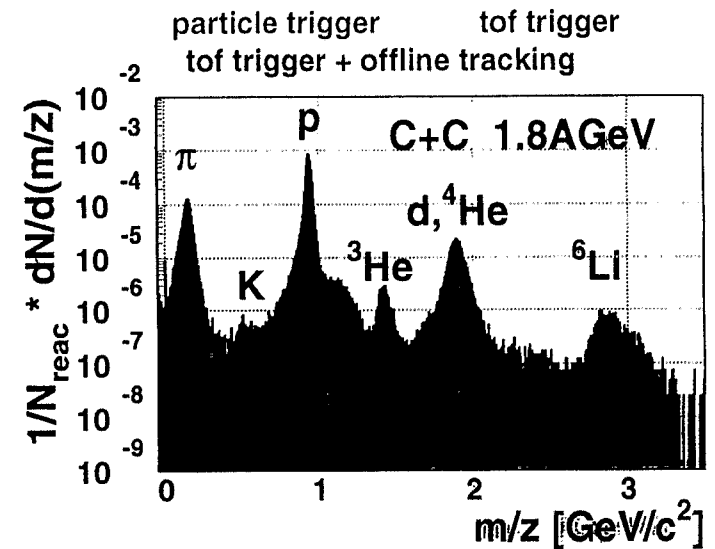
$$\pi\pi \rightarrow K^-K^+$$

$$\pi\Delta \rightarrow K^+Y$$

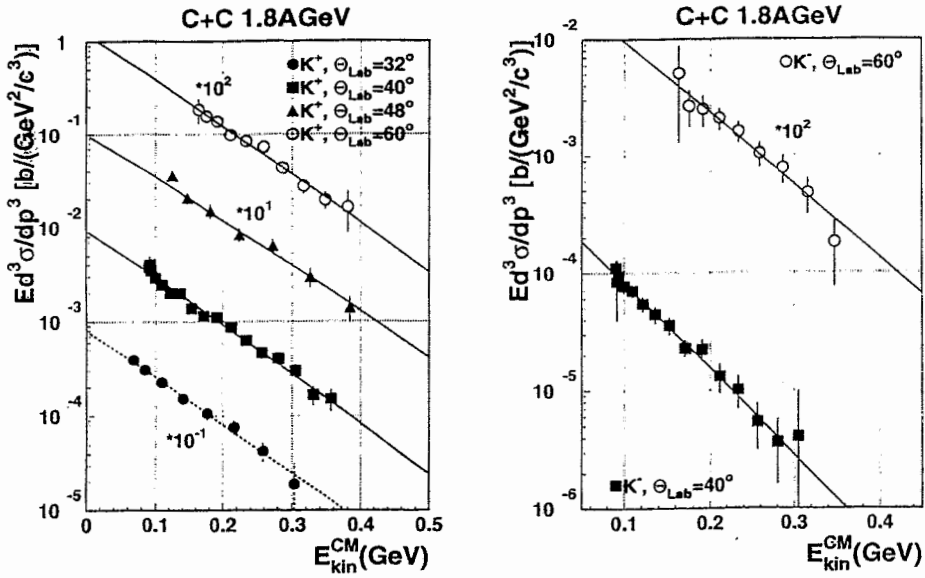
$$\frac{M_{K^+}}{A_{part.}} \propto A_{part.}^{1.8 \pm 0.15}$$

Medium effects are important

- nuclear equation of state (→ Ch. Sturm)
- hadron properties in matter

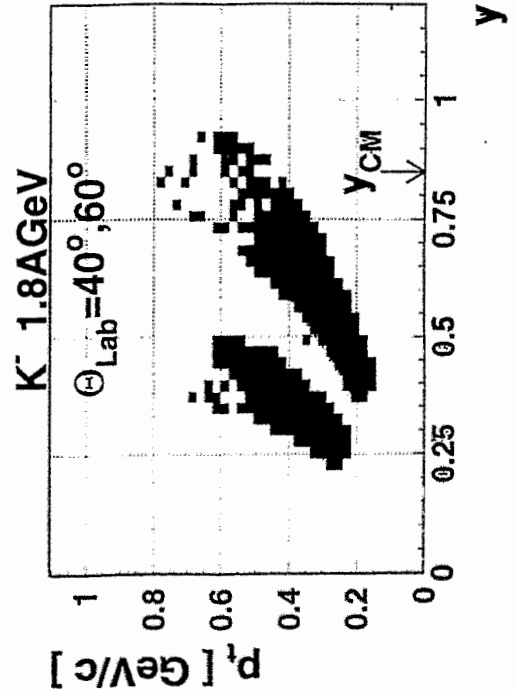
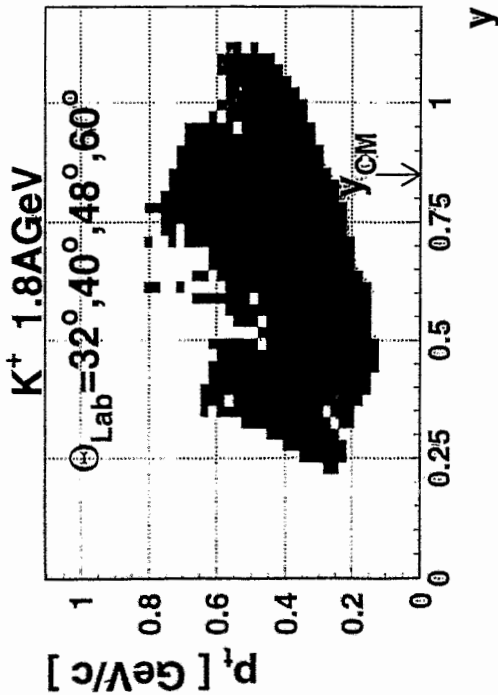


K⁺ and K⁻ Spectra

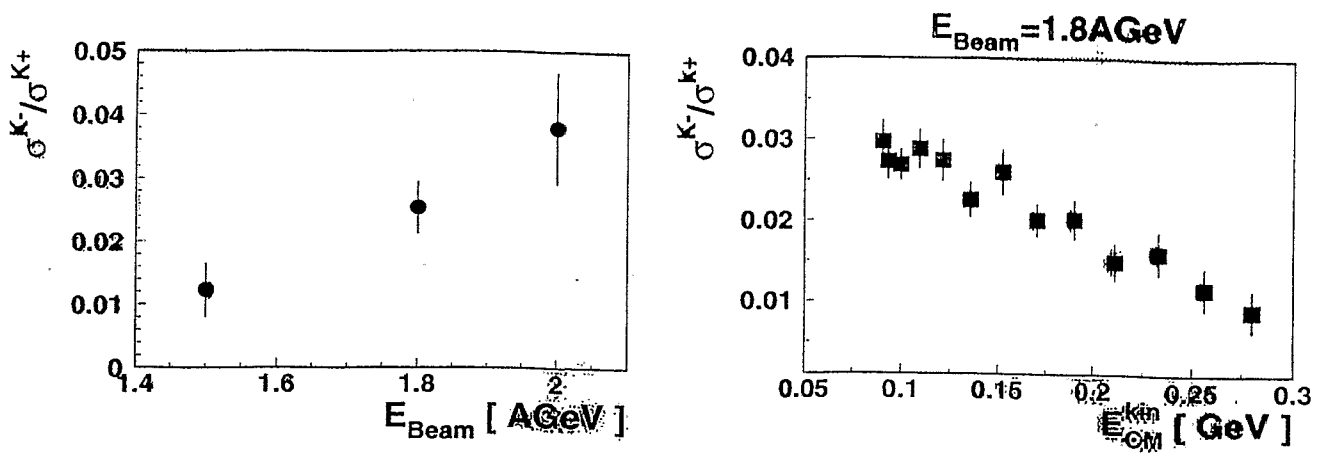


The data can be fitted by Maxwell-Boltzmann distributions.
 In C+C collisions we have data for 0.8, 1.0, 1.2, 1.5, 1.8 and 2.0 AGeV.

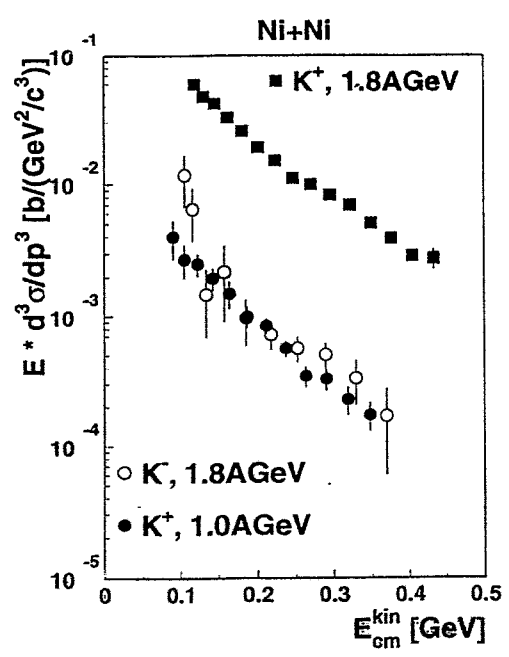
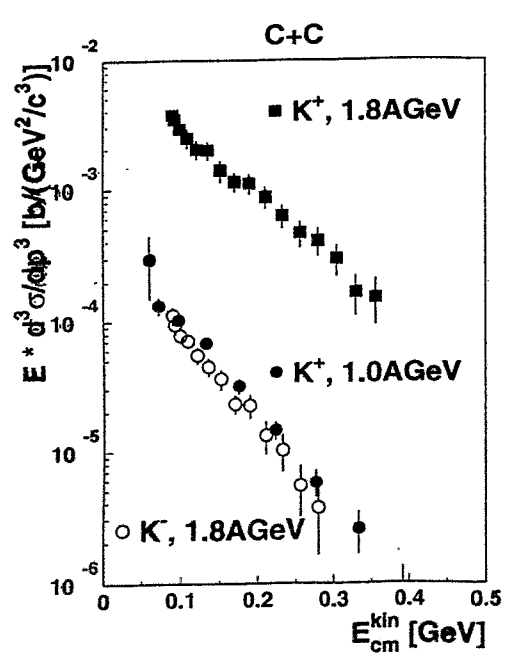
Phasespace Coverage



The K^+/K^- Ratio in C+C

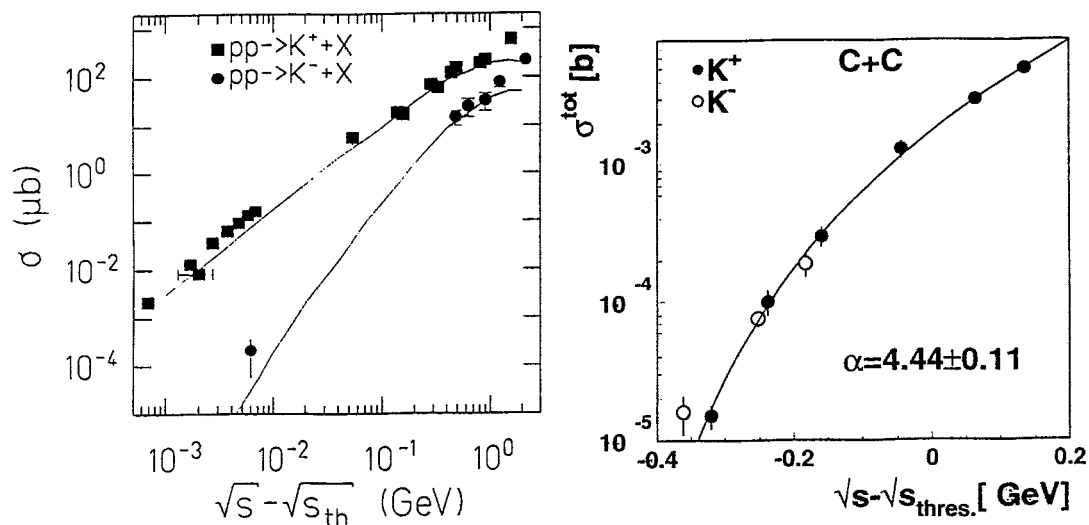


excitation function for K^- is steeper than for K^+
because of the different thresholds



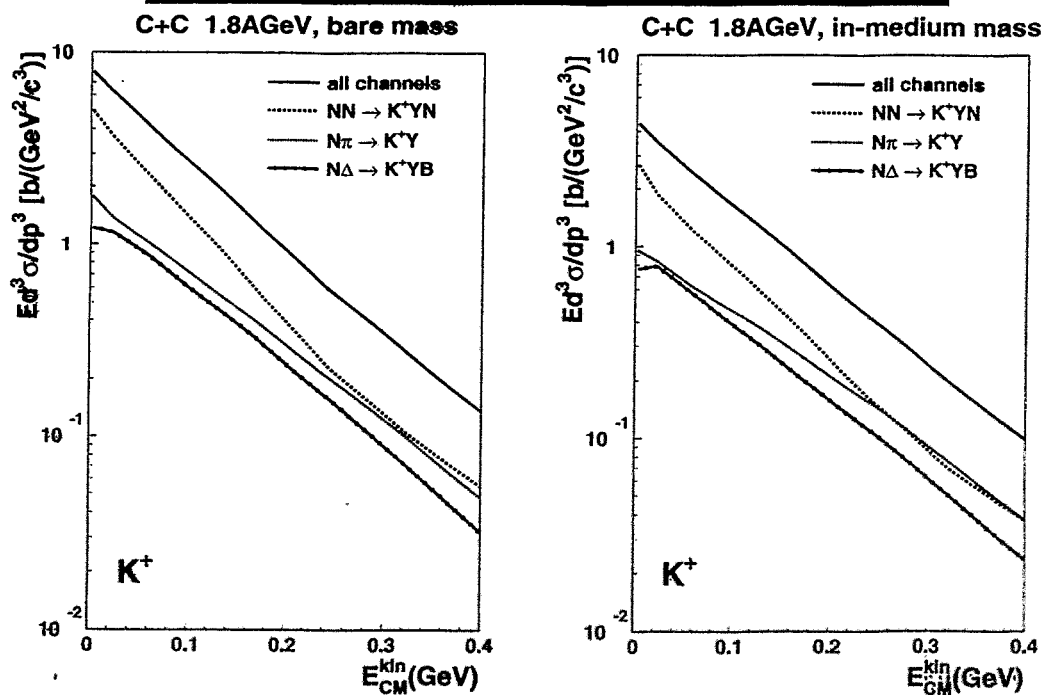
equivalent energies: $\begin{cases} K^+ @ 1.0 \text{ AGeV} : \sqrt{s} - \sqrt{s_{\text{thres}}^{K^+}} \approx -0.23 \text{ GeV} \\ K^- @ 1.8 \text{ AGeV} : \sqrt{s} - \sqrt{s_{\text{thres}}^{K^-}} \approx -0.23 \text{ GeV} \end{cases}$

K[±] Production as a function of Excess-Energy



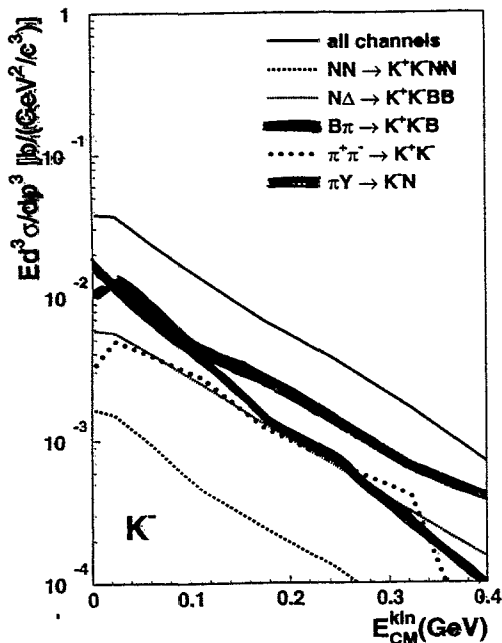
⇒ medium effects are important

RBUU Calculations (Giessen)

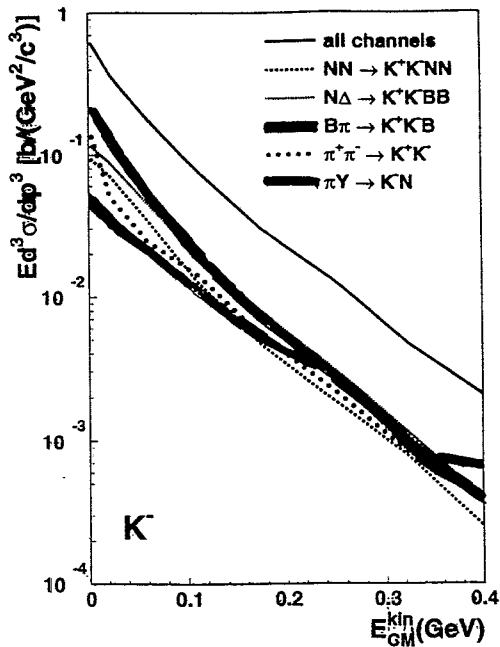


RBUU Calculations (Giessen)

C+C 1.8GeV, bare mass



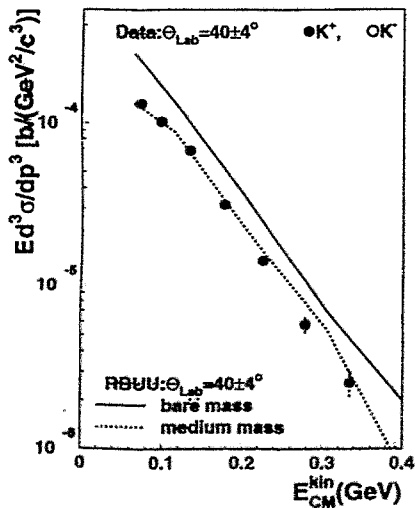
C+C 1.8GeV, in-medium mass



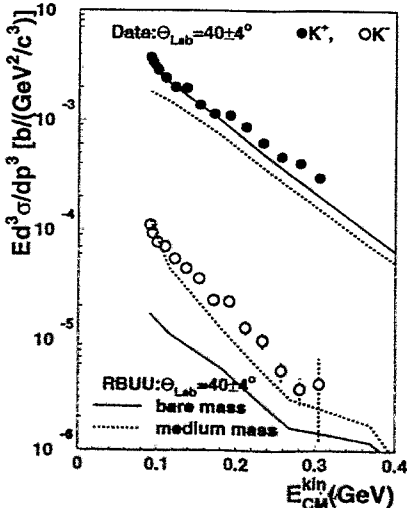
14

Comparison to RBUU

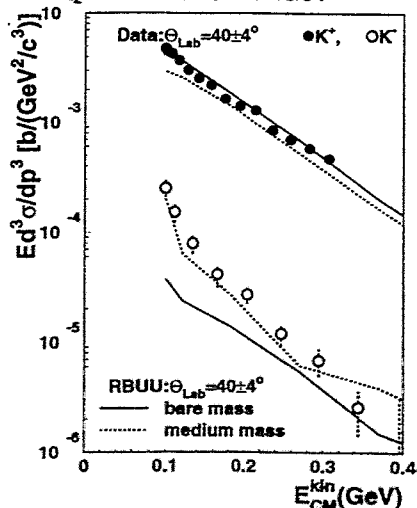
C+C 1.0GeV



C+C 1.8GeV

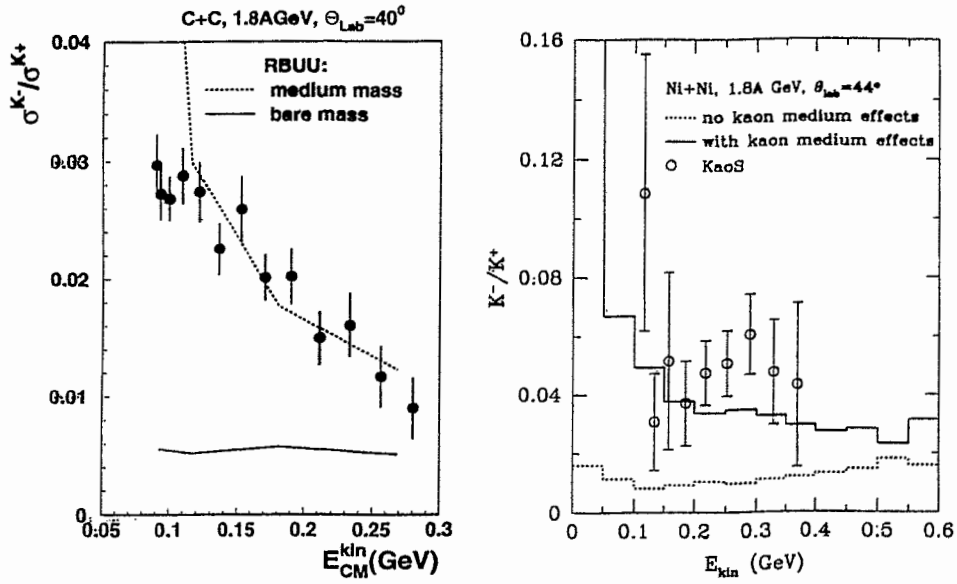


C+C 2.0GeV



16

Comparison to RBUU

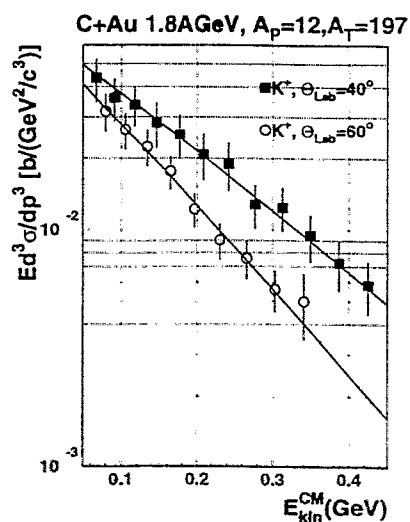
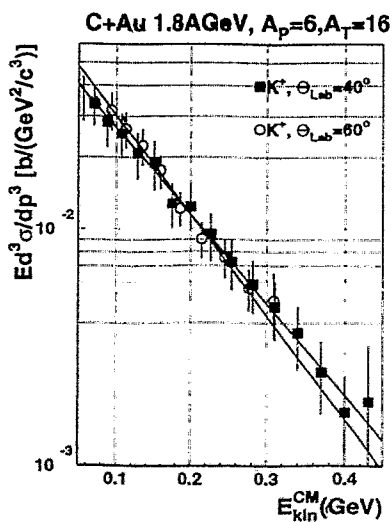
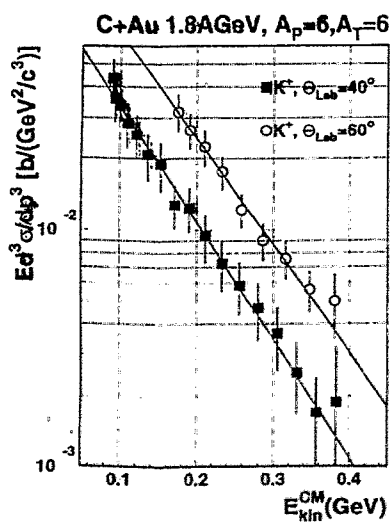


RBUU: C+C [Bra97], Ni+Ni [Li98, Li97]

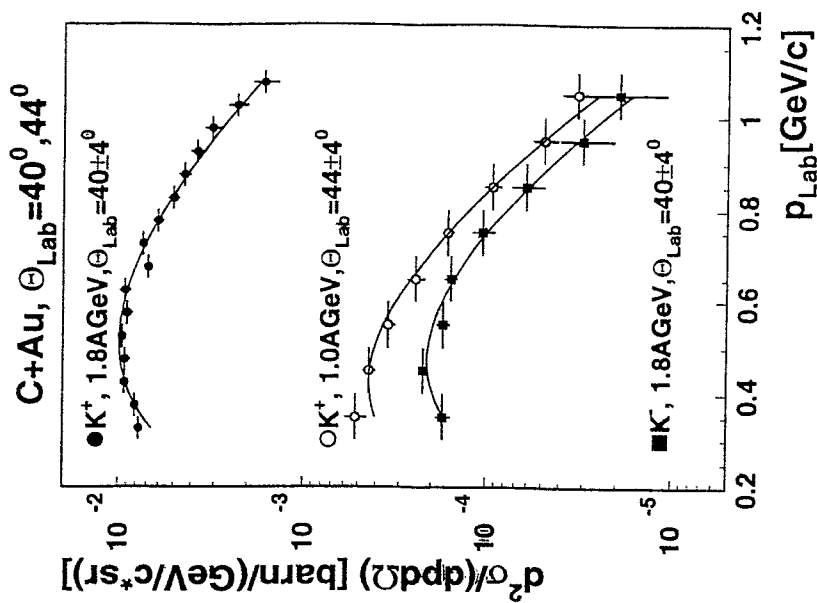
- measurements at low E_{CM}^{kin} , p_T should be performed

Summary

- The C+C data cover a large fraction of the phase space for K^\pm (and π).
- The time of flight trigger allows to study kaons and antikaons even far below threshold.
- K^\pm @ $E_{Beam} = 0.8\text{---}2.0\text{A GeV}$
- K^- @ $E_{Beam} = 1.5\text{---}2.0\text{A GeV}$
- K^\pm spectra can be fitted by Maxwell-Boltzmann distribution (with small correction due to a polar angular distributions).
- ⇒ C.Sturm (next talk)
- K^+ and K^- production cross-sections (and inverse slope parameters) seem to scale with $\sqrt{s} - \sqrt{s_{th}}$ (total yield, shape).
- Transport models can explain the data only by assuming in-medium potentials or by neglecting K^- absorption.



The C+Au System

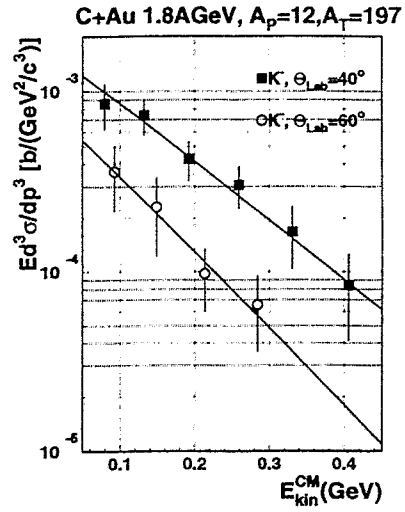
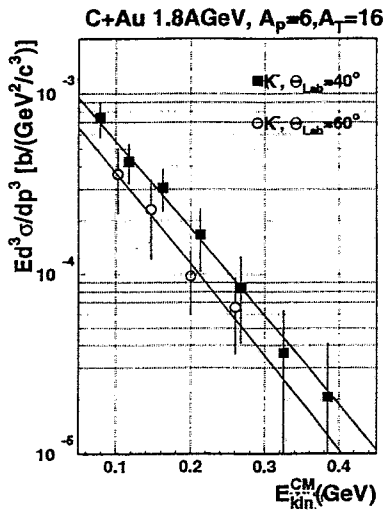
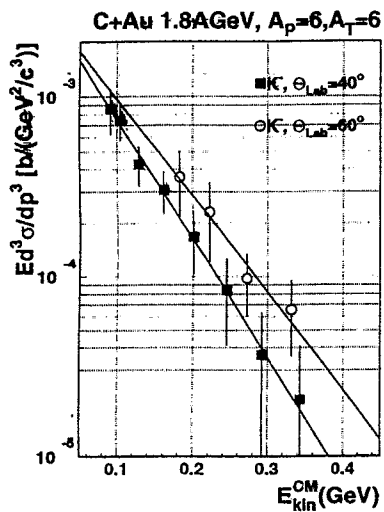


- Why is the C+Au system interesting ?
You can learn about absorption.
- Why is the C+Au system difficult ?
Where is midrapidity ?
Different for each individual collision.

The C+Au System

The C+Au System

22



C. Sturm:

**K⁺ production in heavy-ion reactions as a probe for
the nuclear equation of state**

K^+ Production in Heavy Ion Reactions

as a Probe for the Nuclear Equation of State

C. Sturm (TU Darmstadt)

for the

KaoS Collaboration

method:

the comparison of the K^+ production excitation function in a heavy and light collision system

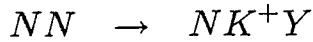
Outline

- Can K^+ serve as a probe for the EOS?
- Experimental results of the collision systems Au+Au and C+C
 - Spectral distributions
 - Polar angle distributions
 - Excitation functions
- Summary

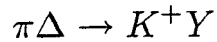
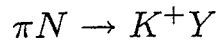
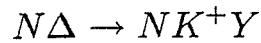
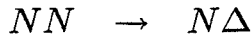
K⁺ - a Probe for the High-Density Phase

Production

- direct production



- two-step production



⇒ multi-step processes

Emission

- K⁺ mean free path at ρ_0 :

$$\lambda_{K^+} \approx 5 \text{ fm}$$

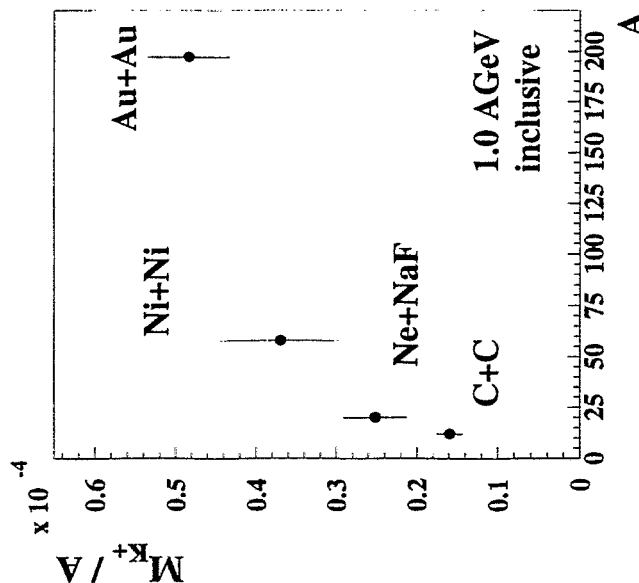
- no absorption

due to strangeness conservation

⇒ direct information

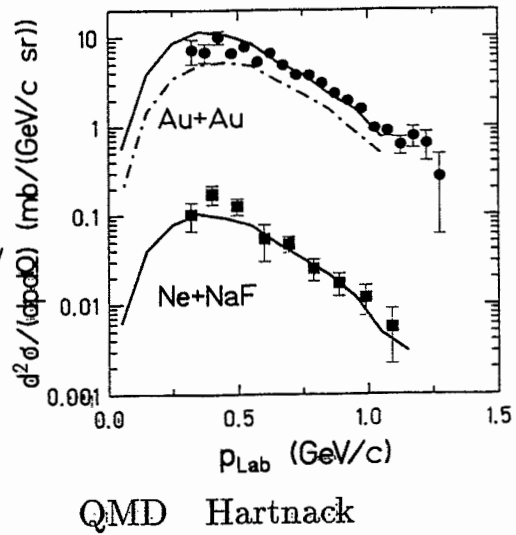
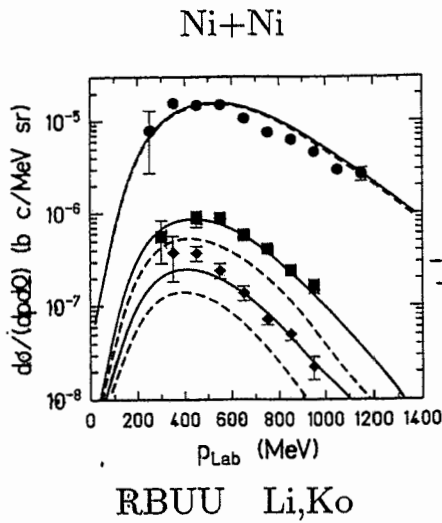
K⁺ Production in A+A Collisions

via Collective Effects



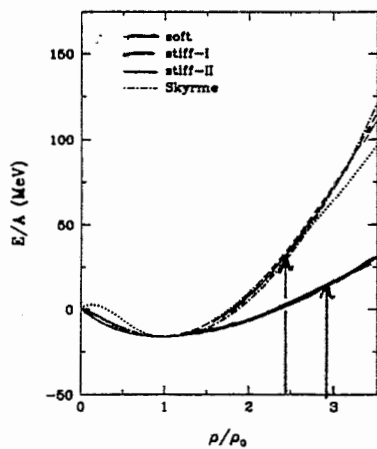
$$M_{K^+} = \frac{\sigma(K^+)}{\sigma_{\text{react}}}$$

Dependence of Incident Energy and System Size



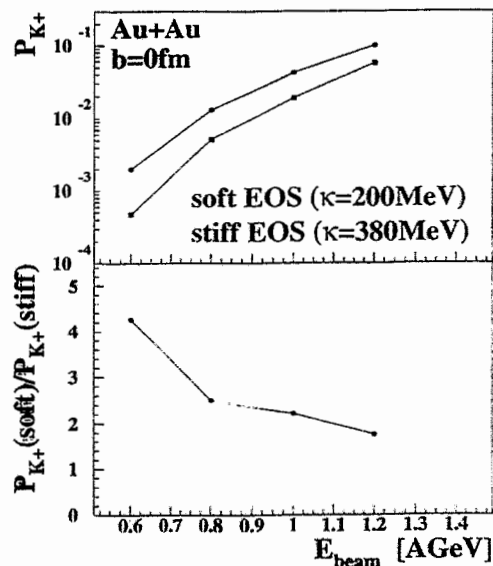
K⁺ Production and the EOS

RBUU: G.Q. Li and C.M. Ko, Physics Letters B 349 (1995)

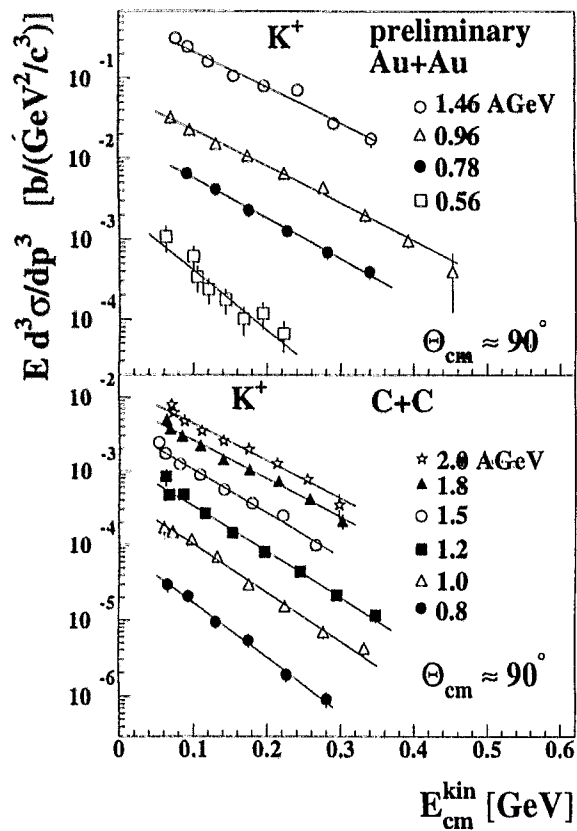


$$(\rho_{max}/\rho_0)_{stiff} \cong 2.4$$

$$(\rho_{max}/\rho_0)_{soft} \cong 2.9$$



K⁺ Spectral Distributions

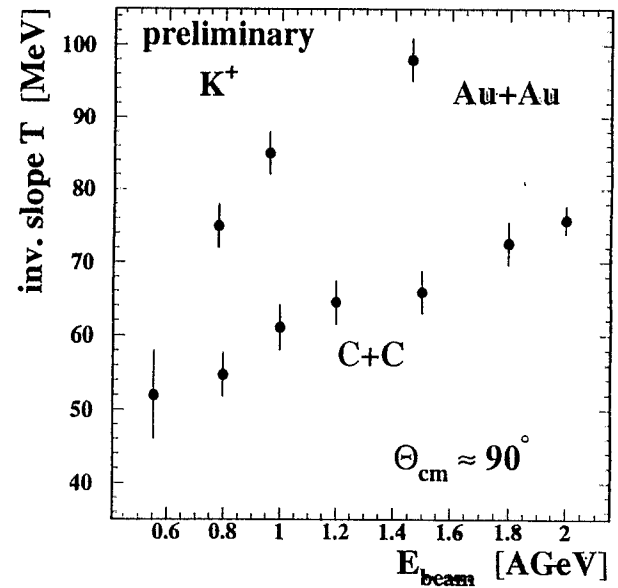


Au+Au, 0.56 AGeV:
I.Böttcher, Uni. Marburg

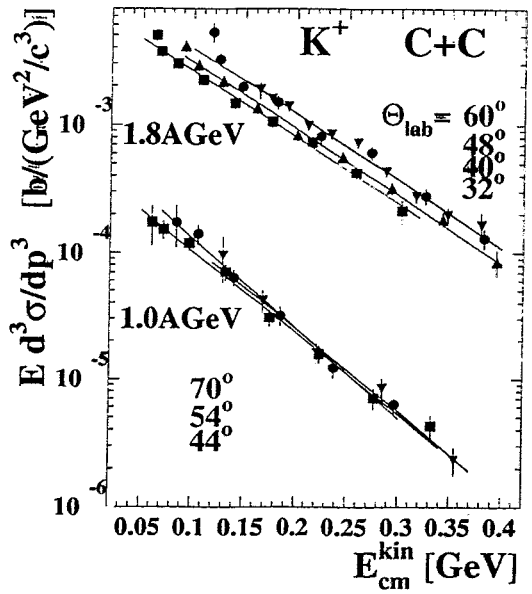
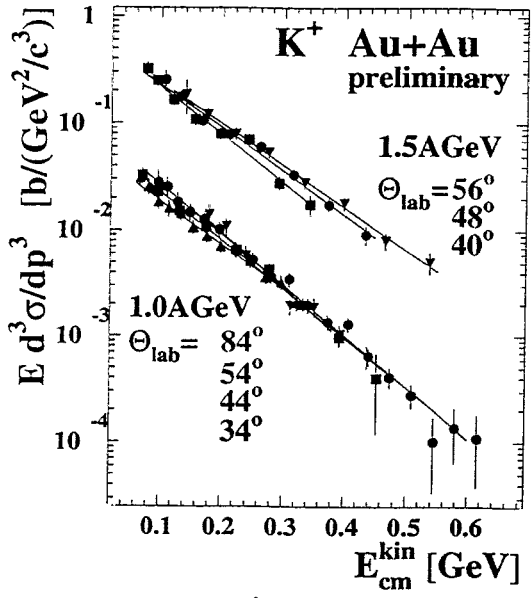
K⁺ Slope Parameters

Boltzmann distribution

$$\frac{d^3 \sigma}{dp^3} \propto \exp\left(\frac{-E}{T}\right)$$



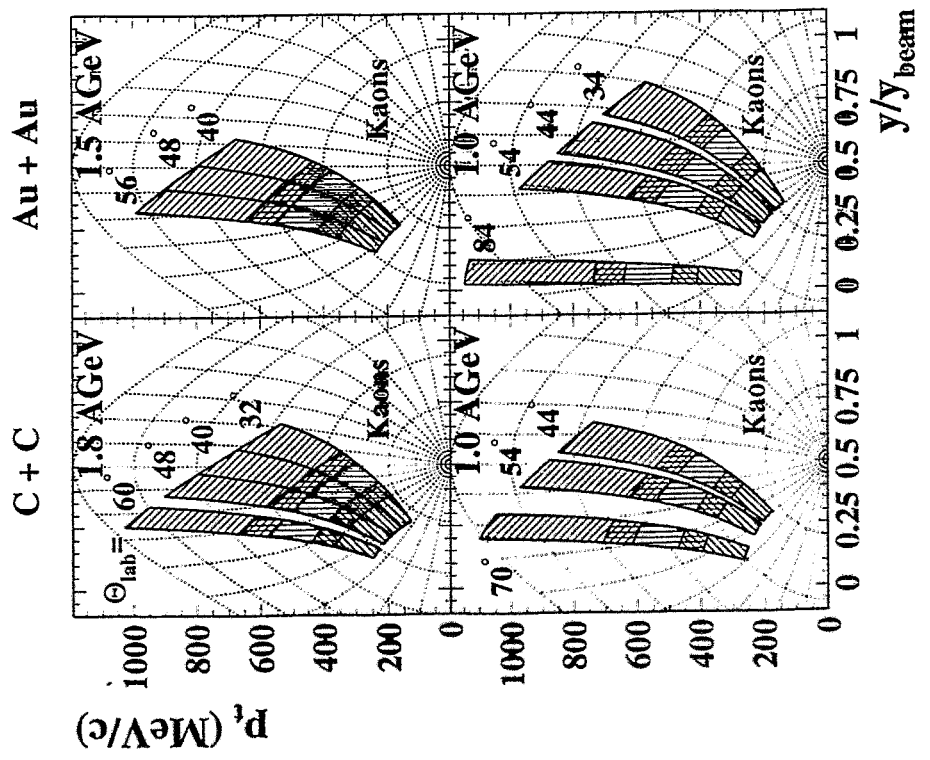
K⁺ Spectral Distributions



1.0 AGeV, 84° I.Böttcher

1.8 AGeV, 60° +
1.0 AGeV, 70° F.Laue

Phase Space Coverage

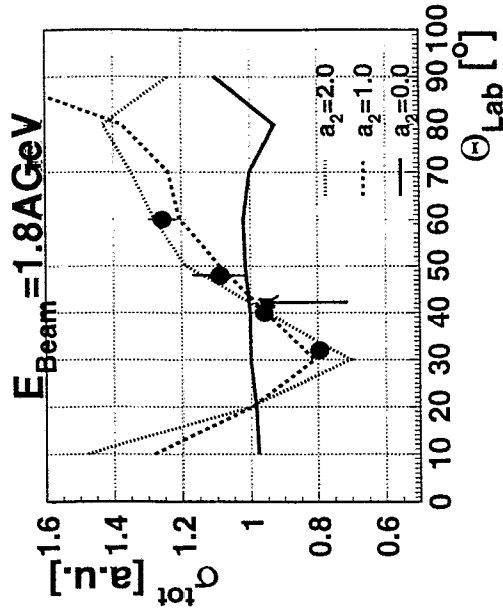


Total Cross Sections

Monte Carlo Simulation:

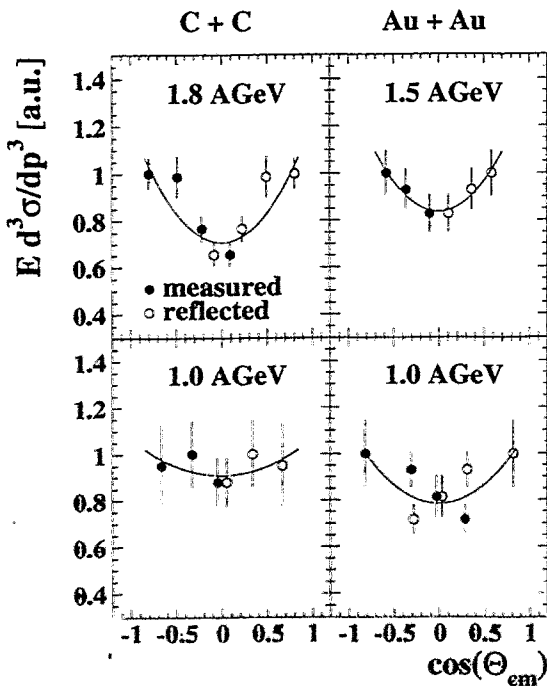
thermal source + anisotropic polar emission

$$\frac{d\sigma}{d\Theta_{cm}} \propto 1 + a_2 \cdot \cos^2(\Theta_{cm})$$

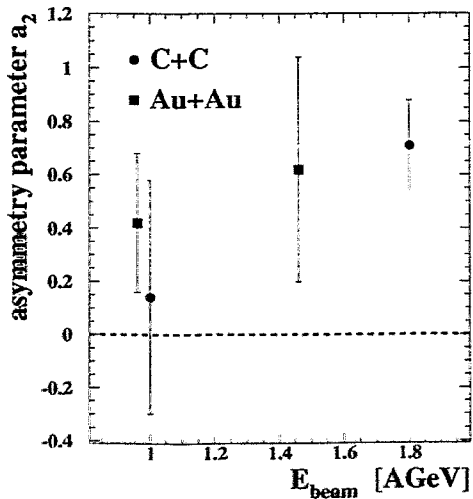


(F.Laue, PHD)

K⁺ Polar Angle Distribution



$$E \cdot \frac{d^3\sigma}{dp^3} \propto 1 + a_2 \cdot \cos^2(\Theta_{cm})$$



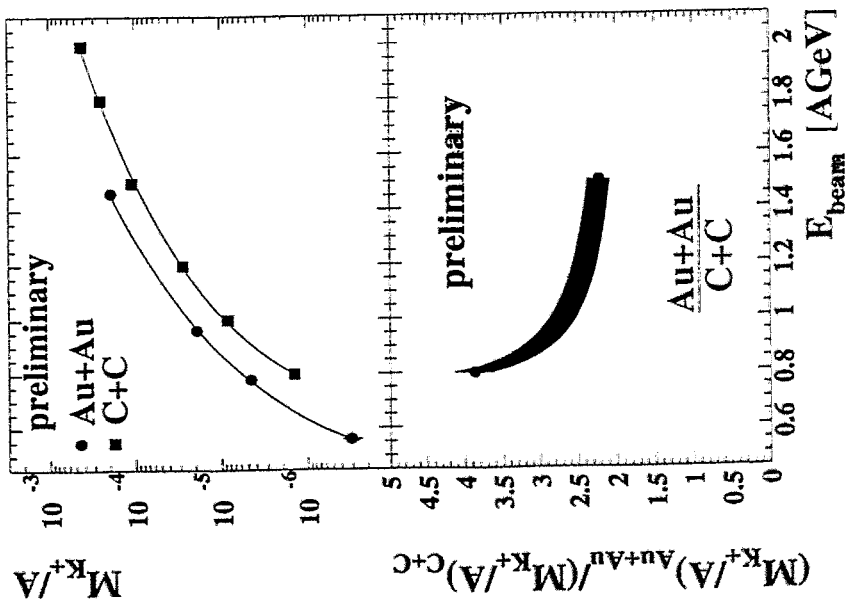
for $a_2 \approx 0.5$:

$$\sigma_{tot} \approx 1.2 \cdot 4\pi \cdot \left(\frac{d\sigma}{d\Omega}\right)_{\Theta_{cm}=90^\circ}$$

Summary

- A new observable sensitive to the EOS:
comparison of the K^+ -production in a heavy and a light collision system - experimental and theoretical uncertainties are strongly reduced
- Rise of $\frac{K^+(Au+Au)}{K^+(C+C)}$ with decreasing incident energy
 \Rightarrow evidence for a soft EOS
- K^+ production excitation functions
 - in Au+Au (0.56 - 1.46 AGeV) (0.38 mb - 230 mb)
 - in C+C (0.8 - 2.0 AGeV) (0.017 mb - 5.0 mb)
- K^+ polar angle distributions:
slight forward backward peaked

K⁺ Excitation Functions



\Rightarrow evidence for a soft EOS
 \rightarrow comparison with transport model calculations

The KaoS Collaboration

I. Böttcher^c, M. Dębowski^f, F. Dohrmann^f,
A. Förster^b, E. Grosse^{f,g}, P. Koczoń^a,
B. Kohlmeyer^c, F. Laue^a, M. Menzel^c, L. Naumann^f,
H. Oeschler^b, F. Pühlhofer^c, Ch. Schneider^f,
E. Schwab^a, P. Senger^a, Y. Shin^d, J. Speer^a,
W. Scheinast^f, H. Ströbele^c, Ch. Sturm^b, G. Surowka^e,
F. Uhlig^b, K. Völkel^d, A. Wagner^h, W. Waluś^e

^a GSI Darmstadt, ^b TU Darmstadt, ^c Univ. Marburg,

^d Univ. Frankfurt, ^e FZ Rossendorf,

^f TU Dresden, ^g Univ. Kraków, ^h NSCL MSU

Wanted ...

... detailed transport calculations which describes the available observables:

- K^+ -Production
 - K^+ production excitation functions for $C + C$ and $Au + Au$ collisions
 - K^+ polar angle distributions
- π -Production
 - π -production excitation functions
 - spectral distributions
 - angular distributions

K.R. Schubert:

**Recent results on symmetry breaking in the K^0
system**

K. R. Schubert, TU Dresden
Kaon Workshop Rossendorf, 19/12/98

2

Introduction

Neutral K mesons have played important roles in uncovering the properties of the weak interaction. Six highlights:

- 1956 P violation because of $K^0 \rightarrow \pi^+ \pi^-$, $\pi^+ \pi^-$
Dalitz; Lee + Yang ...
- 1961 $K^0 - \bar{K}^0$ oscillations Pais, Good ...
- 1963 $\sin^2 \theta_c (K^0 \rightarrow e^+ \pi^- \nu) + \cos^2 \theta_c (K^0 \rightarrow \mu^+ \nu)$
 $= 1 (K^+ \rightarrow e^+ \nu)$ Cabibbo
- 1964 $K_L^0 \rightarrow \pi^+ \pi^-$, SP. Cronin, Fitch
- 1964 $K_L^0 \rightarrow \mu^+ \mu^-$, FENC Bj, Glushko
- 1973 $A_m(K_L^0 - K_S^0) \rightarrow m_c \approx 2.6 \text{ GeV}$ Ellis et al

Recent Results
on Symmetry Breaking
in the K^0 System.

Introduction.

SEP, X, and CPT in $K^0 \bar{K}^0$ Oscillations.

Oct. 98: Direct T Violation in CPLEAR.

Oct. 98: Direct T Violation in KTeV.

Conclusion.

Summary on CP, P and CPT-properties

in K^0 Decays and Oscillations. 1964-71

Oscillations $K^0 \leftrightarrow 2\pi, 3\pi, \eta, \bar{c}\bar{c} \leftrightarrow \bar{K}^0$ lead to two eigenstates of time evolutions like in coupled pendulae of classical mechanics.

$$K_S = (1+\epsilon+\delta) K^0 + (1-\epsilon-\delta) \bar{K}^0$$

$$K_L = (1+\epsilon-\delta) K^0 - (1-\epsilon+\delta) \bar{K}^0$$

CP symmetry $\Rightarrow \epsilon = \delta = 0, K_L \not\rightarrow \pi^+ \pi^-$.

$$1964 \text{ seen. } \eta_{+-} = \frac{K_L \rightarrow \pi^+ \pi^-}{K_S \rightarrow \pi^+ \pi^-} = \epsilon - \delta \neq 0.$$

Origin in $K^0 \bar{K}^0$ oscillations, Δm & $\Delta \Gamma$.

Four possible contributions to $\eta = \frac{2}{3} \eta_{+-} + \frac{1}{3} \eta_{00}$

- 1.) CPT conserved, \cancel{P} in Δm , $\text{Re } \epsilon + \gamma m \epsilon$
- 2.) $-\cancel{P}$ \cancel{P} in $\Delta \Gamma$, $\text{Re } \epsilon - \gamma m \epsilon$
- 3.) T conserved, CPT in Δm , $\text{Re } \delta - \gamma m \delta$
- 4.) $-\cancel{P}$ CPT in $\Delta \Gamma$, $\text{Re } \delta + \gamma m \delta$

Experimental Separation in 1970/71

K.R. Schubert et al, PL 31B (1970) 662

+ Proc. Int. Conf. HEP Amsterdam (1971) 333

using Bell-Steinberger Unitarity Relation:

$$i \cdot \Delta m (K_L - K_S) \cdot \langle K_S | K_L \rangle = \sum_f \langle f | T | K_S \rangle^* \langle f | T | K_L \rangle$$

$$\text{Re } \epsilon + \gamma m \epsilon = (2,7 \pm 0,3) 10^{-3} \quad \leftarrow$$

$$\text{Re } \epsilon - \gamma m \epsilon = (0,1 \pm 0,4) 10^{-3} \quad \checkmark$$

$$\text{Re } \delta - \gamma m \delta = (0,0 \pm 0,5) 10^{-3} \quad \checkmark$$

$$\text{Re } \delta + \gamma m \delta = (-0,2 \pm 0,2) 10^{-3} \quad \checkmark$$

CPT is conserved and T is violated

in "Virtual" (Δm) part of $K^0 \bar{K}^0$ oscillations.

Max. CPT contribution = $\frac{1}{3} \cancel{P}$ contribution.

Uses unitarity, i.e. all decaying K mesons decay into observable final states.

Well known result. Remember:

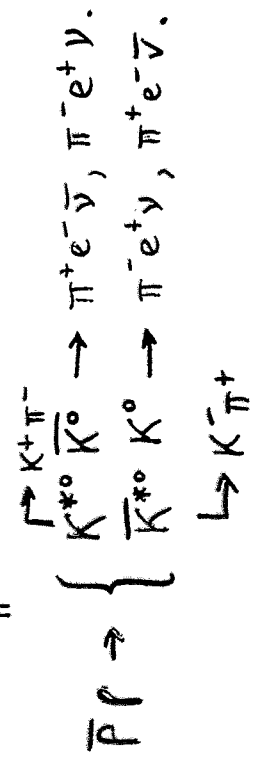
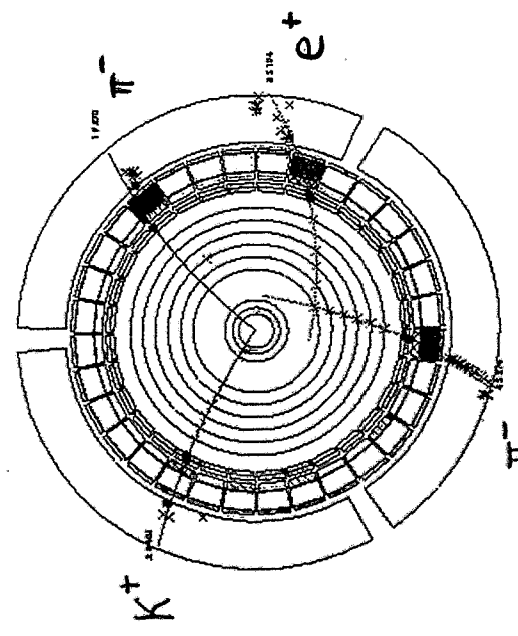
$$\Gamma(\bar{K}^0 \rightarrow K^0) \geq \Gamma(K^0 \rightarrow \bar{K}^0) \quad \cancel{CP}, \cancel{P}$$

$$K_L = p K^0 + q \bar{K}^0 \quad \text{with } |p| > |q|.$$

More "direct" observations of T violation in the K^0 system came only this October (apart from conference contributions from CPLEAR a few years ago).

Direct T Violation in CPLEAR

LEAR @ CERN: 200 MeV/c \bar{p} into H_2 gas

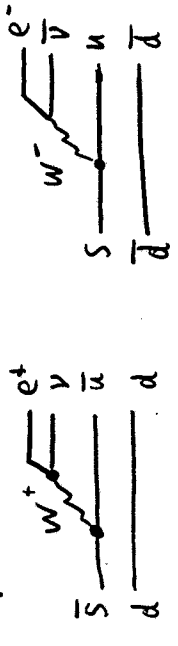


$12 \cdot 10^6$ tagged π ev decays with $t > 1 \tau_c$

Four classes of events $K^0, \bar{K}^0 \rightarrow \pi^+ e^- \bar{\nu}, \pi^- e^+ \nu$.

Time dependence confirms " $\Delta S = \Delta Q$ " with

high precision:



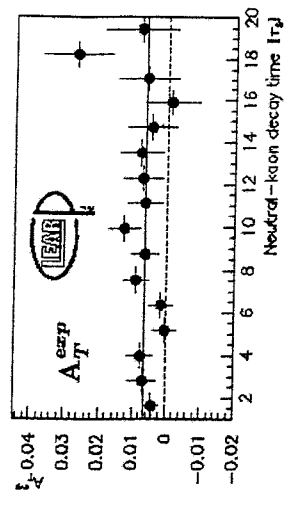
Lepton charge tags K flavour at t decay.

Kaon charge ($K^\pm \pi^\mp$) tags $||$ at t production.

CP- and T- violating result:

Direct measurement of T violation

$$A_T = \frac{R(\bar{K}^0 \rightarrow K^0) - R(K^0 \rightarrow \bar{K}^0)}{R(\bar{K}^0 \rightarrow K^0) + R(K^0 \rightarrow \bar{K}^0)} = 4\text{Re}\epsilon$$



$\text{Re } \epsilon = (1.65 \pm 0.32 \pm 0.25) \cdot 10^{-3}$

Not new, but new way.

$A_T = (6.6 \pm 1.3_{stat.} \pm 1.0_{sys.}) \cdot 10^{-3}$

This result, called "direct" by CPLEAR assumes CPT in the decay and tests CPT in oscillations. Result: All CP is T.

In a second paper

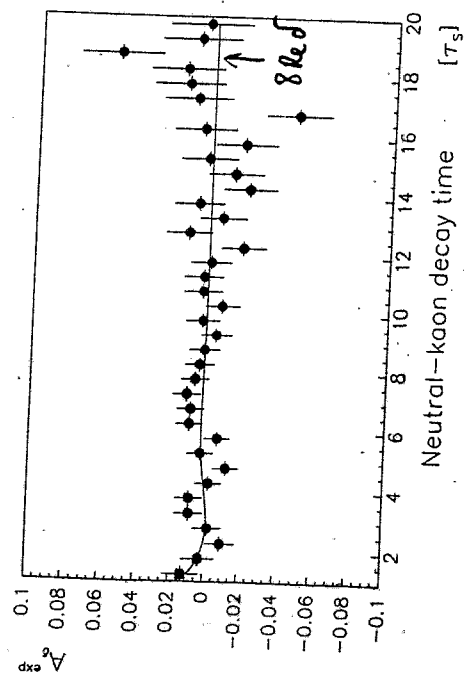
A. Angelopoulos et al, CERN-EP/98-154, 12/10/98

CPLEAR gives up CPT assumption in semileptonic decays. "Nicer" result:

$Re \delta = (0,30 \pm 0,33 \pm 0,06) \cdot 10^{-3}$ CPT ✓

Using all four observed rates.

$Im \delta = (-15 \pm 23) \cdot 10^{-3}$ CPT ✓
 $= (-0,9 \pm 2,9) \cdot 10^{-3}$ if $\Delta S = \Delta Q$ strict.



Direct T Violation in KTeV

Experiment E832 at FNAL, F. Adams et al,

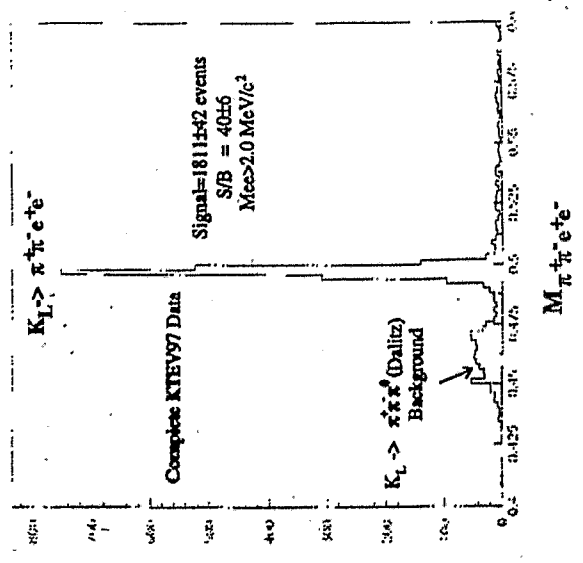
Main goal: $Re(\epsilon'/\epsilon) \pm 3 \cdot 10^{-4}$

1997 data: $2.5 \cdot 10^{10} K_L^0$

Search for $K_L^0 \rightarrow \pi^+ \pi^- e^+ e^-$

$1.3 \cdot 10^8$ triggers with 4 tracks.

1800 events reconstructed, $S/B \approx 40$.

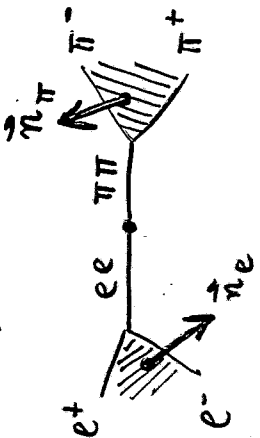


First
 obser-
 vation!

$B = (3,2 \pm 0,4 \pm 0,6) \cdot 10^{-7}$

$B = (3,2 \pm 0,4 \pm 0,6) \cdot 10^{-7}$

$K_L^0 \rightarrow \pi^+ \pi^- \gamma$ has CP-conserving and CP-violating part. Interference leads to γ polarisation. Leads to angular asymmetry in $\pi^+ \pi^- e^+ e^-$.



$$\phi = \angle(\vec{n}_e, \vec{n}_\pi)$$

$$\sin\phi = \frac{[\vec{p}(e^+) \times \vec{p}(e^-)] \cdot [\vec{p}(\pi^+) \times \vec{p}(\pi^-)] \cdot [\vec{p}(\pi^+) + \vec{p}(\pi^-)]}{|\vec{p}(e^+) \times \vec{p}(e^-)| \cdot |\vec{p}(\pi^+) \times \vec{p}(\pi^-)| \cdot |\vec{p}(\pi^+) + \vec{p}(\pi^-)|}$$

The triple product is odd under P ($\vec{p} \rightarrow -\vec{p}$), even under C ($Q \rightarrow -Q$), odd under T ($\vec{p} \rightarrow -\vec{p}$).

An asymmetric distribution around zero of

S, or $\sin\phi$, or $\sin\phi \cos\phi$, or ϕ is

P-violating, CP-violating, T-violating.

L.M. Sehgal et al, PRD 46(1992)1035+5209

predict large effect on the basis of known E.

From
M. Arenton (U Virginia, KTeV)
Heavy Quarks 98

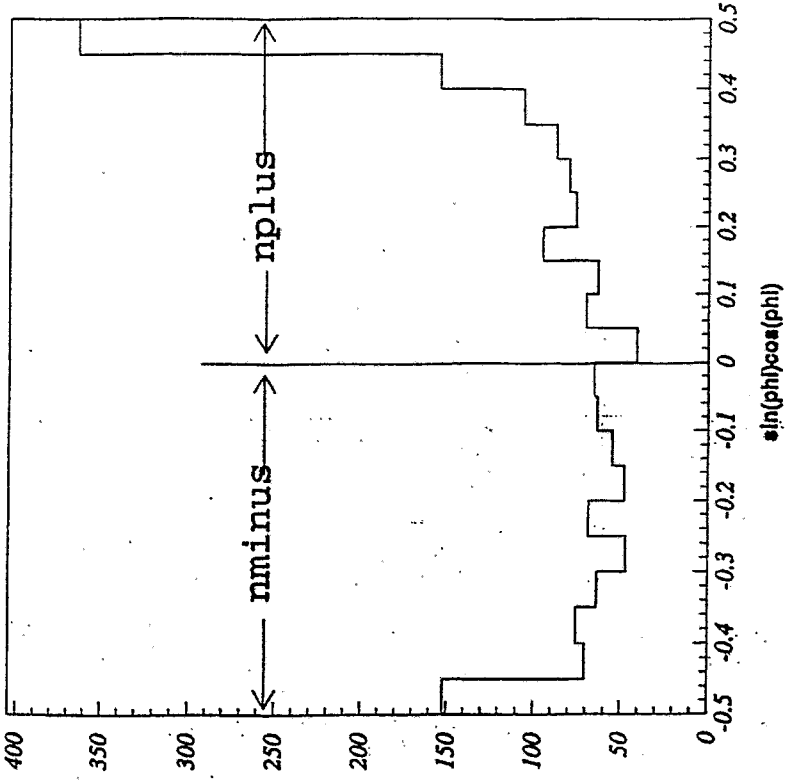


Figure 14: $\sin\phi\cos\phi$ distribution for the total data sample, where nplus and minus are also shown

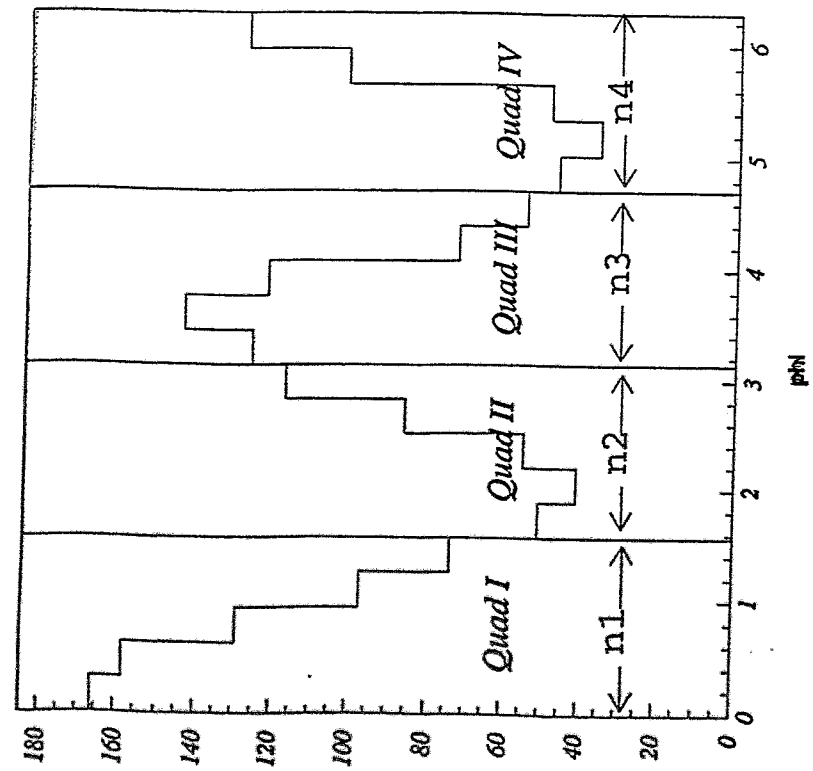


Figure 15: singular distribution for the total data sample, where the Quadrants, n_1 , n_2 , n_3 and n_4 are also shown

$$A = \frac{n_1 + n_3 - n_2 - n_4}{n_1 + n_2 + n_3 + n_4} = (13.5 \pm 2.5 \pm 3.0)\%$$

in perfect agreement with the 1992 prediction of Seghal and the known value of ϵ .

Conclusion

Both new results demonstrate T violation and are, therefore, "ripe" for text books. But they do not contribute to progress in understanding and predicting CP violating effects. All effects so far depend on one parameter ϵ only ($\delta=0, \epsilon'=?$).

In the Standard Model $\epsilon \approx E(m_t, \theta_{12}, \theta_{23}, \theta_{13}, \delta, \dots)$ Knowledge on θ_{13} and δ from other rare K decays like $K^* \rightarrow \pi^+ \nu \bar{\nu}$ and from B decays.

B decays have also the potential to look for non-standard contributions to CP. Cosmology needs them, Standard CP is far too weak to explain antimatter disappearance in the Universe. Each new CP contribution must also be tested for T and CPT.

Theoretical Part

W. Cassing & E. Bratkovskaya:

**The RBUU (HSD) approach to strangeness
production**

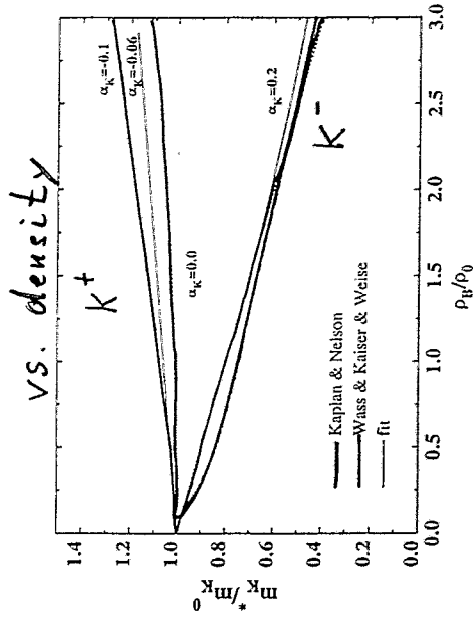
The RBUU (HSD) approach – strangeness production

W. Cassing, E.L. Bratkovskaya

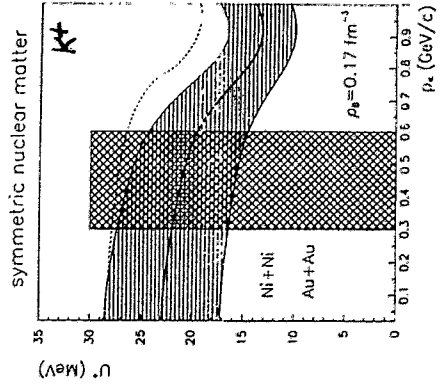
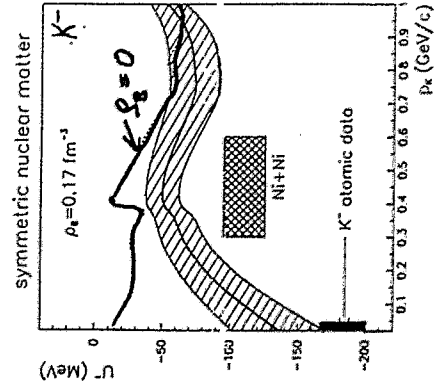
Contents

1. Introduction
2. The HSD approach
3. ss -production and observables
4. Benchmark tests for Ni + Ni at 1.8 A-GeV

K^\pm - potentials



vs. momentum



HSD¹ - a covariant transport approach

W. Ehehalt and W. Cassing, Nucl. Phys. A602 (1996) 449

The covariant transport equations for the phase-space distributions $f_h(x, p)$ of hadron h read:

$$\begin{aligned} & \{ (\Pi_\mu - \Pi_\nu \partial_\mu^p U_h^* - M_h^* \partial_\mu^p U_h^S) \partial_x^\mu + (\Pi_\nu \partial_\mu^p U_h^* + M_h^* \partial_\mu^p U_h^S) \partial_p^\mu \} f_h(x, p) \\ & = \sum_{h_2 h_3 h_4 \dots} \int d^3d^4 \dots [G^I G^J]_{12 \dots 34 \dots} \delta^4(\Pi + \Pi_2 - \Pi_3 - \Pi_4 \dots) \\ & \times \{ f_{h_3}(x, p_3) f_{h_4}(x, p_4) \bar{f}_h(x, p) \bar{f}_{h_2}(x, p_2) \\ & - f_h(x, p) f_{h_2}(x, p_2) \bar{f}_{h_3}(x, p_3) \bar{f}_{h_4}(x, p_4) \} \dots \end{aligned}$$

with the quasi-particle dispersion relation

$$\delta(\Pi_\mu \Pi^\mu - M_h^{*2}) \quad (1)$$

with effective mass and momentum given by

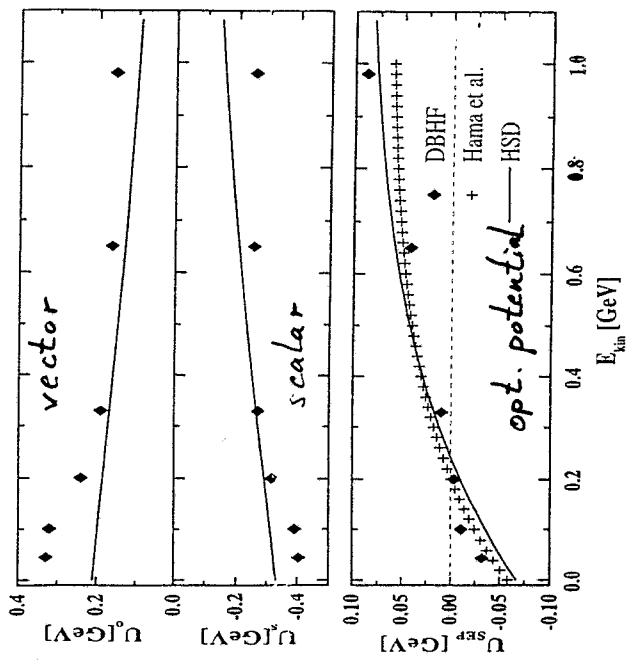
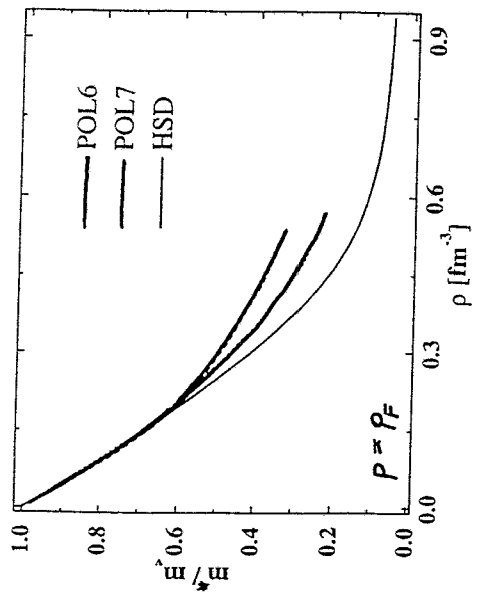
$$\begin{aligned} M_h^*(x, p) &= M_h + U_h^S(x, p) \\ \Pi^\mu(x, p) &= p^\mu - U_h^\mu(x, p) \end{aligned}$$

and scalar and vector self-energies $U_h^i(x, p)$ ($i = 0, 1, 2, 3$) for all hadrons. The phase-space factors

$$\bar{f}_h(x, p) = 1 \pm f_h(x, p) \quad (2)$$

are responsible for fermion Pauli-blocking or Bose enhancement, respectively.

$$M^* = m_v + U_S(S_3, p)$$



quasi-particles in the medium

$$(w - u_0(x, p))^2 = (\vec{p} - \vec{u}(x, p))^2 + (m_0 + u_s(x, p))^2$$

or $\vec{\pi}(x, p)$

$$w^2 = \vec{p}^2 + m_0^2 + \pi(x, p, S_B, S_S) \quad (\text{mesons})$$

equations of motion:

$$\dot{x} = \frac{\partial w}{\partial p_x} \quad \dot{p}_x = -\frac{\partial w}{\partial x}$$

$$\dot{y} = \frac{\partial w}{\partial p_y} \quad \dot{p}_y = -\frac{\partial w}{\partial y}$$

$$\dot{z} = \frac{\partial w}{\partial p_z} \quad \dot{p}_z = -\frac{\partial w}{\partial z}$$

Hamilton Eq.

treatment of collisions:

$$\text{impact parameter } b \leq \sqrt{\frac{R_1 R_2}{M}}$$

formation time $\tau_f \approx 0.5 \text{ fm}/c$

+ energy - momentum conservation

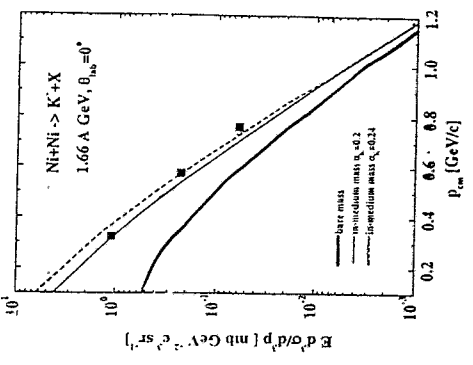
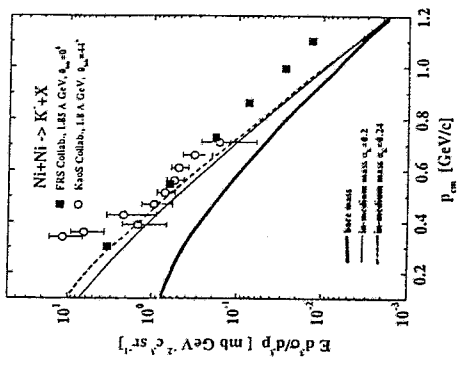
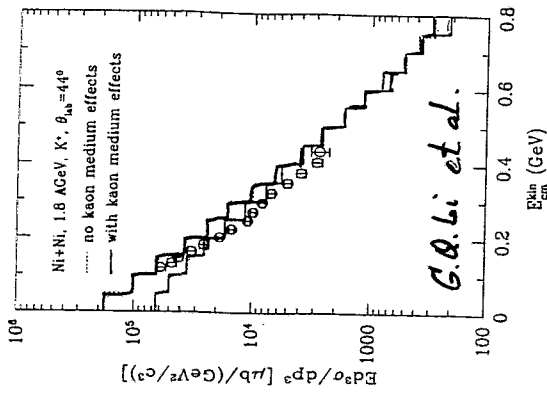
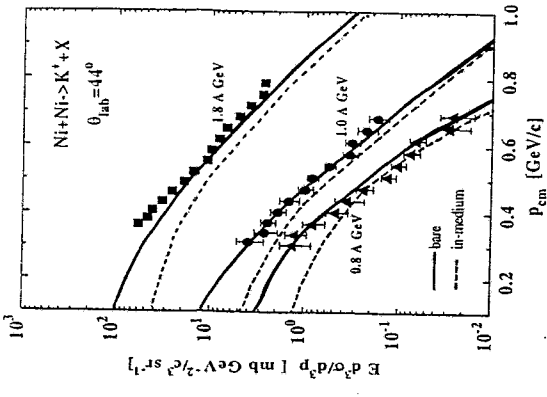
$$w_1(x, p) + w_2(x, p) = w_3(x, p_3) + w_4(x, p_4) + w_5(x, p_5)$$

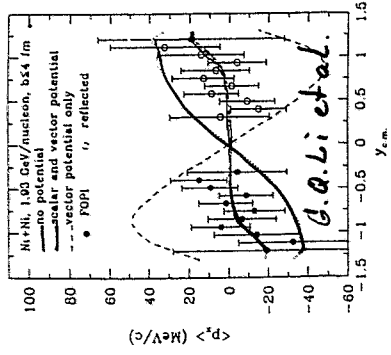
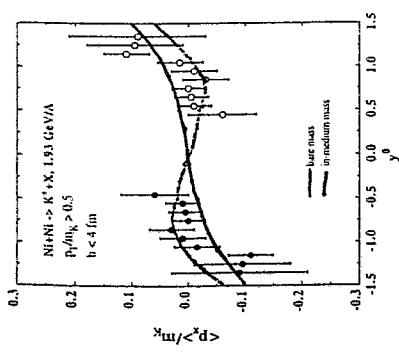
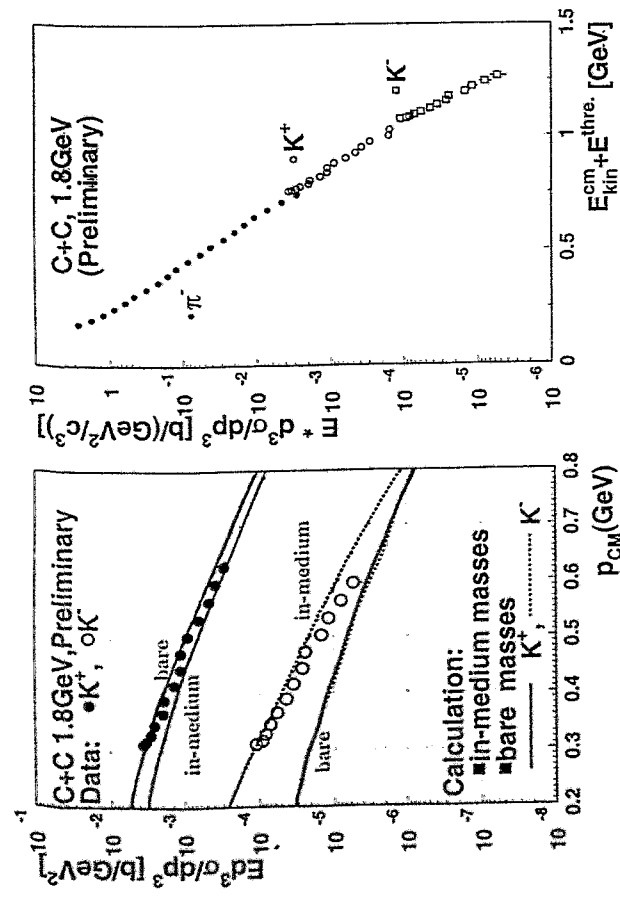
$$\vec{\pi}_1(x, p_1) + \vec{\pi}_2(x, p_2) = \vec{\pi}_3(x, p_3) + \vec{\pi}_4(x, p_4) + \vec{\pi}_5$$

'historical' treatment of mesons:

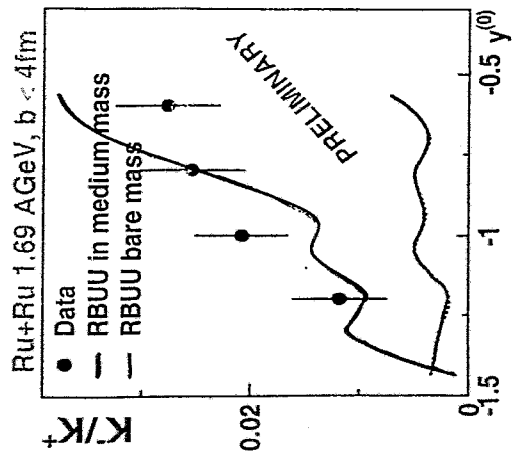
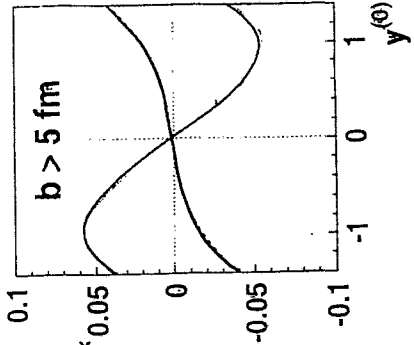
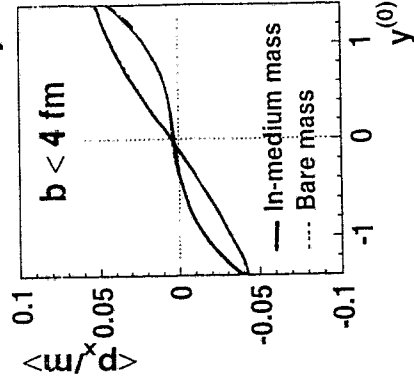
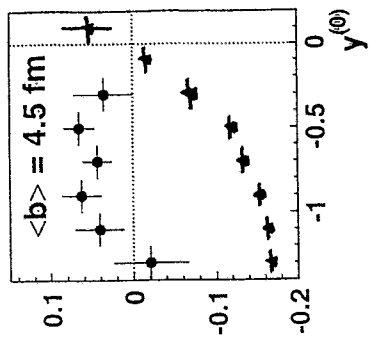
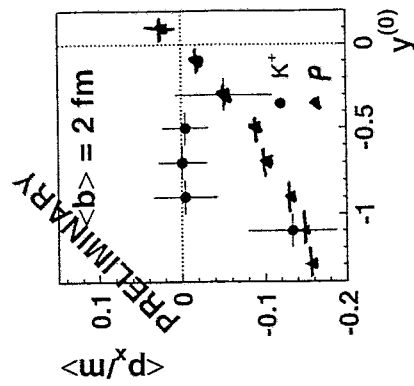
$$\pi(x, p) = M^{*2}(x, p) - m_0^2, \quad M^* = m_0(1 - \alpha_m S_B(x)/S_0)$$

with coefficient α .

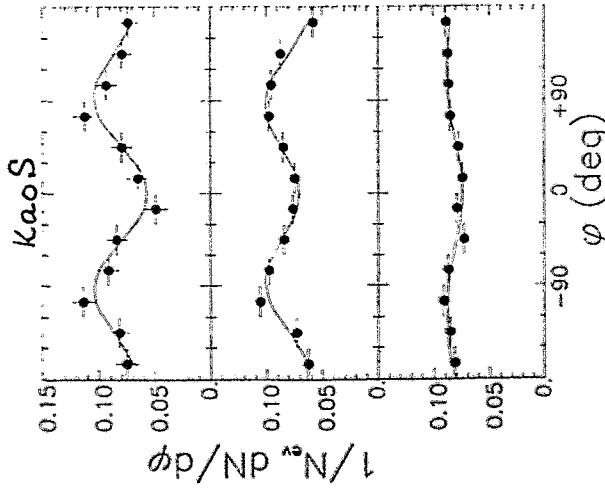




in-plane K^+ -flow



K^+ azimuthal angular distribution for



peripheral

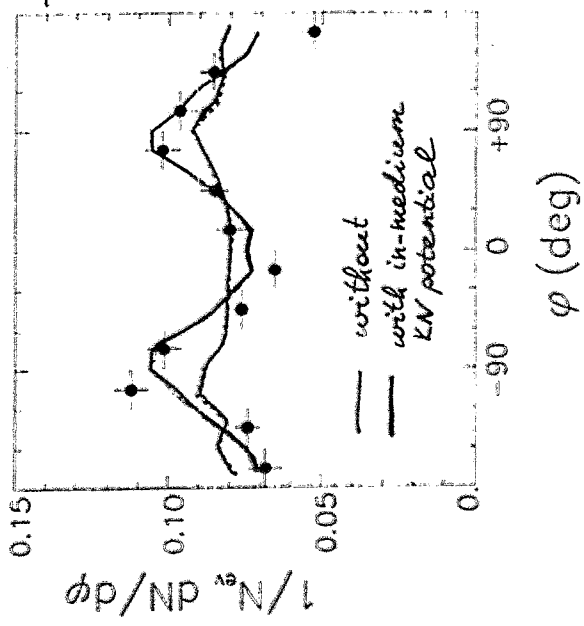
semi-central

central collisions

$$0.2 \leq \frac{y}{y_{proj}} \leq 0.8$$

$$0.2 \leq P_t \leq 0.8 \text{ GeV}/c$$

Au+Au, 1 A.Gel.



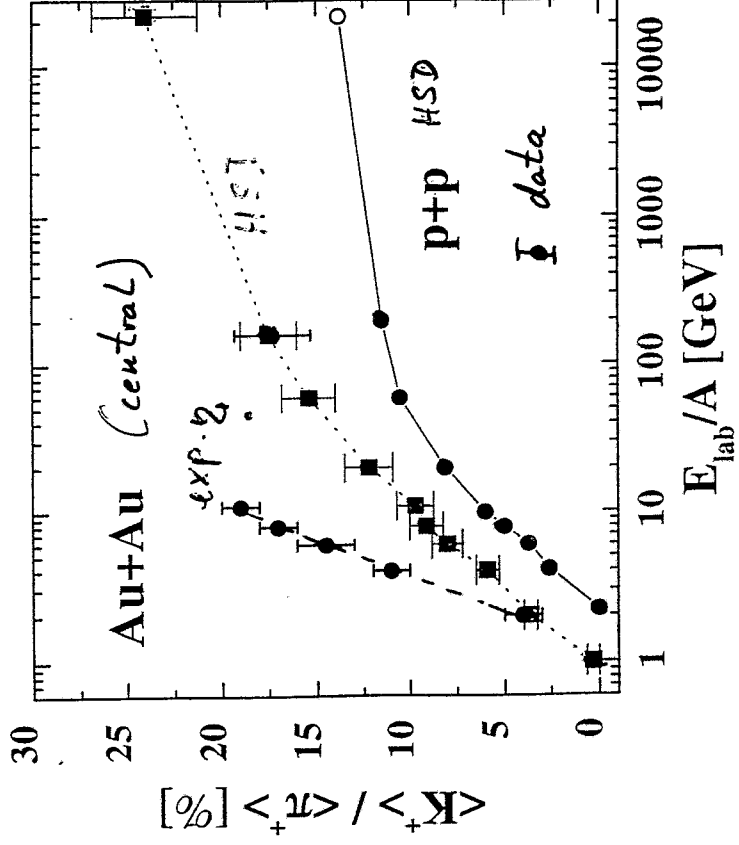
• semi-central Au+Au, 1 A.G.

RBM collected:

G. Li, C.H. Ko, and G.E. Brown
Phys. Lett. B 381 (1996) 17.

— without
— with in-medium KN potential

$\frac{K^+}{\pi^+}$ at midrapidity



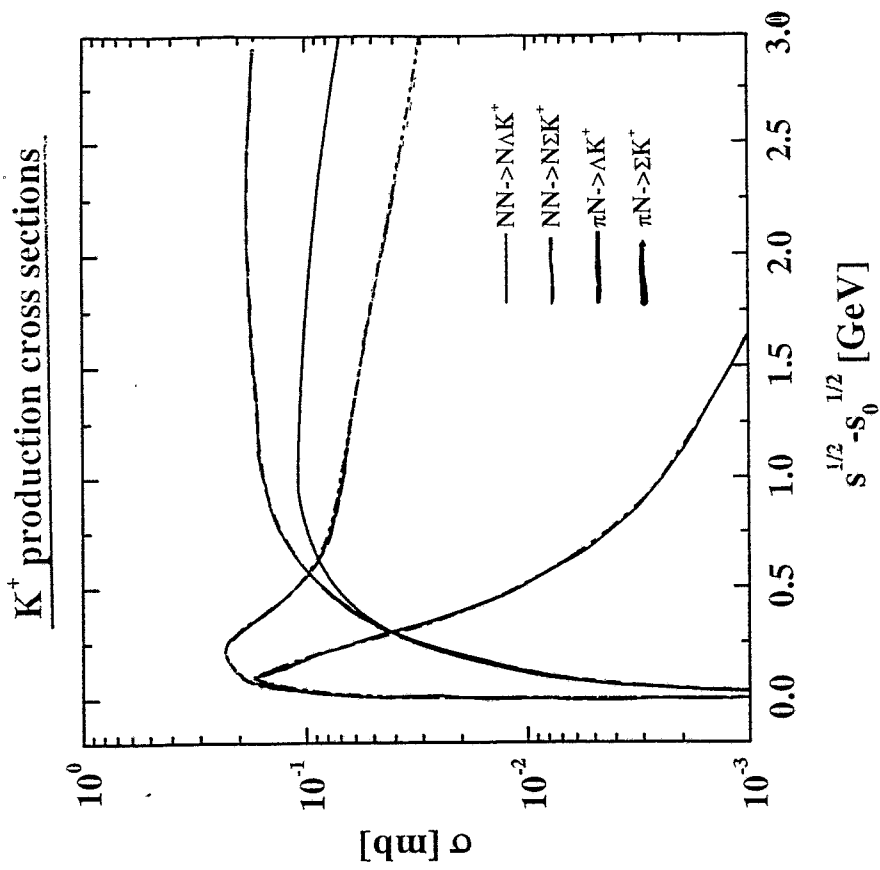
→ chiral symmetry restoration?
parton degrees of freedom?

Benchmark tests.

Ni+Ni at 1.8 A.GeV, b=2 fm

Included processes for K^+ and K^- productions:

1. a) $NN \rightarrow N\Lambda K^+$
2. b) $NN \rightarrow N\Sigma K^+$
3. c) $N\Delta \rightarrow N\Lambda K^+$
4. d) $N\Delta \rightarrow N\Sigma K^+$
5. e) $\Delta\Delta \rightarrow N\Lambda K^+$
6. f) $\Delta\Delta \rightarrow N\Sigma K^+$
7. g) $\pi N \rightarrow \Lambda K^+$
8. h) $\pi N \rightarrow \Sigma K^+$
9. i) $\pi\Delta \rightarrow \Lambda K^+$
10. k) $\pi\Delta \rightarrow \Sigma K^+$
11. l) $NN \rightarrow NNK^+K^-$
12. m) $N\Delta \rightarrow NNK^+K^-$
13. n) $\Delta\Delta \rightarrow NNK^+K^-$
14. o) $\pi N \rightarrow NK^+K^-$
15. p) $\pi\Delta \rightarrow NK^+K^-$
16. q) $\pi\Lambda \rightarrow NK^-$
17. r) $\pi\Sigma \rightarrow NK^-$
18. s) $N\Lambda \rightarrow NNK^-$
19. t) $N\Sigma \rightarrow NNK^-$
20. u) $\pi\pi \rightarrow K^+K^-$

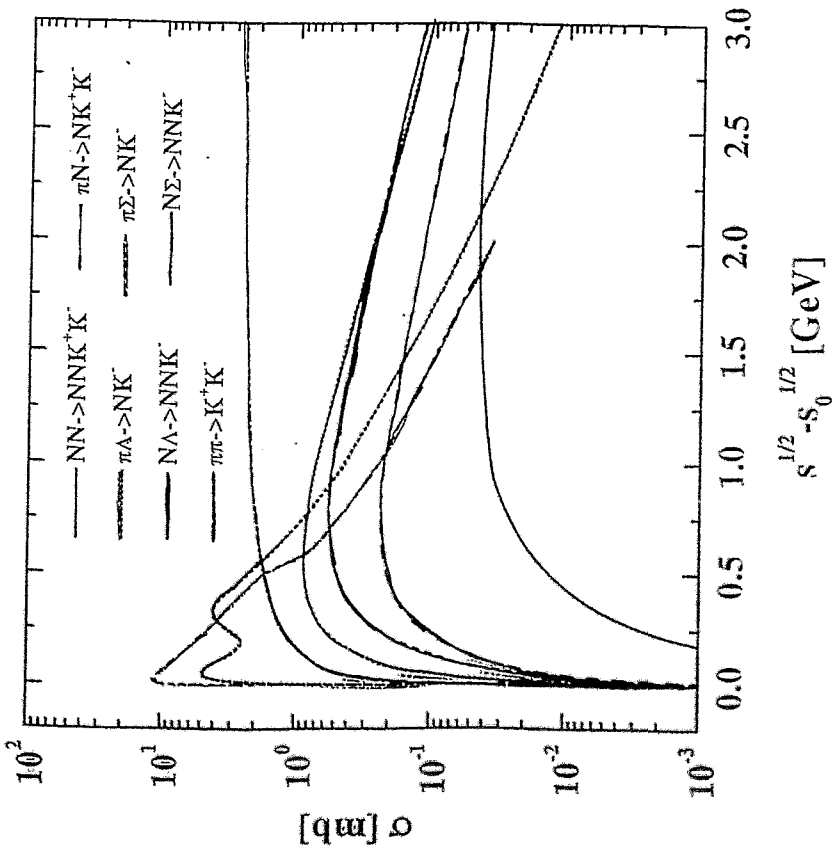


$$\sigma(N\Delta) \approx \frac{3}{4} \sigma(NN)$$

$$\sigma(\Delta\Delta) \approx \frac{1}{2} \sigma(NN)$$

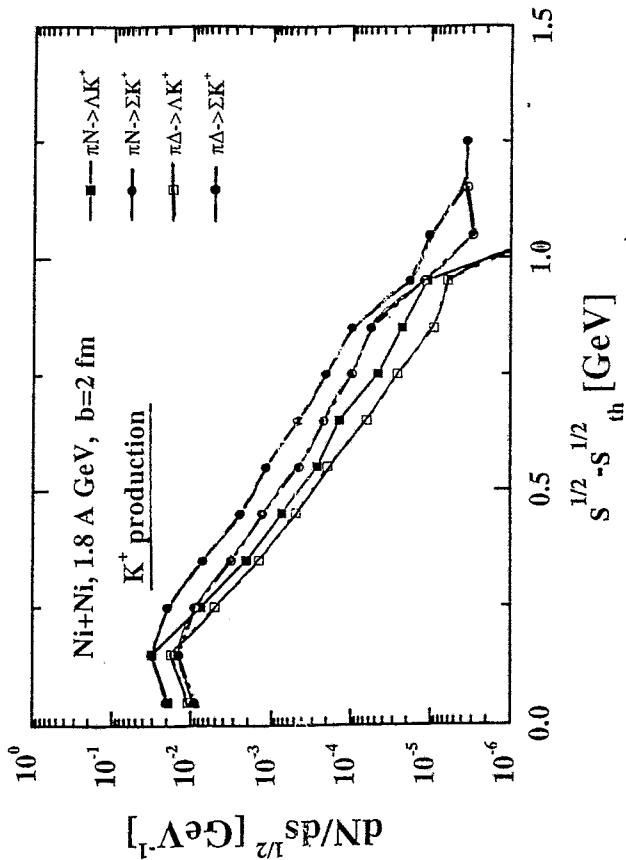
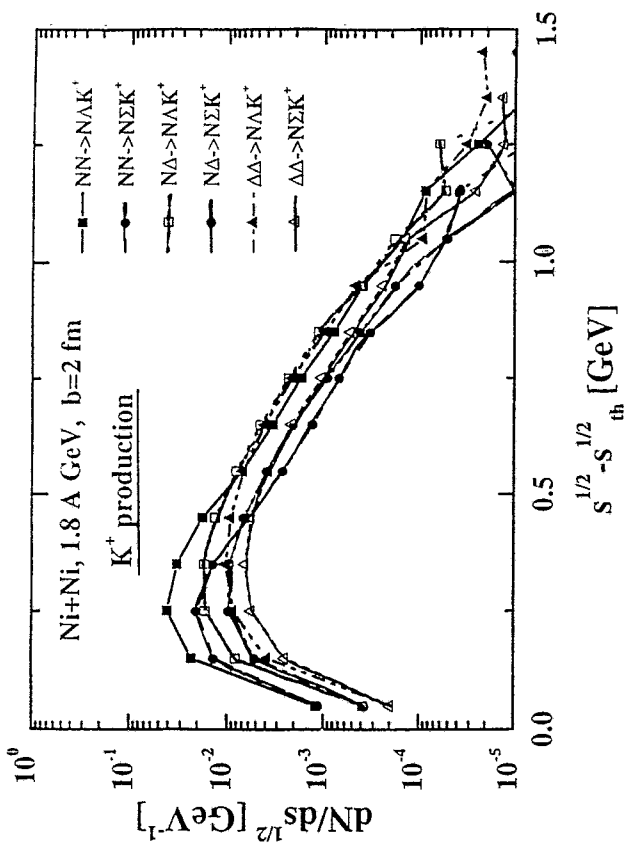
$$\sigma(\pi\Delta) = \sigma(\pi N)$$

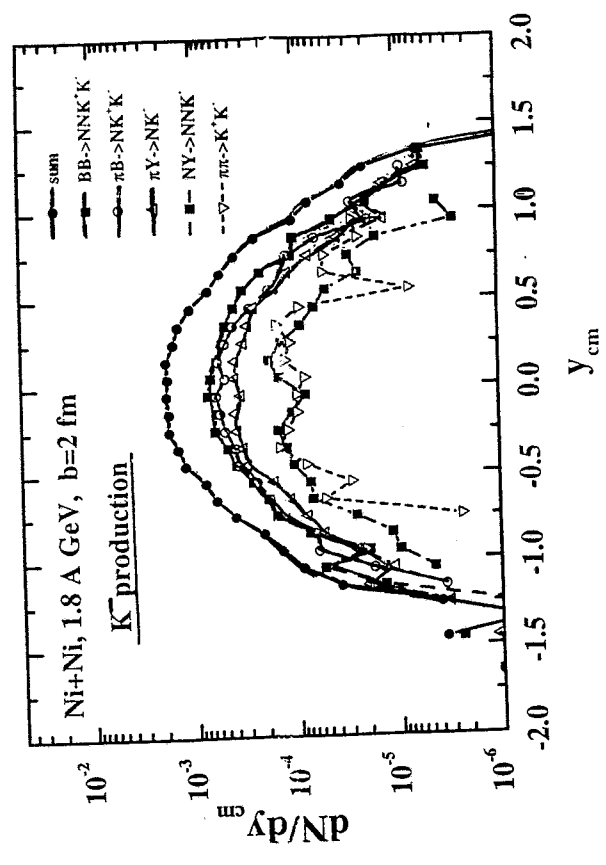
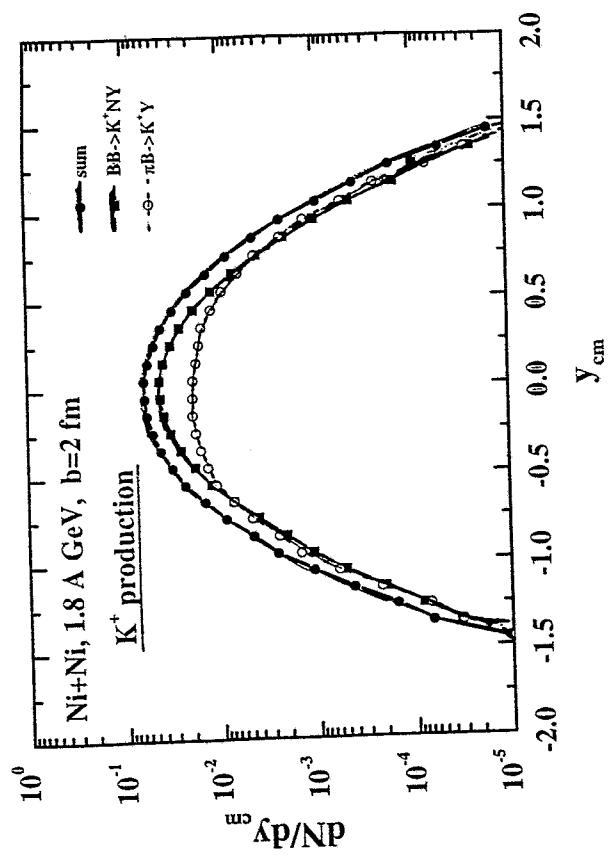
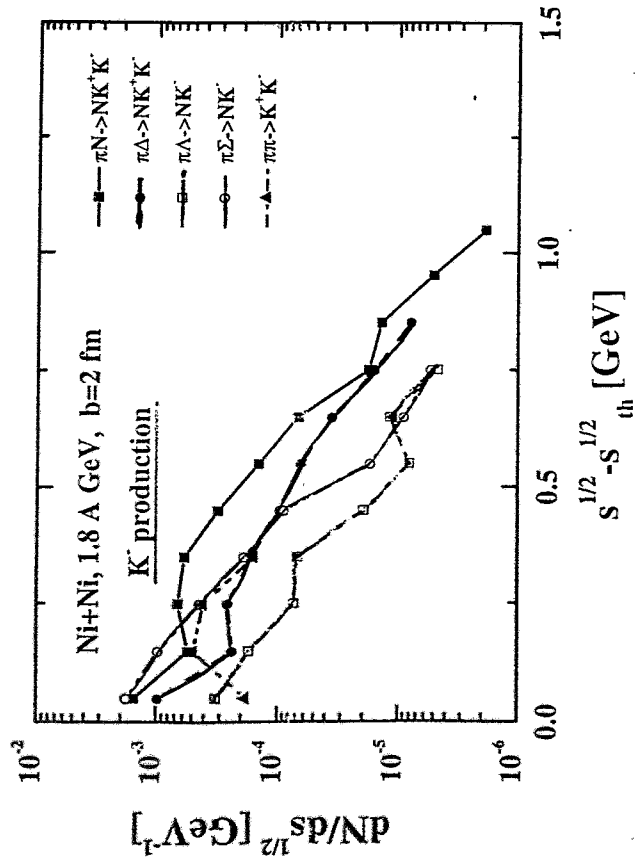
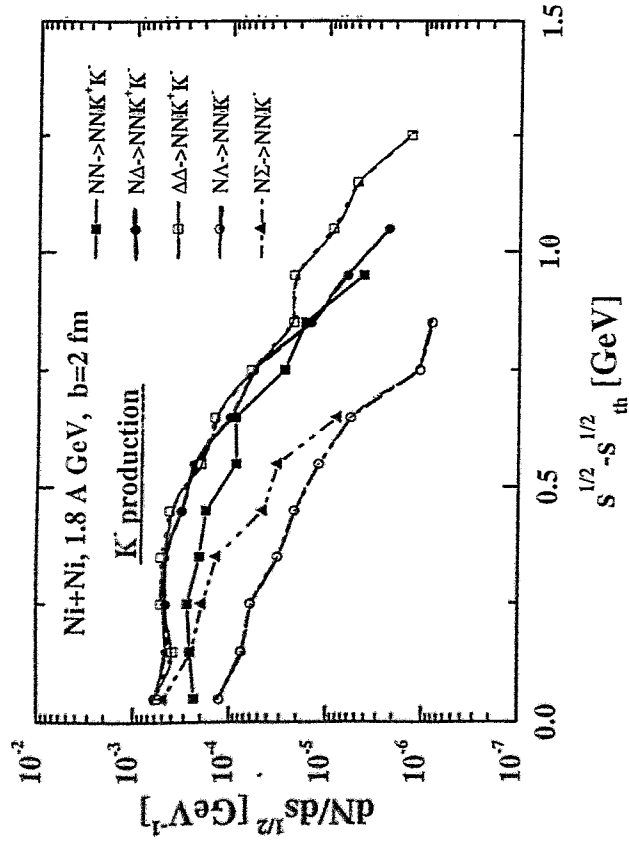
K⁻ production cross sections

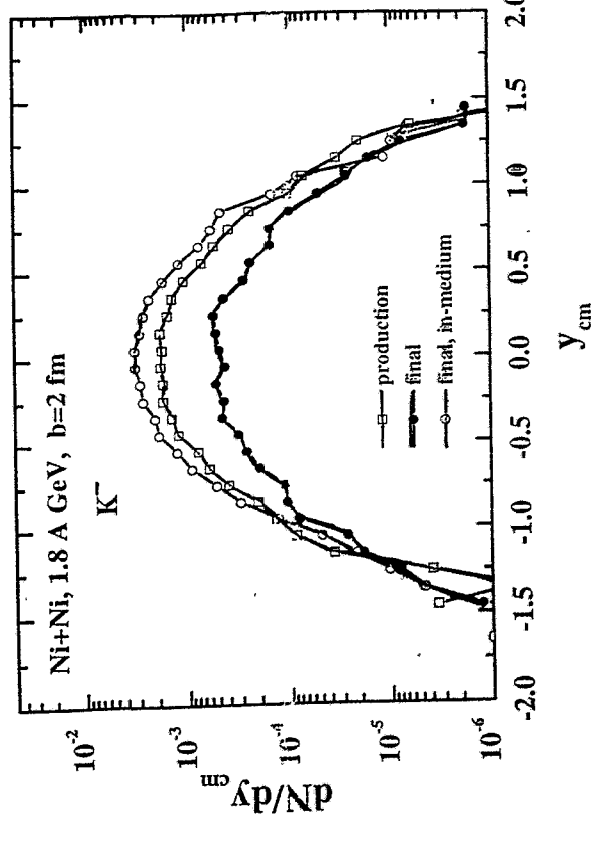
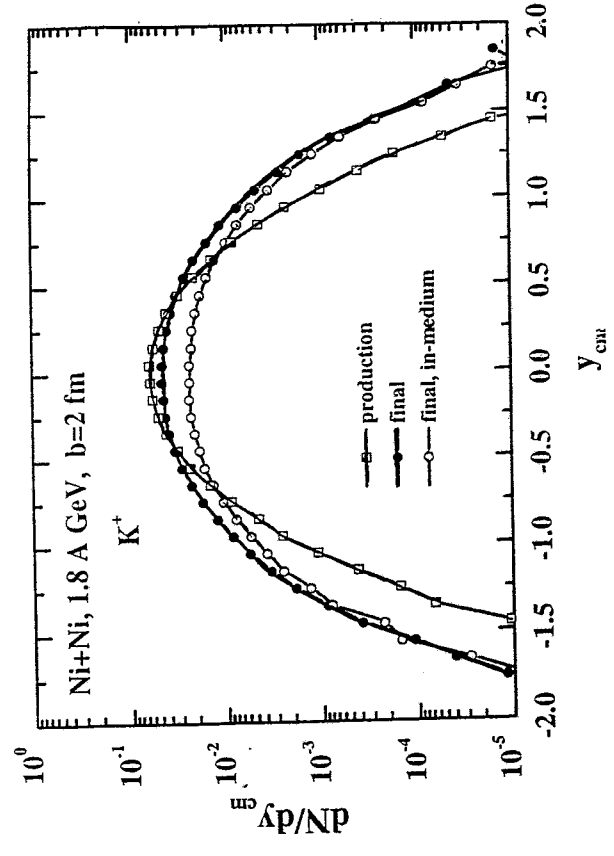
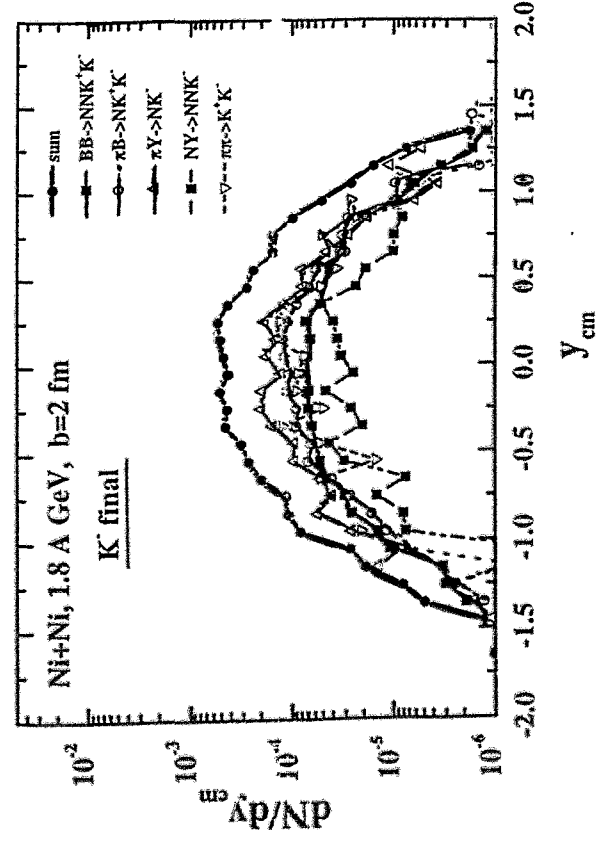
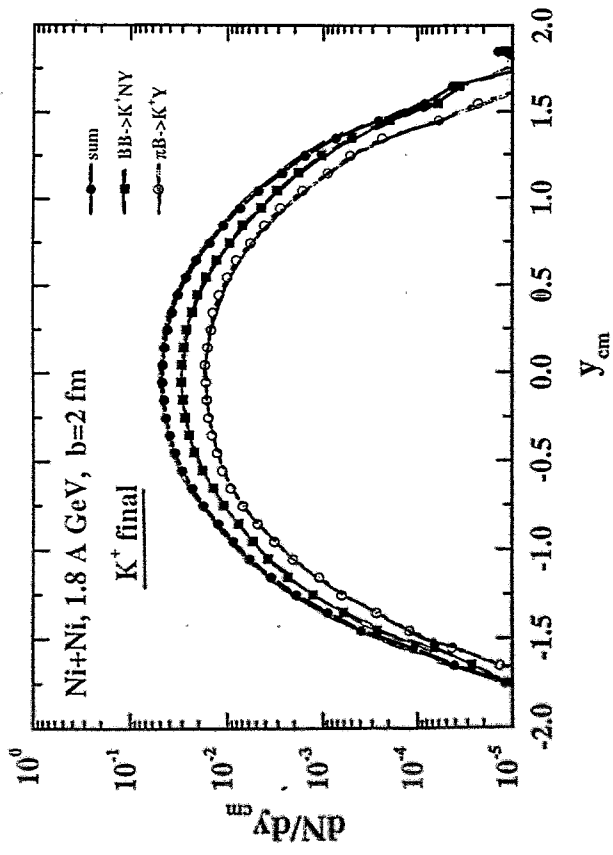


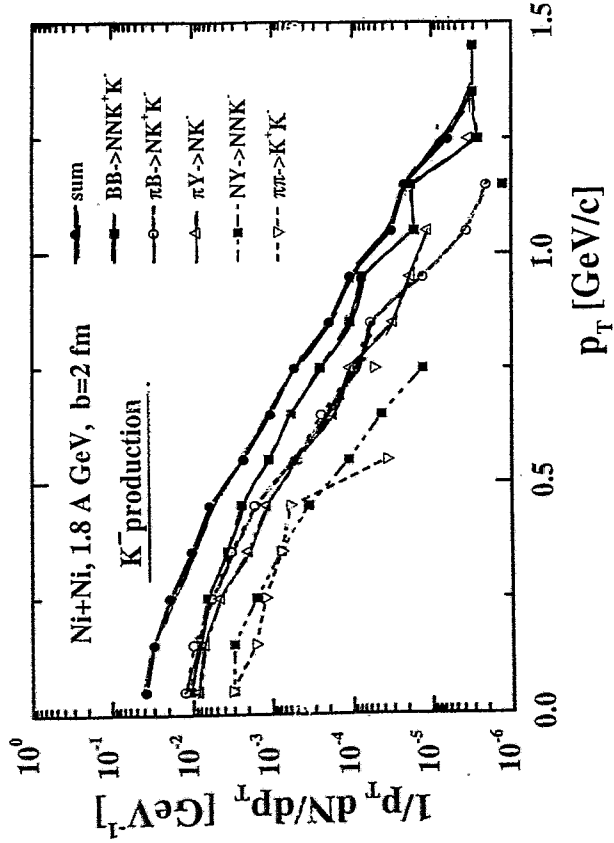
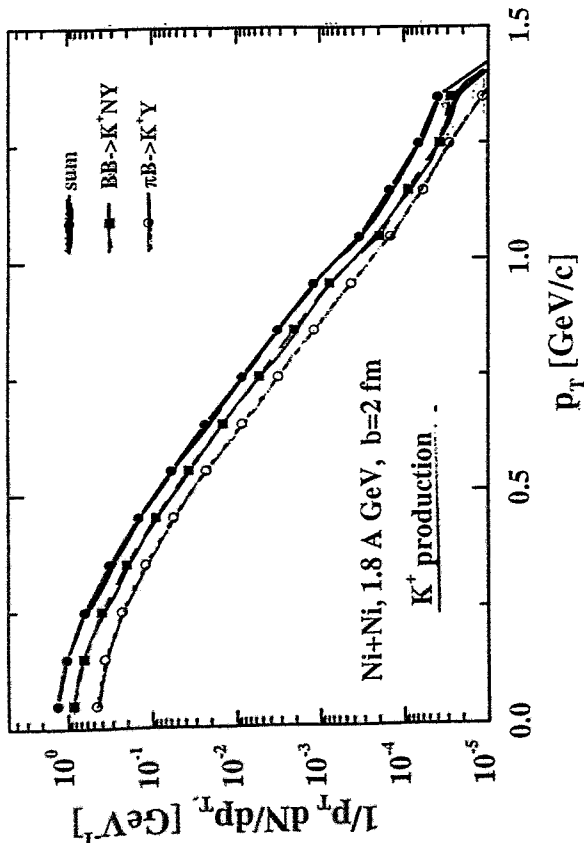
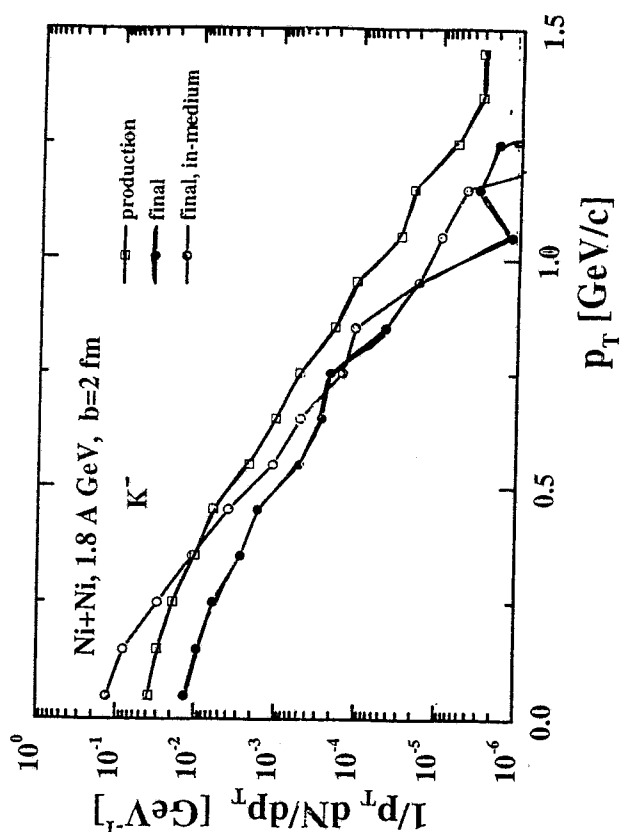
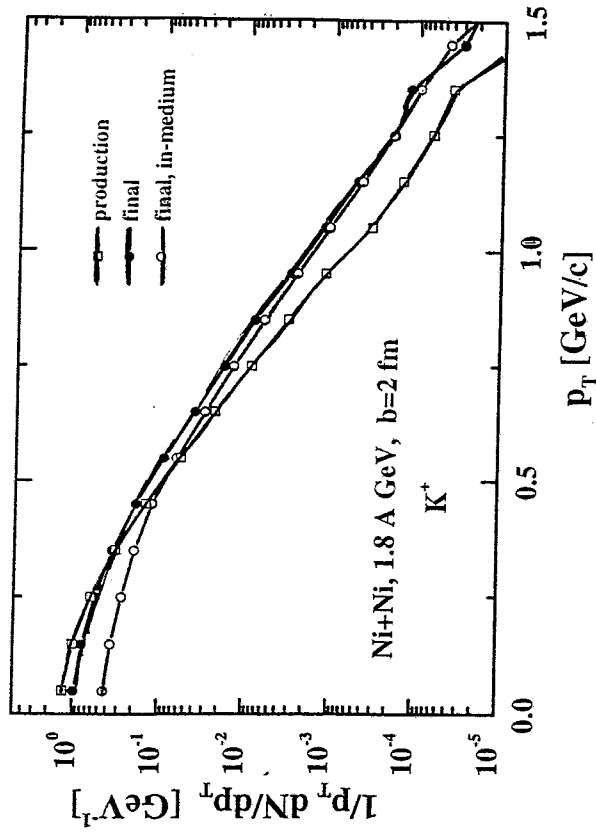
$$\sigma(N\Delta) = \sigma(\Delta\Delta) = \sigma(NN)$$

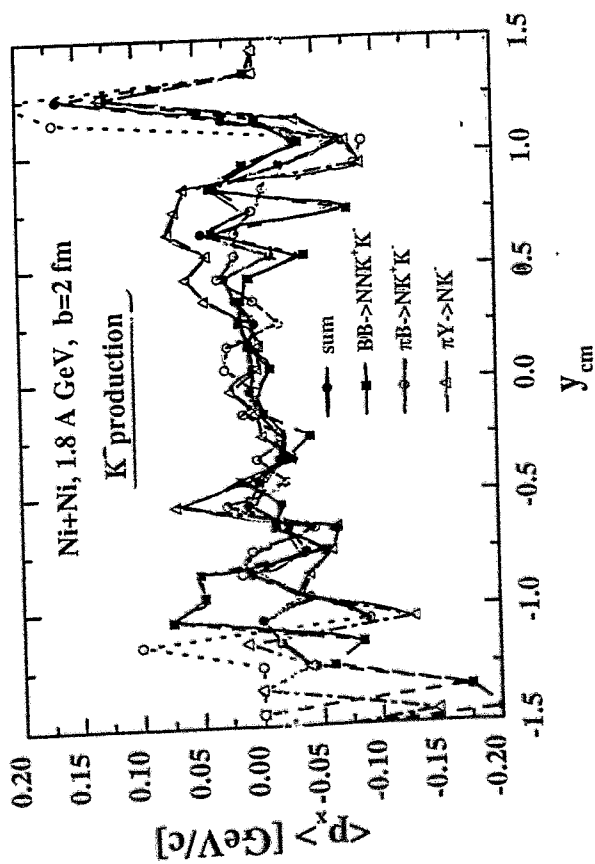
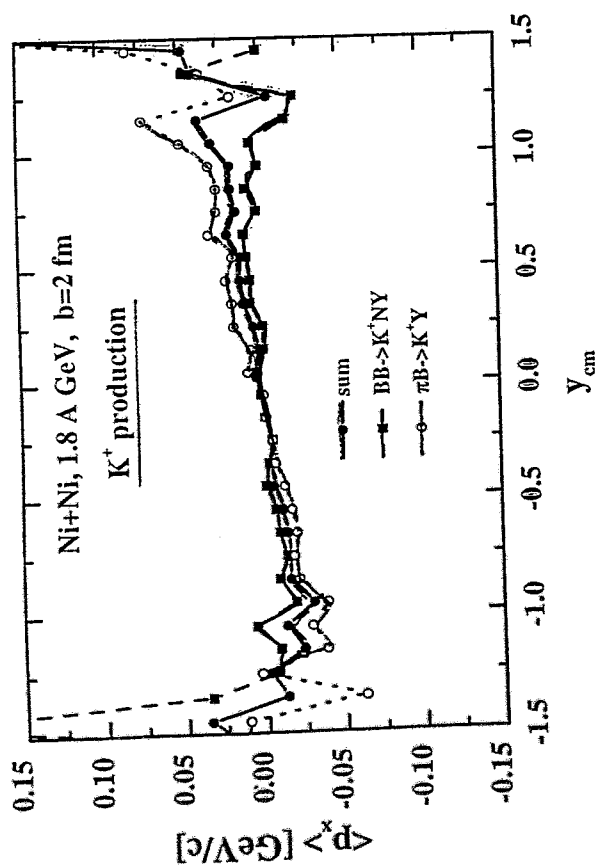
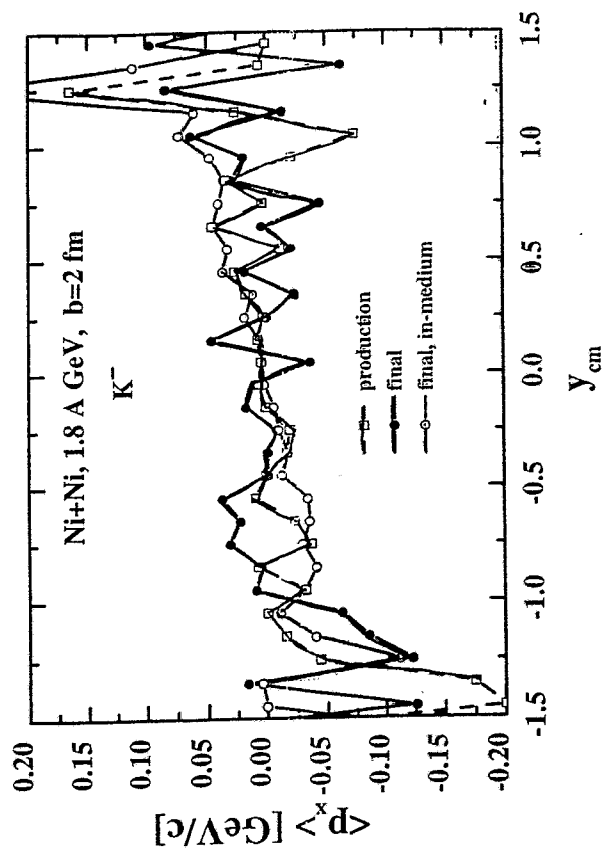
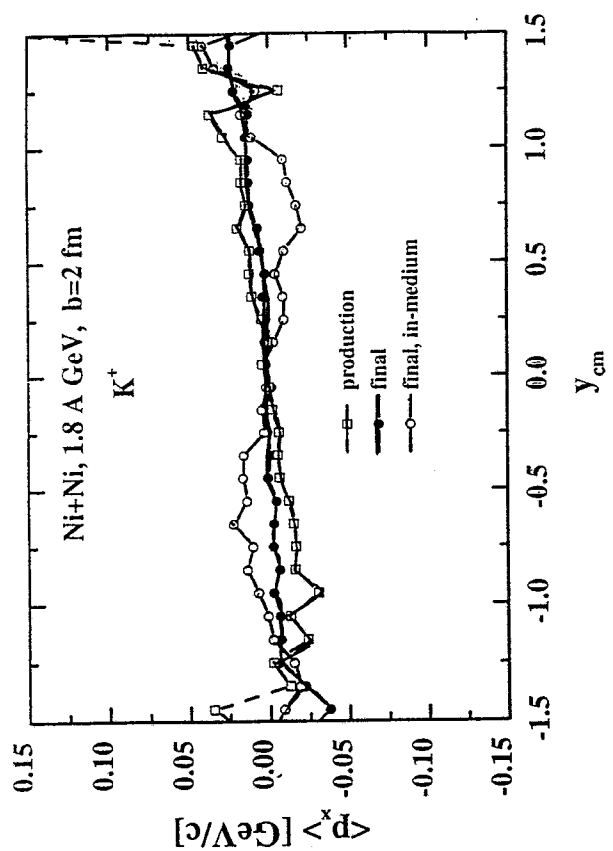
$$\sigma(\pi\Delta) = \sigma(\pi N)$$

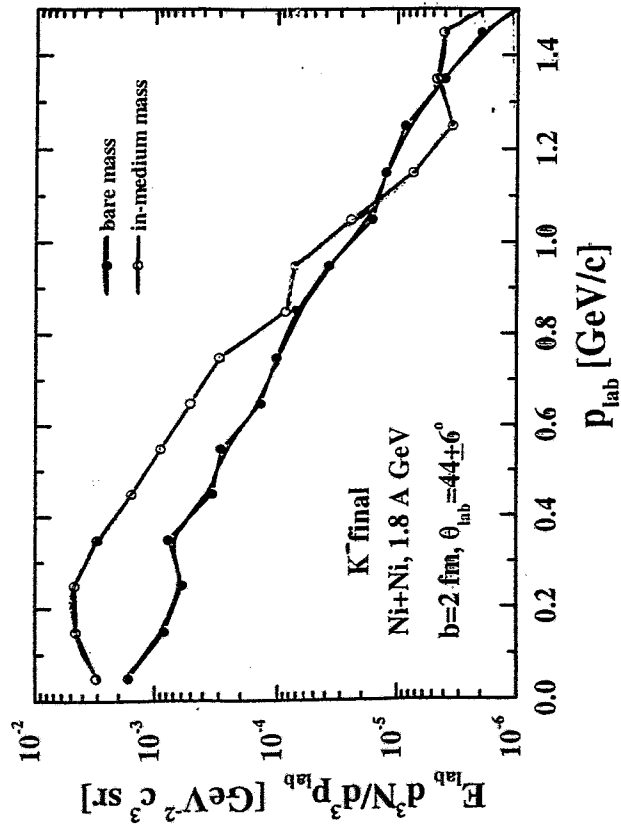
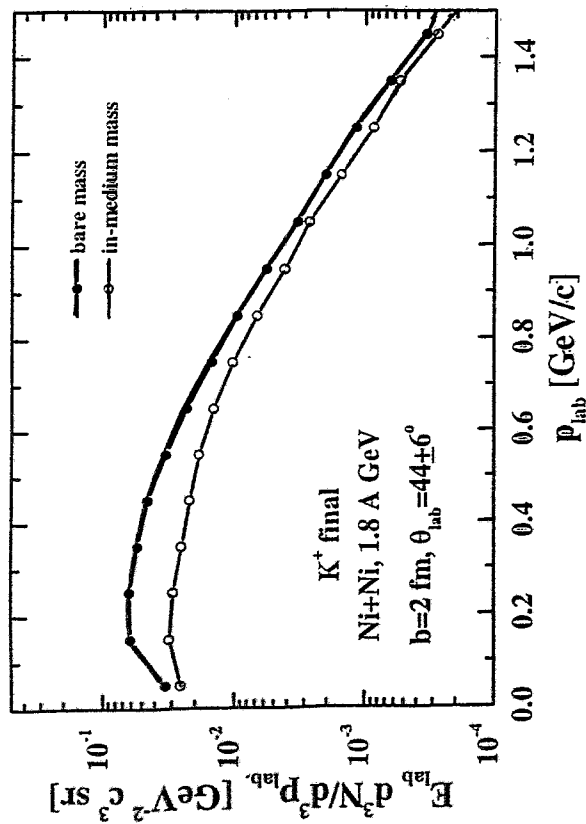












C.-H. Lee:

Bechmark test of the RVUU model

- G.E. Brown -

Benchmark Test of

RVLL Transport Model.

You have to say

" I just get into Transport Code.

So, I came here to learn

from Older and Wiser people

Chang-Hwan Lee
SUMY at Stony Brook

Then, they won't give you
hard time.

* based on

Guoqiang Li's code.

NPA 625 (1997) 37R.

RVLL model

$$\frac{1}{P_0^*} \left\{ (\partial_x^\mu - \partial_x^\nu \Sigma_V^\nu - \partial_x^\nu \Sigma_V^\mu) \partial_\nu^{\rho^*} \right\} P_\mu^* + m^* (\partial_x^\mu m^*) \partial_\mu^{\rho^*} \} f(\alpha, p^*) = I_C$$

$$I_C = \frac{1}{(2\pi)^3} \int d^3 p_2^* \int d^3 p_3^* \int d\Omega_2 \frac{d\Omega}{dR} \delta^3(p^* + p_2^* - p_3^* - p_4^*) \times \left\{ f(\alpha, p_3^*) f(\alpha, p_4^*) [1 - f(\alpha, p^*)] [1 - f(\alpha, p_2^*)] - f(\alpha, p^*) f(\alpha, p_2^*) [1 - f(\alpha, p_3^*)] [1 - f(\alpha, p_4^*)] \right\}$$

$$\frac{dx}{dt} = \frac{p^*}{E^*}$$

$$\frac{dP}{dt} = -\nabla_x (E^* + \left(\frac{g_w}{m_w}\right)^2 P_N)$$

O-w model.

$$\mathcal{L} = \mathcal{T} \left[i \not{\partial} - m - g_0 \sigma - g_w \gamma_\mu w^\mu \right] \psi + \frac{1}{2} (\partial^\mu \sigma)^2 - \frac{1}{2} m_0^2 \sigma^2 - \frac{1}{3} b \sigma^3 - \frac{1}{4} c \sigma^4 - \frac{1}{4} (\partial_\mu w^\nu - \partial_\nu w^\mu)^2 + \frac{1}{2} m_w^2 w_\mu^2$$

$$M^* = m - \Sigma_S, \quad \Sigma_S = g_0 \langle \sigma \rangle$$

$$P_\mu^* = p_\mu - \Sigma_{V\mu}, \quad \Sigma_{V\mu} = g_w \langle w_\mu \rangle$$

$$m_0^2 \langle \sigma \rangle + b \langle \sigma \rangle^2 + c \langle \sigma \rangle^3 \approx g_0 \rho_S$$

$$\langle w_\mu \rangle = (g_w / m_w)^2 \rho_M$$

$$\rho_S = \int \frac{d^3 p}{(2\pi)^3} f(\alpha, p^*) \frac{m^*}{E^*}$$

$$\rho_M = \int \frac{d^3 p}{(2\pi)^3} f(\alpha, p^*) \frac{p_\mu^*}{E^*}$$

$$E^* = (m^{*2} + p^{*2})^{1/2}$$



parameter we used

$$C_\sigma = \left(\frac{g_\sigma}{m_\sigma}\right) m \approx 13.95$$

$$C_\omega = \left(\frac{g_\omega}{m_\omega}\right) m \approx 8.498$$

$$B = b/g_\rho^3 m = 0.0199$$

$$C = c/g_\rho^4 = -0.00296$$

$$e/A (\rho = \rho_0) = -15.96 \text{ MeV}$$

$$K \quad K|_{\rho_0} = 200 \text{ MeV}$$

$$\frac{g_{\rho^2}}{m|_{\rho_0}} = 0.88$$

$$m_\sigma = 550 \text{ MeV}$$

$$m_\omega = 783 \text{ MeV}$$

KN interaction

(density dependent Kaon Mass)

$$\begin{aligned} \mathcal{L}_K = & \partial_\mu \bar{K} \partial^\mu K - (m_K^2 - g_{\sigma K} m_K \sigma) \bar{K} K \\ & + i g_{\omega K} \omega_0 \bar{K} \vec{\sigma} \cdot \vec{\sigma} K \end{aligned}$$

$$\omega_K = [m_K^2 + k^2 - g_{\sigma K} m_K \sigma + (g_{\omega K} \omega_0)^2]^{1/2} + g_{\omega K} \omega_0$$

$$\omega_{\bar{K}} = [m_{\bar{K}}^2 + k^2 - g_{\sigma K} m_{\bar{K}} \sigma + (g_{\omega K} \omega_0)^2]^{1/2} - g_{\omega K} \omega_0$$

$$\sigma = \langle \sigma \rangle$$

$$\omega_0 = \langle \omega \rangle$$

$$g_{\omega K} / g_{\omega N} = 1/3$$

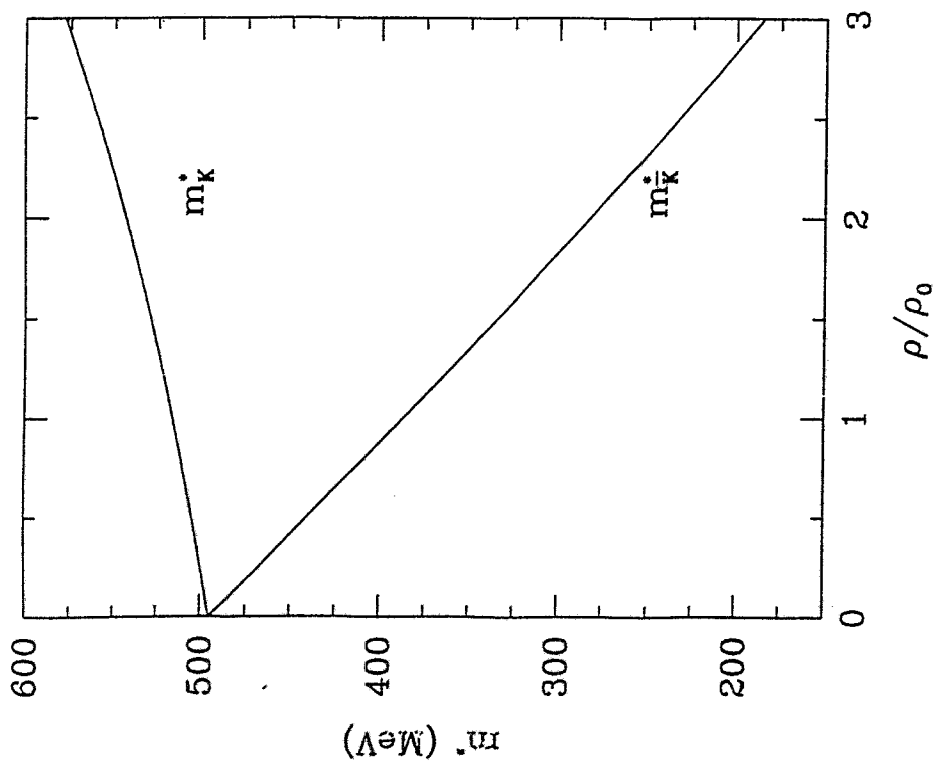
Processes in our code

K^+ production

20~30%

- a) $NN \rightarrow N\Lambda K$, $N\Lambda\pi K$, $N\Lambda\pi\pi K$
- b) $NN \rightarrow N\Sigma K$, $N\Sigma\pi K$, $N\Sigma\pi\pi K$
- c) $ND \rightarrow N\Lambda K$, $N\Lambda\pi K$, $N\Lambda\pi\pi K$
- d) $ND \rightarrow N\Sigma K$, $N\Sigma\pi K$, $N\Sigma\pi\pi K$
- e) $\Delta\Delta \rightarrow N\Lambda K$, $N\Lambda\pi K$, $N\Lambda\pi\pi K$
- f) $\Delta\Delta \rightarrow N\Sigma K$, $N\Sigma\pi K$, $N\Sigma\pi\pi K$
- g) $\pi N \rightarrow \Lambda K$, $\Lambda\pi K$
- h) $\pi N \rightarrow \Sigma K$, $\Sigma\pi K$
- i) $\pi\Delta \rightarrow \Lambda K$, $\Lambda\pi K$
- k) $\pi\Delta \rightarrow \Sigma K$, $\Sigma\pi K$

20~30% increase
in K^+ -production



BB Cross Sections

[NPA 625 (1997) 372]

K^- production

- l) $NN \rightarrow NNK^+K^-$, $NN\pi KK$, $NN\pi\pi KK$
- m) $N\Delta \rightarrow N\pi KK$, $NN\pi KK$ "
- n) $\Delta\Delta \rightarrow NNKK$, $NN\pi KK$ "
- o) $\pi N \rightarrow NKK$, $N\pi KK$
- p) $\pi\Delta \rightarrow NKK$, $N\pi KK$

- q) $\pi\Lambda \rightarrow N\bar{K}$
- $\pi\Sigma \rightarrow N\bar{K}$

K^- annihilation

- r) $N\bar{K} \rightarrow \pi\Lambda$
- $\pi\Sigma$

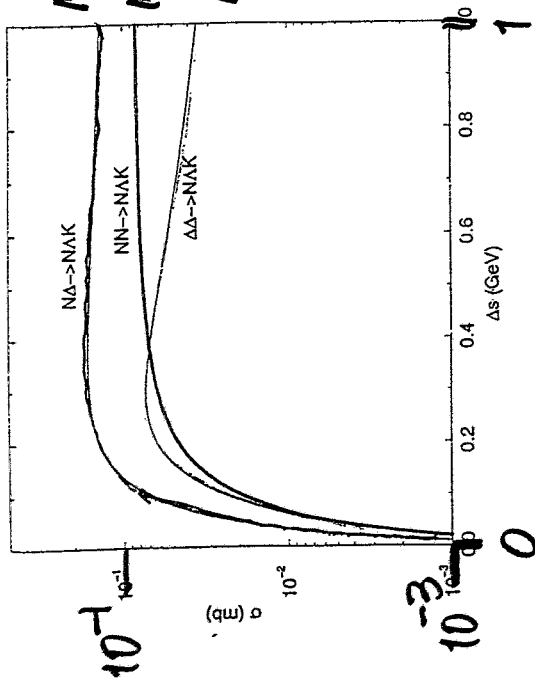
Quite Important.

$$\sigma_{BB \rightarrow N\pi K} = \frac{a (\sqrt{s} - \sqrt{s_0})^2}{b + (\sqrt{s} - \sqrt{s_0})^2} \text{ mb}$$

	a	b	x
$NN \rightarrow N\Lambda K$	0.0865	0.0345	2.0
$N\Sigma K$	0.1499	0.167	2.4
$N\Delta \rightarrow N\Lambda K$	0.1397	0.0152	2.3
$N\Sigma K$	0.3221	0.107	2.3
$\Delta\Delta \rightarrow N\Lambda K$	0.0361	0.0137	2.9
$N\Sigma K$	0.0965	0.014	2.3

* done by Guoqiang Li

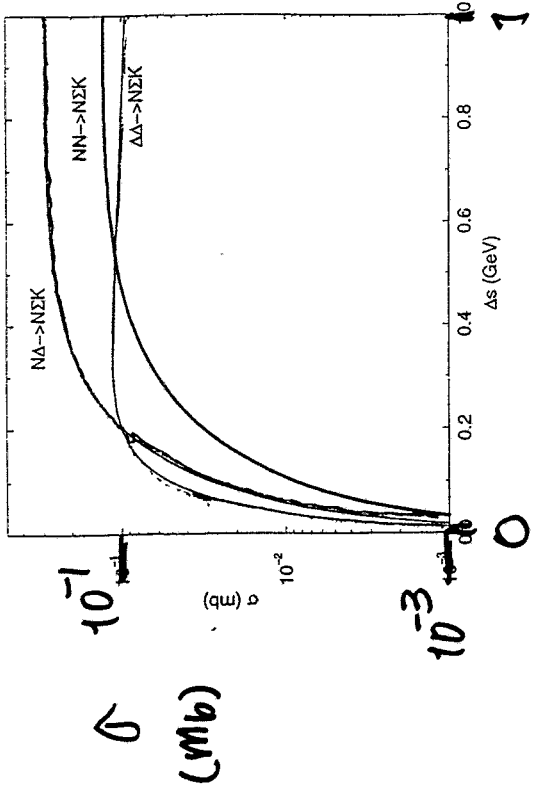
I. $BB \rightarrow NAK$ PRODUCTION CROSS SECTIONS



$NA \rightarrow NAK$
 $NN \rightarrow NAK$
 $AA \rightarrow NAK$

$\sqrt{s} - \sqrt{s_0}$ (GeV)

II. $BB \rightarrow NEK$ PRODUCTION CROSS SECTIONS

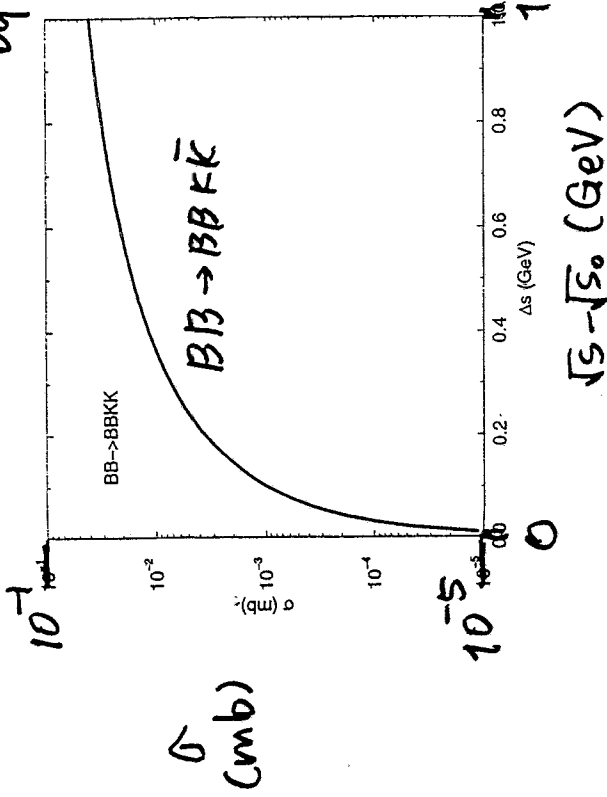


$NA \rightarrow NEK$
 $NN \rightarrow NEK$
 $AA \rightarrow NEK$

$\sqrt{s} - \sqrt{s_0}$ (GeV)

IV. $BB \rightarrow BBKK$ PRODUCTION CROSS SECTIONS

by Guoqiang Li.

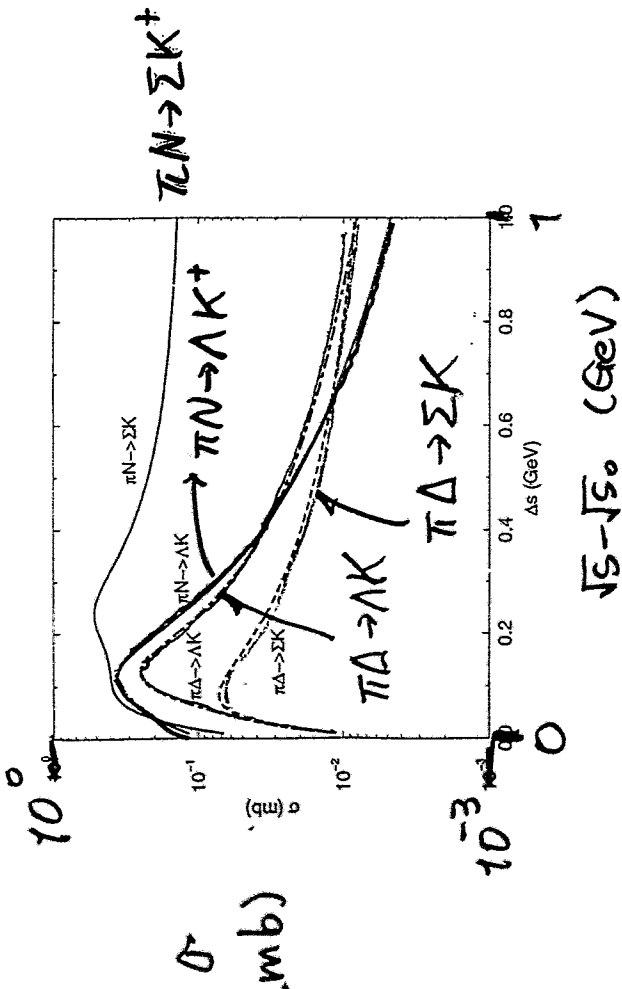


Used the name cross sections



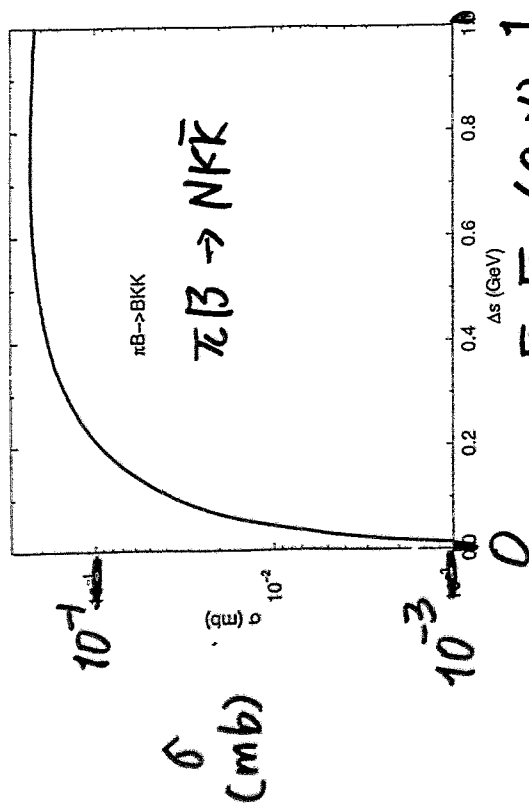
$$\sigma = \frac{5}{4} \cdot 0.19 \left(1 - \frac{s_0}{s}\right)^2 \left(\frac{s_0}{s}\right)^{0.31} \text{ mb}$$

III. $\pi B \rightarrow A, \Lambda K$ PRODUCTION CROSS SECTIONS



[Tsushima, Huang, Faessler.
 PLB 337 (1994) 245
 J. Phys. G 21 (1995) 33.]

V. $\pi B \rightarrow BKK$ PRODUCTION CROSS SECTIONS

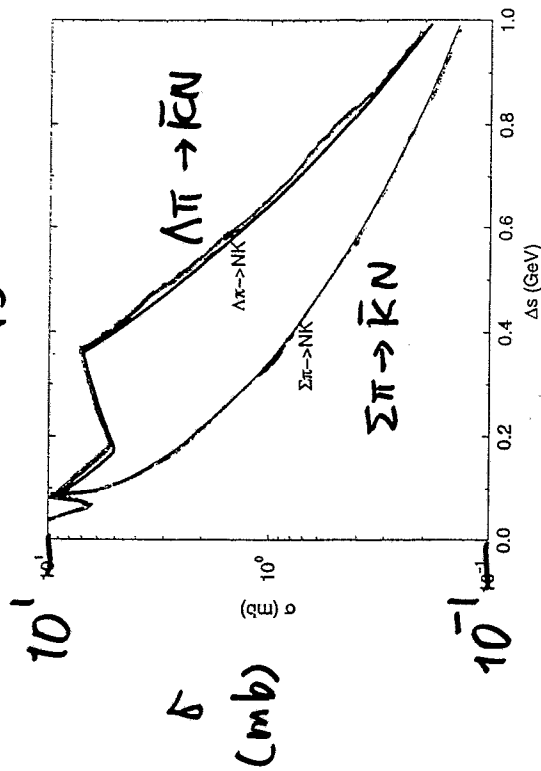
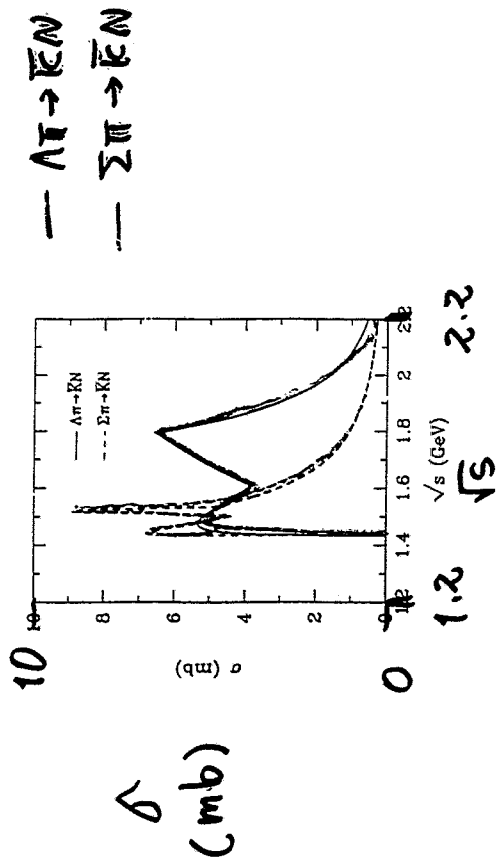


$\sqrt{s} - \sqrt{s_0} \text{ (GeV)} = 1.$

$\sigma = 3.363 \left(1 - \frac{s_0}{s}\right)^{1.86} \left(\frac{s_0}{s}\right)^2 \text{ mb}$

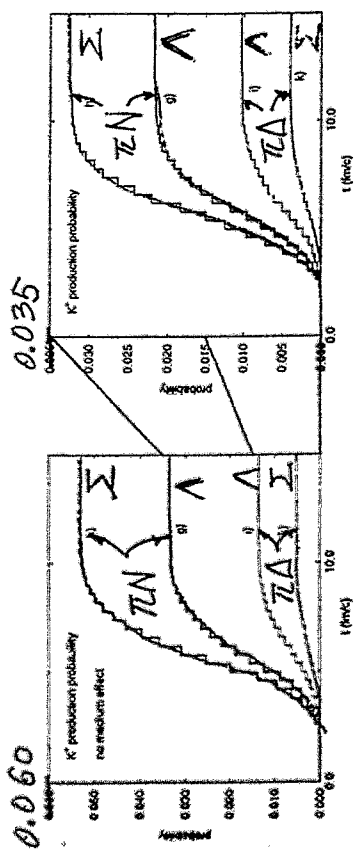
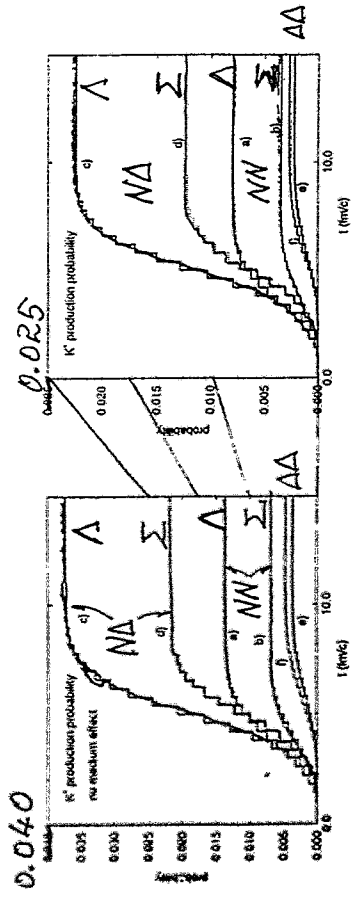
* The name for $\pi N, \pi \Delta$ by Guoqiang NPA 625 (87) 372.

VI. $\Lambda, \Sigma \pi \rightarrow N\bar{K}$ PRODUCTION CROSS SECTIONS



K⁺ production

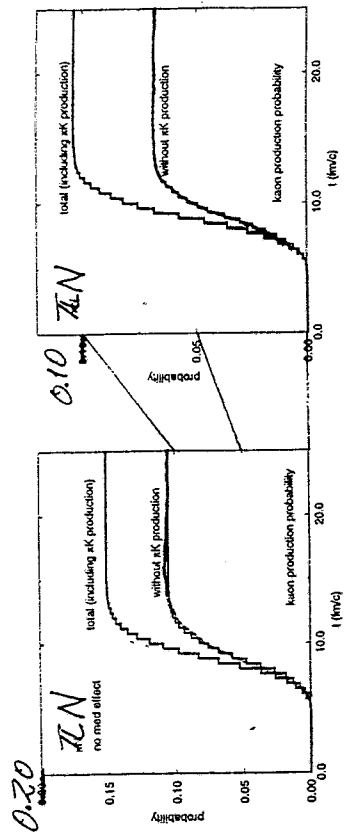
A. K⁺ production without/with KN optical potential



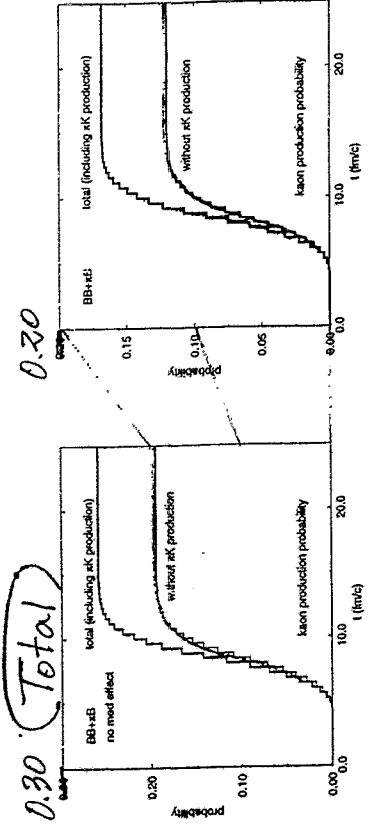
↑
No KN opt pot with KN opt-pot.
↑

* $\pi N \rightarrow HK^+$, $N\Delta \rightarrow NHK^+$ dominant.

M. K⁺ production probability with/without $\pi\beta \rightarrow Y\pi K^+$ channel.

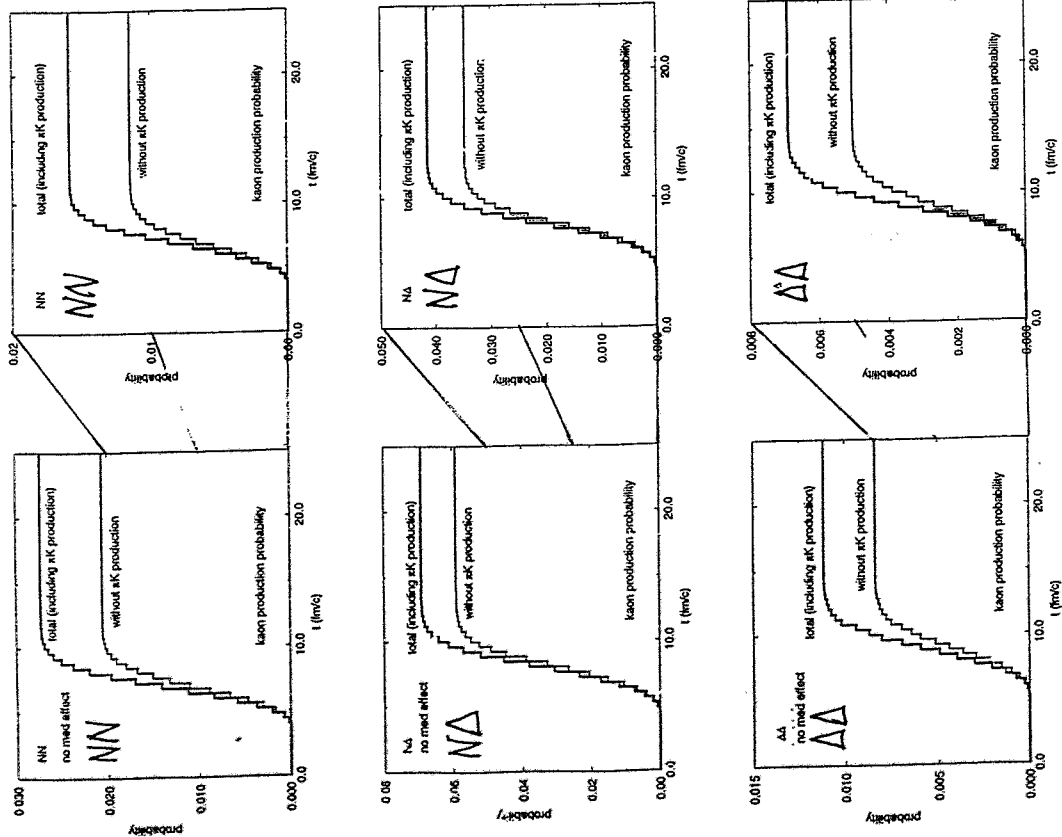


N. Total K⁺ prod. with/without $XX \rightarrow Y + \pi K^+$.



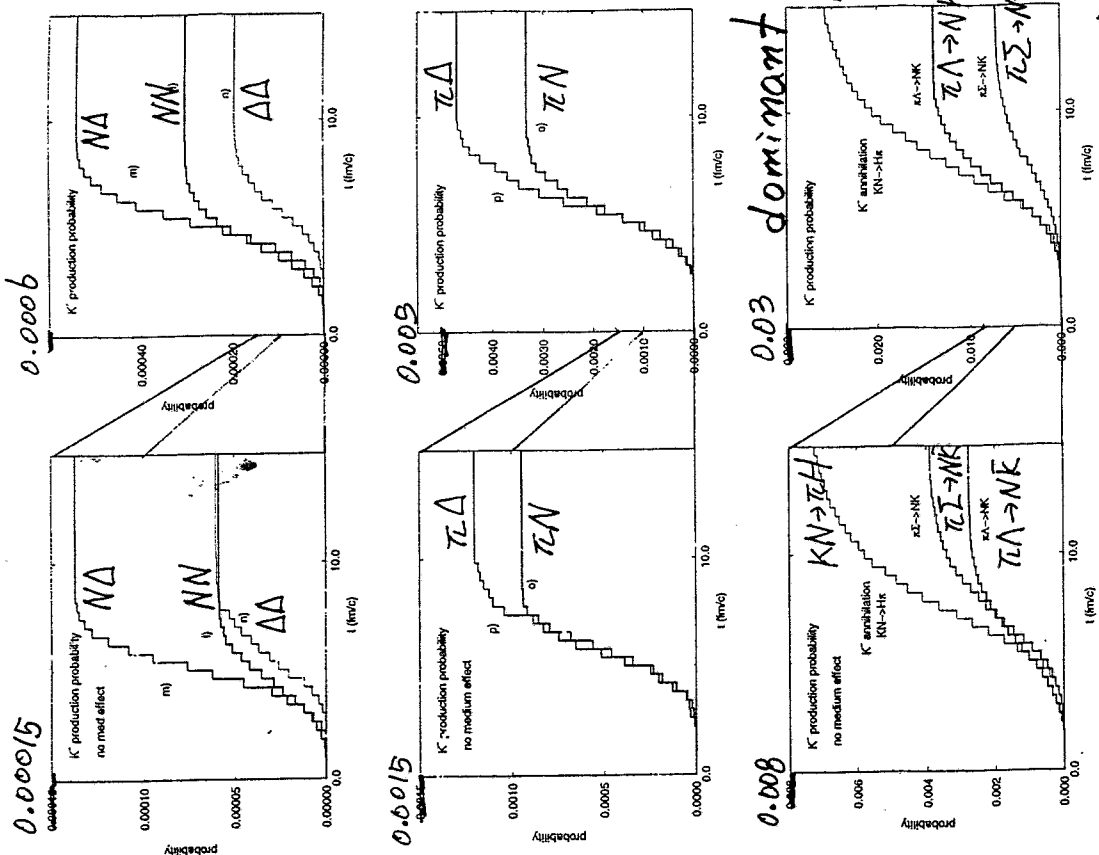
* upper curve : with $NN \rightarrow NH\pi K, NH\pi\pi K$
lower curve : without " "

L. K^+ production probability with/without $BB \rightarrow Y\pi K^+$ channel.

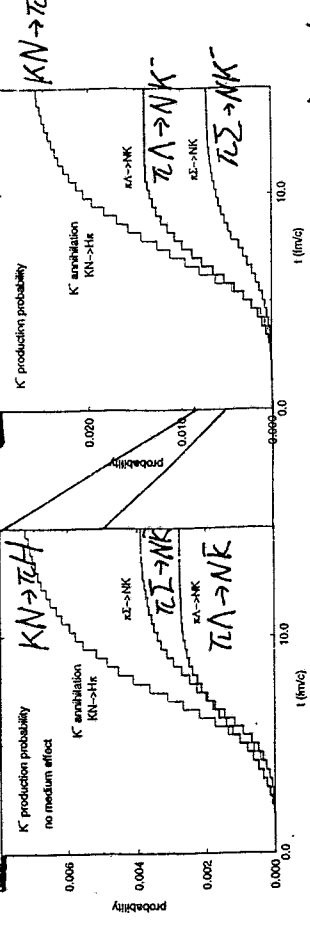


K^- production

B. K^- production and annihilation probability



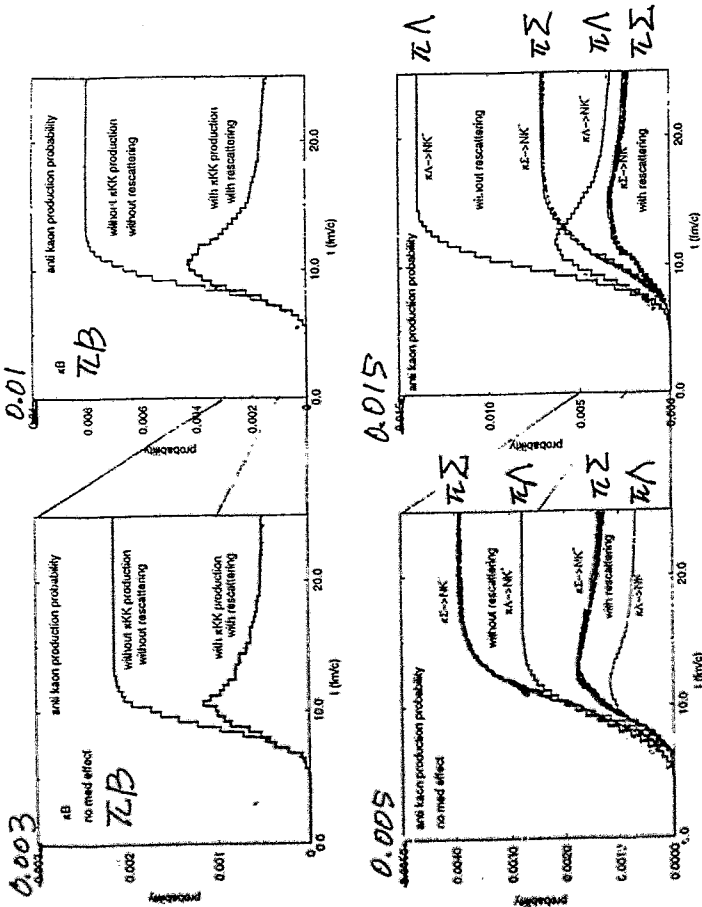
0.03 dominant!



Kaon Absorption is important.

Effect of Rescattering

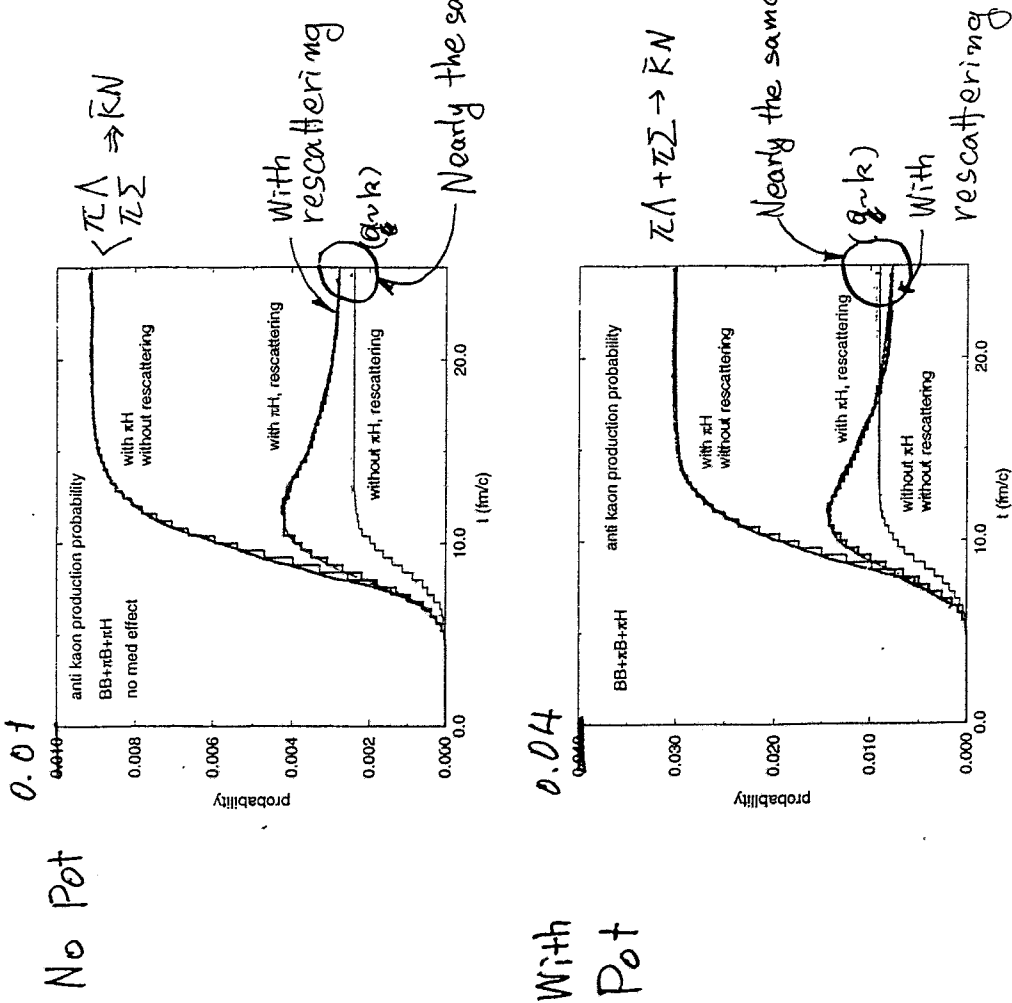
P. $\pi B \rightarrow X K K$ probability with/without rescattering



↑ No KN opt-pot with KN opt pot. ↑

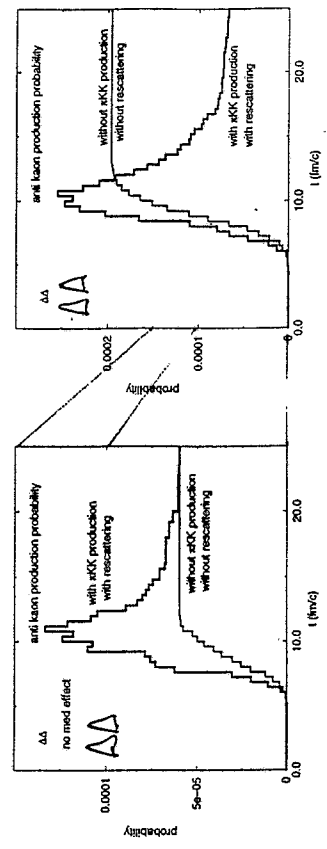
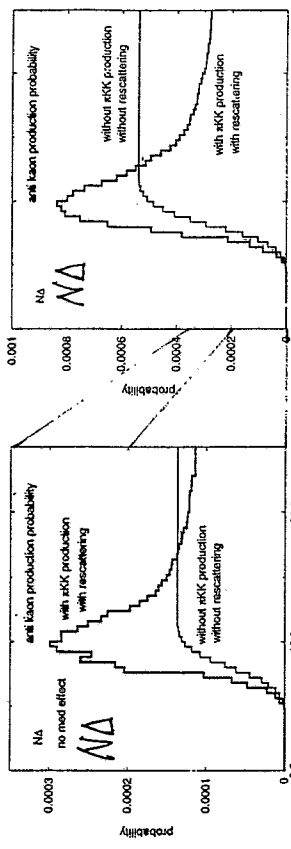
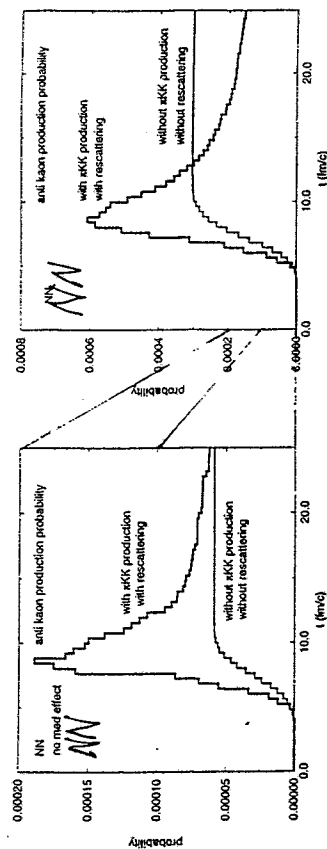
Total K^-

Q. Total and $\pi \Lambda, \Sigma \rightarrow K^- N$ channel K^- production probability.



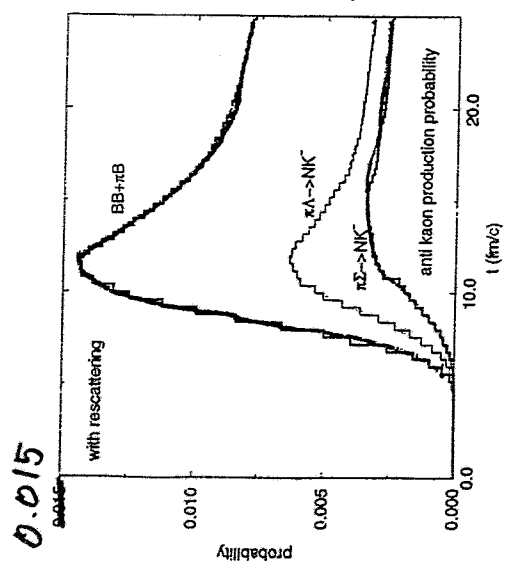
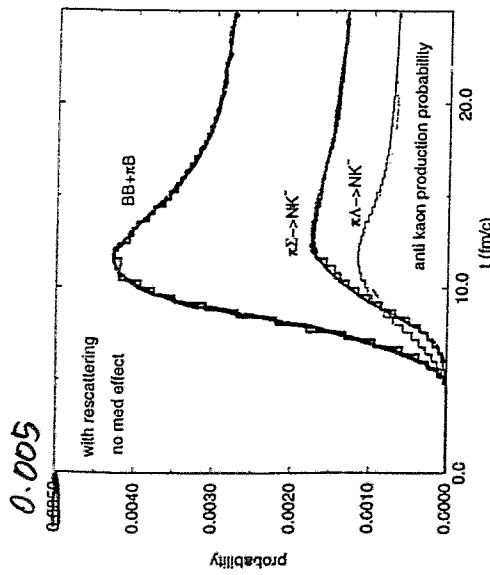
* Total & (a-k) gives the same # of K^- But Rapidity & P_T Spectrum will change

$O. BB \rightarrow XKK$ probability with/without rescattering



Total
 $\pi \Sigma \rightarrow N\bar{K}$
 $\pi \Lambda \rightarrow N\bar{K}$

Total
 $\pi \Lambda \rightarrow N\bar{K}$
 $\pi \Sigma \rightarrow N\bar{K}$

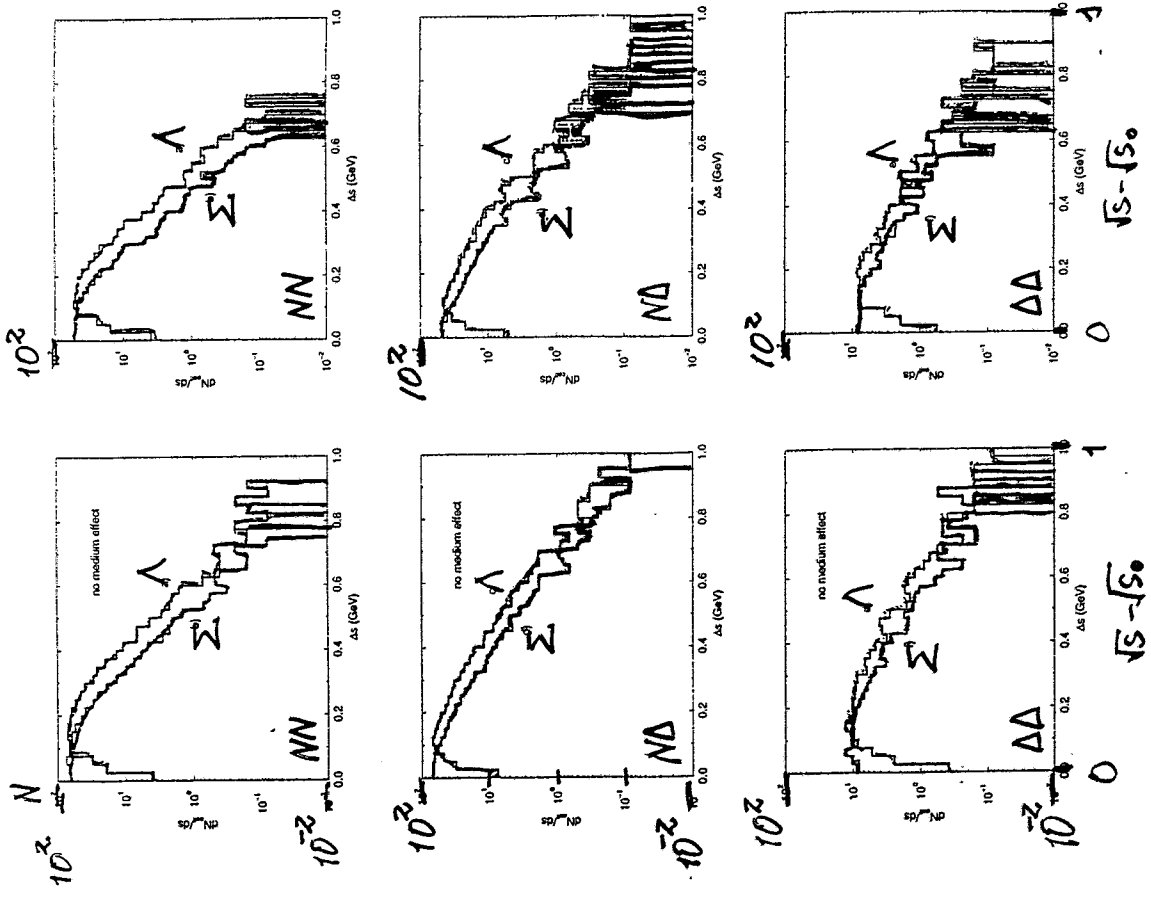


No Pot

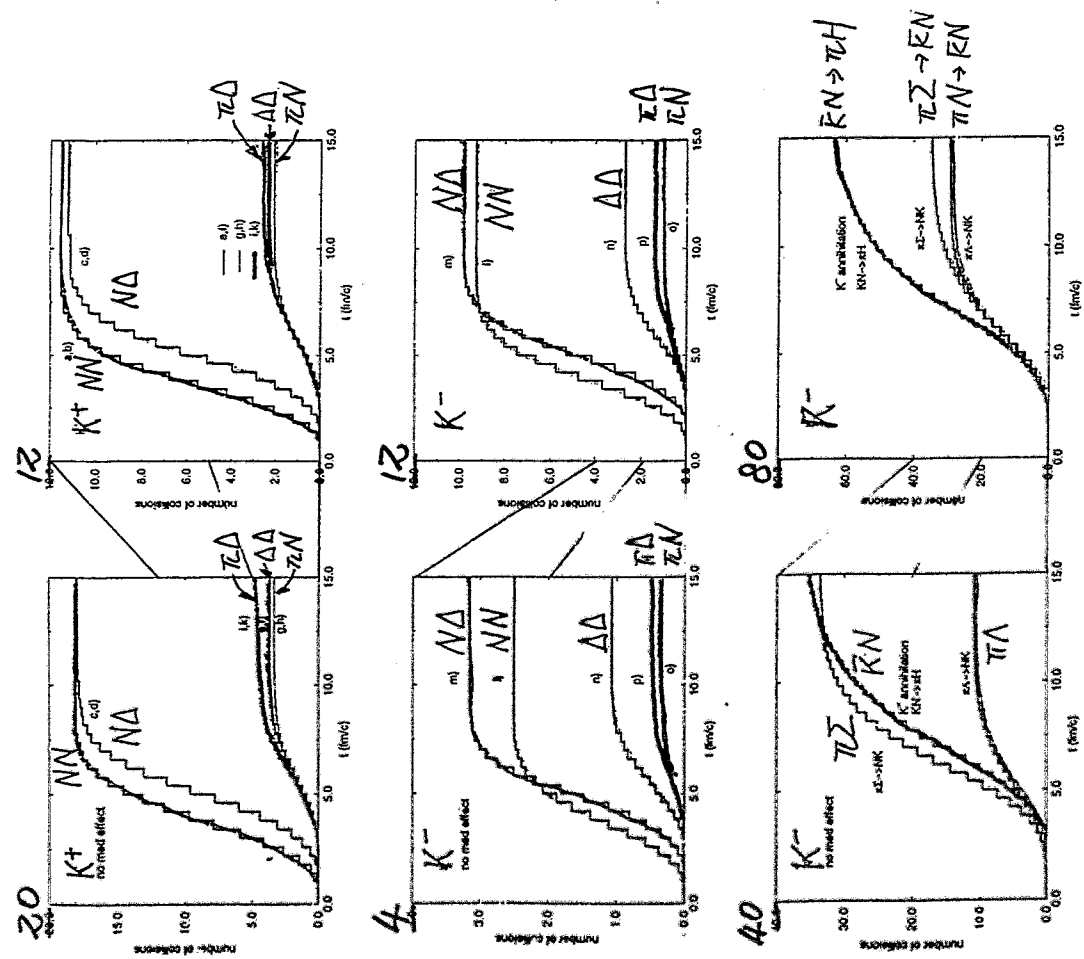
With Pot.

$dN/d\sqrt{s}$

D. $dN/d\sqrt{s}$: Number of collisions for K^+ production (a-f)

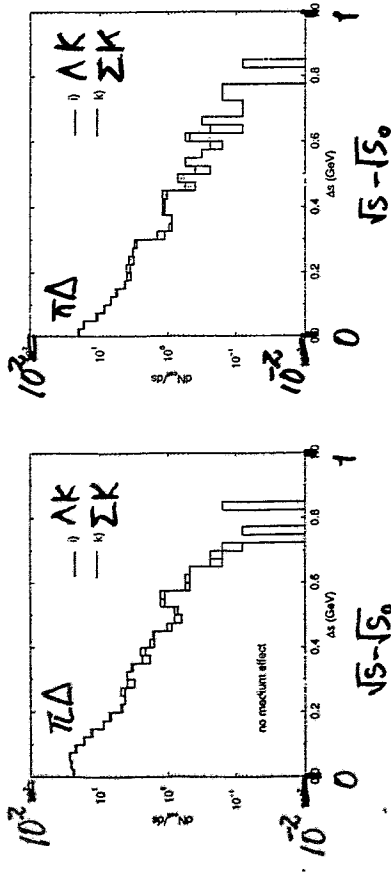
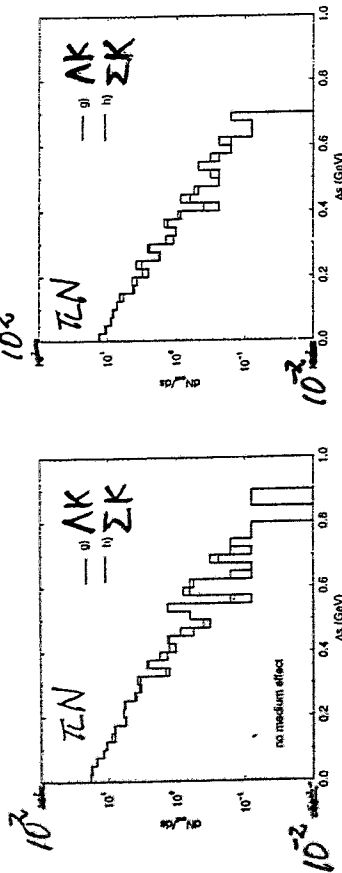


C. Number of collisions for K^\pm production



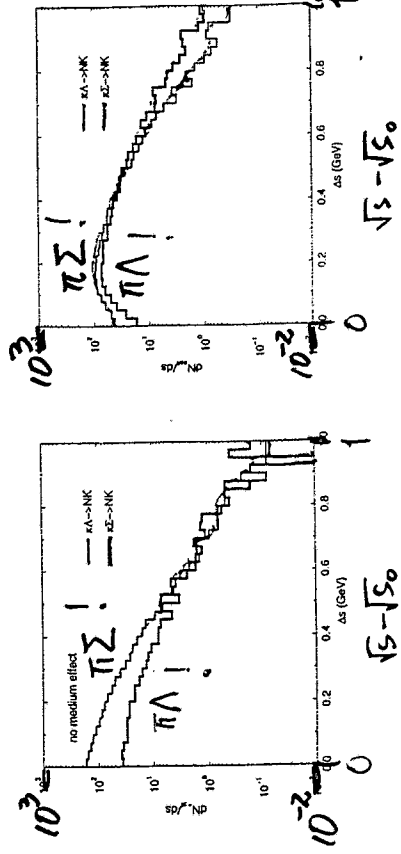
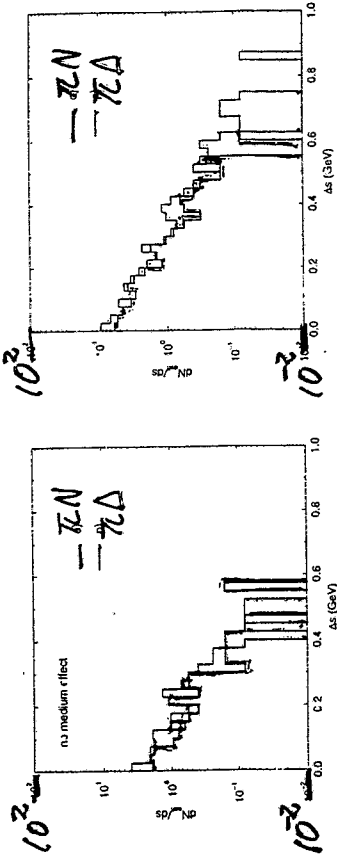
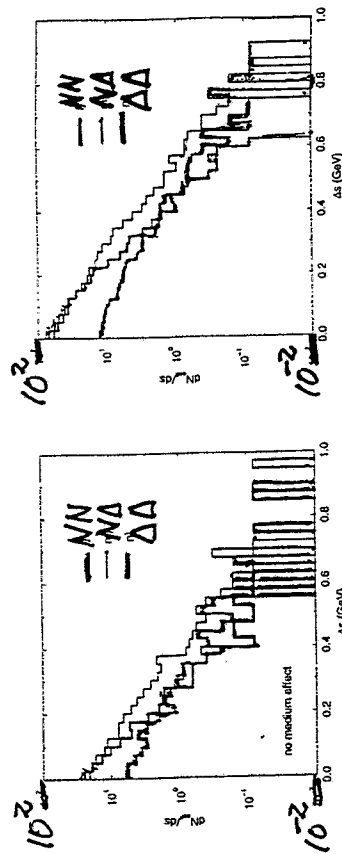
$\frac{dN}{d\Omega ds}$

E. $\frac{dN}{d\Omega ds}$: Number of collisions for K^+ production (g-k)



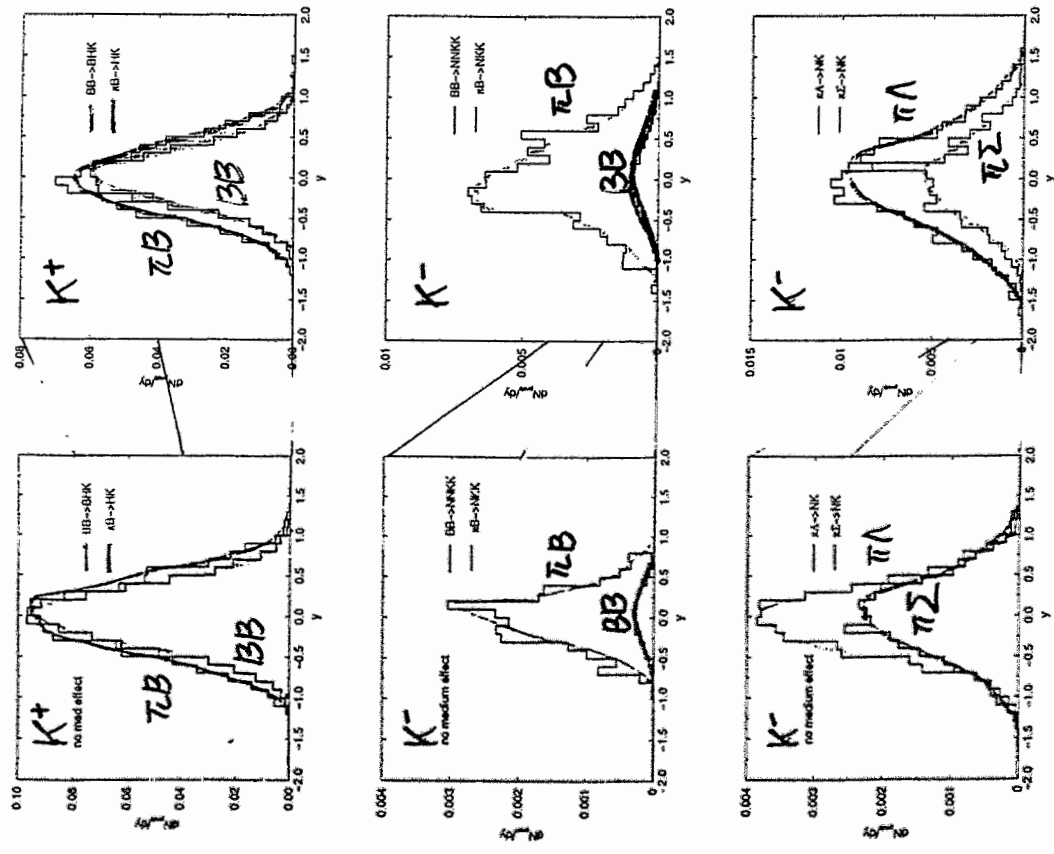
K^- prod

F. Number of collisions for K^- production and annihilation



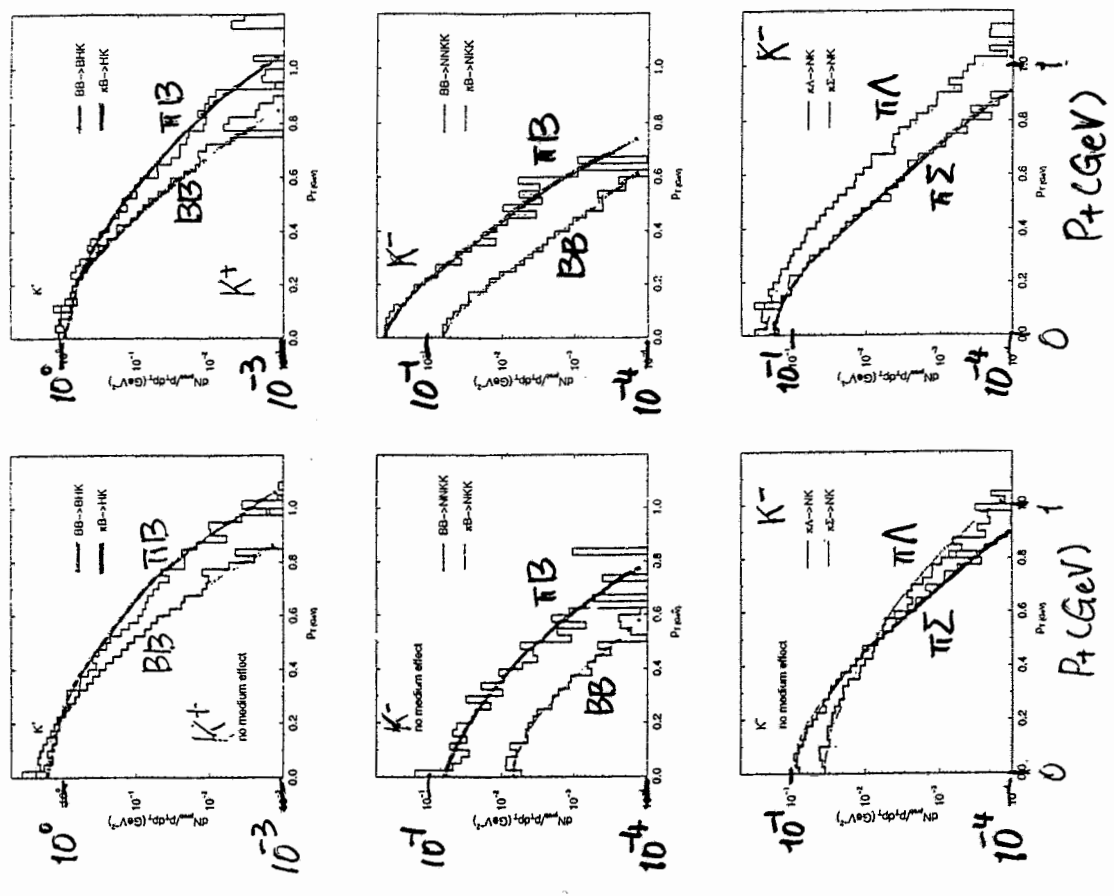
Rapidity dist. dN/dy

G. dN_{prod}/dy : Rapidity distribution (K^\pm)



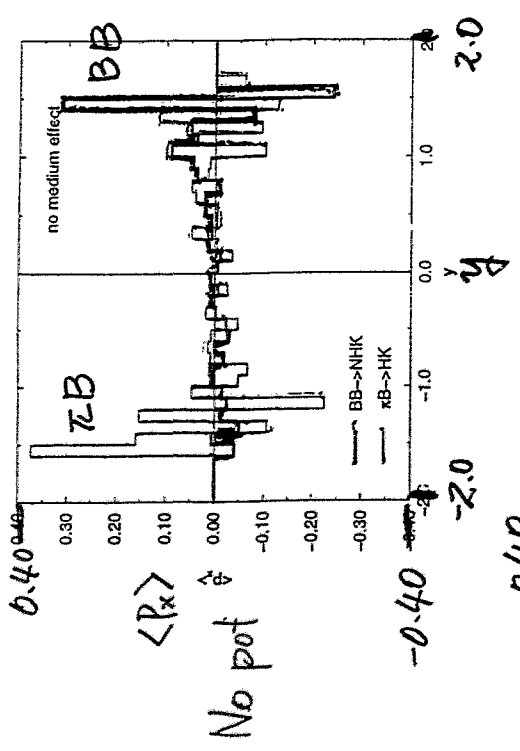
dN/dp_T

H. $dN_{prod}/p_T dp_T$: Transverse momentum distribution (K^\pm)

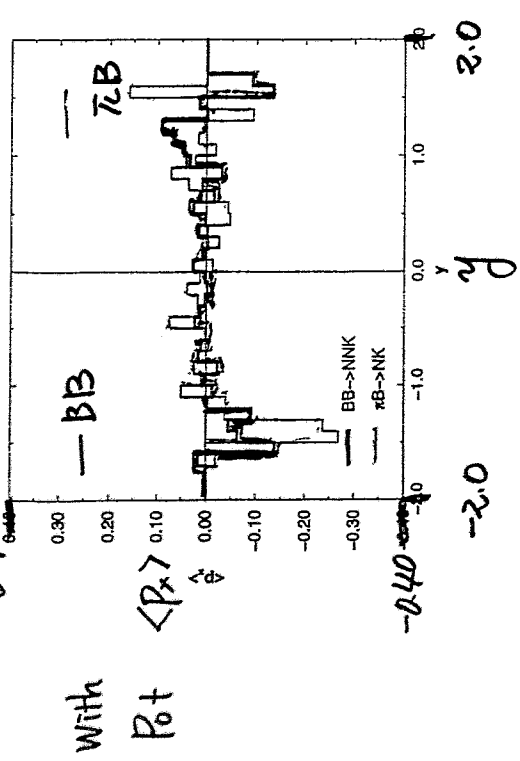


Kaon flow

I. Kaon flow

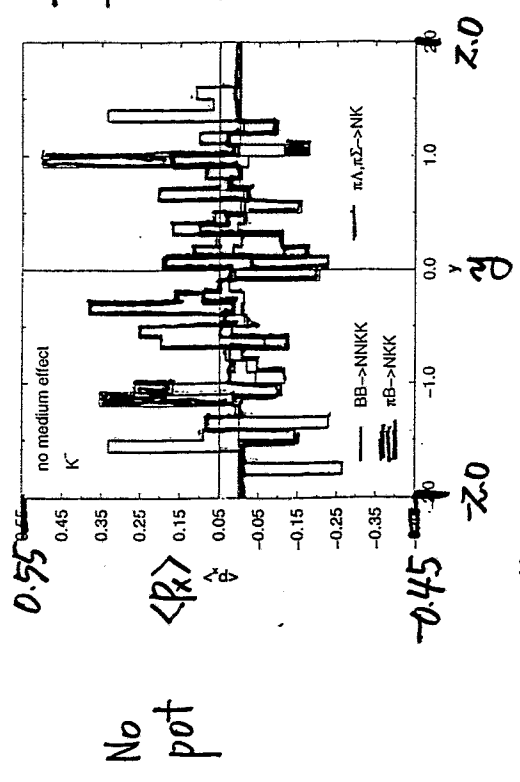


No pot

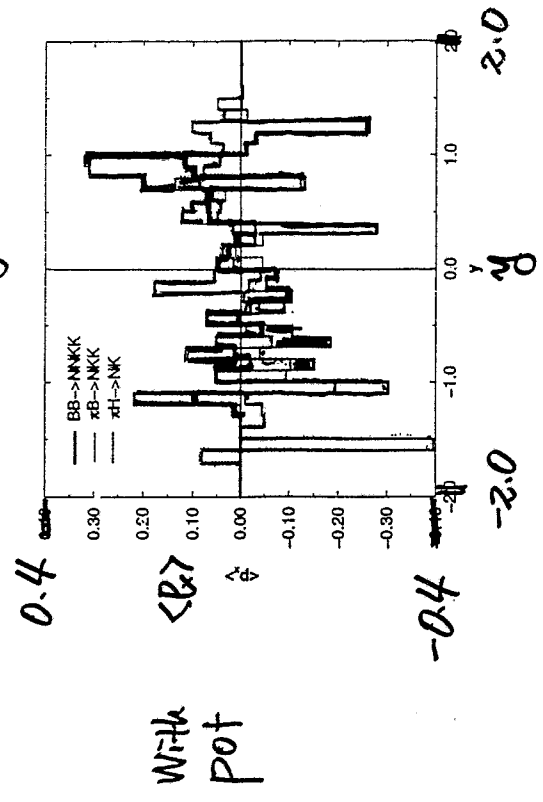


With Pot

Anti Kaon Flow



No pot

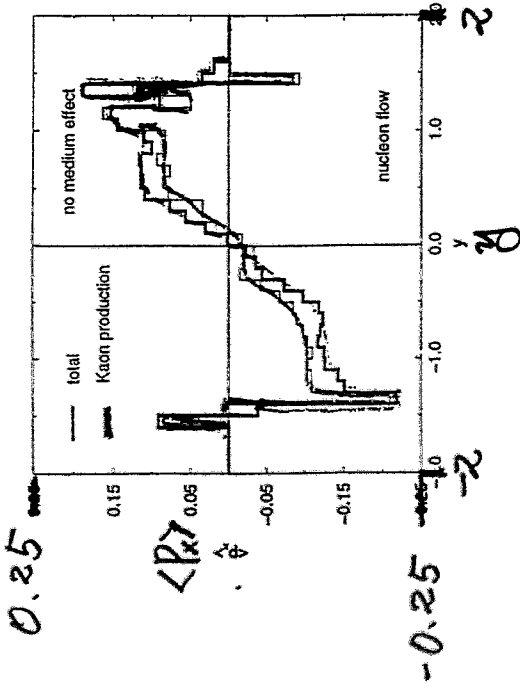


With pot

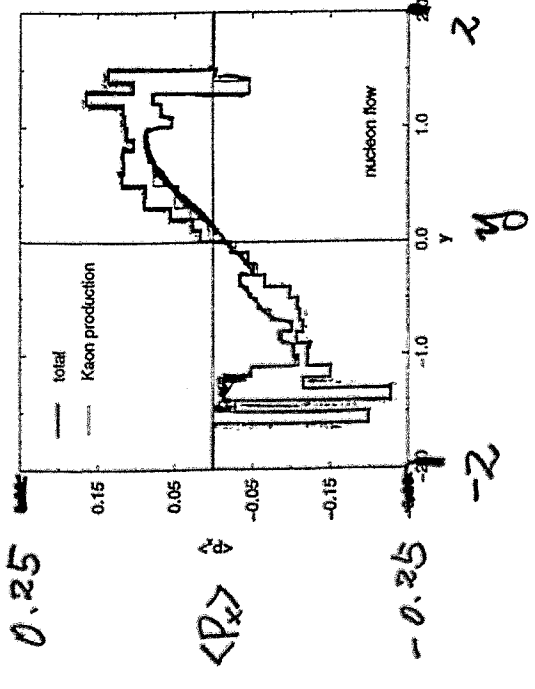
$\pi B \rightarrow \pi K$
 $\pi A \rightarrow \pi K$
 $\pi B \rightarrow \pi K$

Nucleon Flow

J. Nucleon flow



No Pot

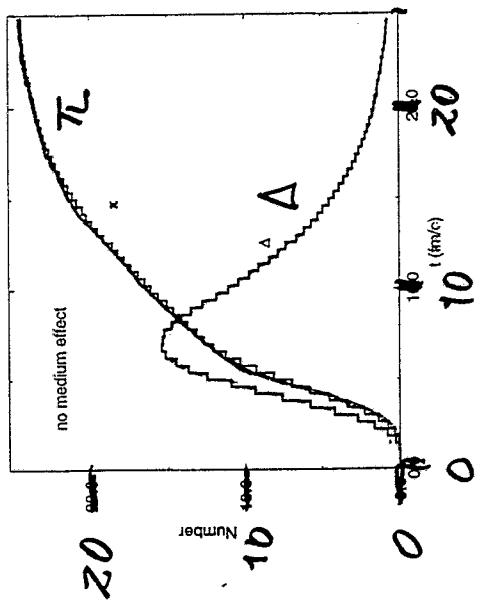


With Pot

— N : K-prod
 - - total

of π, Δ

K. Number of pions and deltas



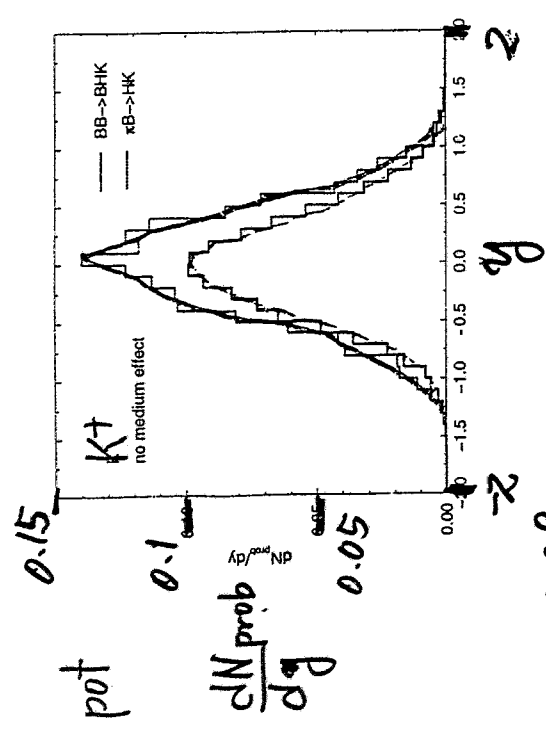
+ (fm/c)

Indep. of KN optical pot.

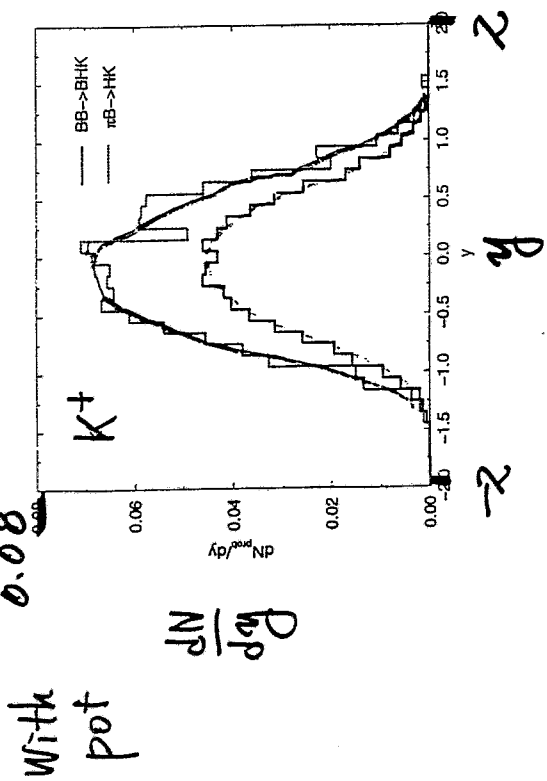
* Dynamics of N, π, Δ is independent of K^\pm, Λ, Σ production.

Final K^+ rapidity distribution

1. Final K^+ rapidity distribution

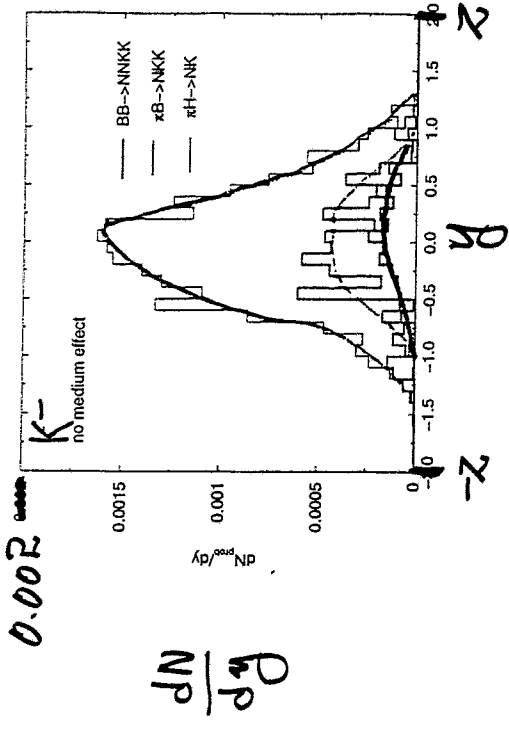


$\pi B \rightarrow \pi HK$
 $BB \rightarrow BHK$

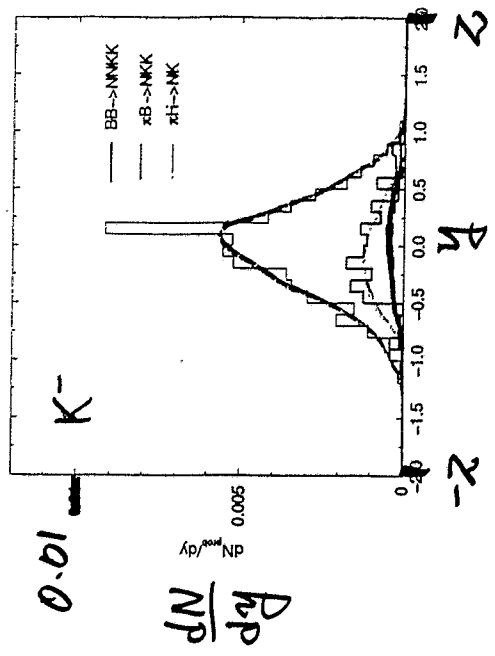


with
pot

Final K^- rapidity dist.



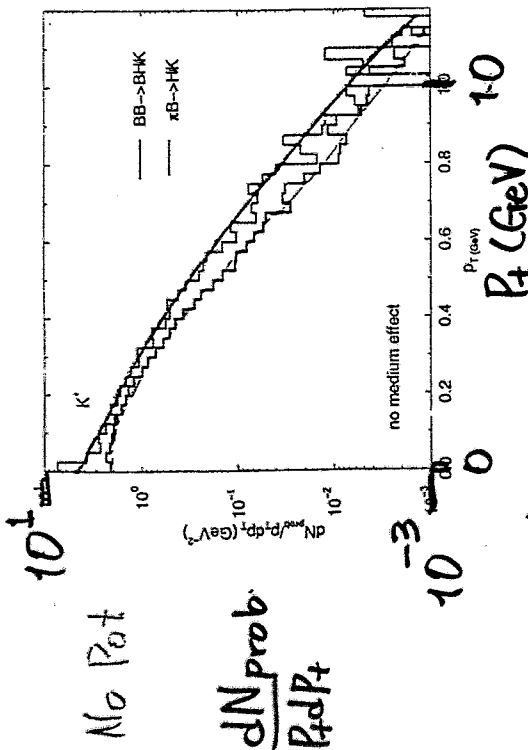
$\pi H \rightarrow \pi NK$
 $\pi B \rightarrow \pi NK$
 $BB \rightarrow \pi NK$



$\pi H \rightarrow \pi NK$
 $\pi B \rightarrow \pi NK$
 $BB \rightarrow \pi NK$

Final K^+

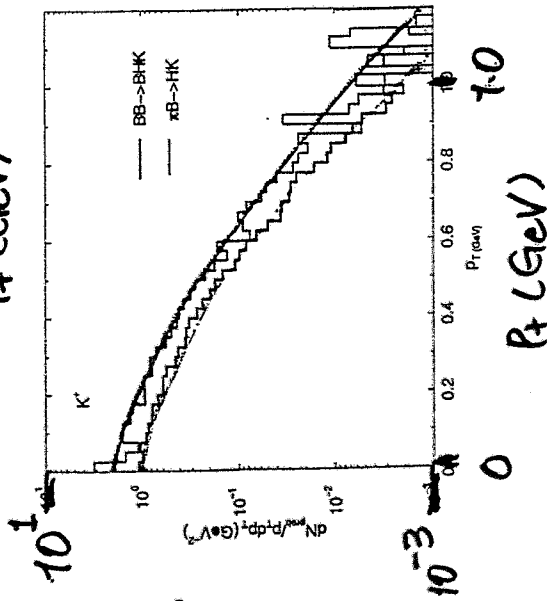
S. Final transverse momentum distribution



— $\pi B \rightarrow HK$
— $BB \rightarrow BHK$

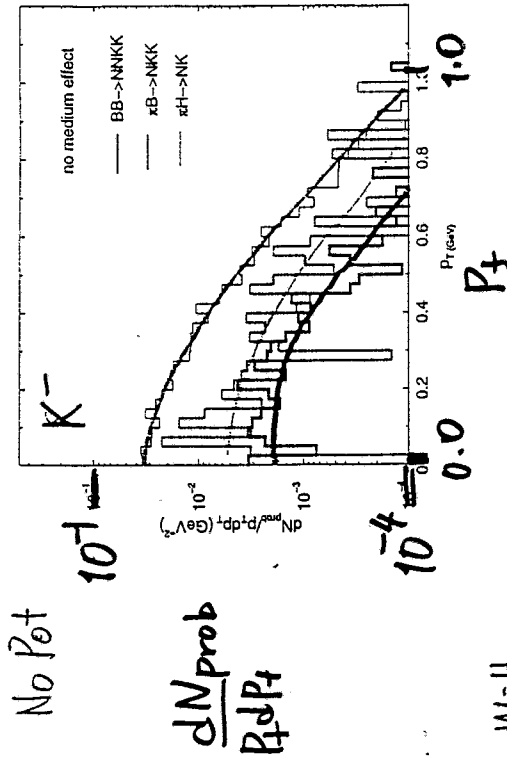
With
Pot

$\frac{dN_{\text{prob}}}{P_T dP_T}$



— $\pi B \rightarrow HK$
— $BB \rightarrow BHK$

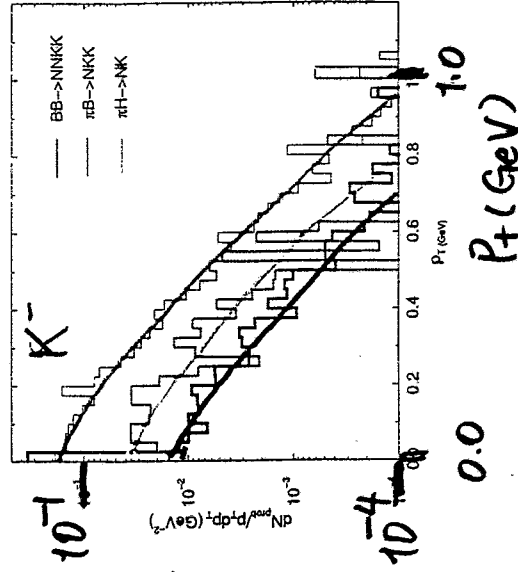
Final K^-



— $\pi H \rightarrow NK$
— $\pi B \rightarrow NKK$
— $BB \rightarrow NNKK$

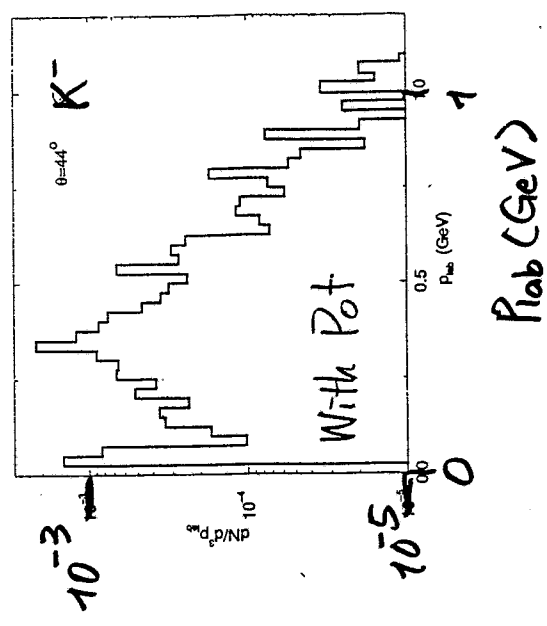
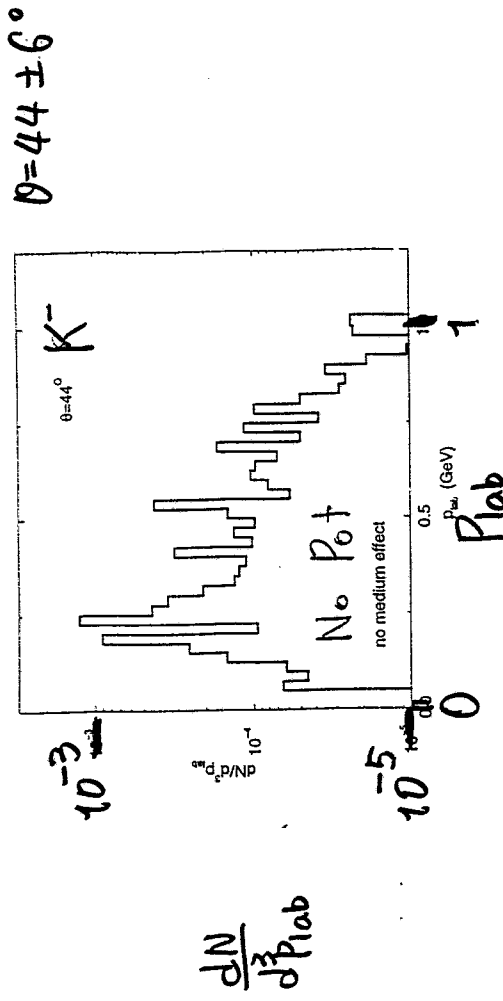
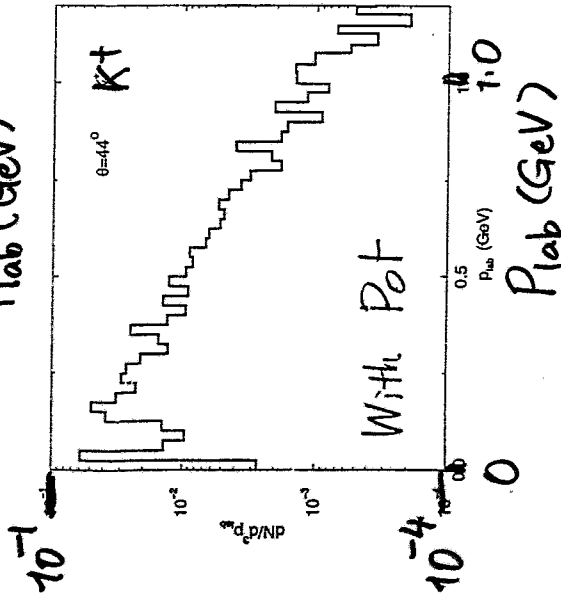
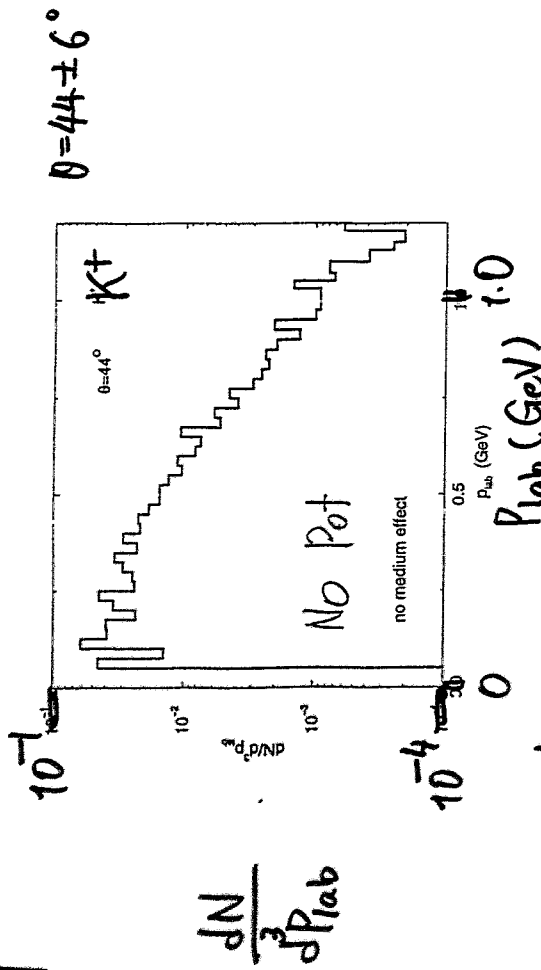
With
Pot

$\frac{dN_{\text{prob}}}{P_T dP_T}$



— $\pi H \rightarrow NK$
— $\pi B \rightarrow NKK$
— $BB \rightarrow NNKK$

T. Final lab momentum distribution



Discussion.

1. KN optical potential is crucial for K^- production
2. $\pi\Lambda, \Sigma \rightarrow K^-N$ is dominant for K^- production
3. $K^-N \Rightarrow \pi\Lambda, \Sigma$ (\bar{K} annihilation) is very important for K^- production.

For The Reunification
of South & North Korea.

Thank you.

J. Aichelin:

QMD

Kaonen - Workshop

QMD

C. Hartnagel, C. David, J.R.

What influences the kaon production

- cross sections $a+b \rightarrow K+x$
- K-N potentials (H.M.I. (1) : angular distribution
- Influence of NN potential
comparison QMD - RBUU
- Lifetime of Δ resonance

Nonrelativistic reduction of the DIRAC equation

$$m^* = m = \Sigma_0; \vec{p} = \vec{p} = \Sigma_0, \alpha = \begin{pmatrix} \Phi \\ \chi \end{pmatrix}$$

$$\begin{pmatrix} E - m^* - \Sigma_0 & -\vec{\sigma} \cdot \vec{p} \\ -\vec{\sigma} \cdot \vec{p} & E + m^* - \Sigma_0 \end{pmatrix} \begin{pmatrix} \Phi \\ \chi \end{pmatrix} = 0$$

Assumption: Φ is the Schrodinger two component spinor

$$((E - \Sigma_0)^2 - m^{*2} - p^{*2})\Phi = 0$$

Hamilton operator for Schrodinger eq.

$$H = \frac{p^2}{2m} + \Sigma_0 + \Sigma_s + \frac{\Sigma_s^2 - \Sigma_0^2}{2m} + \frac{\Sigma_0}{m} E_{kin} + \vec{\sigma}(\vec{p} \times \vec{p}^*)$$

If the Σ 's depend on the density only

$$\rightarrow U_{opt} = u E_{kin}$$

Correct up to $E_{kin} = 200$ MeV but not at higher energies.

In the Dirac Brueckner approach the self energy Σ is defined as

$$\Sigma_{DB}(k) = \int d^3q \frac{m^*(q)}{E^*(q)} \langle kq | G(z) | kq - qk \rangle$$

where $G(z)$ is the relativistic analogon to the Brueckner G-matrix

$$G(q, p, P, z) = v(q, p, P) + \int \frac{d^3k}{(2\pi)^3} v(q, k, P) \left(\frac{m^*(k)}{E^*(k)} \right)^2$$

$$= \frac{Q(k, P)}{E^*(\vec{P} + \vec{k}) - E^*(\vec{P} - \vec{k}) - z} G(k, p, P, z)$$

where

$$E(k) = \sqrt{m^{*2} + k^2}$$

z = energy of entrance channel, $m^* = m + U_s$

Σ is usually complex. It can be presented as

$$\Sigma(k) = \Sigma_s - \gamma_0 \Sigma_0 + \vec{\gamma} \vec{\Sigma}$$

if one neglects tensor and γ_5 contributions.

The RBUU Hamiltonian

$$\omega = \sqrt{(\vec{p} - \vec{\Sigma})^2 + (m - \Sigma_s)^2} + \Sigma_0$$

$$= \sqrt{p^{*2} + m^{*2}} + \Sigma_0 = E^* + \Sigma_0$$

gives the equations of motion:

$$\vec{r} = \frac{\vec{p}}{E^*}$$

$$\vec{p}^* = -(\vec{p}_i - \vec{\Sigma}_i) \frac{\vec{\nabla}_r \Sigma_i + \vec{\nabla} \Sigma_s}{E^*} + \vec{\nabla} \Sigma_0$$

RBUU: mean field approach:

the Σ 's depend on densities only \rightarrow no momentum dependence.

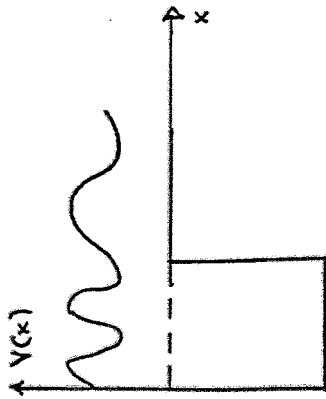
$$\Sigma_0 = \left(\frac{g_\omega}{m_\omega} \right)^2 \rho_B$$

Σ_s is the solution of $a \Sigma_s + b \Sigma_s^2 + c \Sigma_s^3 = g_\sigma \rho_s$

$$\vec{\Sigma} = 0$$

Time delay of wave packets

A) One dimensional potential scattering



No potential:

$$\psi_{\text{free}}(x) = \frac{1}{2i} (e^{ikx} - e^{-ikx}) = \sin(kx)$$

outgoing incoming

with potential

$$\psi_{\text{pot}}(x) = \frac{1}{2i} (e^{ikx + 2i\delta(E)} - e^{-ikx}) = e^{i\delta(E)} \sin(kx + \delta(E))$$

$$\psi_{\text{scatter}} = \psi_{\text{pot}} - \psi_{\text{free}} = \frac{e^{ikx}}{2i} (e^{2i\delta} - 1) \quad \text{outgoing!}$$

→ We can define a scattering amplitude

$$f = \frac{e^{2i\delta} - 1}{2i} \quad \text{with } |f|^2 = \sin^2 \delta$$

Wave packets

$$\psi_{\text{pot}}^{\text{in}} = e^{-ikx} \rightarrow \int dE f(E) e^{-ikx - iEt}$$

$$\psi_{\text{pot}}^{\text{out}} = -e^{ikx + 2i\delta} \rightarrow -\int dE f(E) e^{ikx + 2i\delta - iEt}$$

$$\text{with } \delta(E) = \delta(E_0) + \frac{\partial \delta(E)}{\partial E} \Big|_{E_0} (E - E_0)$$

$$\psi_{\text{pot}}^{\text{out}} = -e^{2i\delta(E_0) - iEt} \int dE f(E) e^{ikx} e^{-i(E - E_0)[t - 2\delta'(E_0)]}$$

$$\psi_{\text{free}}^{\text{out}} = -e^{-iE_0 t} \int dE f(E) e^{ikx} e^{-i(E - E_0)t}$$

⇒ time delay for the outgoing wave

For the scattered wave we find

$$\psi_{\text{scatter}} = \psi_{\text{pot}} - \psi_{\text{free}}$$

$$\psi_{\text{scatter}} = \int dE f(E) e^{ikx - iEt + i\delta} \sin \delta \dots$$

$\psi_{\text{scatter}}(x)$ is maximal at the position where the phase is stationary

$$\nabla_k (kx - Et + \delta(E)) = 0$$

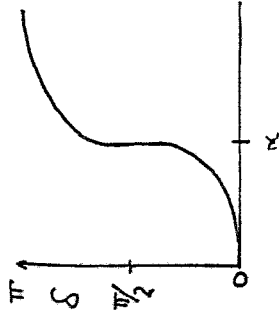
k_0
center of wave packet

$$x = v_0 - \frac{d\delta(E)}{dk} \Big|_{k_0} = v_0 \left(t - \frac{d\delta}{dE} \Big|_{E_0} \right)$$

→ Time delay for outgoing wave. = 2x time delay of scattered wave

In three dim at finite angles one measures $|\psi_{\text{scatter}}|^2$
→ one expects a time delay of $\Delta t = \frac{d\delta}{dE} \hbar$

Resonances



Close to a resonance

$$\delta \approx \tan^{-1} \frac{\beta}{\alpha - k} \quad \frac{1}{\beta} = \frac{d\delta}{dk} \Big|_{k_0}$$

$$f = \frac{e^{2i\delta} - 1}{2i} = \frac{-2i\beta}{(k-\alpha) + i\beta}$$

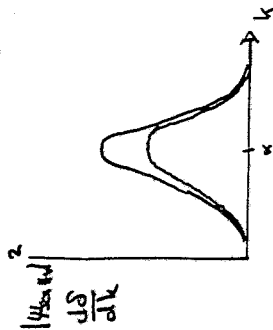
$$k = \sqrt{2mE}$$

$$|\psi_{scat}|^2 = |f|^2 = \frac{\beta^2}{(k-\alpha)^2 + \beta^2}$$

with $\Gamma = \frac{2\alpha\beta}{m}$ and $E - E_R = \frac{\hbar^2 k^2}{m}$

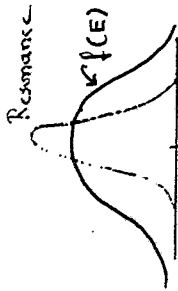
$$= \frac{\Gamma^2/4}{(E - E_R)^2 + \Gamma^2/4}$$

$$\frac{d\delta}{dk} = \frac{\beta}{(k-\alpha)^2 + \beta^2}$$



What is the difference between Γ and ΔE

$$\psi_{scat} \approx \int dE f(E) e^{ikx - iEt} = \underbrace{e^{2i\delta}}_{\text{Resonance}} \frac{1}{E - E_R + i\Gamma/2}$$



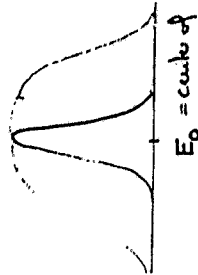
width of resonance $<$ width of w.p. $\hbar k \approx p_R + \frac{m}{p_R} (E - E_R)$

$$f(E) \approx f(E_R)$$

$$\psi_{scat} \approx 2\Gamma f(E_R) e^{i(p_R x - E_R t)} \int dE e^{\frac{i(\frac{x}{v_R} - t)(E - E_R)}{E - E_R + i\Gamma/2}}$$

$$\psi_{scat}(x,t) = 2\Gamma f(E_R) e^{i(p_R x - E_R t)} e^{-\frac{\Gamma}{2}(t - \frac{x}{v_R})}$$

Γ measures the lifetime of the resonant state populated with a wave packet with a large width



$$\delta(E) \approx \delta(E_0) + \delta'(E - E_0)$$

$$\psi_{scat}(x,t) = \int dE f(E) e^{ikx - iEt + \delta(E)} \approx \int dE f(E) e^{ikx - iEt + \delta(E_0) + \delta'(E - E_0)}$$

$$\sim \sin \delta(E)$$

The maximum of the scattered wave is the where the phase is

Stationary

$$x = v_0(t - \delta') = v_0 t - \frac{2\hbar/\Gamma}{\sqrt{2} v_0} \approx \sqrt{2} v_0 \left(t - \frac{\hbar}{\Gamma} \right)$$

Lifetime of Δ 's in simulations

$$\Gamma = \frac{d\sigma}{dE} \text{ if width of wavepacket } \ll \Gamma$$

$$= \frac{\Gamma_0 / v}{(E - E_0)^2 + \Gamma^2 / 4}$$

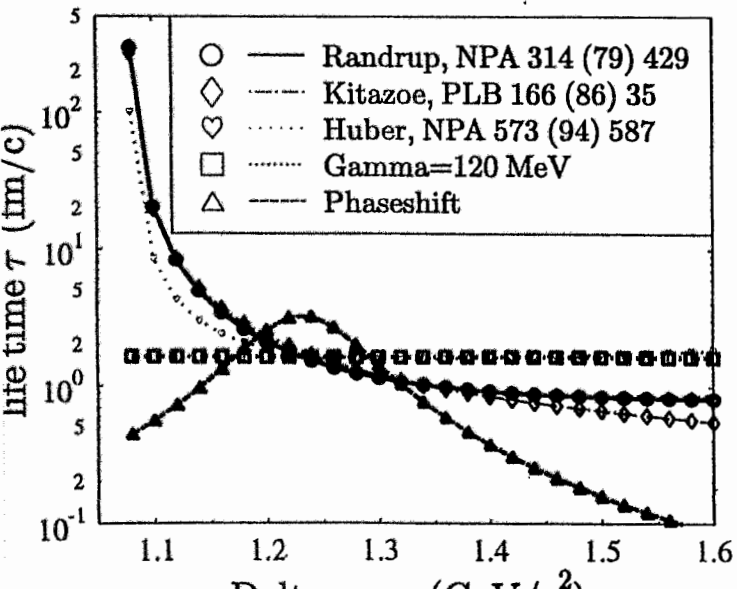
for Breit-Wigner

Up to now

$$\Gamma = \int \frac{d^3 p_f}{E} |M|^2 \delta(p_i - p_f)$$

$$\tau = 1/\Gamma$$

Delta lifetime



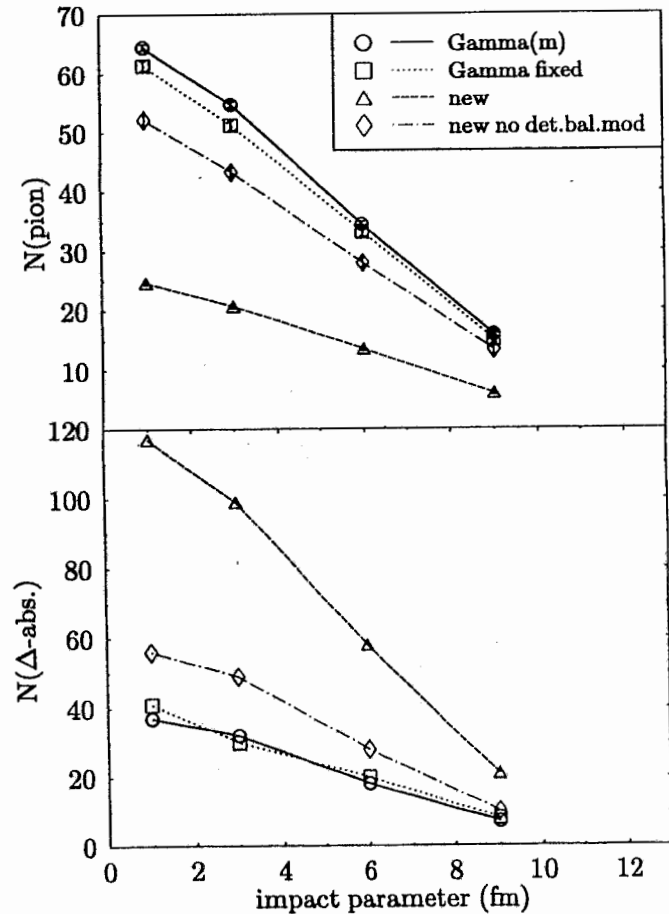
Δ lives much shorter than assumed.

↓
Probability for $\Delta N \rightarrow \Delta N$

small

Pion yield

The new parametrisation yields less pions due to absorption. Au(1AGeV)+Au HM



Creation de kaons

• perturbative :

reference cross section 40 mb

• if each time two hadrons h_1 and h_2 come closer than

$$r = \sqrt{4/\pi} \quad [fm]$$

• a kaon is produced with the probability

$$P_K = \frac{\sigma_{h_1 h_2} \rightarrow K+X}{40 \text{ mb}}$$

• the hadrons continue as if no K were produced!

• at the point of closest distance

the kaons (as all particles) are produced if the hadrons are closest.

• actual production.

• initially we assume that

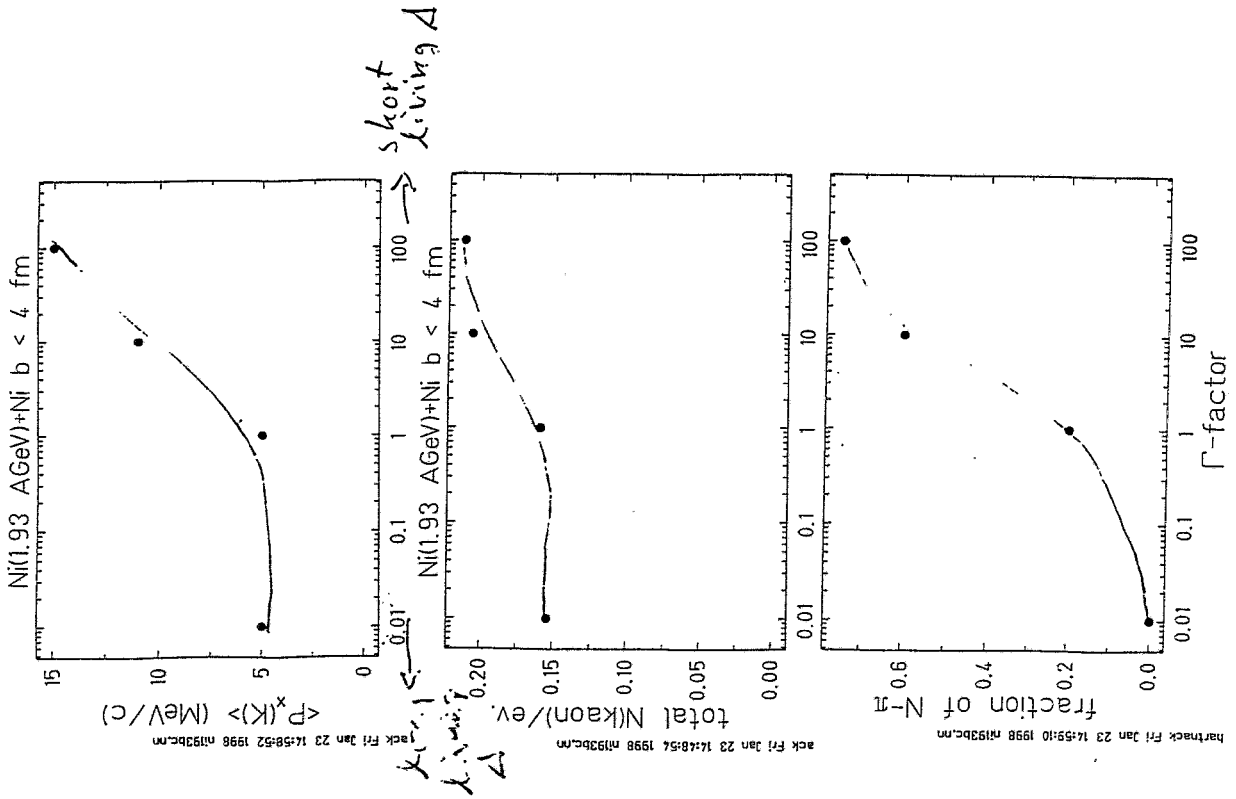
$$V_S = \sqrt{(p^2 + p^2)^2} + \underbrace{Y_{opt}(h_1) + Y_{opt}(h_2)}_{>0}$$

because particles can use this energy

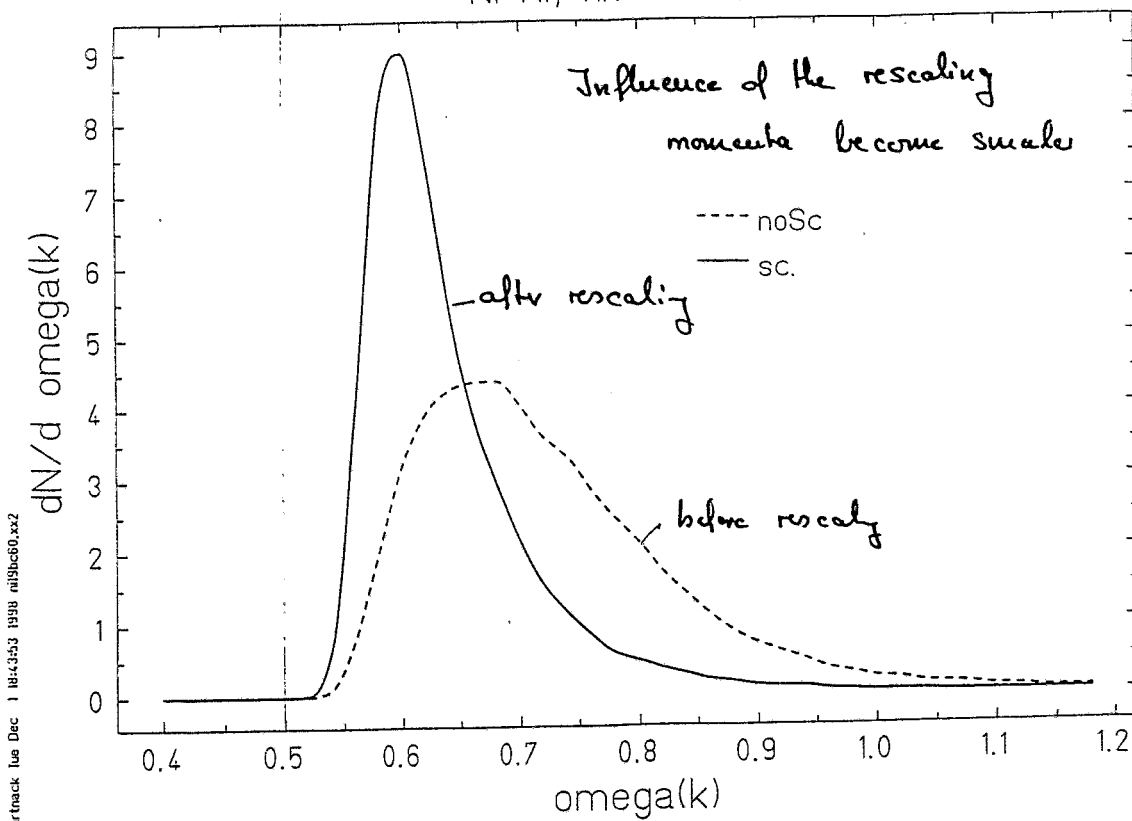
$$\text{threshold} = m_{h_1} + m_{h_2} + m_K(k_K=0) - \underbrace{\left(\frac{V(h_1)}{h_1} + \frac{V(h_2)}{h_2} \right)}_{\text{negative}} / 6$$

$$V_\lambda(g) \approx \frac{2}{3} V_\lambda(g)$$

Cross section σ is calculated with these quantities



Ni+Ni, nk= 78908



hartnack Tue Dec 1 18:43:53 1999 ni99buc60.xx2

The momenta of the kaons and the outgoing hadrons are calculated with their Γ_S assuming that they are determined by phase space

This procedure does not conserve energy because the outgoing hadrons live in an optical potential

↳ iteration procedure.

- rescale all momenta by a factor α
- recalculate

$$V_{opt}(h_1)$$

$$V_{opt}(h_2)$$

$$w(k)$$

- if the energy difference between the incoming and outgoing particles is smaller than 10 MeV assume that we have found the right momenta.

- recalculate the true Γ_S of the reaction

$$\Gamma_S = \sqrt{(p_1^2 + p_2^2)^2 + \Delta V_{opt}(h_1) + \Delta V_{opt}(h_2)}$$

cross section ② is calculated with this Γ_S

Our approach

$$L_{KN} = D_\mu^* \bar{K} D^\mu K - m_K^2 \bar{K} K - g_{\sigma K} m_K \bar{K} K \sigma - g_{\delta K} m_K \bar{K} \vec{\nabla} K \cdot \vec{\delta}$$

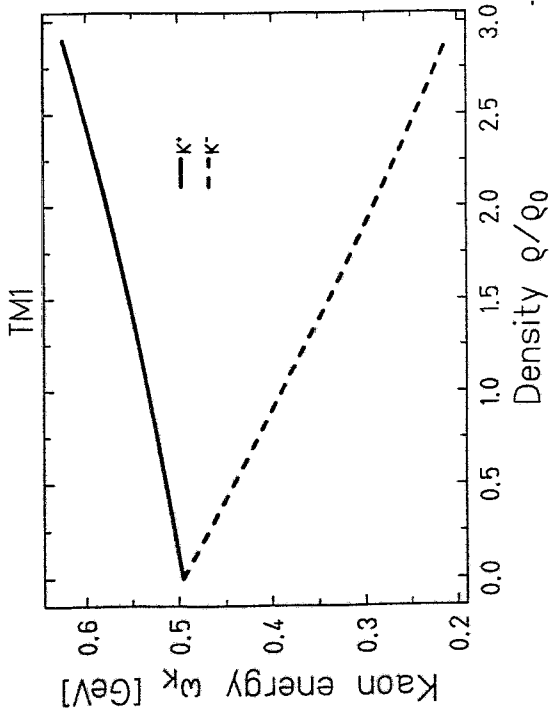
gives in infinite matter the equation of motion

$$(\partial_\mu \partial^\mu + m_K^2 + m_K \Sigma_S + 2(\Sigma_V^0) i \partial^0 - \Sigma_V^2) K = 0$$

$$(-2 \vec{\Sigma}_V \cdot i \vec{\partial}_x)$$

Energy of K , \rightarrow enters for the cross section calculation

$$\text{Optical potential} = \omega - \sqrt{m_K^2 + k^2}$$



Kaon dispersion relation in nuclear medium

$$\omega_K^{*2} = m_K^2 + \vec{p}_K^2 - \frac{\Sigma_{KN}}{f^2} \rho_S \pm \frac{3\omega_K^*}{4f^2} \rho_V$$

$\frac{\Sigma_{KN}}{f^2} \rho_S$ attractive scalar field

$\frac{3\omega_K^*}{4f^2} \rho_V$ vector field:

Repulsive for kaons

Attractive for antikaons (leading to a reduction of energy in medium)

K and \bar{K} energies in medium

$$K^+ \quad \omega_K^* = \sqrt{m_K^{*2} + \vec{p}_K^2 + \left(\frac{3}{8f^2} \rho_V\right)^2} + \frac{3}{8f^2} \rho_V$$

$$K^- \quad \omega_K^* = \sqrt{m_K^{*2} + \vec{p}_K^2 + \left(\frac{3}{8f^2} \rho_V\right)^2} - \frac{3}{8f^2} \rho_V$$

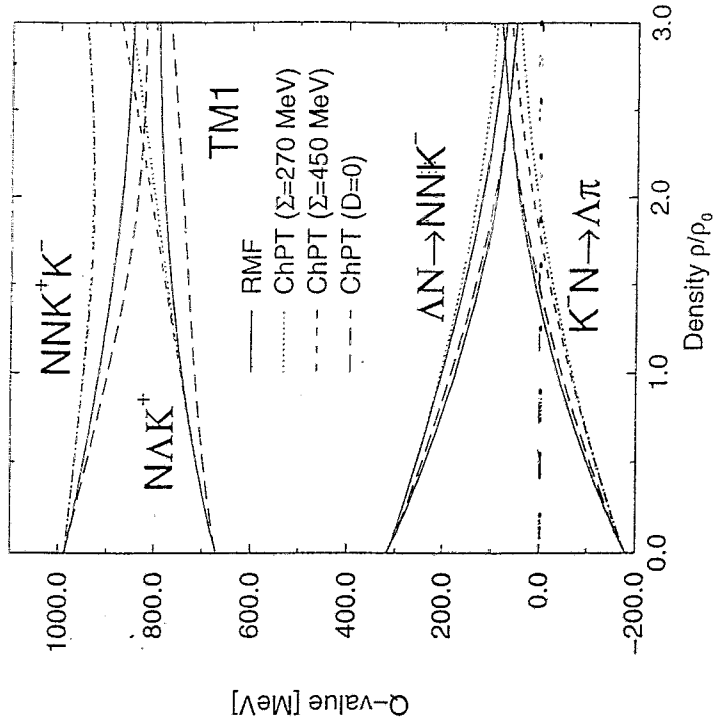
with

$$m_K^{*2} = m_K^2 - \frac{\Sigma_{KN}}{f^2} \rho_S$$

$$U_{\text{opt}} = \omega^* - \sqrt{m_K^{*2} + k^2}$$

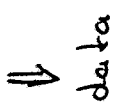
Changes of thresholds in medium

Schaffner et al. ($\vec{k}_{jN} = 0$)



$K^-N - \Lambda\pi$: Q-value > 0

no K^- absorption

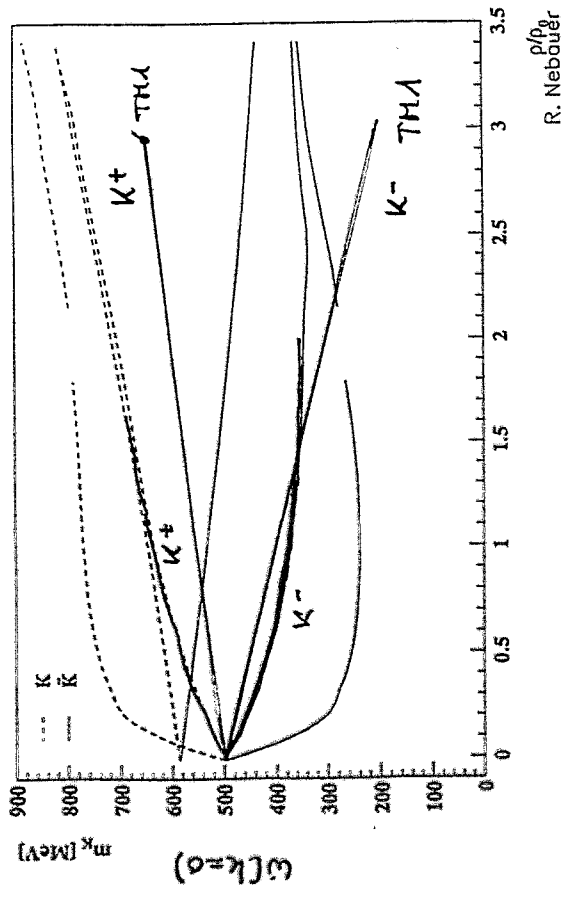


NJL - Kaon masses

Nauber - Jona-Lasinio

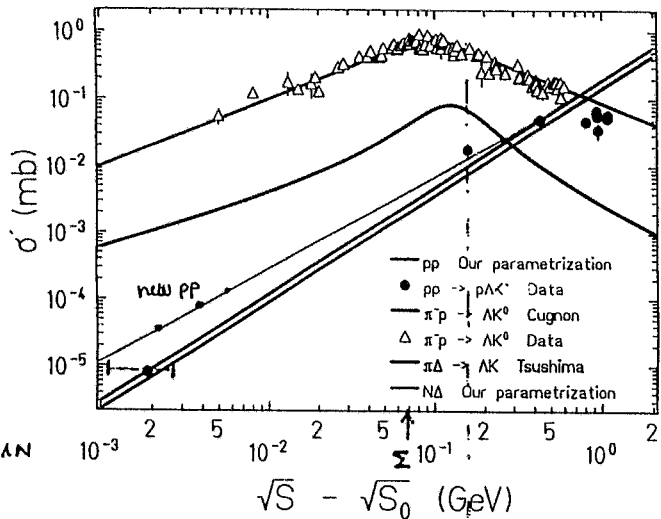
$T=150$ MeV

$T=280$ MeV



$$\sigma_{\pi N \rightarrow AK} = \frac{1}{2} \sigma_{\pi^+ p \rightarrow AK^0}$$

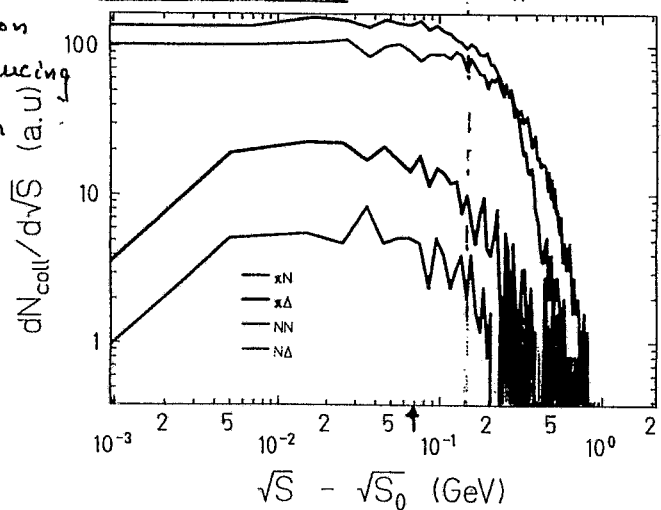
↳ this cross section controls the $\pi N \rightarrow K$ channel



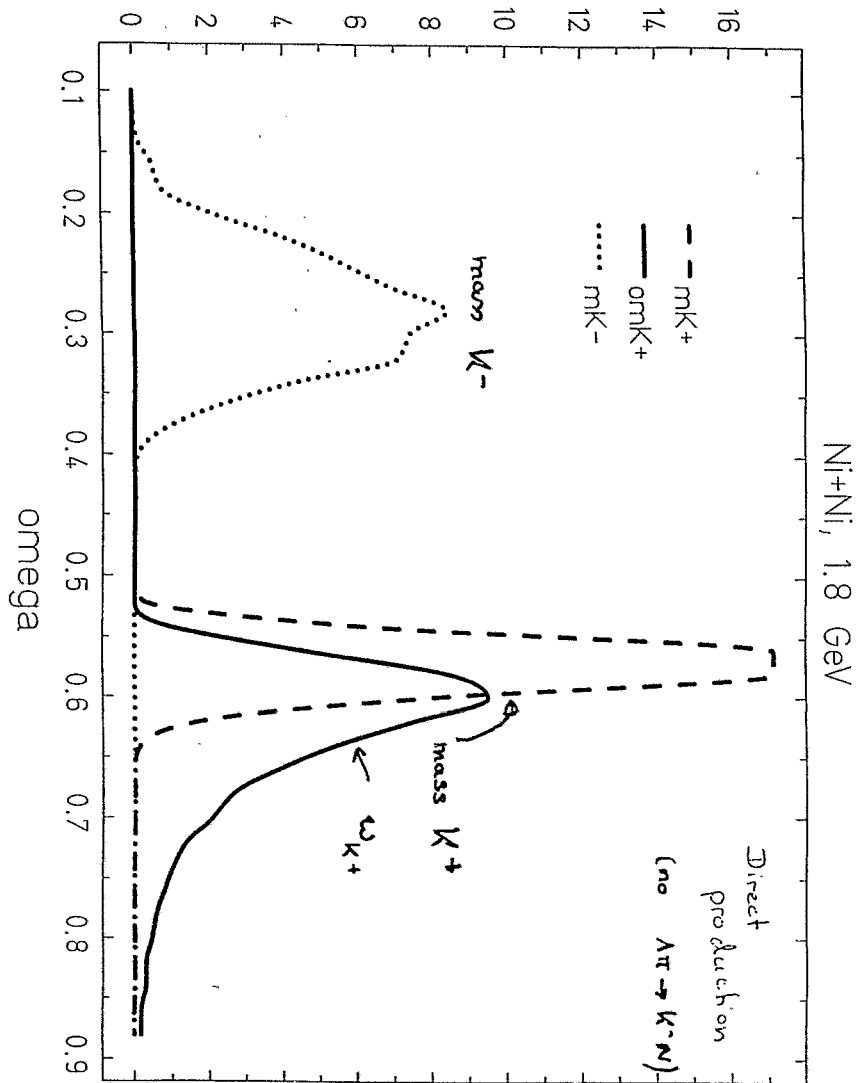
$$\sigma_{NN \rightarrow AKN} = 3\sigma_{pp \rightarrow K^+ \Lambda N}$$

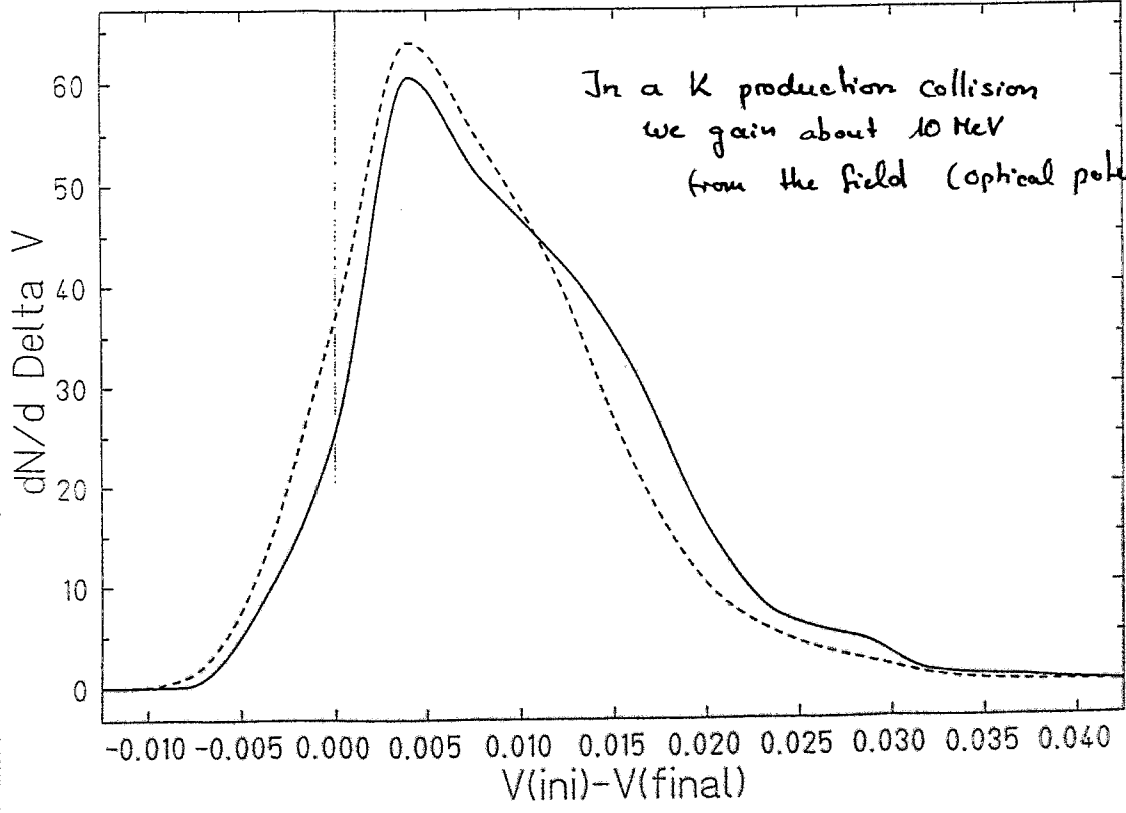
⁵⁸Ni(1.93A GeV)+⁵⁸Ni SM $\Gamma = \Gamma_H$ $b \leq 4$ fm

Its distribution of kaon producing collisions in QMD



dN/d omega

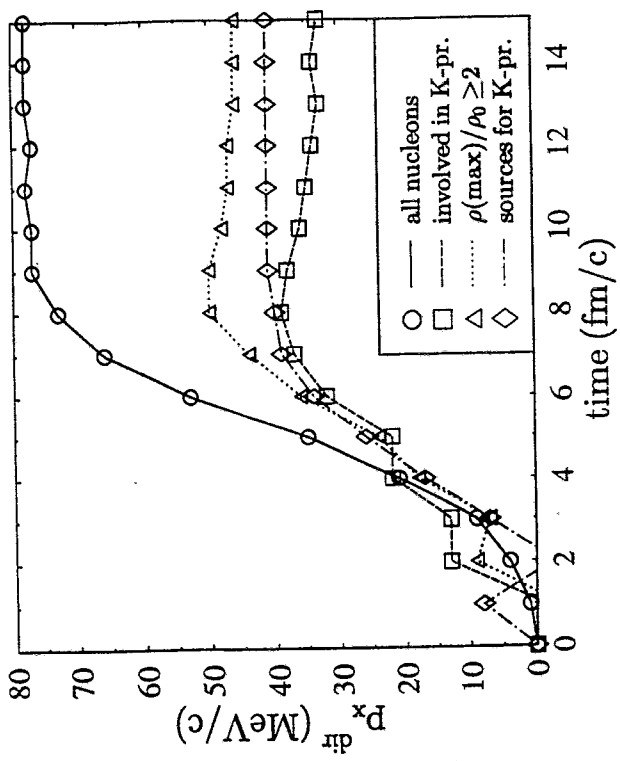




Time evolution of flow

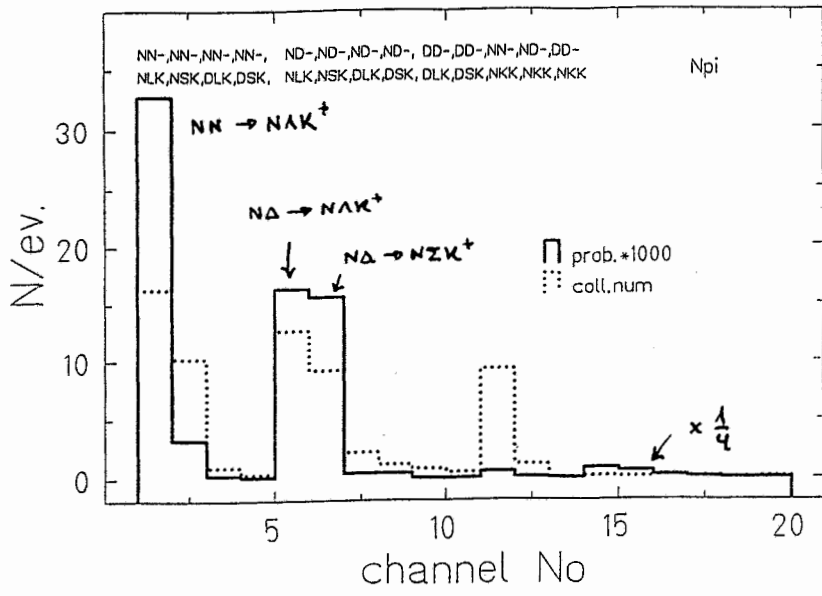
Nucleons involved in kaon production show much less flow than the average of all nucleons.

Ni(1.93 AGeV)+Ni b=2fm



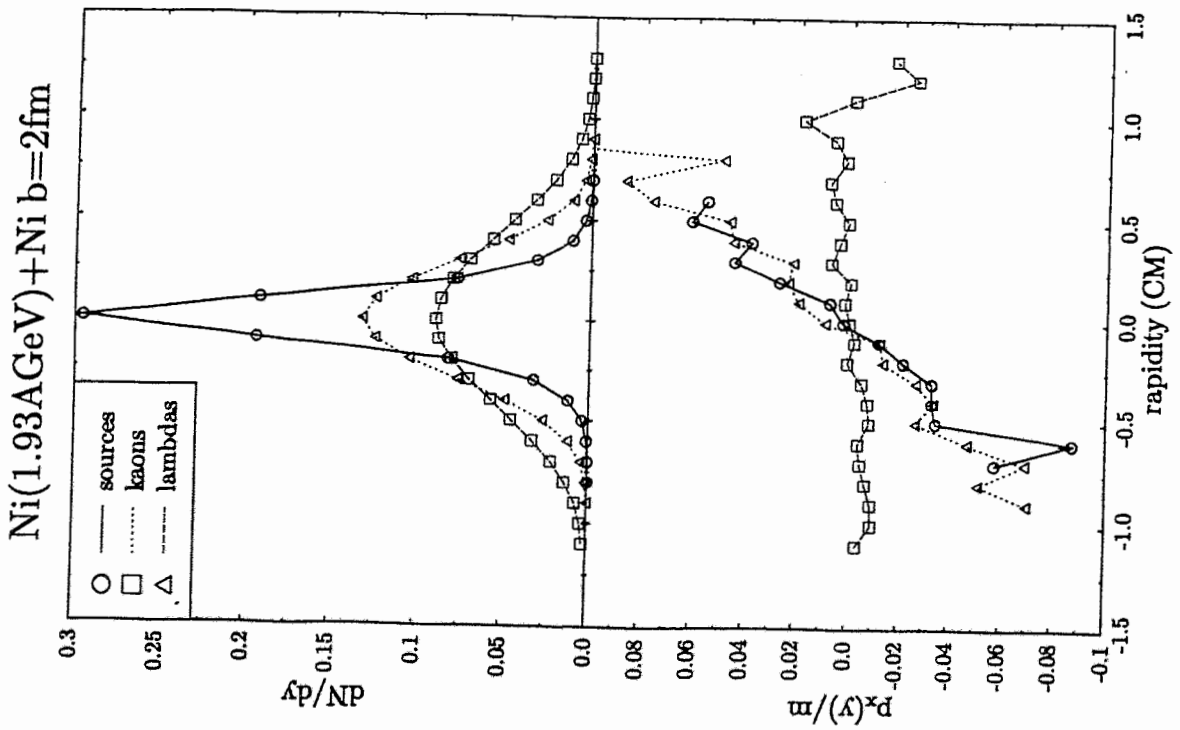
Similarly the flow of particles which felt highest densities is reduced.
The flow of the sources is strongly reduced, if we take into account their higher masses.

58+ 58, E= 1.800 GeV

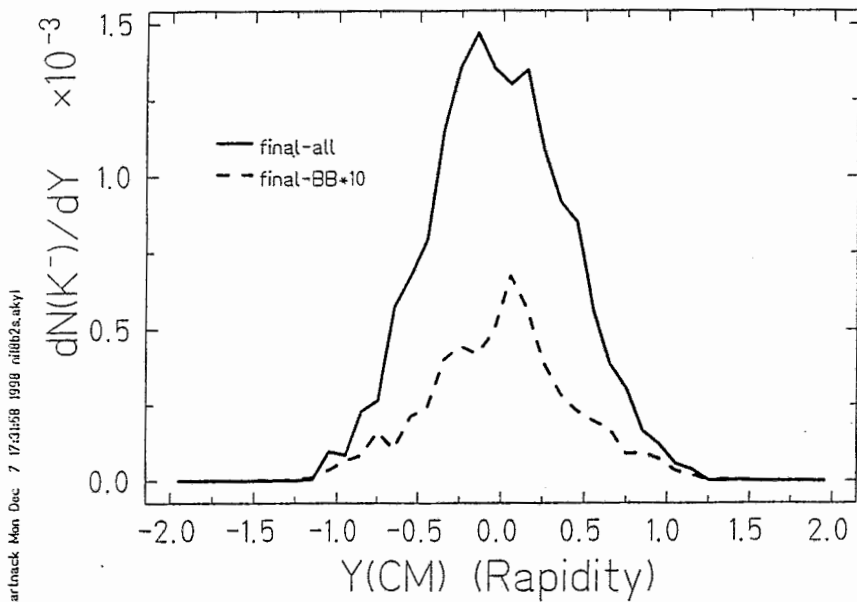


hartnack Mon Dec 7 16:28:44 1998 ni802s.knc2

3 body channels
 $BB \rightarrow NYK$

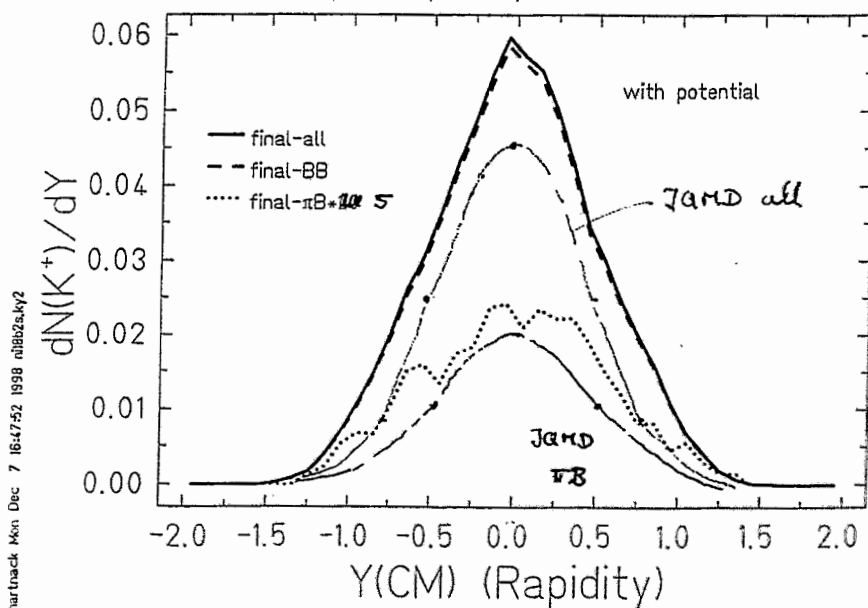


Ni+Ni, b=2, SM, E= 1.800 GeV

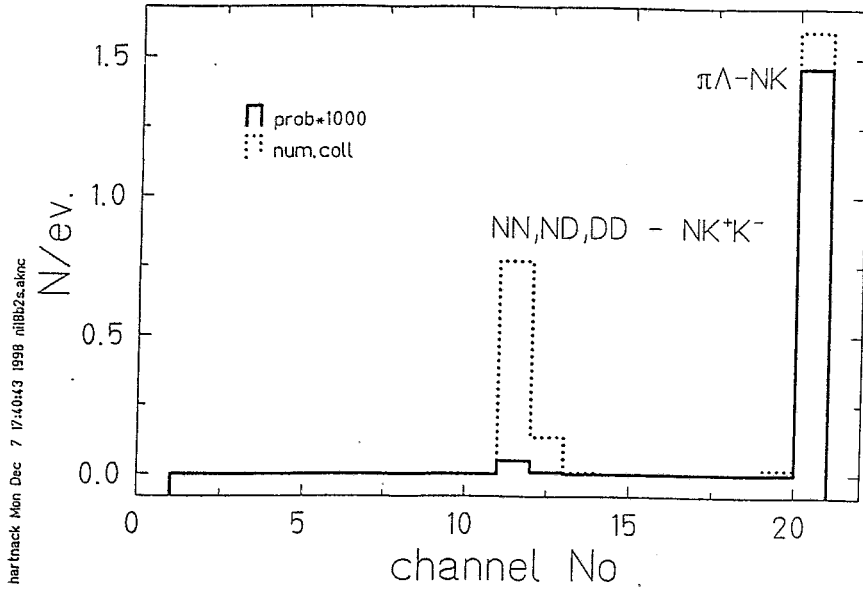


potential. change only
weakly the rapidity
distribution

Ni+Ni, b=2, SM, E= 1.800 GeV

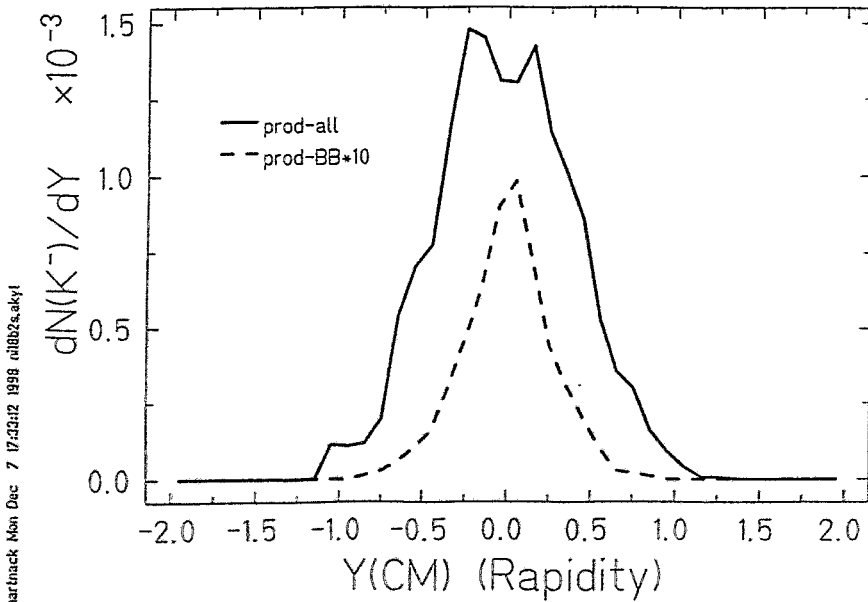


Ni+Ni, b=2, SM, E= 1.800 GeV



K⁻ production channel

Ni+Ni, b=2, SM, E= 1.800 GeV



S. Soff:

**Kaon production at SIS energies in the UrQMD
approach**

Kaon Production at SIS energies in the UrQMD approach

H. Weber, C. Ernst, M. Belkacem, S.S., H. Stöcker, W. Greiner

Inst. f. Theoret. Physik, Universität Frankfurt

— Some ingredients of the UrQMD model.

— Modeling the elementary production channels
Via Resonances

— Example Ni (1.8 AGeV) Ni, $t = 2$ fm

— Standard phase space observables

— Comparison to C. (2.4 GeV) C. ; min. bias

— Classification of production channels:



UrQMD hadron multiplets

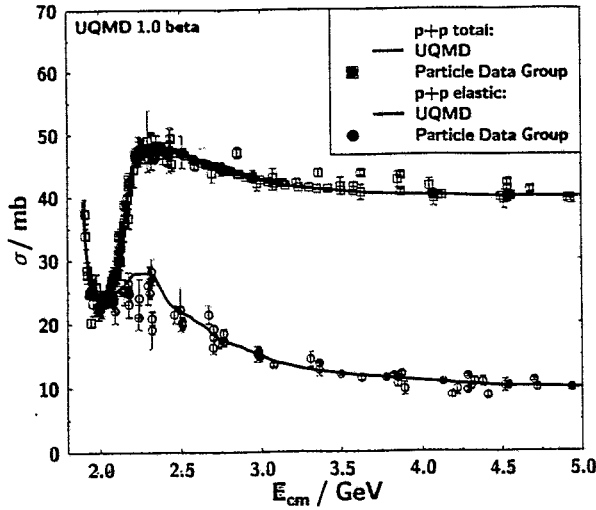
N	Δ	Λ	Σ	Ξ	Ω
938	1232	1116	1192	1317	1672
1440	1600	1405	1385	1530	
1520	1620	1520	1660	1690	
1535	1700	1600	1670	1820	
1650	1900	1670	1790	1950	
1675	1905	1690	1775	2025	
1680	1910	1800	1915		
1700	1920	1810	1940	0 ⁻⁺	1 ^{- -}
1710	1930	1820	2030	\bar{K}	ρ
1720	1950	1830		K^*	K_0^*
1990 [†]		2100		η	ω
2080		2110		η'	ϕ
2190				1 ^{+ -}	2 ^{+ +}
2200				$(1^{--})^*$	$(1^{--})^{**}$
2250				b_1	a_2
				K_1	K_2^*
				h_1	ω
				h_1'	f_2'
				ω 1450	ρ 1700
				K 1680	K 1680
				ω 1662	ω 1662
				ω 1680	ϕ 1900

+ all charge conjugated states

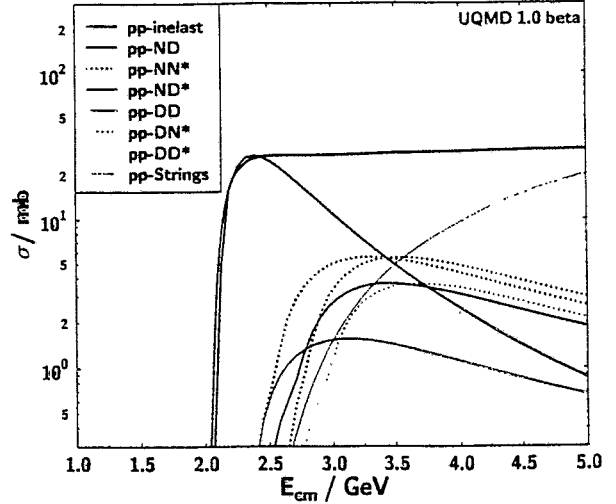
+ meson- & (anti-)baryon-strings

p+p Cross Sections

p+p total and elastic cross sections

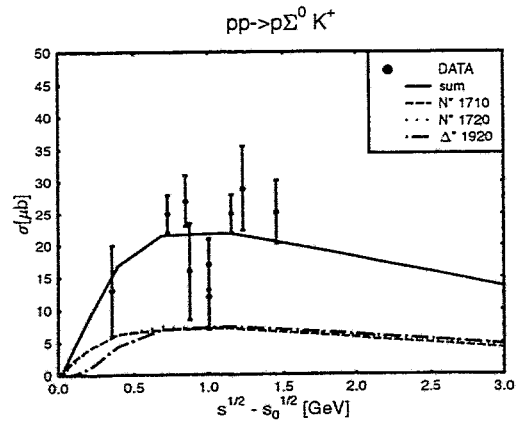
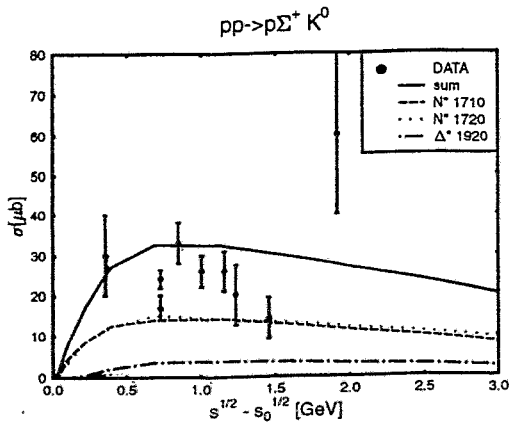


p+p inelastic channels



- total and elastic cross section via table lookup
- inelastic cross sections are parameterized (fixed to data)

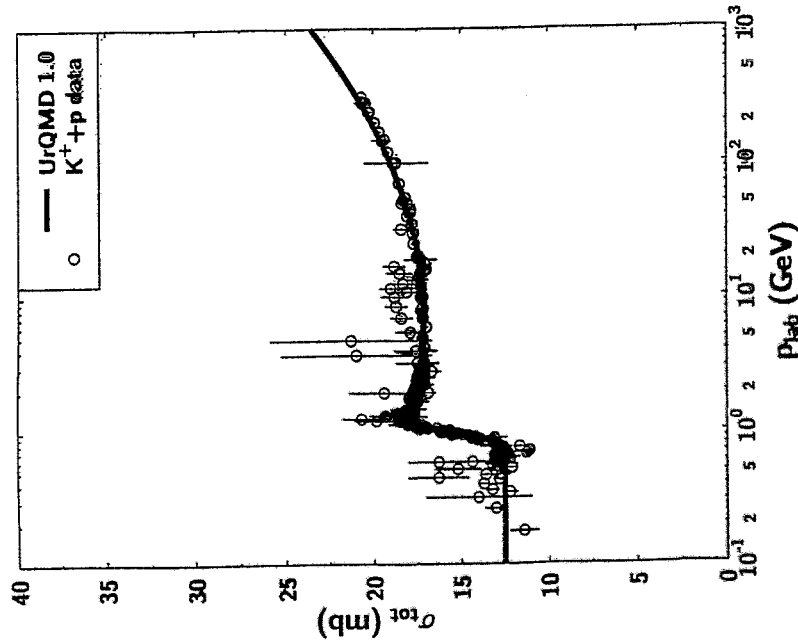
Elementary Kaon Production



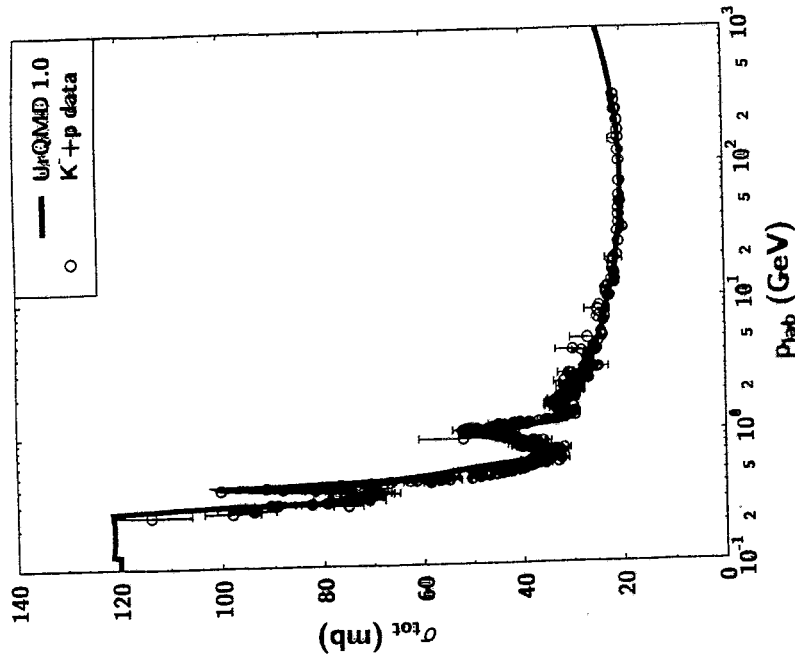
- $pp \rightarrow pN_{1710}^* \rightarrow p\Sigma^+ K^0$
- $pp \rightarrow pN_{1720}^* \rightarrow p\Sigma^+ K^0$
- $pp \rightarrow p\Delta_{1920}^* \rightarrow p\Sigma^+ K^0$

- $pp \rightarrow pN_{1710}^* \rightarrow p\Sigma^0 K^+$
- $pp \rightarrow pN_{1720}^* \rightarrow p\Sigma^0 K^+$
- $pp \rightarrow p\Delta_{1920}^* \rightarrow p\Sigma^0 K^+$

$K^+ p$ cross section parametrized according to experimental data (non-resonant)



$K^- p$ cross section Hyperon Resonances



Ni (1.8 A GeV) Ni $b = 2 \text{ fm}$

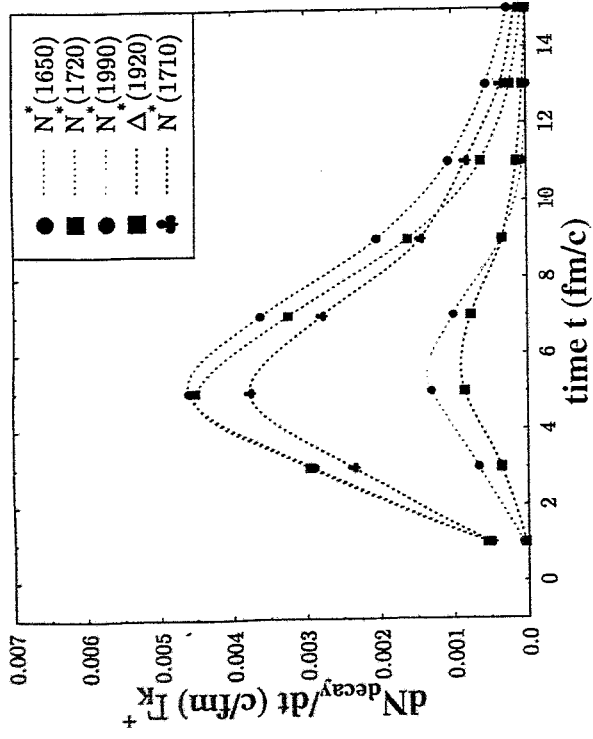
$\sigma = 12.5, 7 \text{ mb}$

- # K^+ produced 0,10 $\rightarrow \sigma \approx 12,8 \text{ mb}$
- # K^- produced 0,01 $\rightarrow \sigma \approx 1,3 \text{ mb}$
- # K^+ absorbed 0,015 $\rightarrow 15\% \text{ of produced}$
- # K^- absorbed 0,008 $\rightarrow 76\% \text{ of produced}$

$\rightarrow K^-$ absorption essential
 K^+ absorption inessential

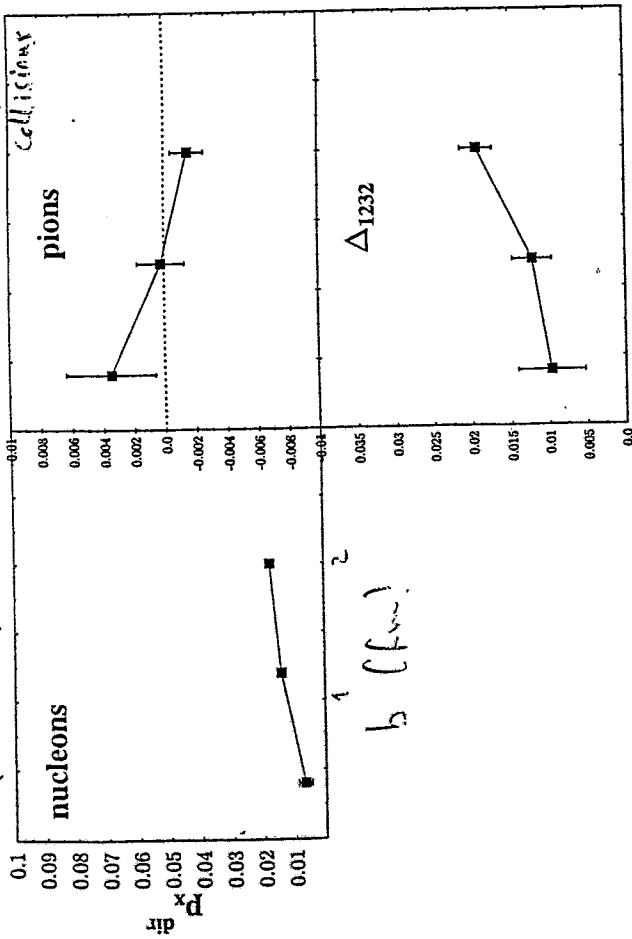
UrQMD, Sven Soff

Ni (1.8 A GeV) Ni



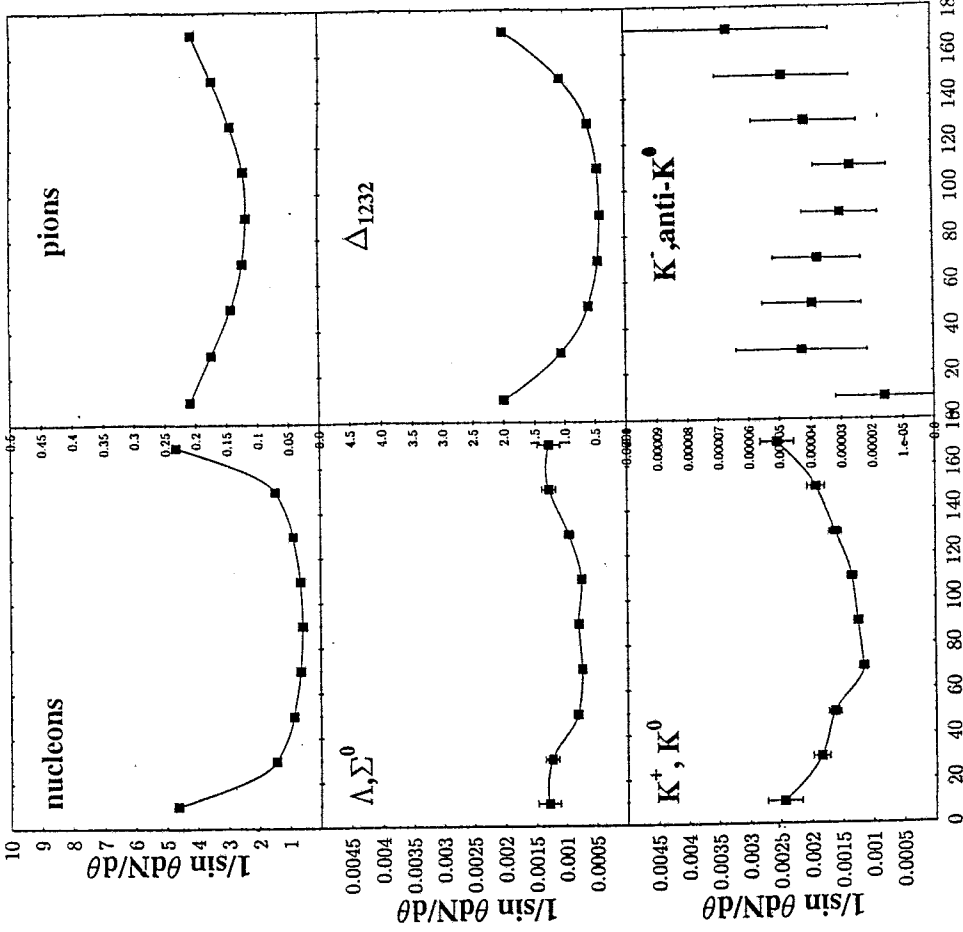
Resonance Abundancies
 weighted with
 branching ratio

C (2 A GeV) C min.bias Negative Fien flow for peripheral collisions

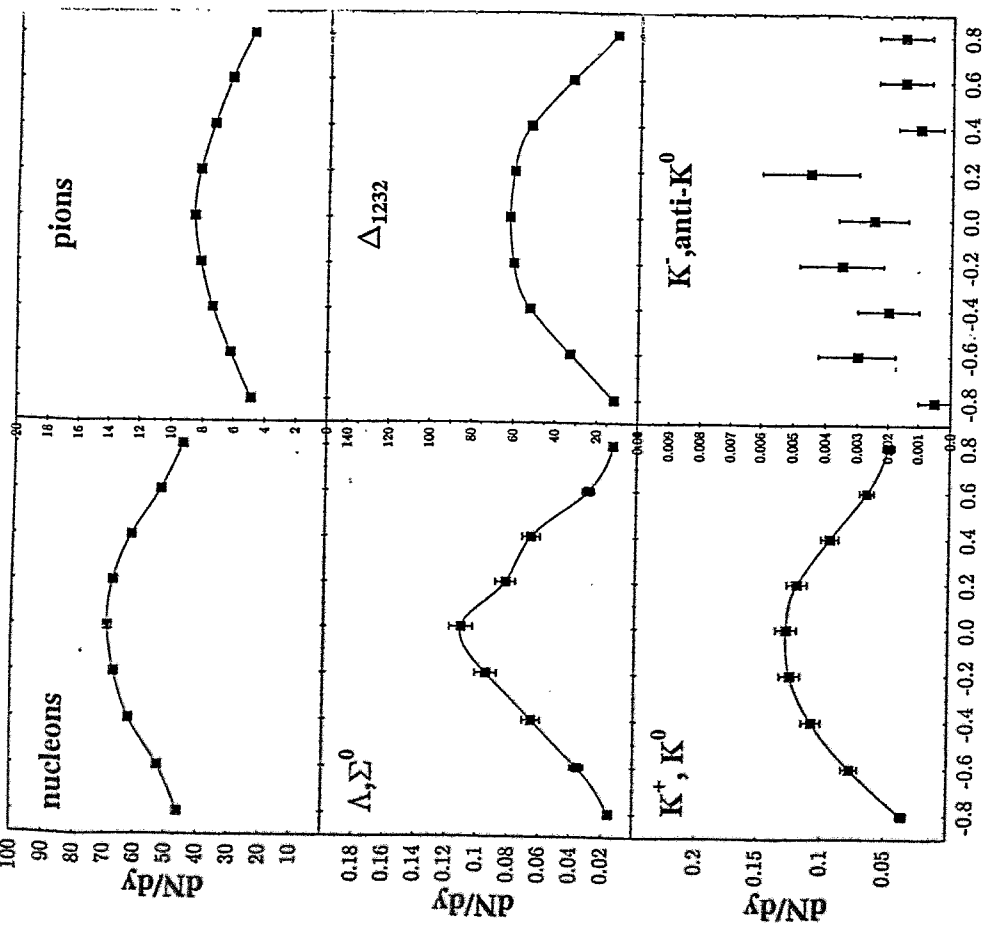


Centrality Dependence of the Strength and Sign of the in-plane flow

Ni (1.8 A GeV) Ni $b=2$ fm

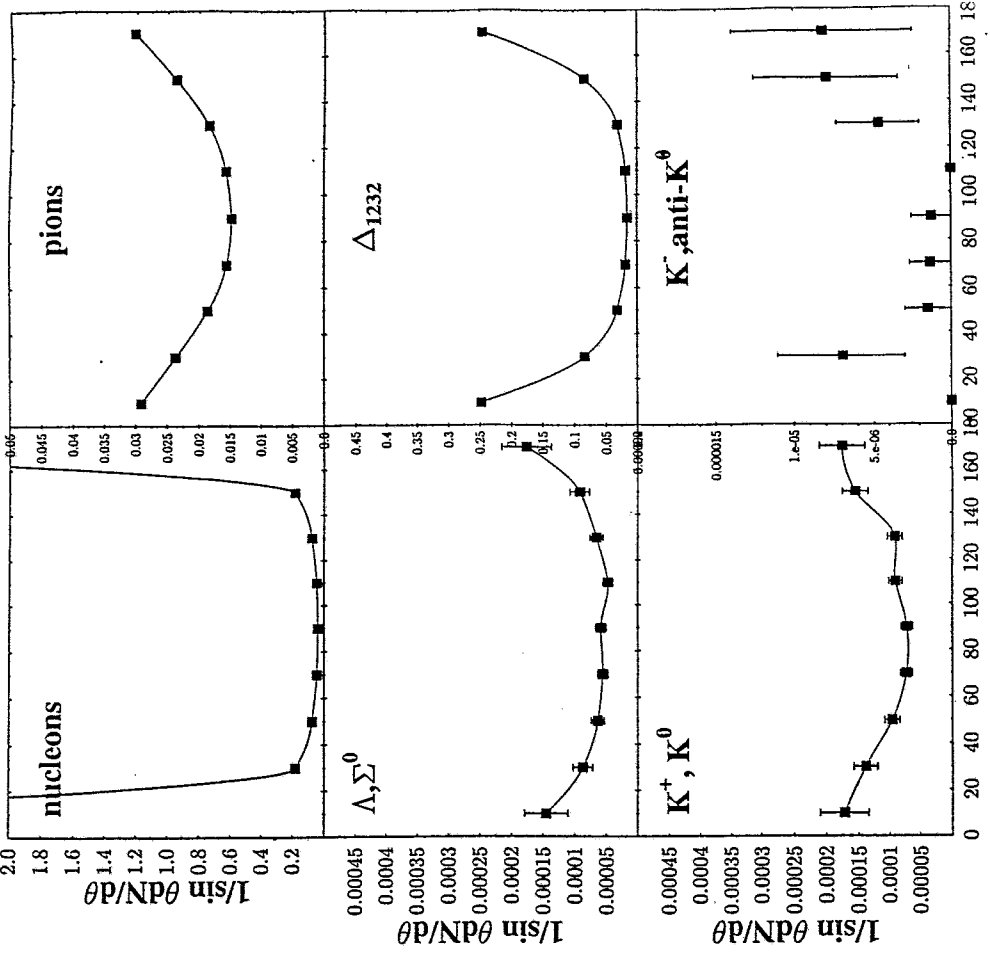


Ni (1.8 A GeV) Ni b=2fm



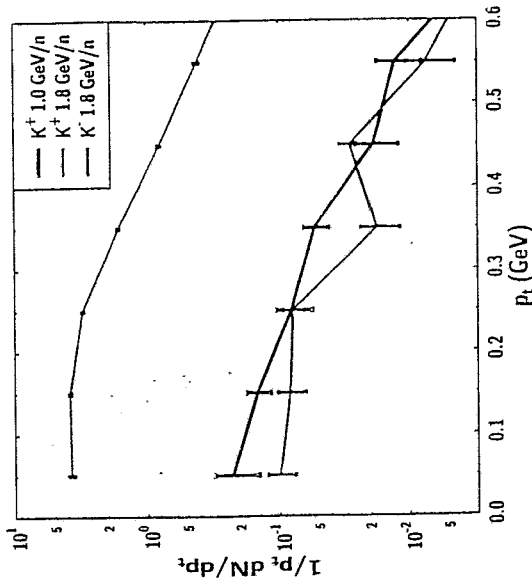
pions are broader than K^+ (than Δ)

C (2 A GeV) C min.bias



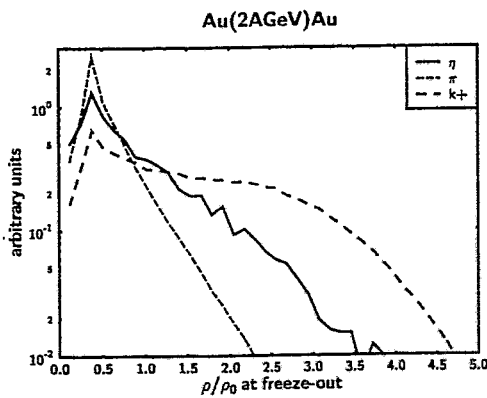
Forward backward peaking already in C + C
 $\approx \frac{(dN/d\theta)_{max}}{(dN/d\theta)_{min}} \approx 2-3$!

**K^- enhancement:
Pion - Hyperon Scattering**

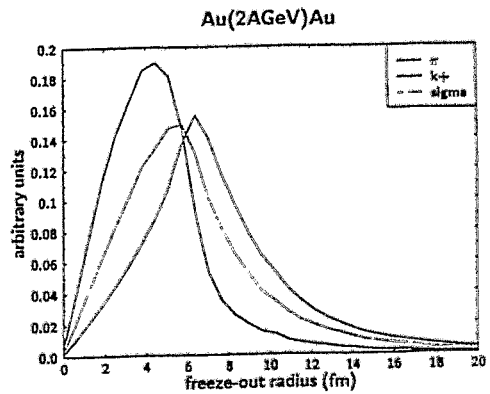


- UrQMD calculation in CASCADE mode
 - at equivalent beam energies strong enhancement of K^- yield
- \Rightarrow enhancement due to $\pi\Sigma \rightarrow \Lambda^* \rightarrow N\bar{K}$

Freeze-out densities and radii



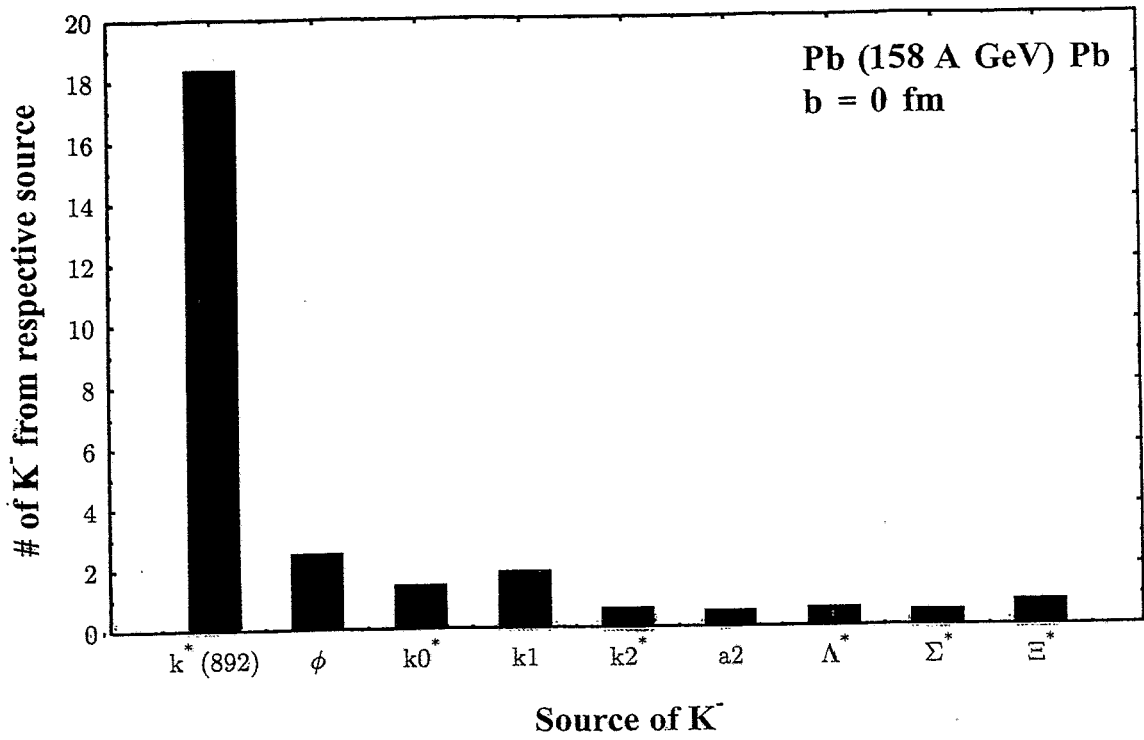
- most pions freeze out below ground state density
- K^+ are a good signal for the high density phase at SIS



- different source sizes for different particle species
- \Rightarrow no global freeze-out radius !
- \Rightarrow no global freeze-out density !

$\approx 60\%$ of last decays from Resonances (40% 'direct')

Last Generation Sources of K^-



Gy. Wolf:

Kaon production – benchmark test

Gy. Wolf

Properties of the model:

- 15 resonances
- varying energy dependent widths good description of meson production in hadron-hadron collisions.
- 5 mesons propagate ($\pi, \rho, \omega, \eta, \omega$)
- potential: Skyrme, $k=240 \text{ MeV}$

kaons

- k^+
- if propagates and rescatters

$$\sigma_{el}^{k^+} = 10 \text{ mb}$$

- creation:

$$\sigma_{pp \rightarrow pK^+} = \frac{1.1 (\sqrt{s} - \sqrt{s_0})^{1.71}}{(0.8 (\sqrt{s} - \sqrt{s_0})^{1.7} + 4.5 \sqrt{(\sqrt{s} - \sqrt{s_0})^2 + 1})} \text{ [m]}$$

Randrup-ko prescription:

$$\sigma_{NA} = \frac{3}{4} \sigma_{NN}$$

$$\sigma_{AA} = \frac{1}{2} \sigma_{NN}$$

$$\sigma_{NR} = \sigma_{NN}$$

Casimir's fit:

$$\sigma_{NN}^{pN} = 4.47 (\sqrt{s} - \sqrt{s_0})$$

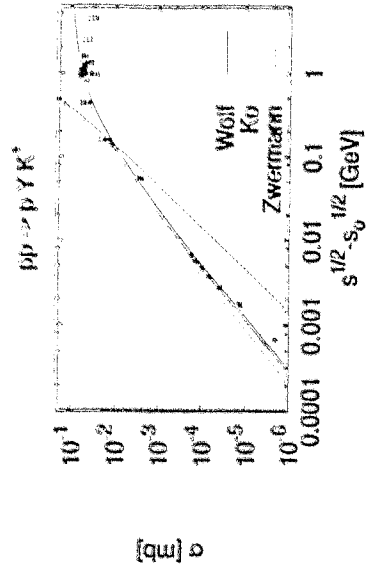
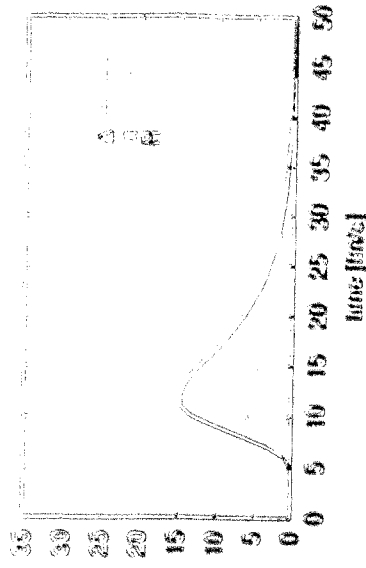
$$\sigma_{NN}^{pN} = 0.0285 / (\sqrt{s} - \sqrt{s_0})$$

$$\sigma_{\pi^+ n} = 2.5 \sigma_{pp} = 4 \sigma_{NN}$$

$$\sigma_{\pi^+ p} = \frac{1}{4} \sigma_{\pi^+ n}$$

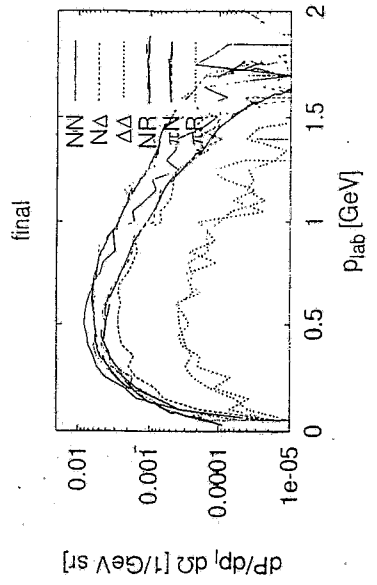
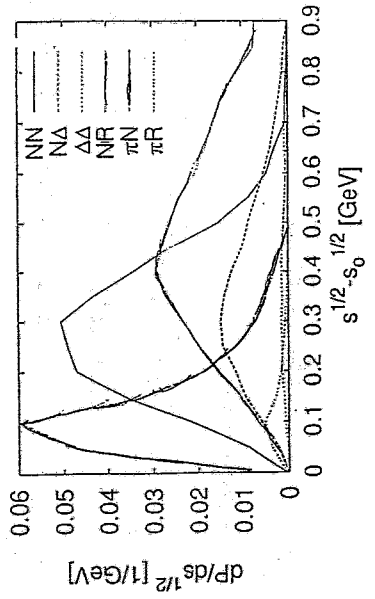
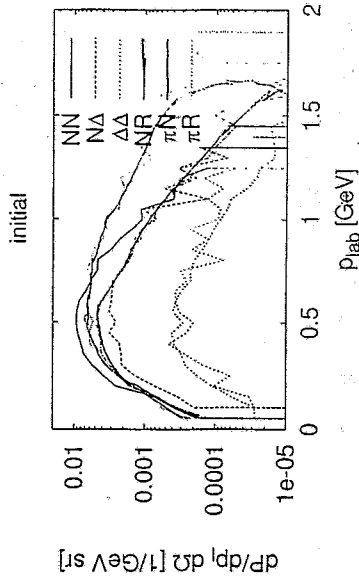
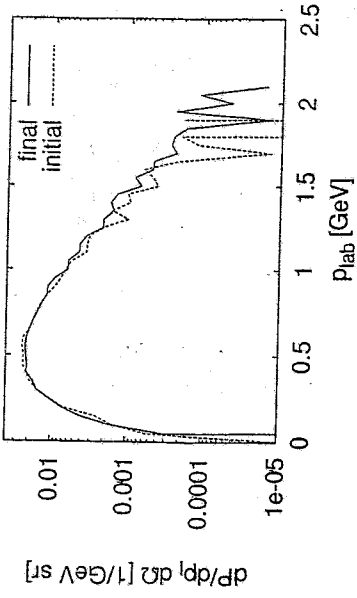
$$\sqrt{s} < 4.7$$

$$\sqrt{s} \geq 4.7$$

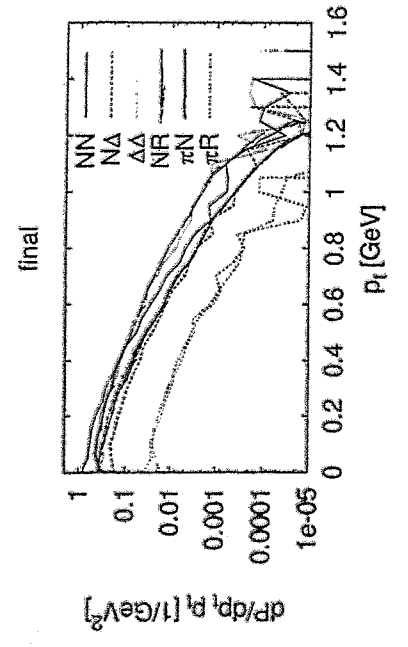
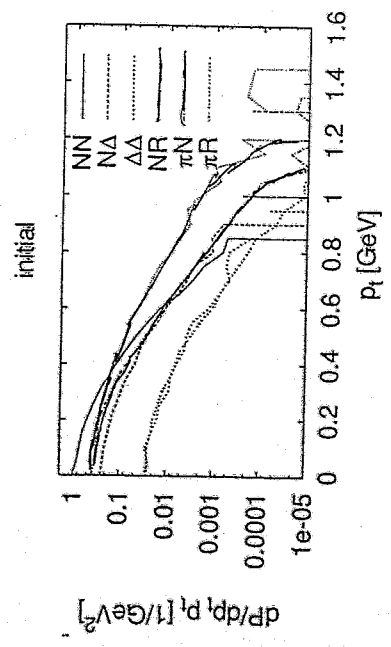
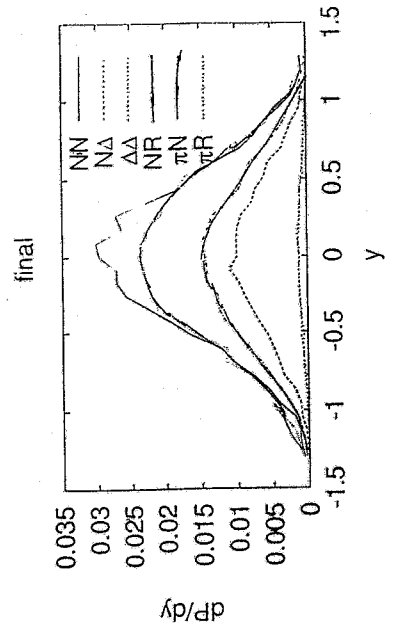
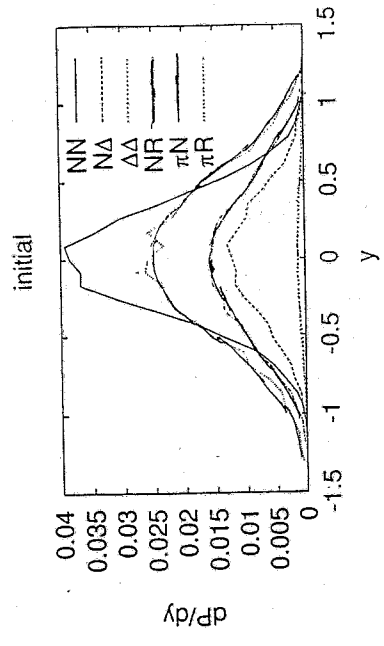


Total probabilities:

NN	0.0175	7553	13076
NA	0.00636	1256	8622
AA	0.000788	3559	4547
NR	0.01621		
πN	0.00879		
πR	0.000829		



Budapest



C. Fuchs:

K⁺ production with Tübingen QMD

K^+ production with

Tübingen QMD

C. Fuchs

Tübingen

Benchmark tests:

$Ni + Ni$, 1.8 A.GeV, $b = 2 \text{ fm}$

QMD, SMDI, $T_{\Sigma} = 120 \text{ MeV}$, $T_{N^*} = 200 \text{ MeV}$

K^+ production:

$BB \rightarrow BYK^+$: Tsushima et al.

nucl-4/9801063

$NN \rightarrow NK^+$, $NN \rightarrow N\Sigma K^+$

$NN \rightarrow \Delta K^+$, $NN \rightarrow \Delta\Sigma K^+$

$N\Delta \rightarrow NK^+$, $N\Delta \rightarrow N\Sigma K^+$

$N\Delta \rightarrow \Delta K^+$, $N\Delta \rightarrow \Delta\Sigma K^+$

$\Delta\Delta \rightarrow \Delta K^+$, $\Delta\Delta \rightarrow \Delta\Sigma K^+$

$\pi B \rightarrow \gamma K^+$

: Tsushima, Huang, Foerster, P-B 337(94)265

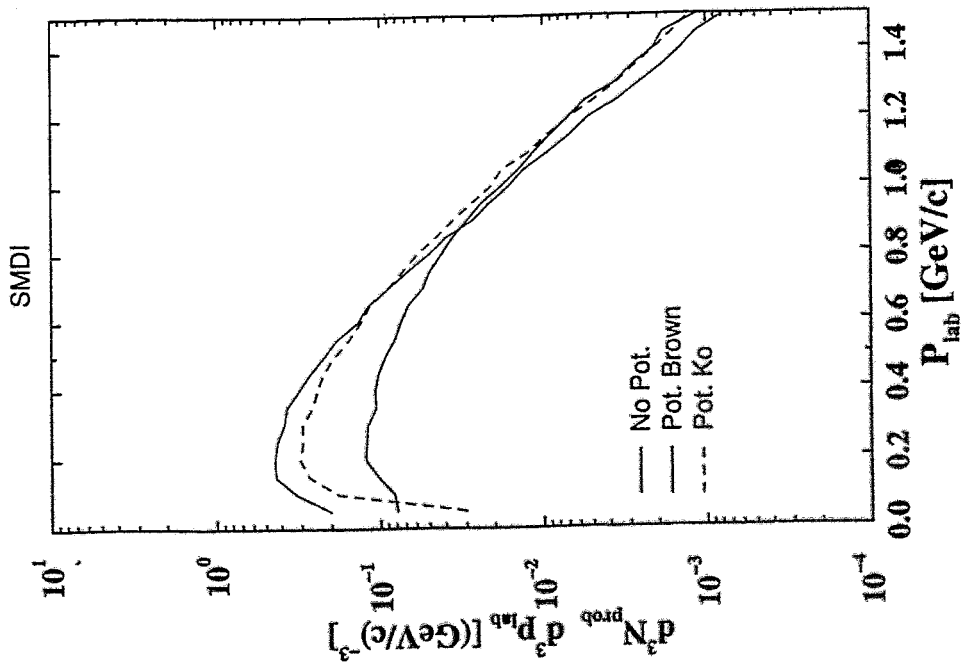
JPG-21(196)33

$\pi N \rightarrow \Sigma K^+$, $\pi N \rightarrow \Sigma K^+$

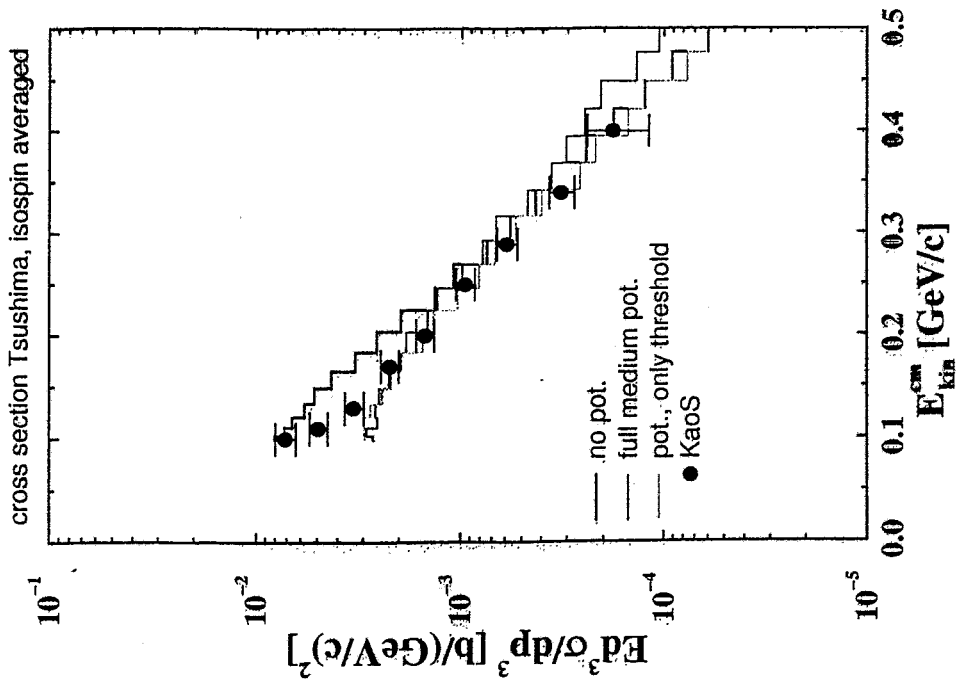
$\pi\Delta \rightarrow \Sigma K^+$, $\pi\Delta \rightarrow \Sigma K^+$

$K^+B \rightarrow K^+B$: Rescattering : Li et al., NPA625(97)372

Ni+Ni, 1.8 A.GeV, b=2fm

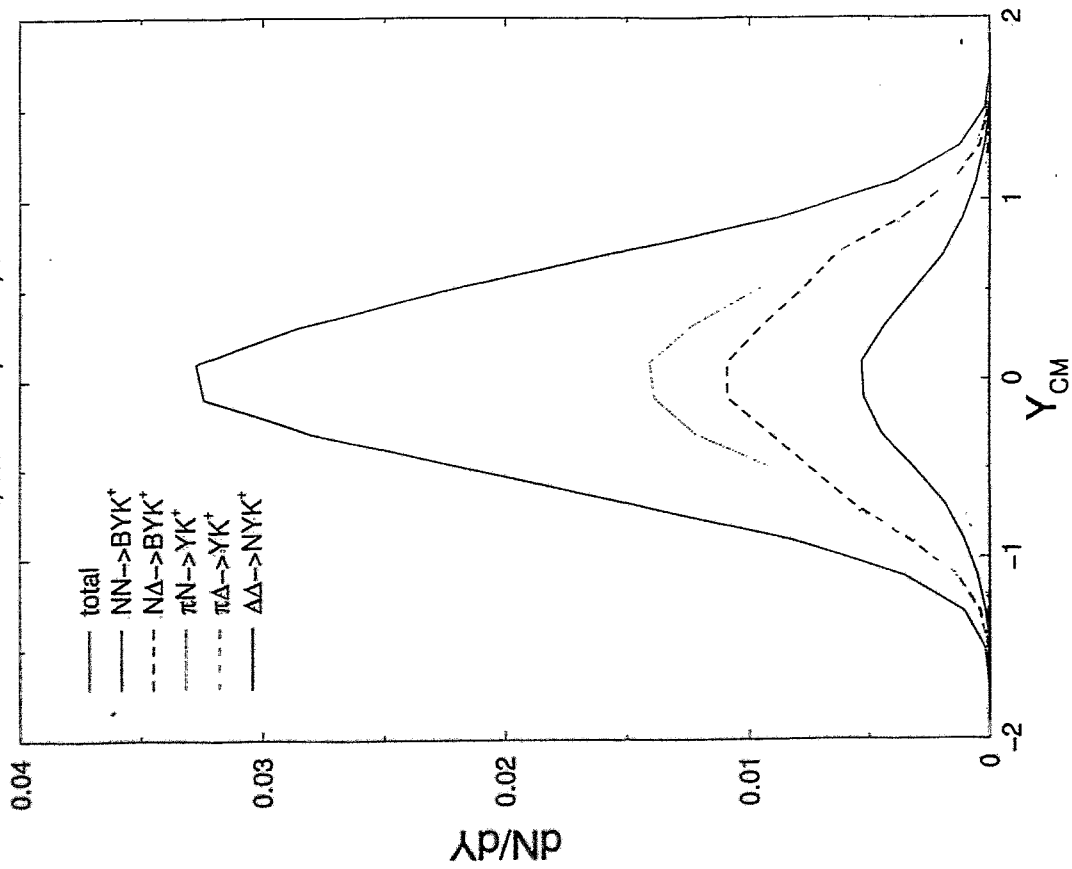


C+C, 2.0 GeV, 40 deg.



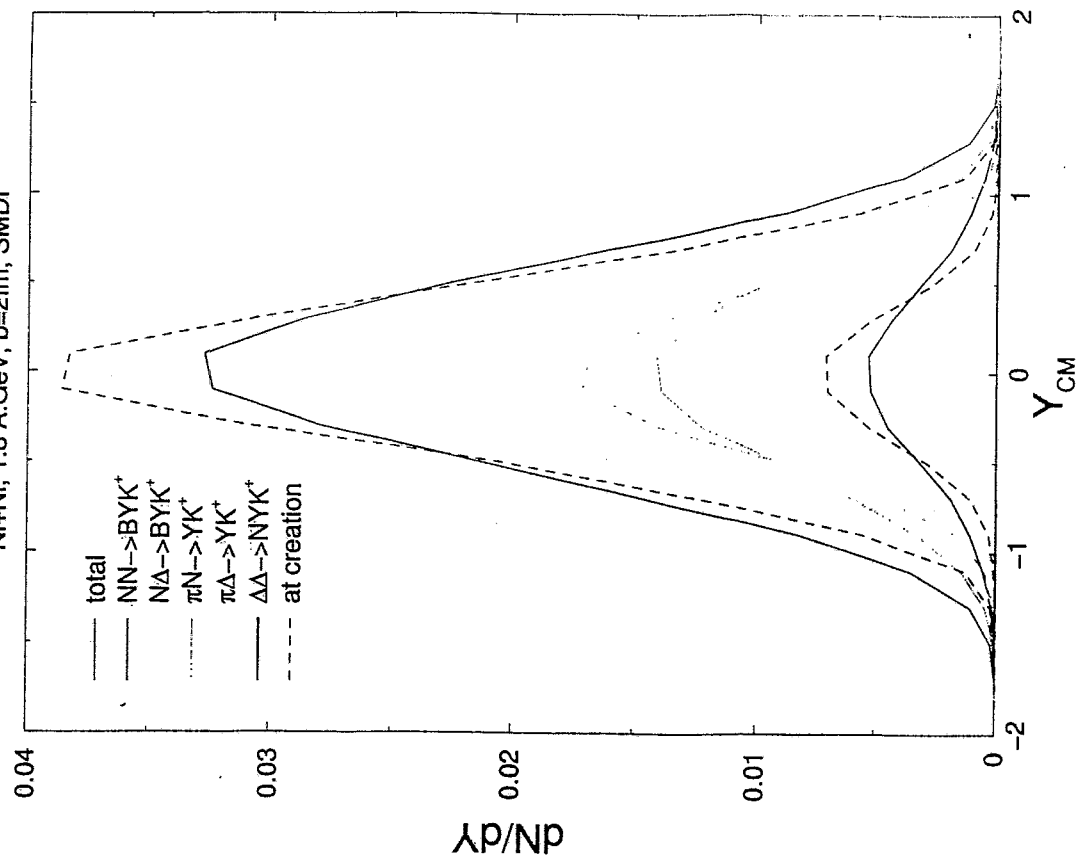
K^+ rapidity dist. , no pot.

Ni+Ni, 1.8 A.GeV, b=2fm, SMDI



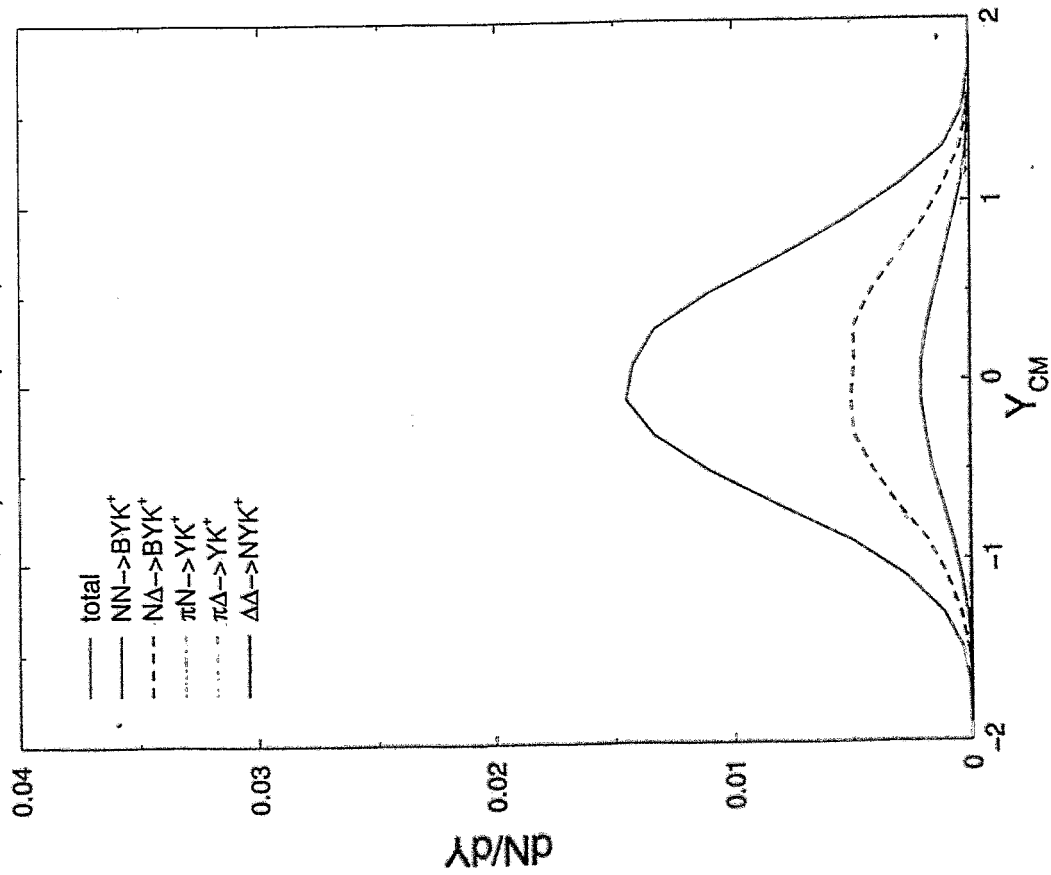
K^+ rapidity final – at creation , no pot.

Ni+Ni, 1.8 A.GeV, b=2fm, SMDI



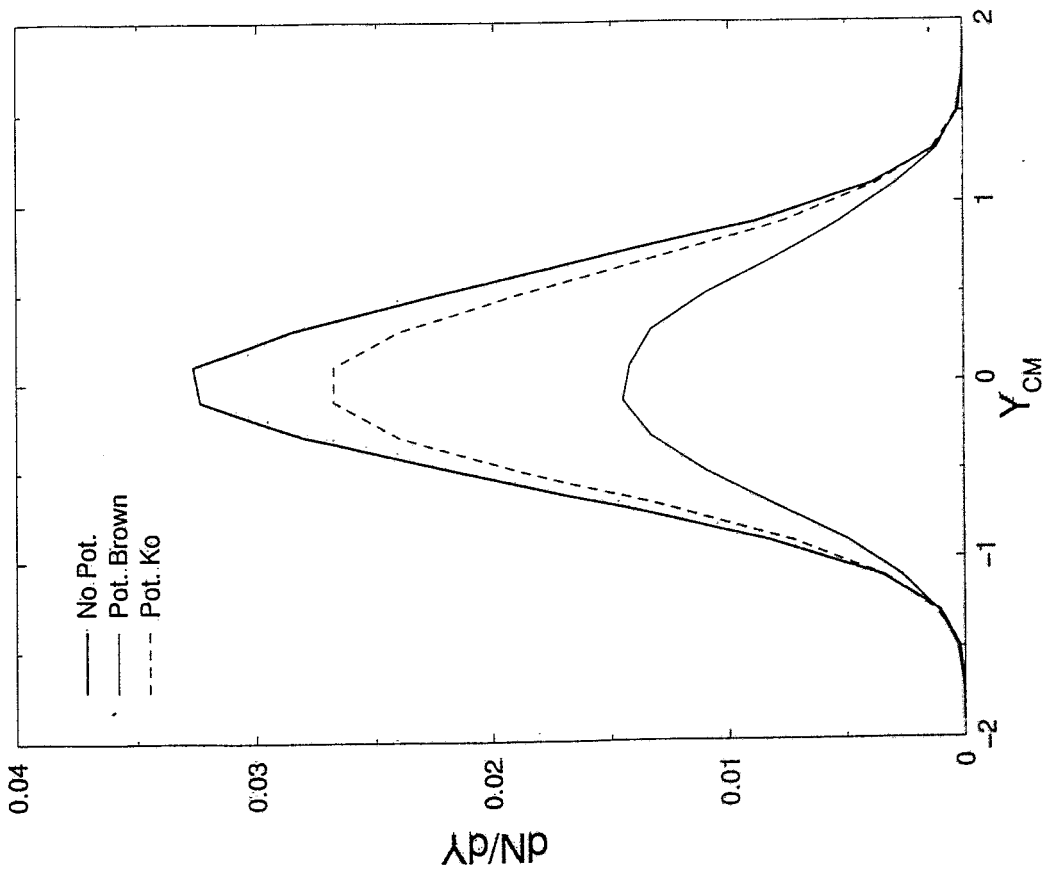
K^+ rapidity dist. , pot. Brown

Ni+Ni, 1.8 A.GeV, b=2fm, SMDI



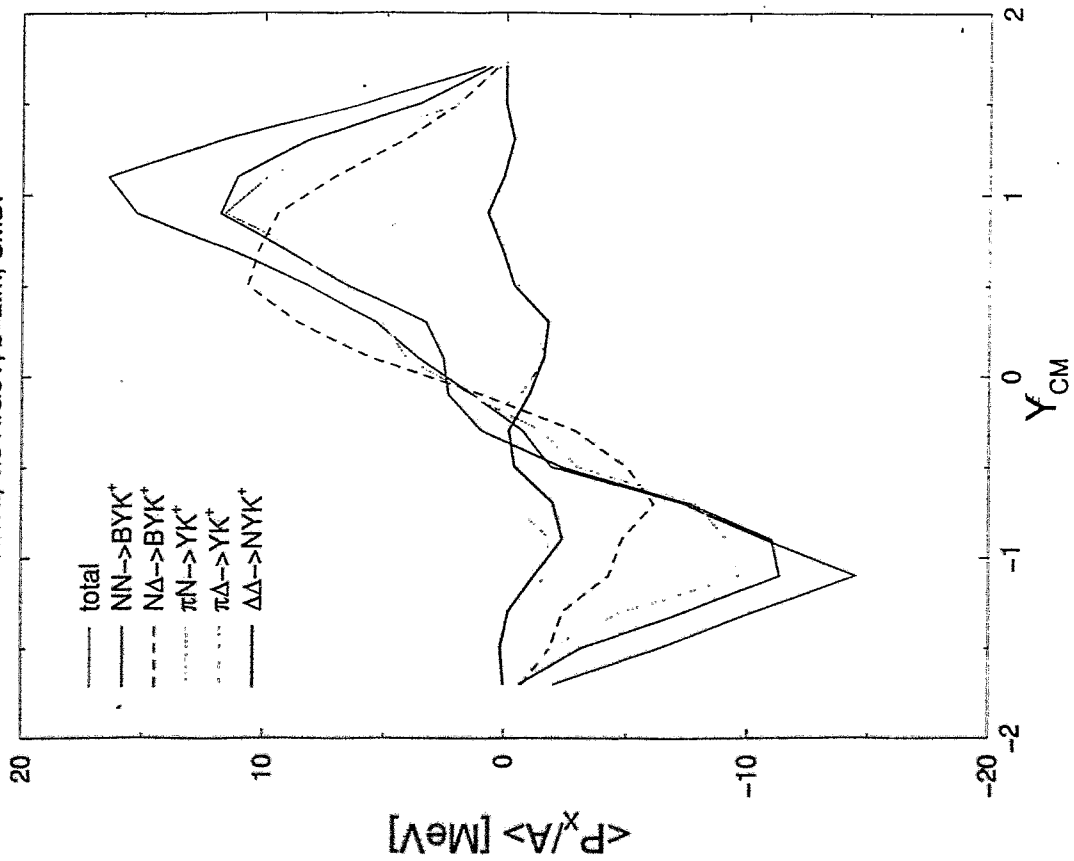
K^+ rapidity

Ni+Ni, 1.8 A.GeV, b=2fm, SMDI



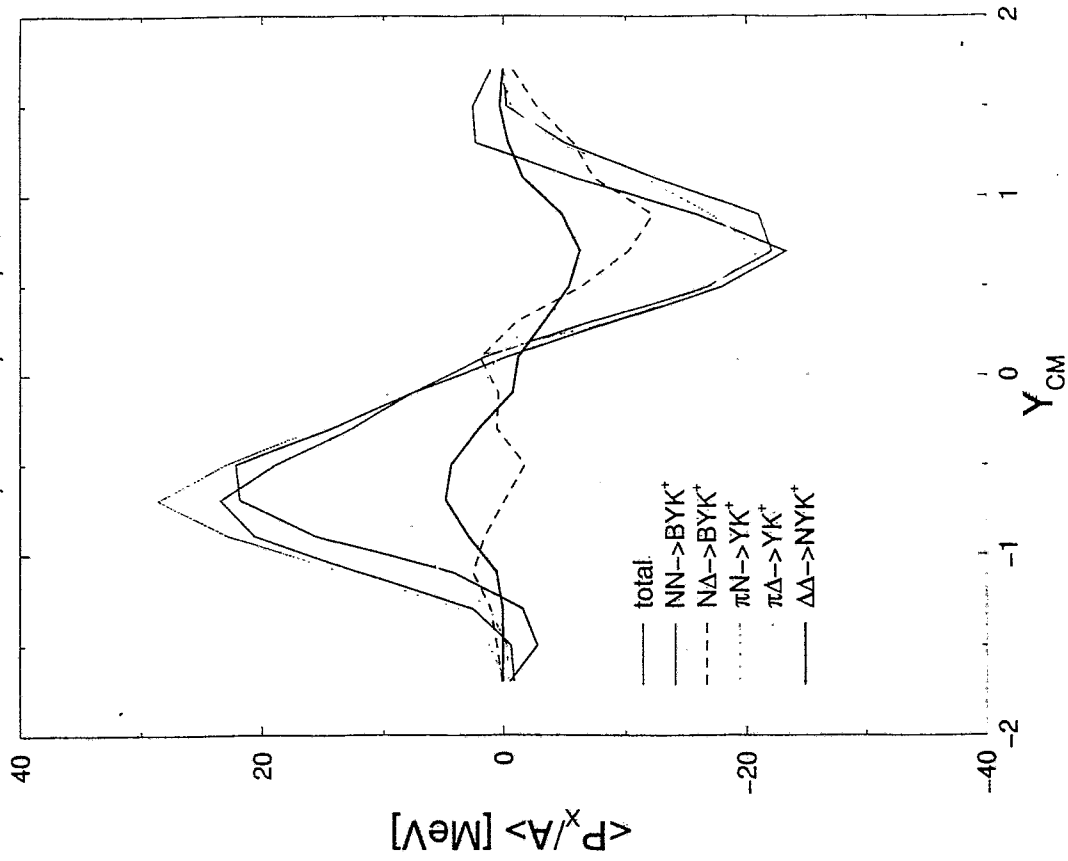
K^+ transverse flow, no pot.

Ni+Ni, 1.8 A.GeV, $b=2\text{fm}$, SMDI

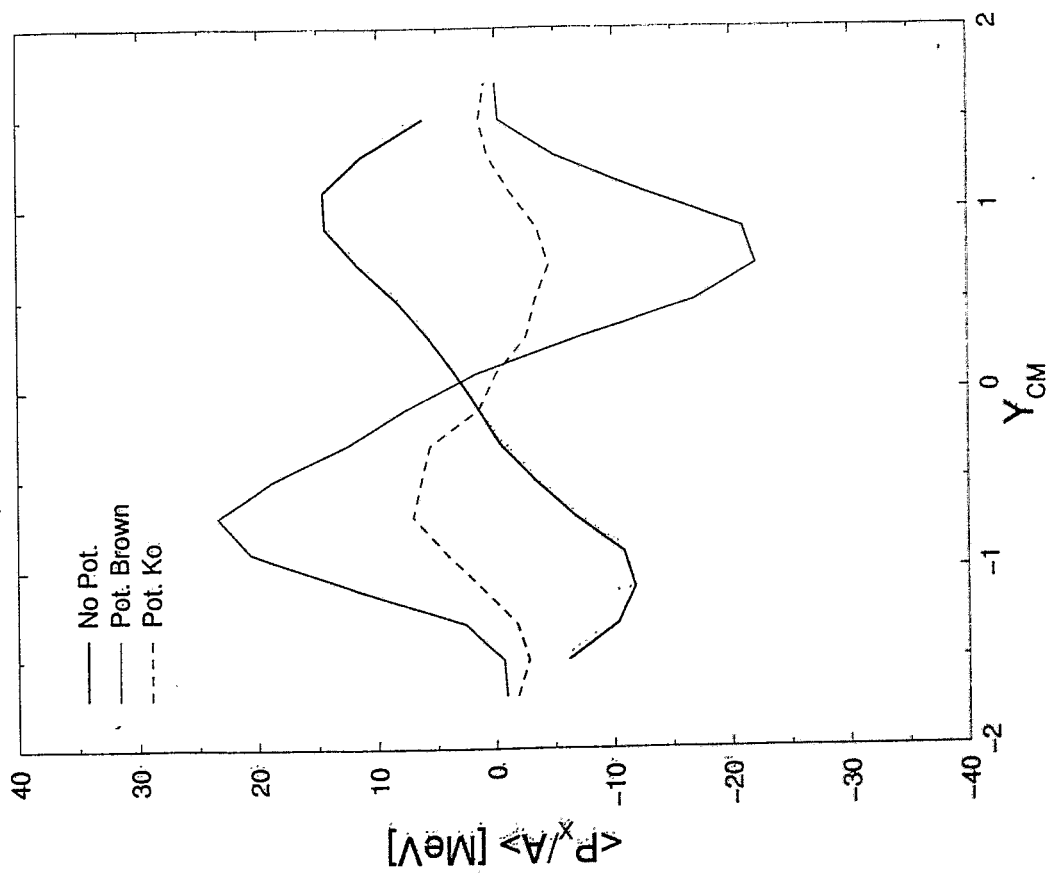


K^+ transverse flow, pot. Brown

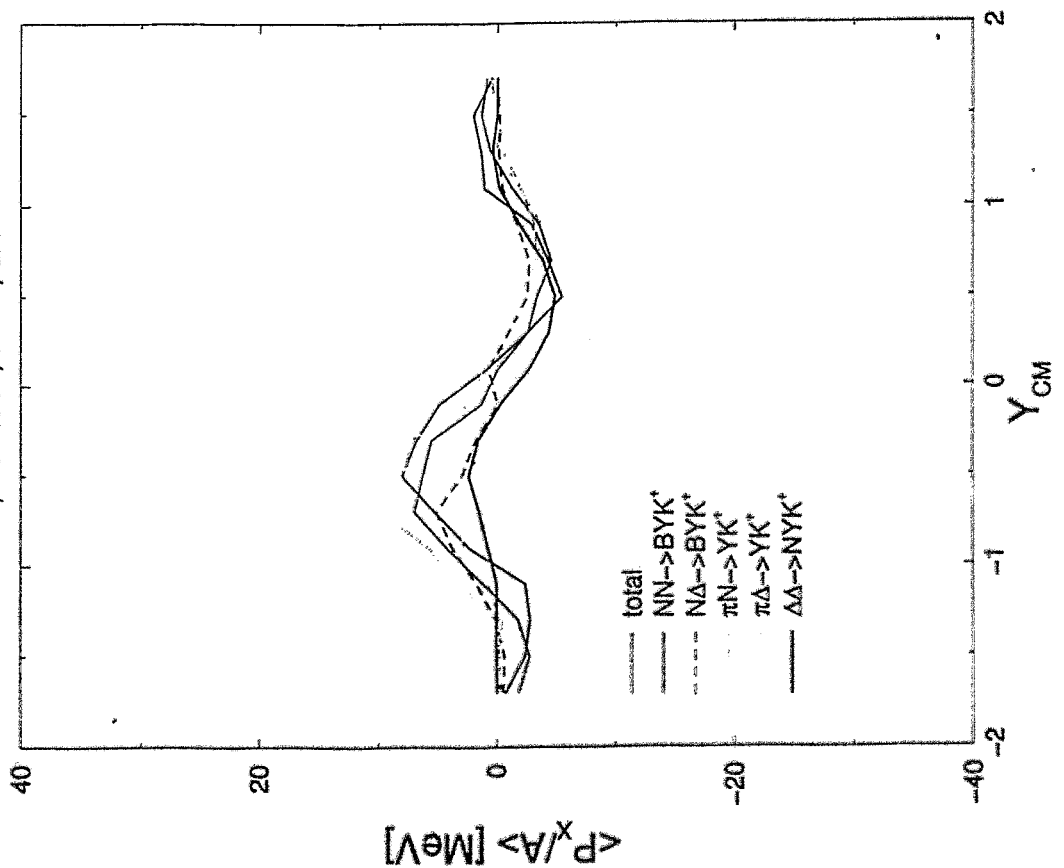
Ni+Ni, 1.8 A.GeV, $b=2\text{fm}$, SMDI



K⁺ transverse flow
 Ni+Ni, 1.8 A.GeV, b=2fm, SMDI



K⁺ transverse flow, pot. Ko
 Ni+Ni, 1.8 A.GeV, b=2fm, SMDI



In-medium potential

Weinberg-Tomozawa

$$V_M = \frac{3}{8\rho^2} j_M$$

Kaplan-Nelson

$$S = \sum_{KK} \frac{g_S}{\rho^2}$$

$$[\partial_\mu \partial^\mu \pm iV_M \partial^\mu + (m^2 - S)] \phi_K = 0$$

Covariant:

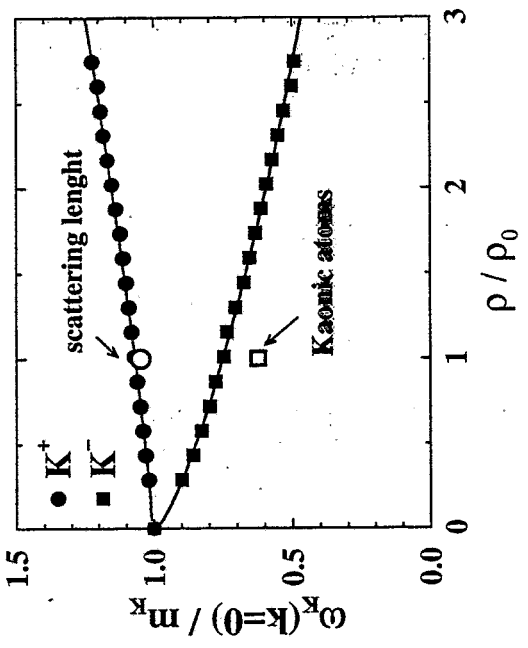
$$[(\partial_\mu \pm iV_M)^2 + (m^2 - S + V^2)] \phi_K = 0$$

$$[(\partial_\mu \pm iV_M)^2 + m^{*2}] \phi_K = 0$$

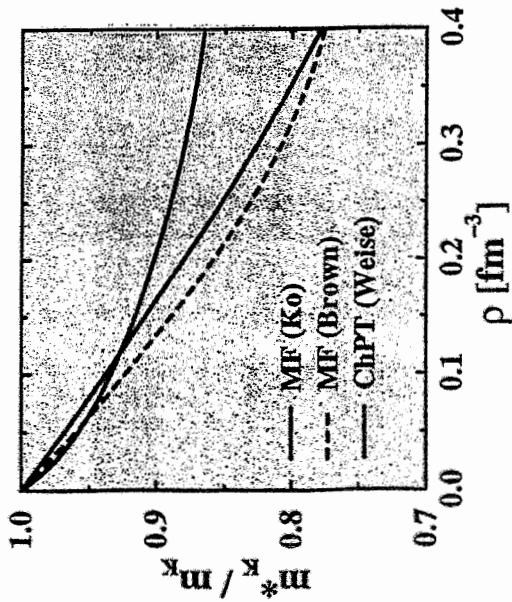
$$[k_\mu^* k^{*\mu} - m^{*2}] \phi_K = 0$$

In-Medium Kaon "Mass"

Waas et al.



In-medium Kaon Mass



$$\frac{d\vec{k}^*}{dt} = \frac{k^*}{m_K^*} \vec{F}^{MD} + \partial_{m_K^*}$$



$$\frac{d\vec{k}^*}{dt} = -\frac{m_K^*}{E^*} \frac{\partial m_K^*}{\partial \vec{q}} \left(\vec{v} \right) \frac{\partial V^0}{\partial \vec{q}} \quad \left. \vphantom{\frac{d\vec{k}^*}{dt}} \right\} -\frac{\partial}{\partial \vec{q}} U$$

$$+ \frac{k^*}{E^*} \vec{E}^* \times \left(\frac{\partial}{\partial \vec{q}} \times \vec{V} \right) \quad \left. \vphantom{\frac{d\vec{k}^*}{dt}} \right\} \text{Lorentz force}$$

Kinetic momenta:

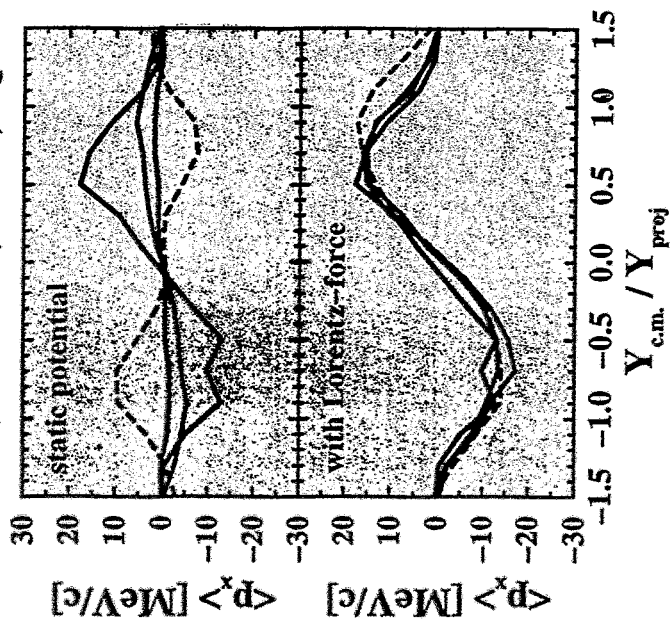
$$\frac{d\vec{k}^*}{dt} = -\frac{m_K^*}{E^*} \frac{\partial m_K^*}{\partial \vec{q}} \left[\vec{v}^0 \pm \beta_1 \frac{\partial V_1}{\partial \vec{q}} \right]$$

$$\approx \pm \frac{3}{8\beta_1^2} (1 - \beta_1 \cdot \beta_N) \frac{\partial \beta_3}{\partial \vec{q}}$$

↑ Kinetic velocities

Influence of Lorentz-Forces on K^+ Flow

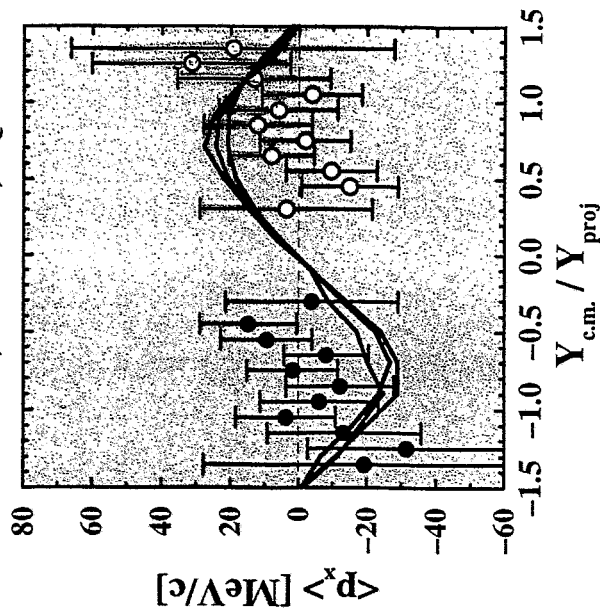
Ni+Ni, 1.93 A.GeV, $b=3$ fm, RQMD



- No pot.
- MF (K0)
- ... MF (Brown)
- ChPT

K^+ Flow (covariant)

Ni+Ni, 1.93 A.GeV, RQMD



- FOPI
- No pot.
- MF (K0)
- ChPT

B. Kämpfer:

Comparison of benchmark tests

Comparison of transport code results

B. KAMPFER

Forschungszentrum Rossendorf

During the preparation of the workshop, J. Alshelmin designed the attached benchmark test for the transport codes. The following theory groups replied by sending to me a lot of data and ps files:

Glessen (W. Cassing, E. Bratkovskaya; RBVU/HSD),

SUNY (C.H. Lee, relying on G.Q. Li's code; RVU),

Nantes (J. Alshelmin, C. Harmaak; QMD),

Frankfurt (S. Sofl and collaborators; UrQMD),

Tuebingen (C. Fuchs; QMD),

Budapest (Gy. Wolf; RVU).

The results have been discussed in the Friday morning session. Here I try to give a compilation of a few comparisons. Note that the groups from Frankfurt, Tuebingen and Budapest focus on K^+ production.

1 Number of pions and deltas

The number of pions and deltas as a function of time is displayed in fig. 1. There are obvious differences in the zero points of time.

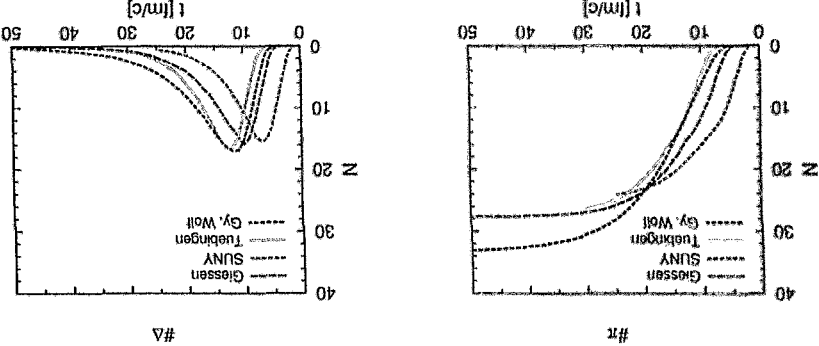


Figure 1: The number of pions (left panel) and deltas (right panel) as a function of time.

2 Elementary cross sections

The cross sections are displayed in figs. 2 - 5. Two groups (Frankfurt, Budapest) have parametrised the $pp \rightarrow p\Lambda K^+$ reaction which describe quite accurately both the

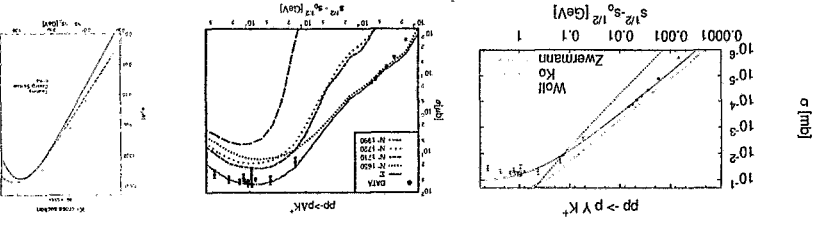


Figure 2: The cross section $pp \rightarrow p\Lambda K^+$ (left panel: Budapest parametrisation, middle: Frankfurt parametrisation, right: Tuebingen (=Tushima)).

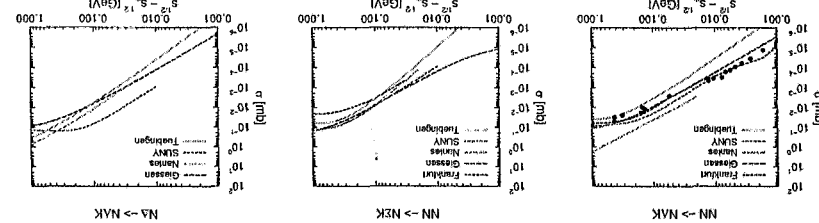


Figure 3: The cross section $NN \rightarrow N\Lambda K^+$.
Figure 4: The cross section $NN \rightarrow N\Sigma K^+$.
Figure 5: The cross section $NN \rightarrow N\Lambda K^+$.

strong point has been made in the discussion by the Glessen group that it would be more appropriate to use the bare production cross sections by removing the final state interaction from the experimental data. The Glessen group is preparing such a parametrisation. As seen in figs. 3 - 5 the elementary cross sections partially deviate noticeably. Reasons for these differences can be the following ones: consistency with previous stages of development of the codes, or compensation for other channels not included explicitly. Sometimes the authors told me that they use the cross sections "as every body", therefore they did not send data files for them. When I display data in the figures (fat dots) one should be aware that these correspond to pp reactions, while the elementary cross sections should refer to isospin averages used in the codes. Due to the too large differences the groups agreed to rely on a unique parameter set in a second round of benchmark test. The Tuebingen and Nantes groups additionally use the cross sections displayed in figs. 23 - 28 instead of the cross sections where in the exit channel a nucleon appears. The Nantes group did not send files for the πX reactions; a few selected points from their input are marked by crosses.

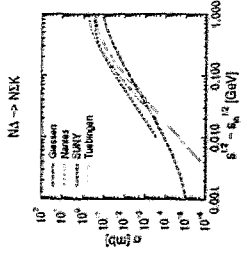


Figure 6: The cross section $N\Delta \rightarrow N\Sigma K^+$.

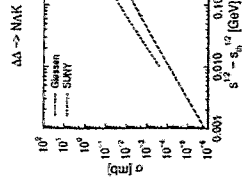


Figure 7: The cross section $\Delta\Delta \rightarrow NAK^+$.

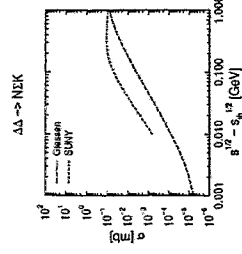


Figure 8: The cross section $\Delta\Delta \rightarrow N\Sigma K^+$.

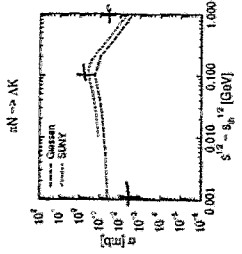


Figure 9: The cross section $\pi N \rightarrow AK^+$.

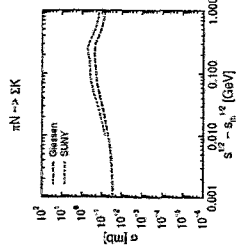


Figure 10: The cross section $\pi N \rightarrow \Sigma K^+$.

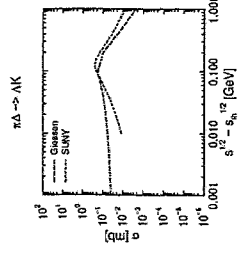


Figure 11: The cross section $\pi\Delta \rightarrow AK^+$.

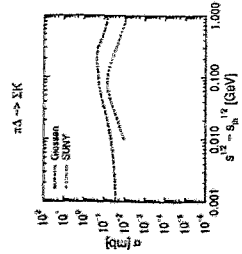


Figure 12: The cross section $\pi\Delta \rightarrow \Sigma K^+$.

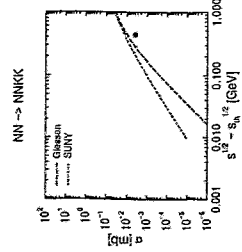


Figure 13: The cross section $NN \rightarrow NNK^+K^-$.

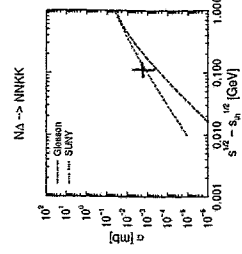


Figure 14: The cross section $N\Delta \rightarrow NNK^+K^-$.

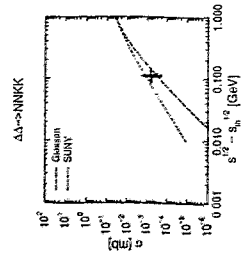


Figure 15: The cross section $\Delta\Delta \rightarrow NAK^+$.

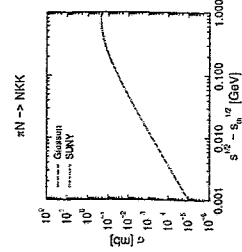


Figure 16: The cross section $\pi N \rightarrow NAK^+$.

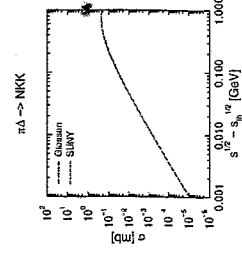


Figure 17: The cross section $\pi\Delta \rightarrow NAK^+$.

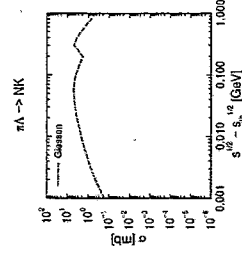


Figure 18: The cross section $\pi A \rightarrow NK^-$.

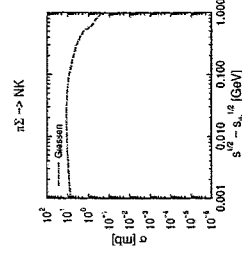


Figure 19: The cross section $\pi\Sigma \rightarrow NK^-$.

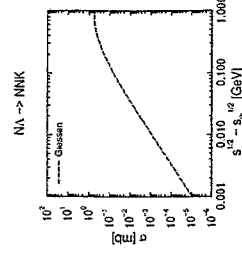


Figure 20: The cross section $N\Delta \rightarrow NNK^-$.

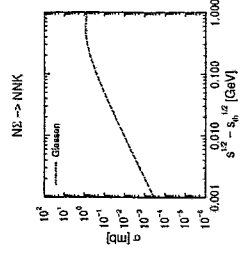


Figure 21: The cross section $N\Sigma \rightarrow NNK^-$.

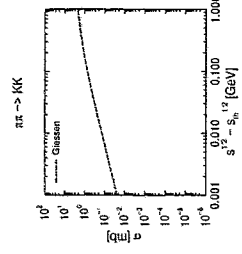


Figure 22: The cross section $\pi\pi \rightarrow K^+K^-$.

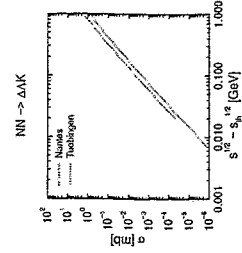


Figure 23: The cross section $NN \rightarrow \Delta AK^-$.

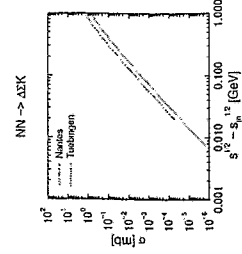


Figure 24: The cross section $NN \rightarrow \Delta\Sigma K^+$.

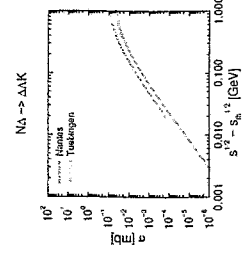


Figure 25: The cross section $N\Delta \rightarrow \Delta AK^-$.

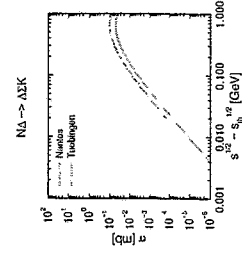


Figure 26: The cross section $N\Delta \rightarrow \Delta\Sigma K^+$.

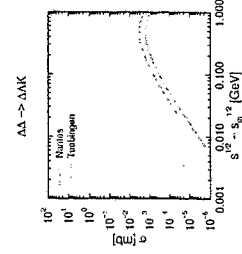


Figure 27: The cross section $\Delta\Delta \rightarrow \Delta AK^+$.

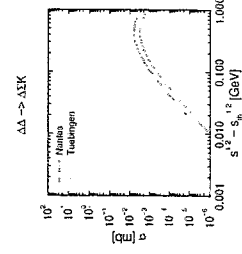


Figure 28: The cross section $\Delta\Delta \rightarrow \Delta\Sigma K^+$.

3 The distribution dN/ds

To see which channels contribute most significantly and which Q values above the corresponding threshold are most important one may inspect the distributions $dN/d\sqrt{s}$ as a function of $\Delta s^{1/2} \equiv s^{1/2} - s_{th}^{1/2}$, displayed in fig. 29. Dominating BB reactions contribute at $\Delta s^{1/2} \sim 300$ MeV in K^+ ($0 - 500$ MeV in K^-) production, while the πB channels have the tendency to peak at small values of $\Delta s^{1/2}$.

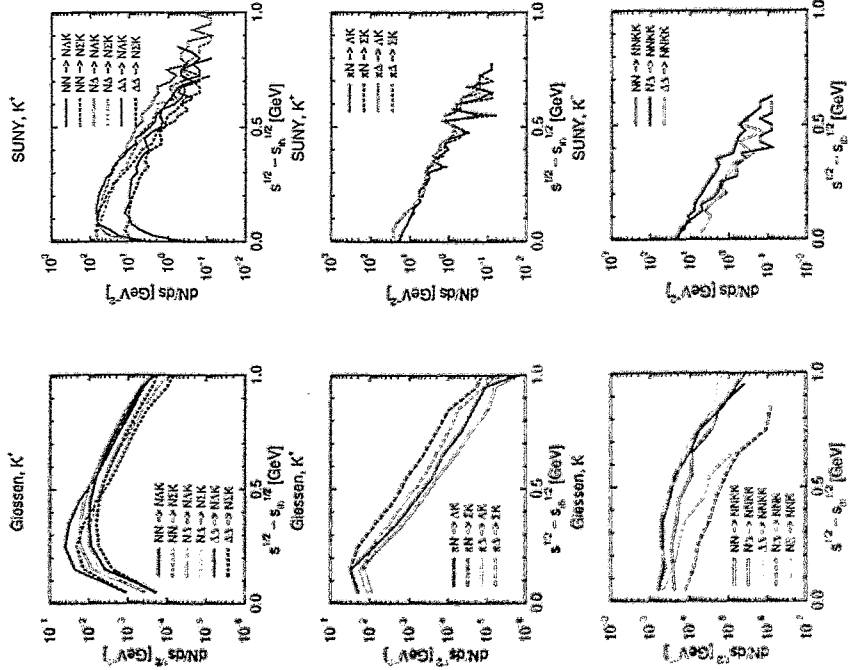


Figure 29: The distribution $dN/ds^{1/2}$ (left panel: Giessen, = probability) and dN/ds (right panel: SUNY, N = collision number) as a function of $\Delta s^{1/2}$.

4 Nucleon flow

The overall nucleon flow and the flow of nucleons involved in kaon production are displayed in fig. 30. The Giessen group communicated that their nucleon flow results are successfully compared in detail with the FOPPI data; the same holds for the Tuebingen results.

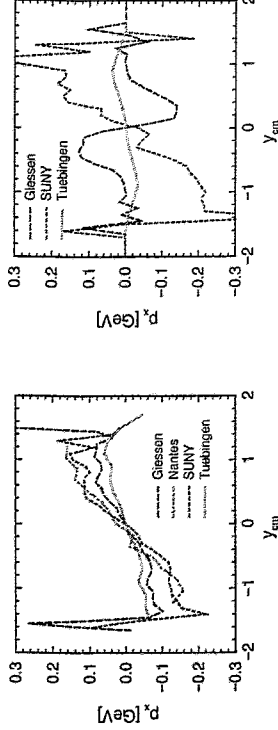


Figure 30: The overall nucleon flow (left panel) and the flow of nucleons involved in kaon production (right panel); the results of the Giessen group are for instant of kaon production, while the groups report results for the final nucleon flow).

5 Rapidity distributions

5.1 At production

The rapidity distributions of bare kaons just in the moment of production are displayed in figs. 31 and 32. Here the summed curves for BB (i.e. baryon-baryon) and MB (i.e. meson (τ)-baryon) channels are displayed. One observes here significant differences, which propagate through the following figures too.

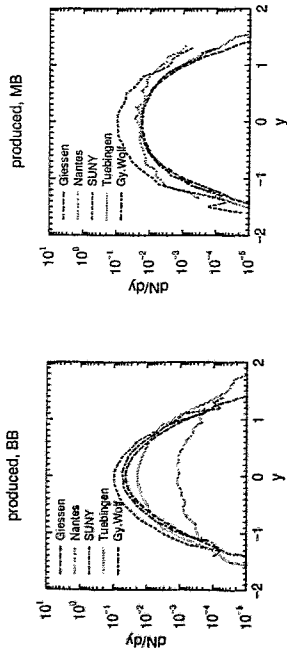


Figure 31: Bare K^+ rapidity distribution at production.

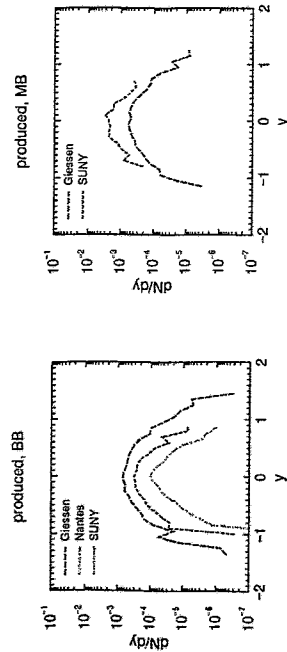


Figure 32: Bare K^- rapidity distribution at production.

5.2 Final distribution

The final rapidity distributions of kaons (with rescattering and in-medium effects) are displayed in figs. 33 and 34.

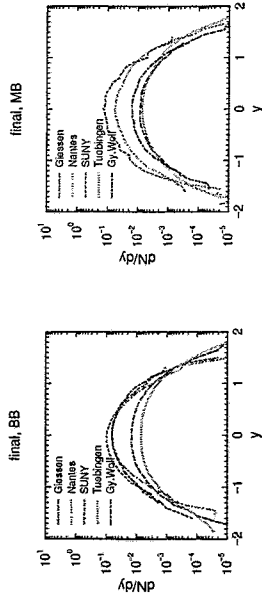


Figure 33: Final K^+ rapidity distribution.

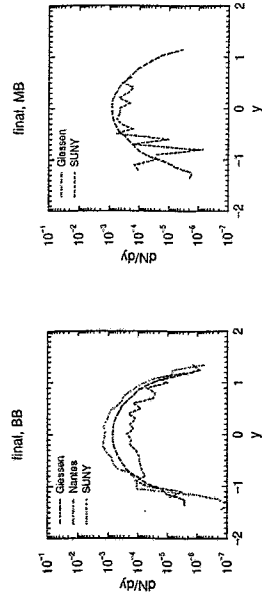


Figure 34: Final K^- rapidity distribution.

6 Transverse momentum distributions

6.1 At production

The transverse momentum distributions of bare kaons at production are displayed in figs. 35 and 36.

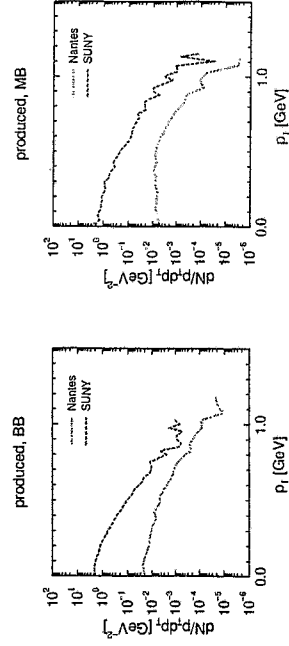


Figure 35: Bare K^+ transverse momentum distribution at production.

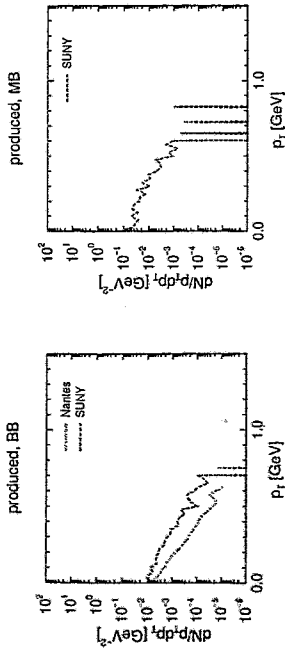


Figure 36: Bare K^- transverse momentum distribution at production.

6.2 Final distribution

The final distributions of kaons (with rescattering and in-medium effects) are displayed in figs. 37 and 38.

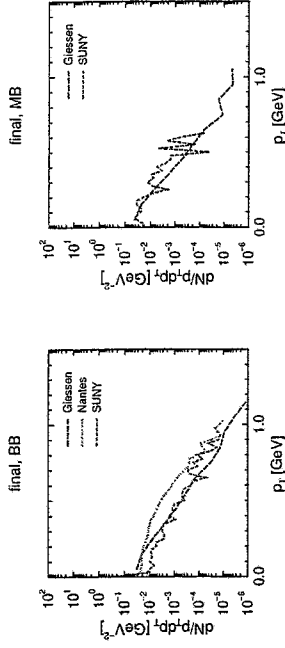


Figure 38: Final K^- transverse momentum distribution.

7 Laboratory transverse momentum distributions

The final laboratory transverse momentum distributions for $\Theta_{lab} = (44 \pm 6)^\circ$ are displayed in figs. 39 and 40 (with rescattering and in-medium effects).

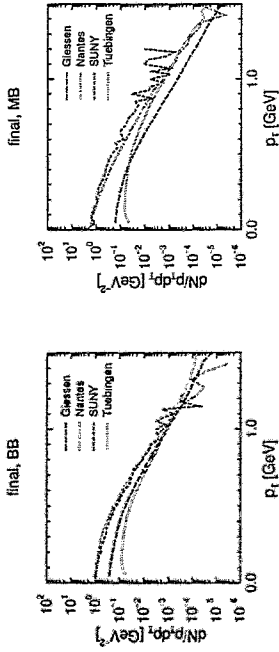


Figure 37: Final K^+ transverse momentum distribution.

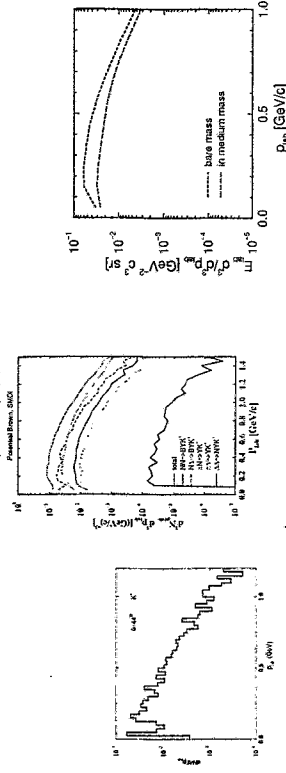


Figure 39: Final K^+ transverse momentum distribution in the lab system (SUNY, Tübingen, Giessen from left to right; the results are obviously differently normalized).

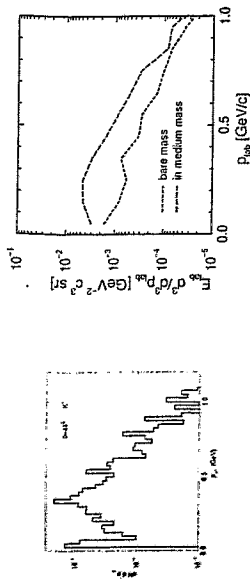


Figure 40: Final K^- transverse momentum distribution in the lab system (left [right] panel: SUNY [Giessen]); the results are obviously differently normalized).

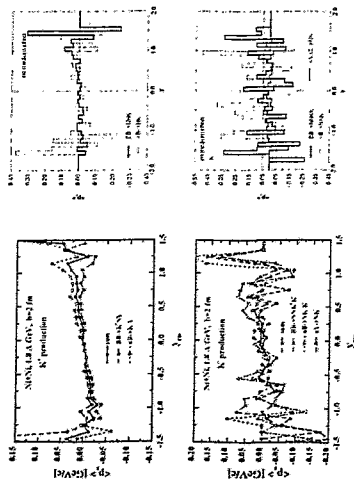


Figure 41: Bare K^\pm flow at production (left [right] panel: Giessen [SUNY]).

8 Kaon flow

Results of the kaon flow are displayed in figs. 41 and 42.

9 Concluding remarks

This is a rough survey on a part of results I received from the active groups. There are obvious differences which must be discussed and clarified in a second round of test calculations relying on a unique input (elementary cross sections).

I hope that in the process of a unifying representation I did not mess up too many data. In a few places one observes obvious different normalizations employed; in a few cases I was asked to scale up/down some contributions and I tried to do so or to indicate in the figure captions these desires.

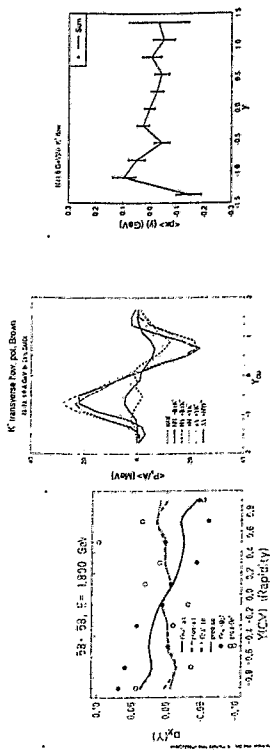


Figure 42: Final K^+ flow (form left to right: Nantes [pion channels must be upscaled by a factor four], Tuebingen, Frankfurt).

Big efforts have been made by the participating groups, and the workshop organizers are grateful to all activists for their attempts. I thank K. Gallmeister for assisting me in the preparation of the figures.

Attachment

KAON WORKSHOP
December 10 – 11, 1998
Forschungszentrum Rossendorf near Dresden
(homework for transport models)
J. Aichelin

In recent times it has been observed that the results of the simulations of the K^+ and K^- production in heavy ion collisions differ much more than expected from fluctuations. Therefore we find it appropriate to ask all groups which work in this field to discuss with us the details of their approaches in order to understand more about the origin of the differences. For this purpose we would like to invite you to come to Rossendorf.

Of course a comparison is only meaningful if all groups present results on a reaction which can be compared. We have chosen the reaction

Reaction : $1.8 \text{ GeV}/N \text{ Ni} + \text{Ni b} = 2 \text{ fm}$, $\Gamma_{\text{delta}} = 120 \text{ MeV}$ energy independent.

In order to allow for a meaningful comparison between the programs and to find the differences of the different programs as fast as possible we would like to ask you to communicate the numbers and spectra to Burkhard Kampfer (kempfer@fz-rossendorf.de) until 4th of December. All quantities should be in mb and GeV and for K^+ resp K^- production only. (Please do not include the K^0 's).

It would be preferable if you can send PS files as well as data files. This would allow to prepare figures which contains the results of the different groups.

A) K^+ PRODUCTION

- 1) Which of the following processes are included
 - a) $NN \rightarrow NAK$ b) $NN \rightarrow N\Sigma K$
 - c) $N\Delta \rightarrow NAK$ d) $N\Delta \rightarrow N\Sigma K$
 - e) $\Delta\Delta \rightarrow NAK$ f) $\Delta\Delta \rightarrow N\Sigma K$
 - g) $\pi N \rightarrow AK$ h) $\pi N \rightarrow \Sigma K$
 - i) $\pi\Delta \rightarrow AK$ k) $\pi\Delta \rightarrow \Sigma K$
- 2) Fig. of the isospin average cross section for (γ -log scale) of a-k (if included in your calculation) as a function of $\sqrt{s} - \sqrt{s_{threshold}}$.
- 3) Time integrated kaon production probability and number of collisions for the processes a-k.
- 4) $\frac{dN_{prod}}{dV_s}$ for the processes a-k as a function of $\sqrt{s} - \sqrt{s_{threshold}}$ (γ -log scale)
- 5) Rapidity distribution $\frac{dN_{prod}}{dy}$ of kaons immediately after creation for πB (g-k) and BB (a-f) collisions separately (N_{prod} = number of kaons weighted with their production probability).
- 6) Transverse momentum distribution $\frac{dN_{prod}}{P_T dy}$ of the kaons (γ -log scale) separated for a-g and h-k
- 7) In plane flow ($p_T(y)$) as a function of y of the kaons separated for a-g and h-k.
- 8) In plane flow for all nucleons and separately for those which are involved in a kaon production collision.
- 9) Number of pions and deltas as a function of time.

B. FINAL K^+ DISTRIBUTION

- 1) Final kaon rapidly distribution $\frac{dN_{prod}}{dy}$ separated for a-g and h-k without KN potential (rescattering only).
- 2) Same as 1) but with KN optical potential (if included in the program)

3) Final transverse momentum distribution $\frac{dN_{prod}}{P_T dy}$ separated for a-g and h-k without KN potential.

4) Same as 3) but with KN optical potential.

5) $\frac{dN_{prod}}{d^2p_{sub}} (\theta_{sub} = 44 \pm 6^\circ)$ (γ -log scale)

C. K^- PRODUCTION

1) Which of the following production processes are included?

- l) $NN \rightarrow NNK^+K^-$
- m) $N\Delta \rightarrow NNK^+K^-$
- n) $\Delta\Delta \rightarrow NNK^+K^-$
- o) $\pi N \rightarrow NK^+K^-$
- p) $\pi\Delta \rightarrow NK^+K^-$

2) Same as A) 2-8 for l-n and o-p, respectively.

3) Same as B) 1-5 for l-n and o-p, respectively.

For questions please contact Joerg Aichele (Aichele@subatech.in2p3.fr), tel. +33 (0) 251 85 84 09.

E.E. Kolomeitsev:

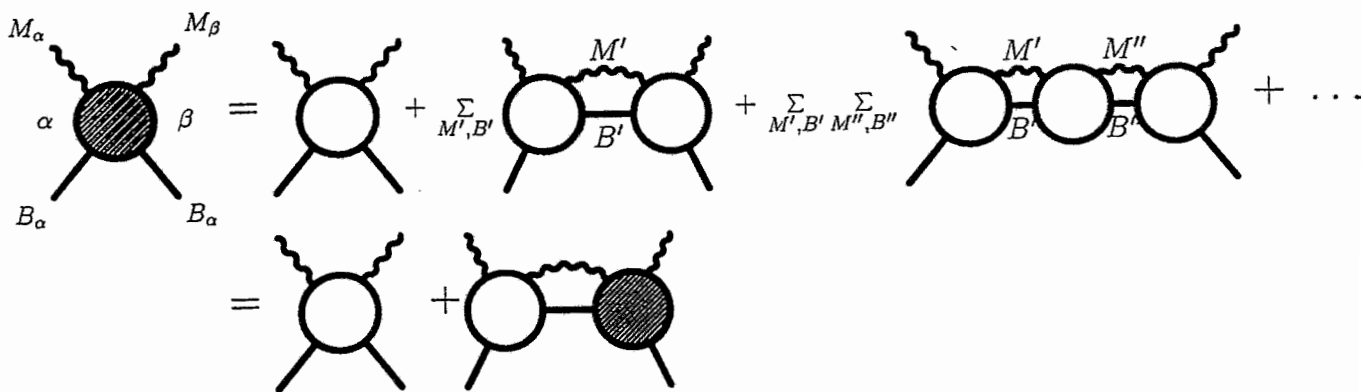
Kaonic excitation in HICs

Kaonic Excitations in HIC

M. Lutz , E.E.K. , D.N. Voskresensky , B. Kämpfer
(GSI, MEPhI, FZR)

- ✓ World of KN interaction
- ✓ Kaon In-medium Dynamics
- ✓ "Scaled mass" vs. Spectral Density
- ✓ Strangeness in HIC

Coupled Channel Equations



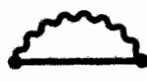
Ingredients:

- CHANNEL SET $\{M_\alpha, B_\alpha\}$ $\alpha = 1, 2 \dots$ (KN ; $\pi\Sigma$; $\pi\Lambda \dots$)

- BARE COUPLINGS



- LOOP REGULARIZATION



$$\rightarrow \int_0^\Lambda \frac{d^4 p}{(2\pi)^4} \dots,$$

Λ cut-off parameter

Model Solution of Coupled Channel Equation

Matrix equation

$$T = V + (V \cdot J \cdot T)$$

Isospin 0 : channels $\{KN, \pi\Sigma\}$

Isospin 1 : channels $\{KN, \pi\Sigma, \pi\Lambda\}$

can be solved analytically in the approximations

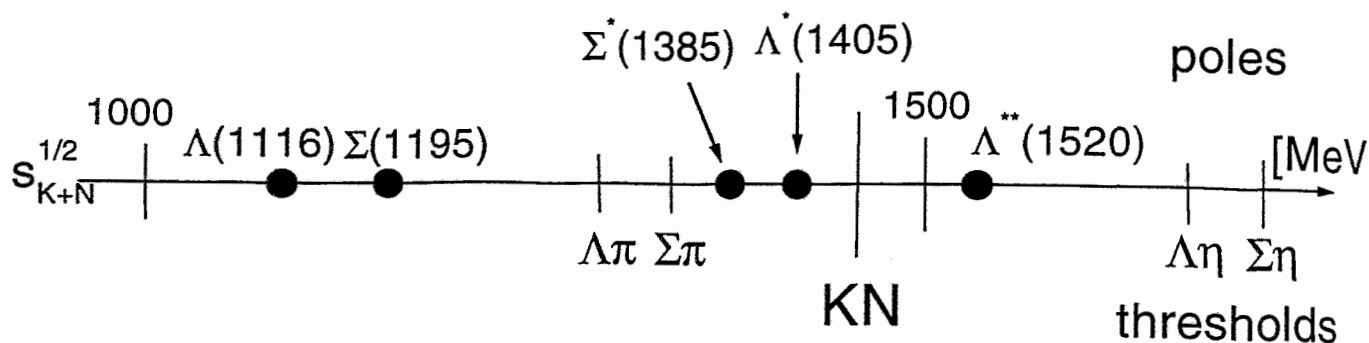
$$V = V(s) = V_0 + R s \text{ where } R \text{ is range term}$$

Parameters V_0 and R are adjusted to reproduce experimental data on $K^- p \rightarrow K^- p, \rightarrow \bar{K}^0 n, \rightarrow \pi^{\pm 0} \Sigma^{\mp 0}, \rightarrow \pi^0 \Lambda$ scattering for $I=0$

$$T = \begin{pmatrix} T_{KN;KN} & T_{KN;\pi\Sigma} \\ T_{\pi\Sigma;KN} & T_{\pi\Sigma;\pi\Sigma} \end{pmatrix} \quad V = \begin{pmatrix} V_{KK} & V_{K\Sigma} \\ V_{K\Sigma} & V_{\Sigma\Sigma} \end{pmatrix} \quad J = \begin{pmatrix} J_{KN} & 0 \\ 0 & J_{\pi\Sigma} \end{pmatrix}$$

$$T_{KN \rightarrow KN}^{(0)} = \frac{V_{KK} + \frac{V_{K\Sigma}^2 J_{\pi\Sigma}}{1 - V_{\Sigma\Sigma} J_{\pi\Sigma}}}{1 - V_{KK} J_{KN} - \frac{V_{K\Sigma}^2 J_{\pi\Sigma}}{1 - V_{\Sigma\Sigma} J_{\pi\Sigma}} J_{KN}}$$

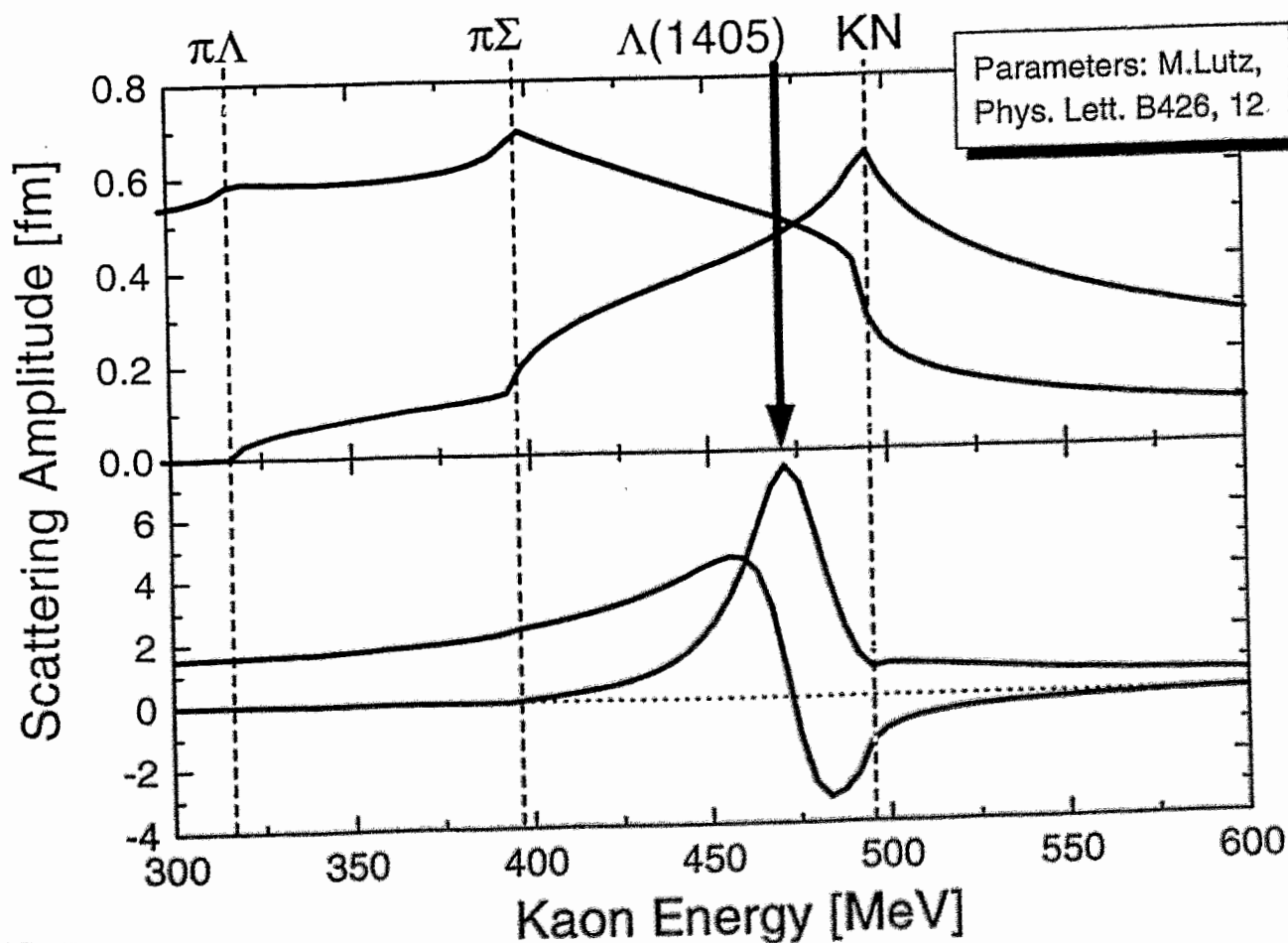
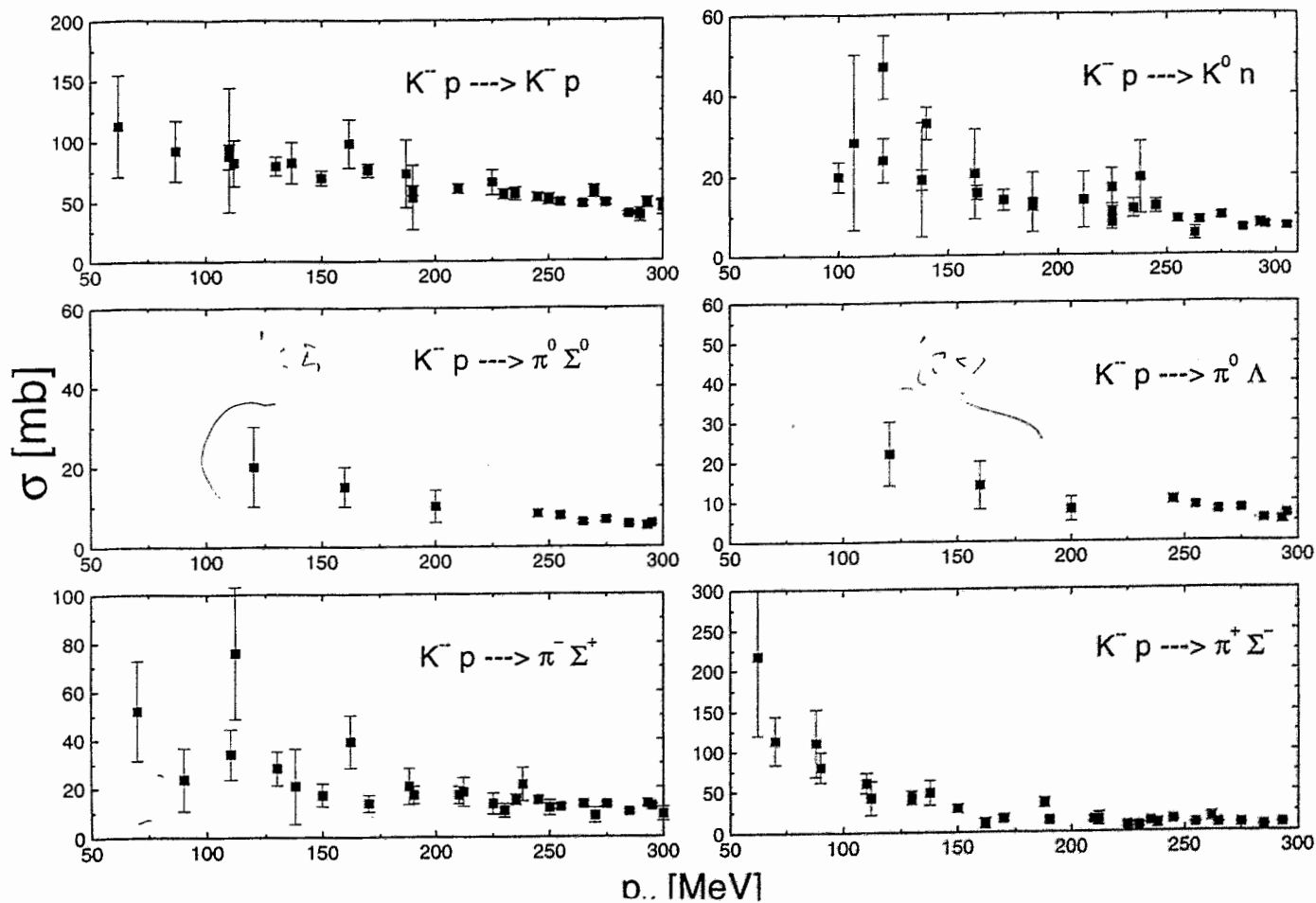
World of K^-N interaction



S wave : $\Lambda^*(1405) \leftarrow \Sigma\pi, KN, \Lambda\eta$ thres. dynamics

P wave : $\Lambda(1116), \Sigma(1195), \Sigma^*(1385)$

D wave : $\Lambda^{**}(1520)$

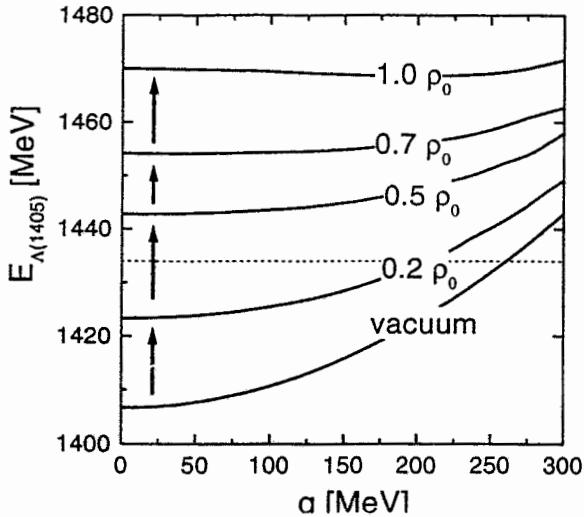


$\Lambda(1405)$ in Medium. Pauli Blocking

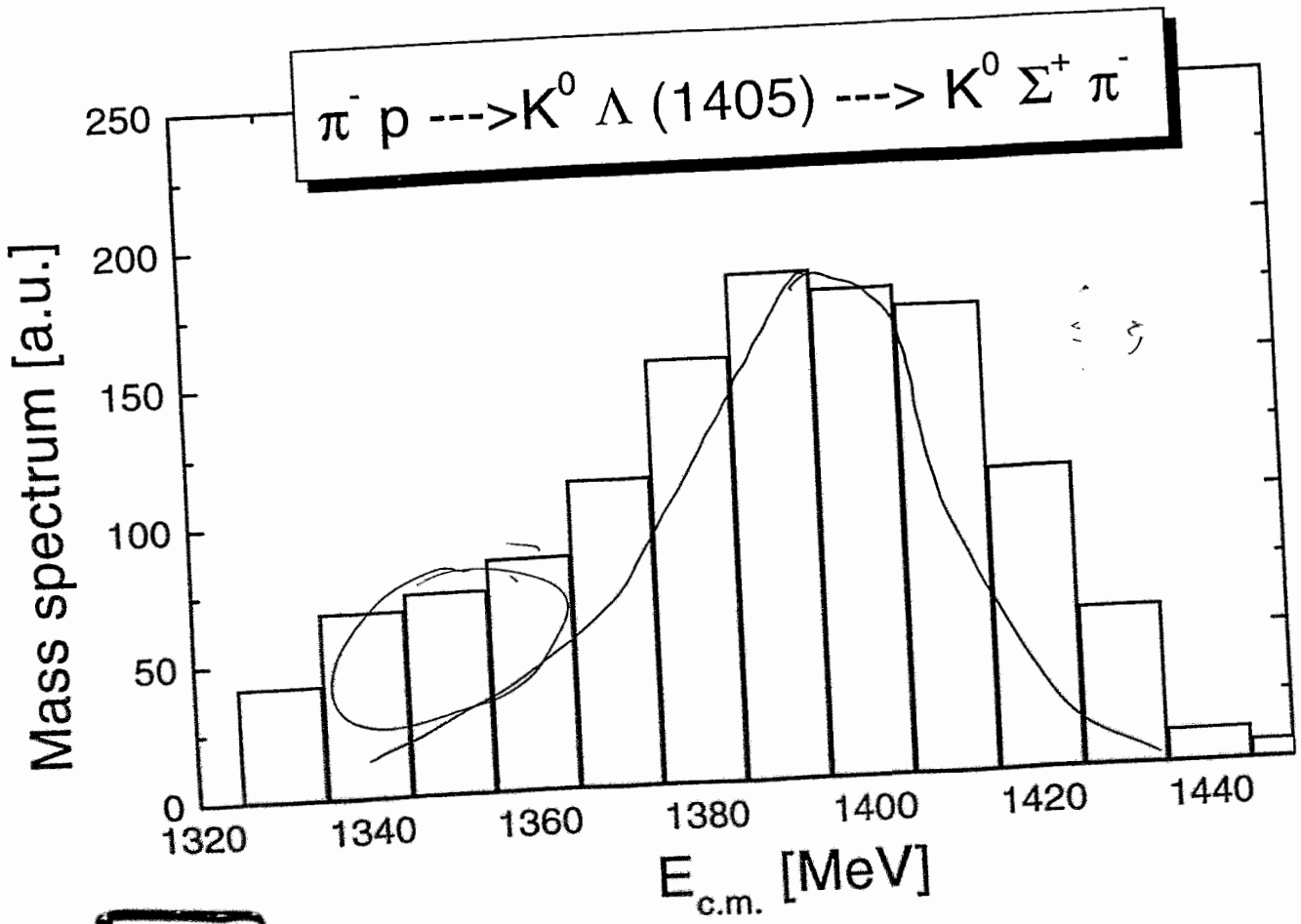
Equation for the Bound State

$$\text{Re} \left\{ 1 - V_{KK} \underline{J}_{KN} - \frac{V_{K\Sigma}^2 J_{\pi\Sigma}}{1 - V_{\Sigma\Sigma} J_{\pi\Sigma}} J_{KN} \right\} = 0$$

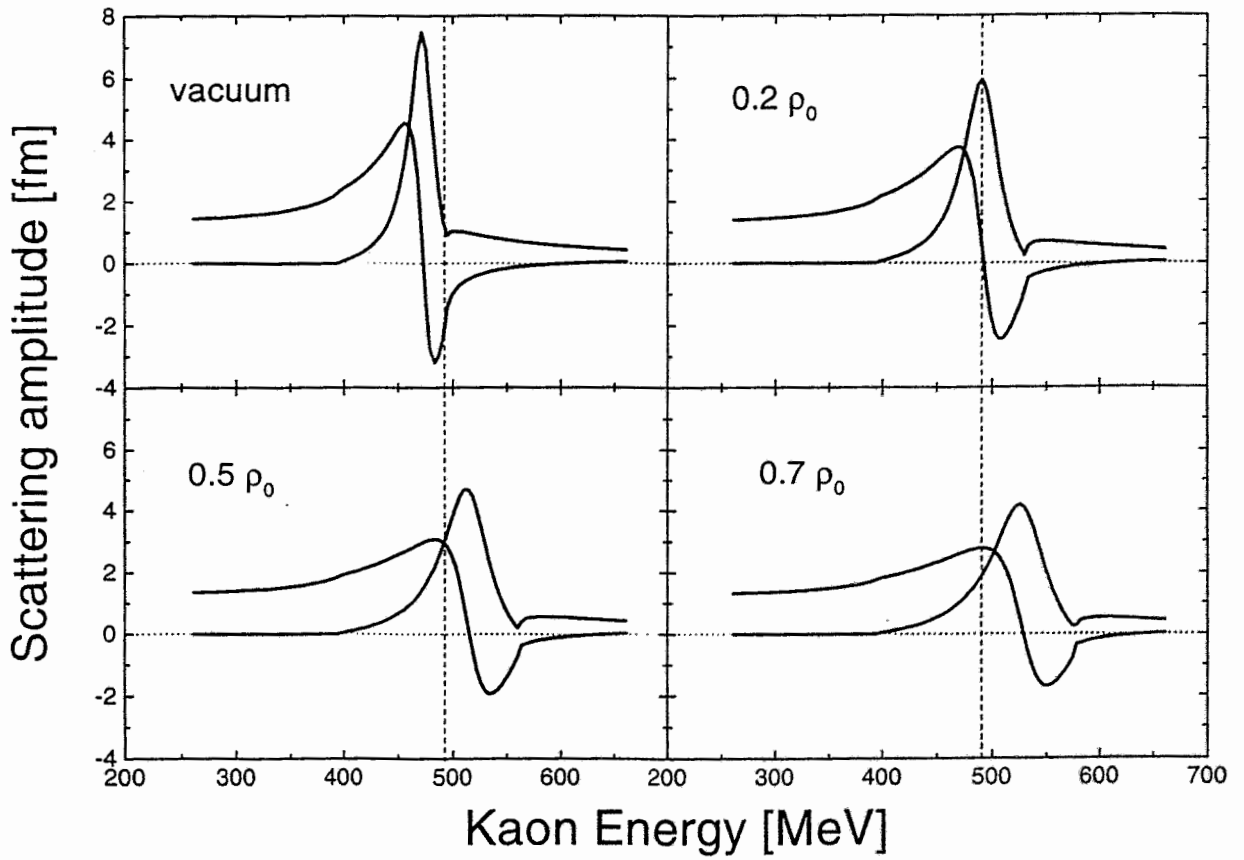
in nuclear medium $J_{KN}(s) \rightarrow J_{KN}(\omega, q) = \int_{p_F}^{\Lambda} \frac{d^3 p}{(2\pi)^3} \frac{m_N}{E_N(p)} D_K^{\text{vac}}(\omega - E_N(p), \vec{q} - \vec{p})$



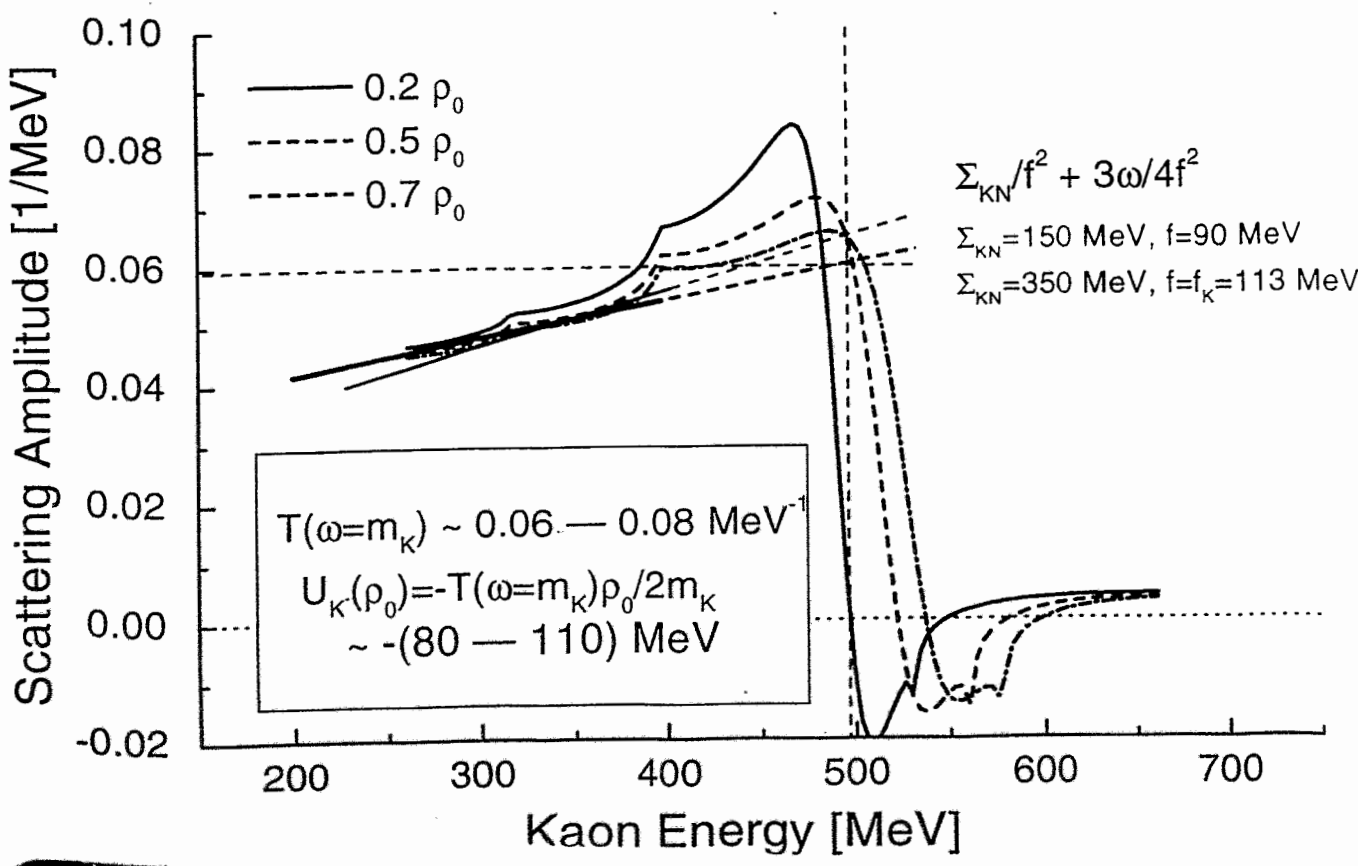
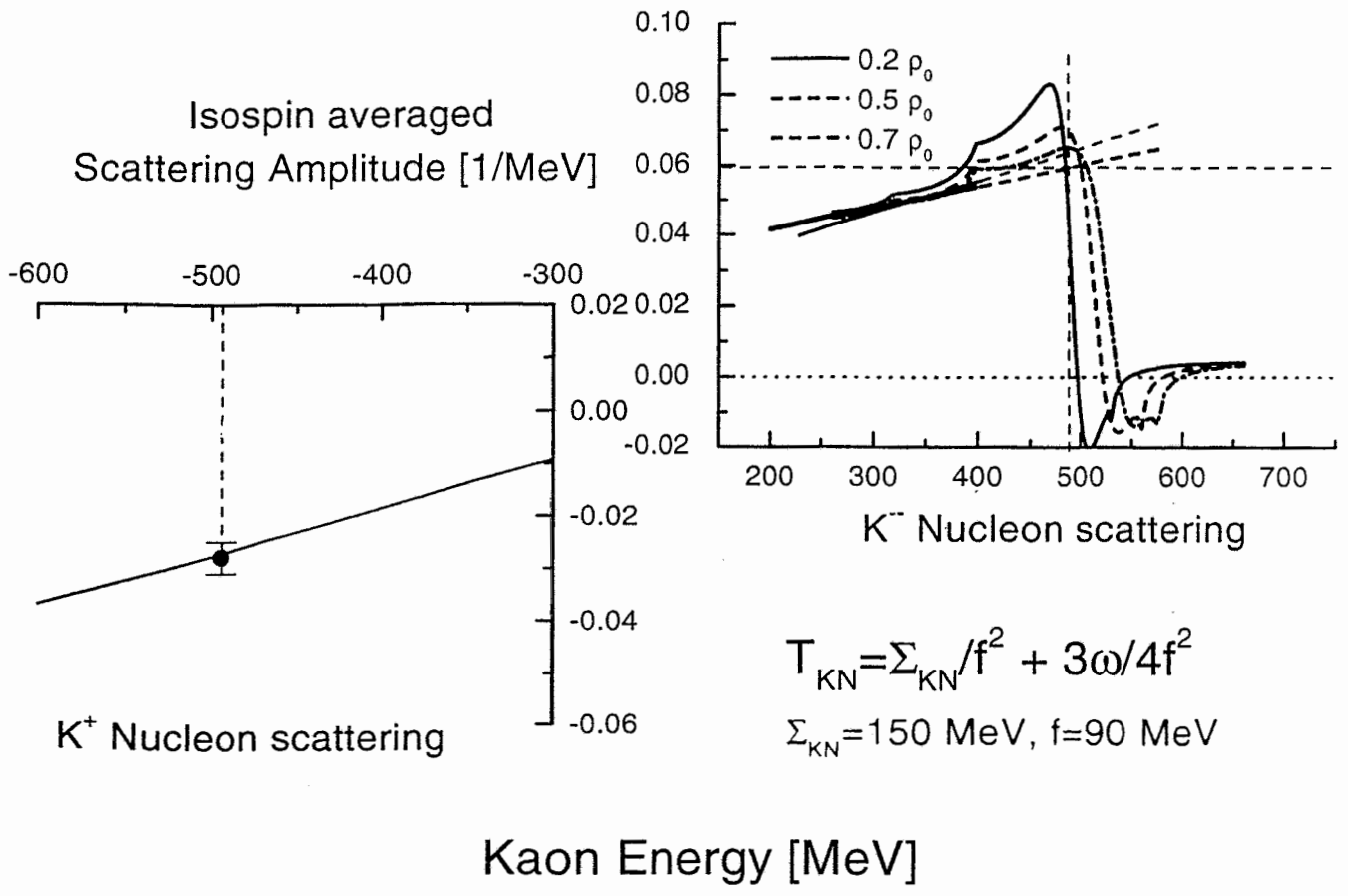
Pole position is shifted above KN threshold



Anti-Kaon Nucleon (Isospin=0) $q=0$

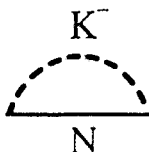


Due to the Pauli blocking
 $\Lambda(1405)$ moves above KN threshold

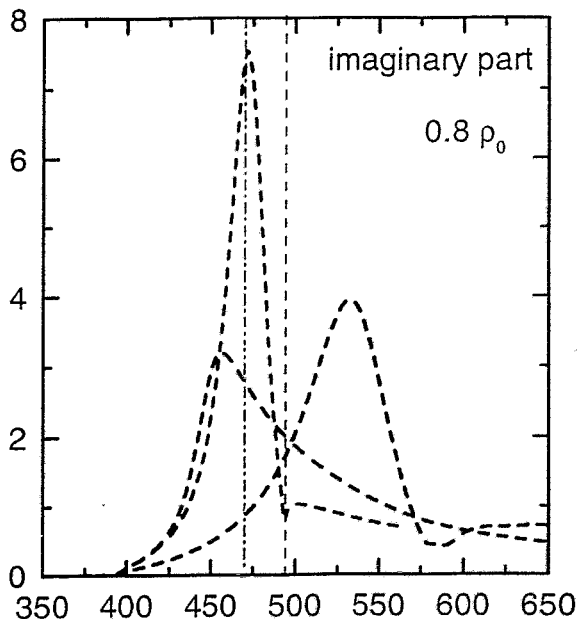
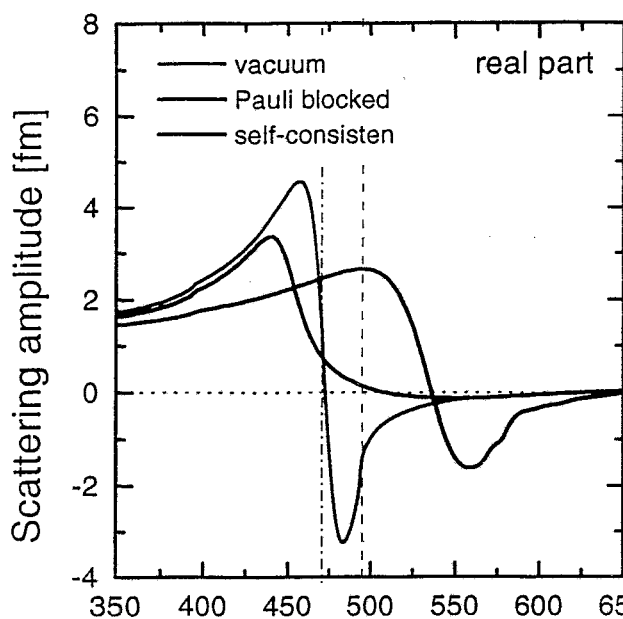


Self-Consistent Amplitude

Kaon Nucleon Loop



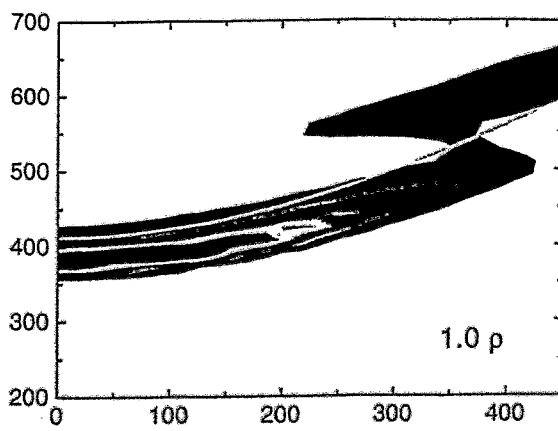
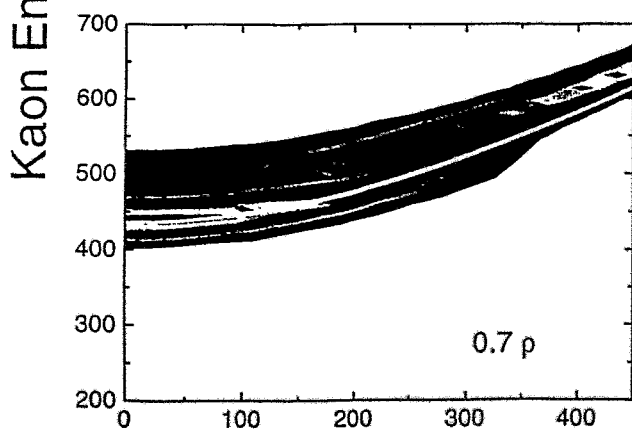
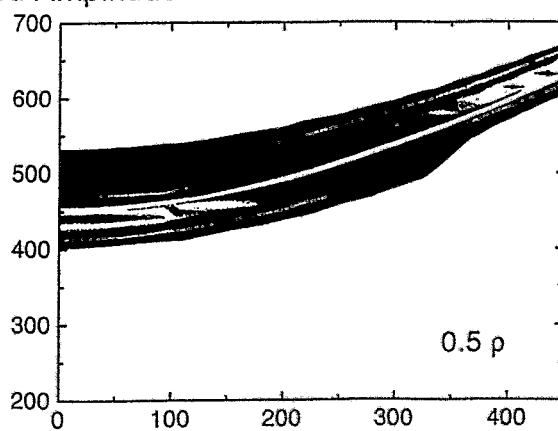
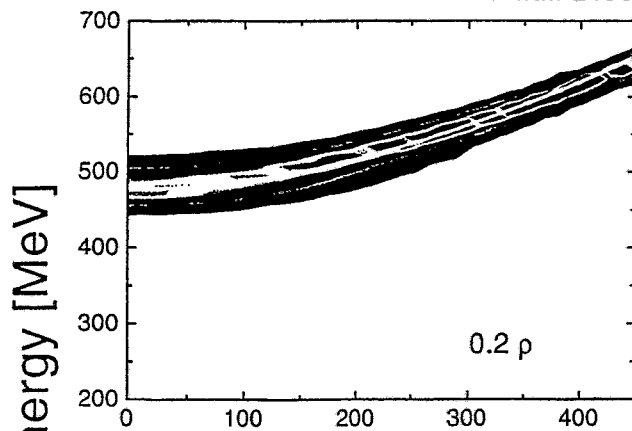
in-medium kaon Green's function



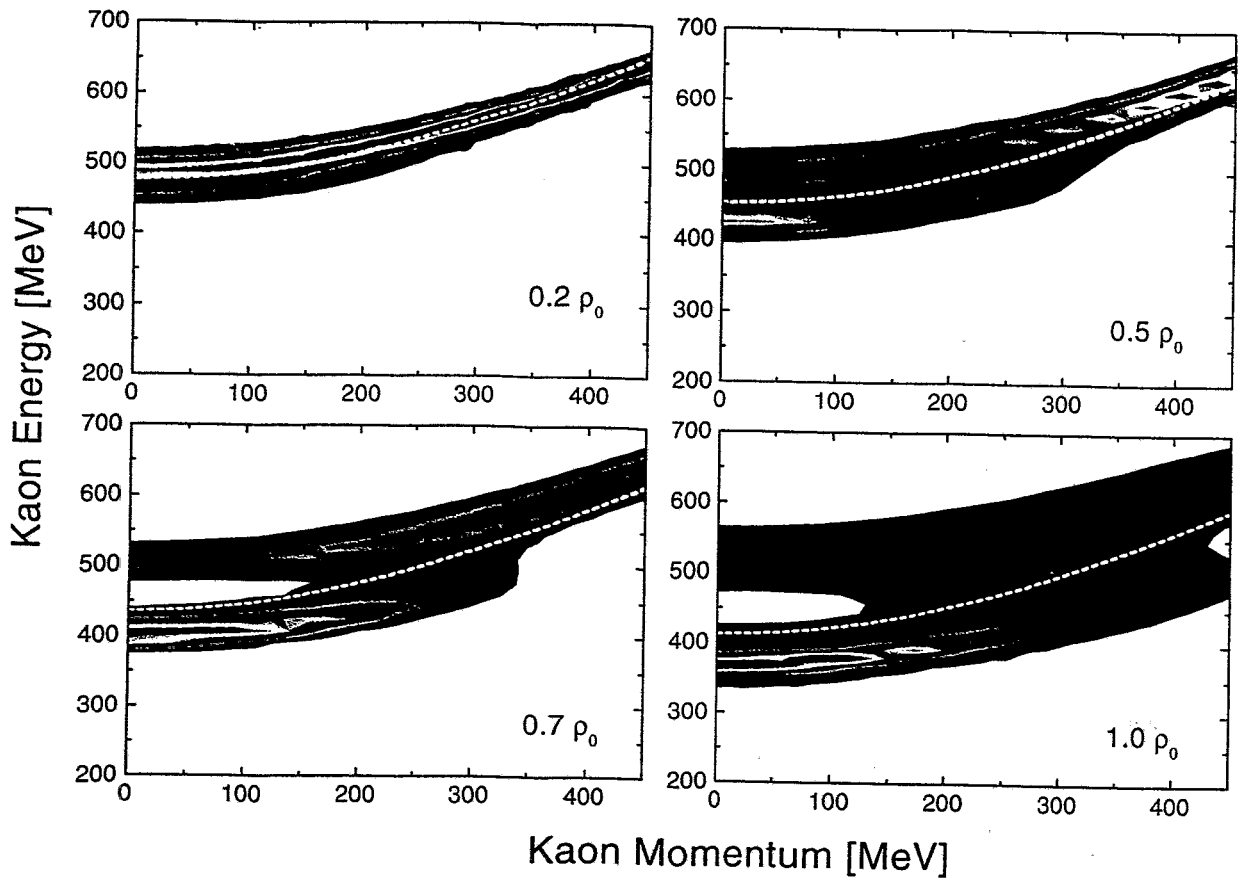
Kaon Energy [MeV]

M. Lutz Phys. Lett B462, 12

Pauli Blocked Amplitude



Kaon Momentum [MeV]



" $\Lambda(1405)$ " stays below KN threshold !!!

I

$$\omega^2 = k^2 + m_K^2 + \Pi, \quad \Pi = V_1 + V_2 \omega + (V_3 \omega^2)$$

OR. $(\omega + V)^2 = m_K^2 + k^2 - S$

** Reasonably adjusted potentials can imitate the effects of $K-N$ interaction in integral observables

** In transport eq. $\frac{d p_{K^-}}{dt} = -\nabla_K U_{K^-}$

instead of. $U_{K^-} = \sqrt{m_K^2 + k^2} S - V - \sqrt{m_K^2 + k^2} \tilde{\epsilon}$
 one should use $\tilde{U}_{K^-} \sim \frac{\text{Re} \Pi(\sqrt{m_K^2 + k^2}, k)}{2\omega - \frac{\partial \text{Re} \Pi}{\partial \omega}} \Big|_{\omega = \sqrt{m_K^2 + k^2}}$ (near mass shell)
 refraction effects

Λ(1405) in-medium dynamics generates non-trivial energy dependence

Equilibrium Number of K^- Mesons

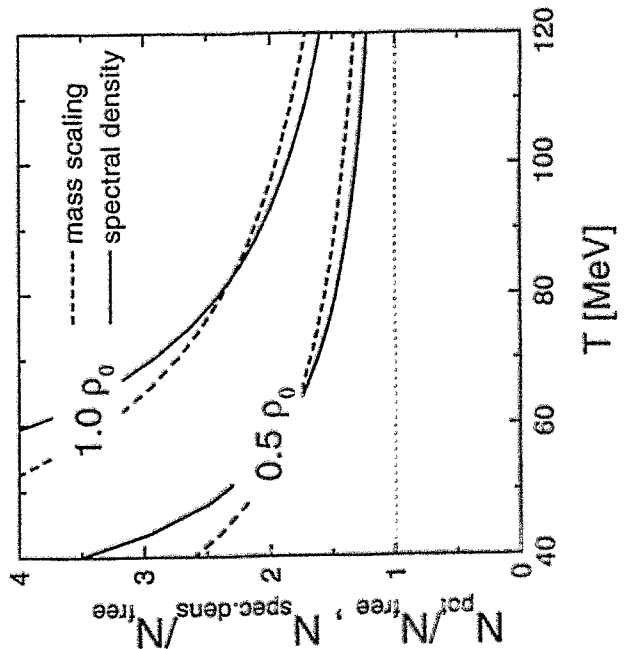
$$N_{\text{free}}(T) = \int \frac{d^3 p}{(2\pi)^3} \text{Exp} \left[-\frac{\sqrt{m_K^2 + p^2}}{T} \right]$$

$$N_{\text{pot}}(T, \rho) = \int \frac{d^3 p}{(2\pi)^3} \frac{2 E_{K^-}(p, \rho)}{2 E_{K^-}(p, \rho) + 3\rho/8 f_\pi^2} \text{Exp} \left[-\frac{E_{K^-}(p, \rho)}{T} \right]$$

$$E_{K^-}(p, \rho) = \sqrt{m_K^2 + p^2 - \frac{\Sigma_{KN}}{f_\pi^2 \rho} + \left(\frac{3\rho}{8 f_\pi^2} \right)^2}$$

$$N_{\text{spec. dens.}} = \int \frac{dE}{\pi} \int \frac{d^3 p}{(2\pi)^3} (E A_{K^-}(E, p)) \text{Exp} \left[-\frac{E}{T} \right]$$

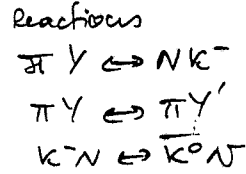
$A_{K^-}(E, p)$ spectral den



II

base interaction
(somehow constrained)

coupled
channels



parameter
ization
in code

coupled
channels

$K^- N \rightarrow K^- N$
Amplitudes
(vacuum)

in-medium
dynamics

"effective"
"potentials"
at $s > 0.2 \text{ GeV}^2$
in code

UNITARITY
LINK

can be broken for
the randomly chosen
"eff. potentials" !

** In medium resonance dynamics can be consistently treated only in the coupled channel approach.

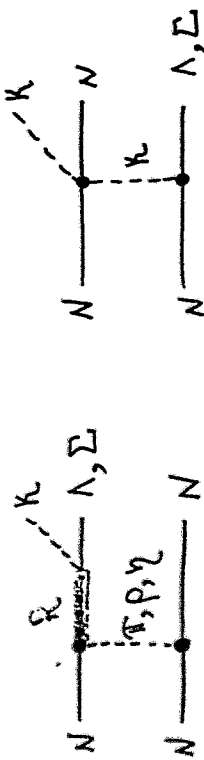
A. Sibirtsev:

Theoretical news on strangeness production in $p + p$ collisions

Theoretical News on strangeness production from p+p collisions

A. Sibirtsev, W. Cassing, K. Terauchi
A. Thomas

Giepen & Adelaide University



R: $N^*(1650)$, $N^*(1710)$,
 $N^*(1720)$, Δ (1920)

$KN \rightarrow KN$ scattering
amplitude from data

[fix with $\pi N \rightarrow KN$,
 $\pi N \rightarrow K\Sigma$ data]

J.M. Laget, Phys. Lett. B 227 (1989) 24

R = 14:1 = 14 SATURNE data

A. Sibirtsev, Phys. Lett. B 333 (1994) 20

R = 19.6:1.3 = 15 total cross sections
 $N\bar{N} \rightarrow K\bar{N}$ and $K\bar{\Sigma}$

✓ SU(6) R = 3cot ϵ = 27!!!

ϵ -mixing angle between Λ and Σ contents of the nucleon $\epsilon = 18.4^\circ$

✓ Dispersion analysis (ambiguities $K^0, \bar{K}^0, \eta, \eta'$, etc.)
total sections and real part of the forward scattering amplitudes (data)

R = 13.9:3.3 = 4.2

A. Sibirtsev, W. Cassing, Nucl. Phys. A 641 (1998) 478

Final State Interaction

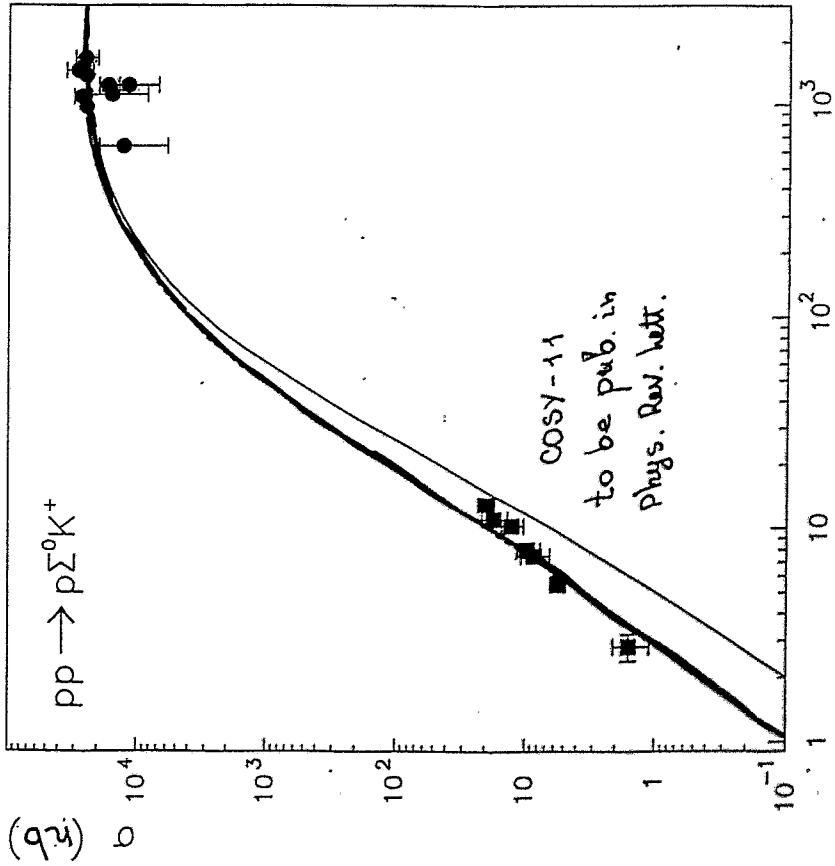
Most functions $\sim \frac{q+i\mathbb{P}}{q-id} \rightarrow 1$ @ large q

$a_s = \frac{d+\mathbb{P}}{d-\mathbb{P}}$ $r_s = \frac{2}{d+\mathbb{P}}$ effective range expansion

$q \cot \delta = \frac{1}{a_s} + \frac{1}{2} r_s q^2 + \dots$

γN -Jülich model $a_s = -2.28 \text{ fm}$ $r_s = 5.15 \text{ fm}$ BUT for $\Sigma^+ p \rightarrow \Sigma^+ p$

Nucl. Phys. A 500 (1989)
485; A 570 (1994) 543



E (MeV)

The role of the P_{11} (1710)

A. S. Ibratsev, K. Tsuchida, W. Cassing, A. W. Thomas,
 nucl-th/9810070, sub. to. Nucl. Phys.

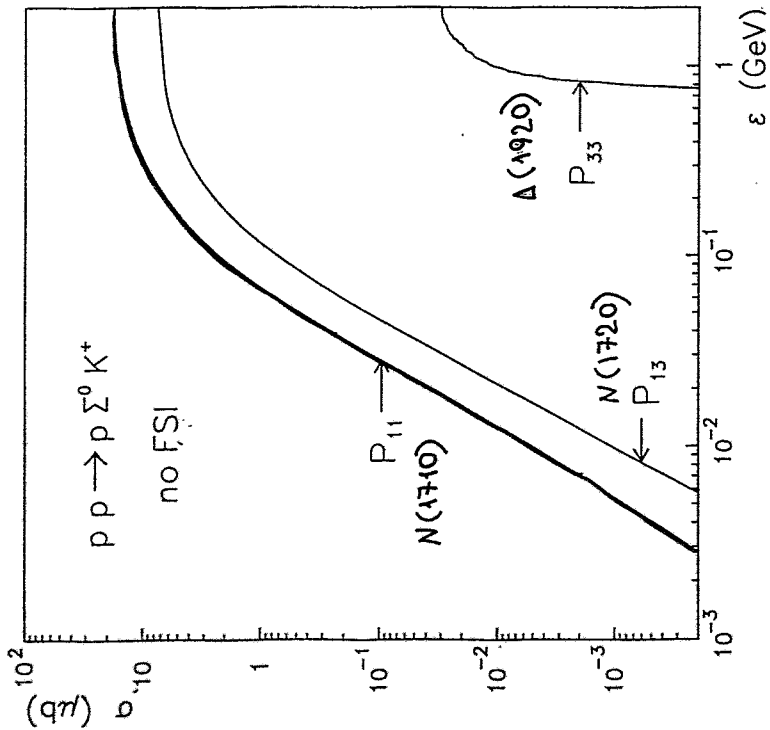
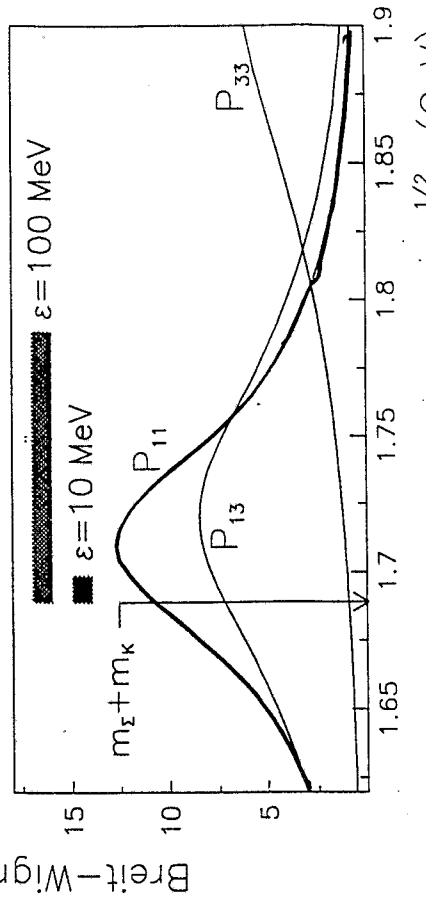
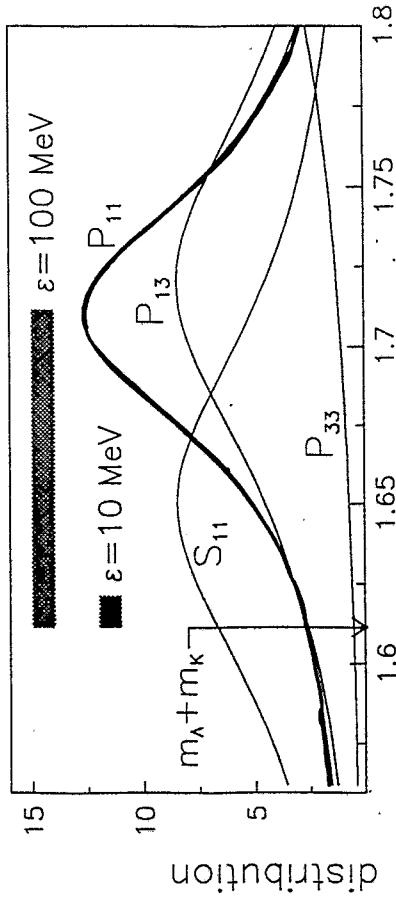


Figure 2: Decomposition of the total cross section in terms of individual resonance contributions, $N(1710)$ (P_{11}), $N(1720)$ (P_{13}) and $\Delta(1920)$ (P_{33}) resonances for the $pp \rightarrow p \Sigma^0 K^+$ reaction. The calculation was performed without the inclusion of final state interactions.

The role of the $N^*(1710)$

for $pp \rightarrow p \Sigma^0 K^+$ $N(1650)$, $N(1710)$, $N(1720)$
 contribute with \sim equivalent
 rates

$pp \rightarrow p \Sigma^0 K^+$ $N(1710)$ $\Delta(1920)$

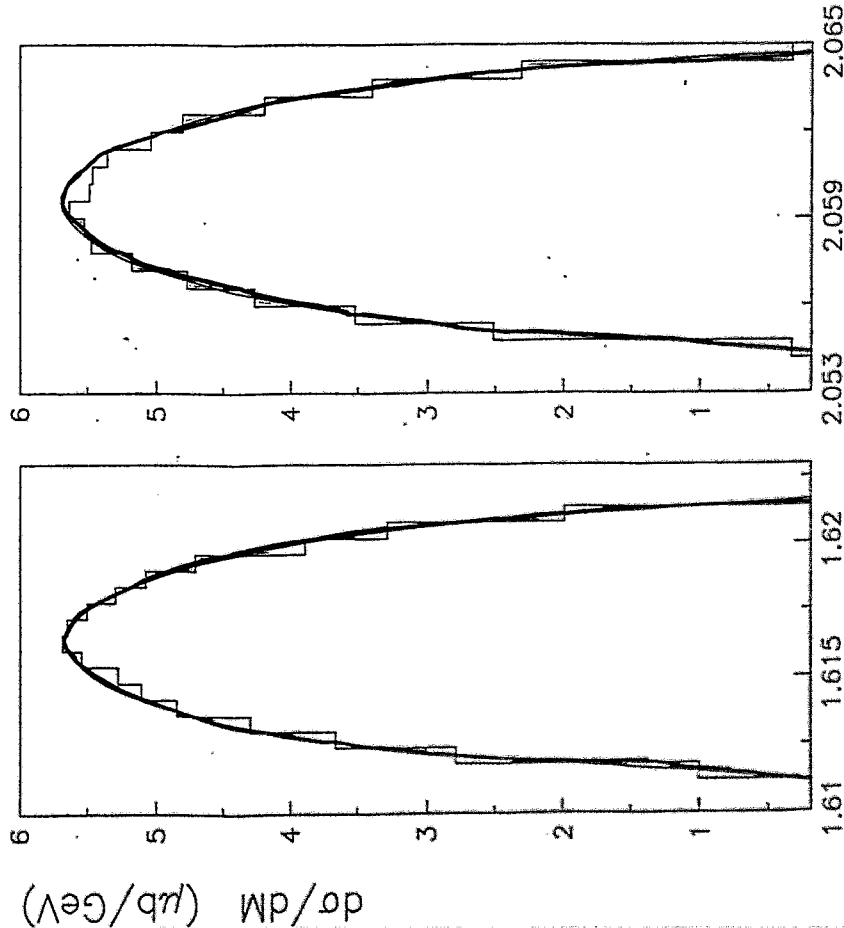


Do $R \rightarrow \Lambda K^+$ possible to detect by ΛK^+ invariant mass distribution?

A.S., K. Tsuchida, A.M. Thomas,
Phys. Lett. B 421 (1998) 59

— real one boson Exchange calculations } No difference
 — phase space } confirmed experimentally

$pp \rightarrow p \Lambda^0 K^+$ at $\epsilon = 10$ MeV



$pp \rightarrow p \Sigma^0 K^+$

Dominant contribution from

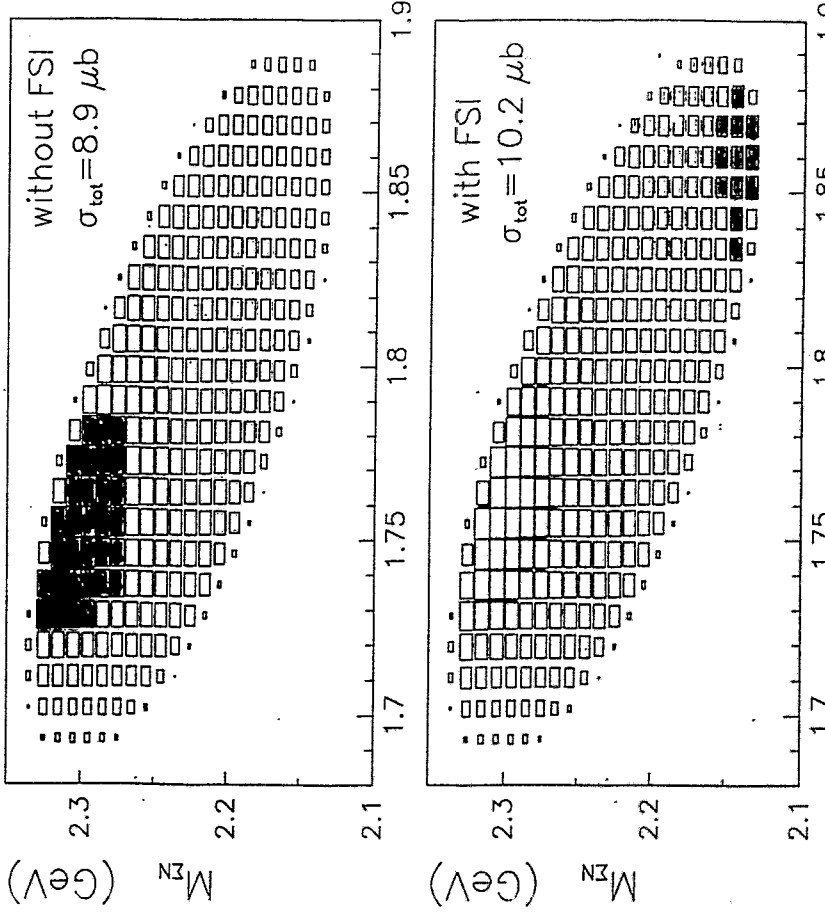
$R_{11} (1710) \quad \Gamma_{\text{tot}} = 199 \text{ MeV}$

$\rightarrow \Lambda K \quad 15\%$

$\rightarrow \Sigma K \quad 8\%$

fixed by studying $\pi N \rightarrow \Lambda K, \pi N \rightarrow \Sigma K$
 total + differential cross sections

$pp \rightarrow p \Sigma^0 K^+$ at $\epsilon = 200$ MeV



FSI and Cost function.

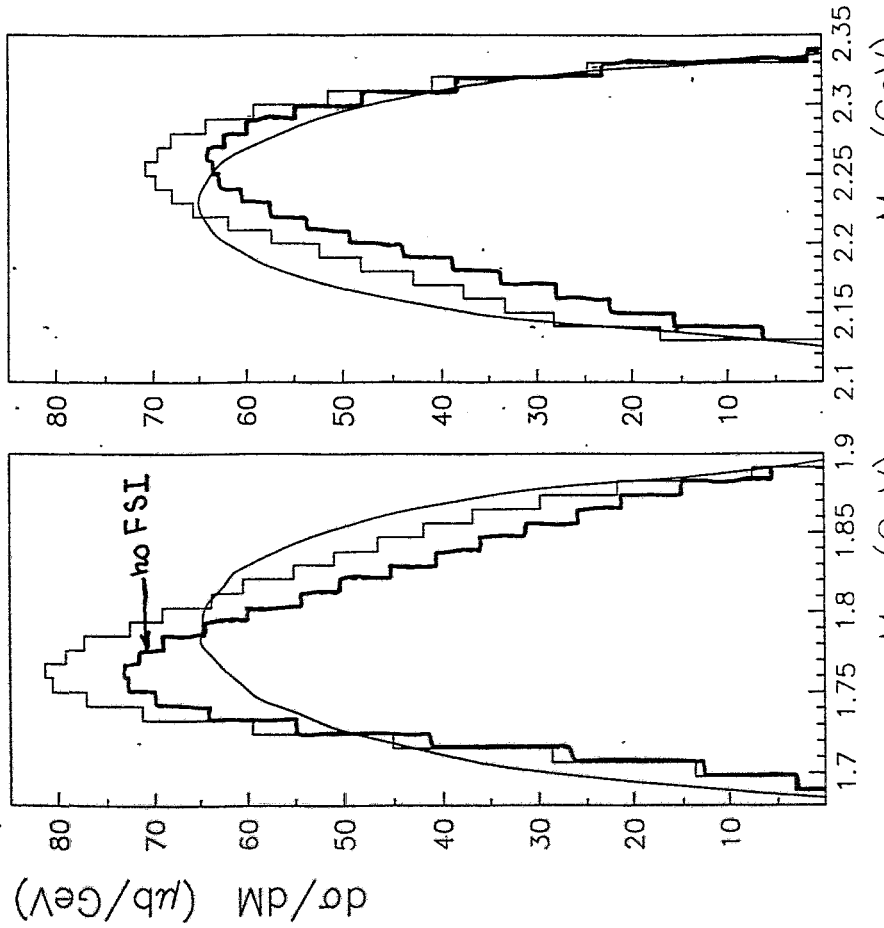
A.S. and V. Cassing, Eur. Phys. J. A2 (1998) 333

FSI and Watson-Migdal approximation

A.S. and V. Cassing, nucl-th/9802025

A.S., Int. J. Phys. Part. (1998)

$pp \rightarrow p\Sigma^0 K^+$ at $\epsilon = 200$ MeV



$\chi^2/\text{dof} = 1.7$

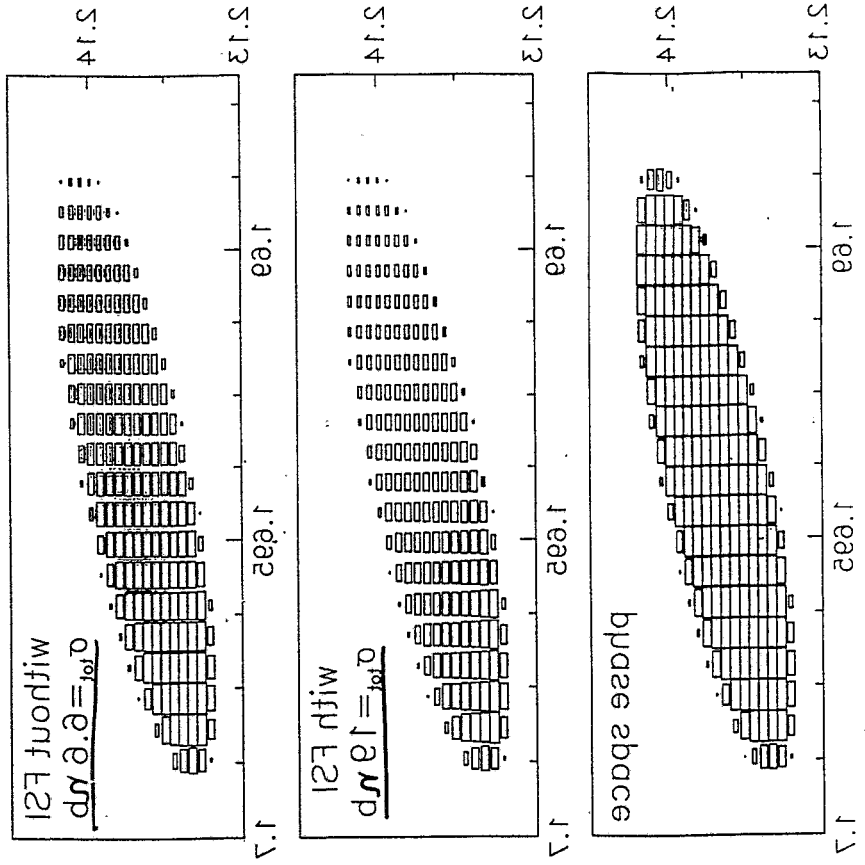
modelos usados em diferentes pontos
 para se ajustar aos dados de ICF, ICF
 e dados

$V_{EM} O_1 = 3$ to

$\Lambda^+ K^+ \rightarrow p p$ ref. $\Lambda^+ K^+ \rightarrow p p$ $\Lambda^+ K^+ \rightarrow p p$
 $\Lambda^+ K^+ \rightarrow p p$ $\Lambda^+ K^+ \rightarrow p p$ $\Lambda^+ K^+ \rightarrow p p$

2 events $O_1 = \text{exchange total}$

$V_{EM} O_1 = 3$ to $K^0 \Sigma^0 \leftarrow q q$

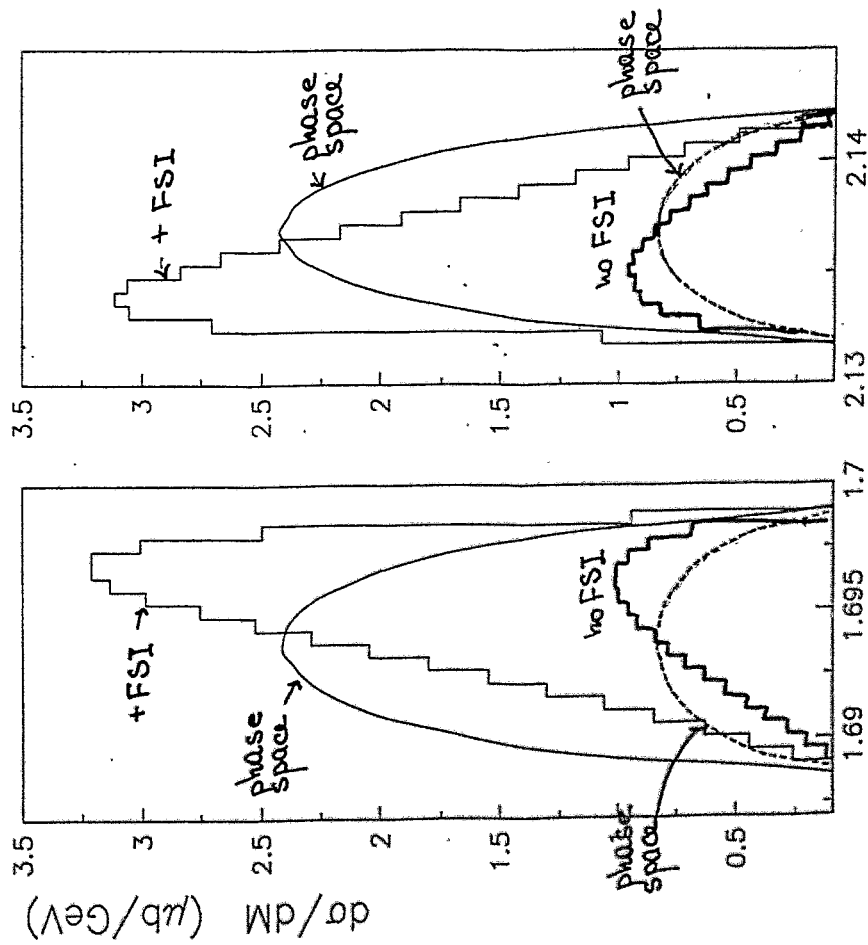


strong deviation from phase space @ $\epsilon = 10$ MeV for $pp \rightarrow p\Sigma^0 K^+$

both: with FSI and without FSI

total relative errors

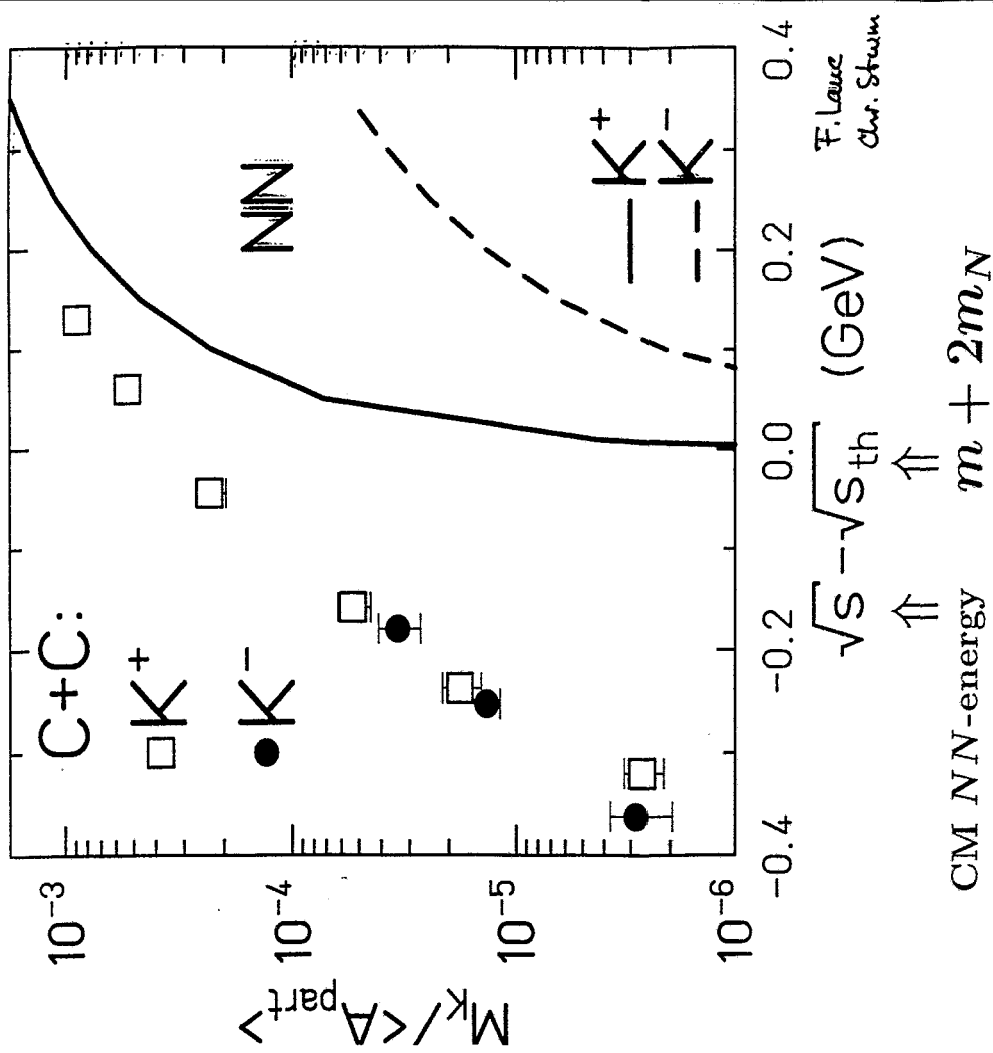
$pp \rightarrow p\Sigma^0 K^+$ at $\epsilon = 10$ MeV



J. Knoll:

Transport kinetics of broad resonances

Threshold Mass Scaling



Transport kinetics
of
broad resonances

J. Knoll

GSI Darmstadt

Y. Ivanov

ANN. PHYS. 249 (1996) 532

D. Voskresensky

HEP-PH/980

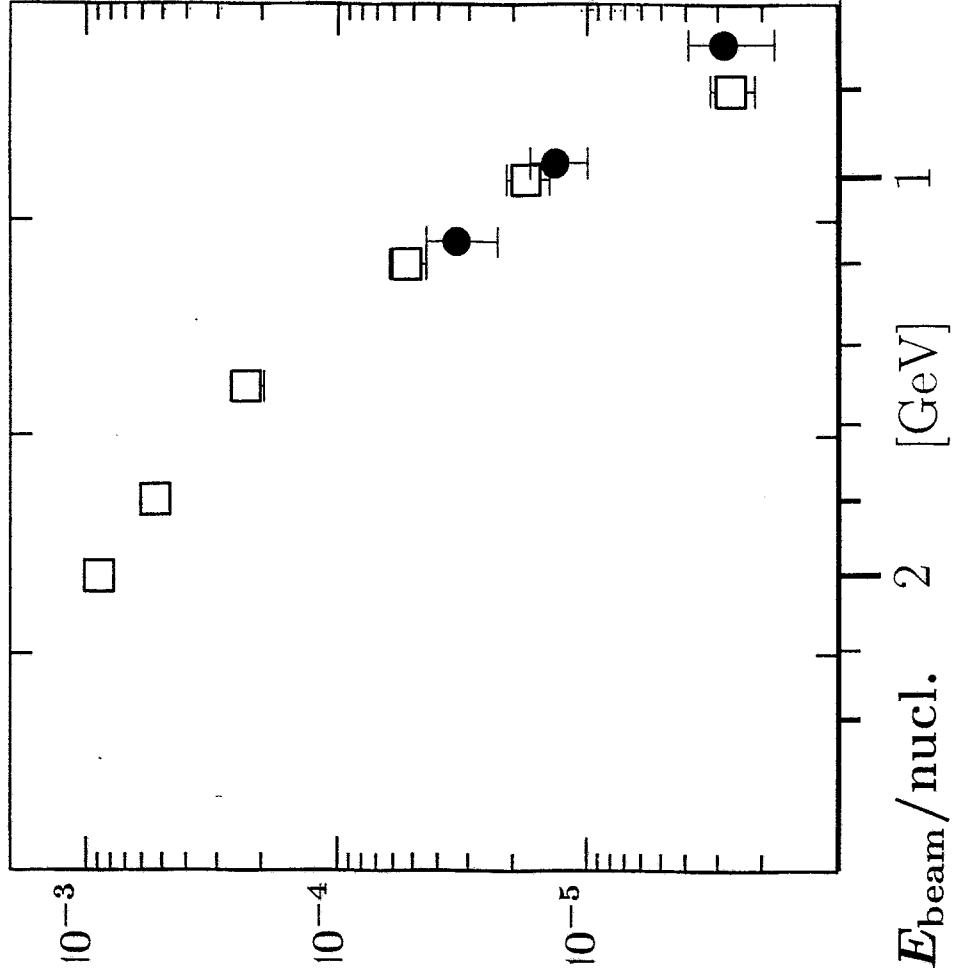
H. van Hees

TFT-98: HEP-PH/981

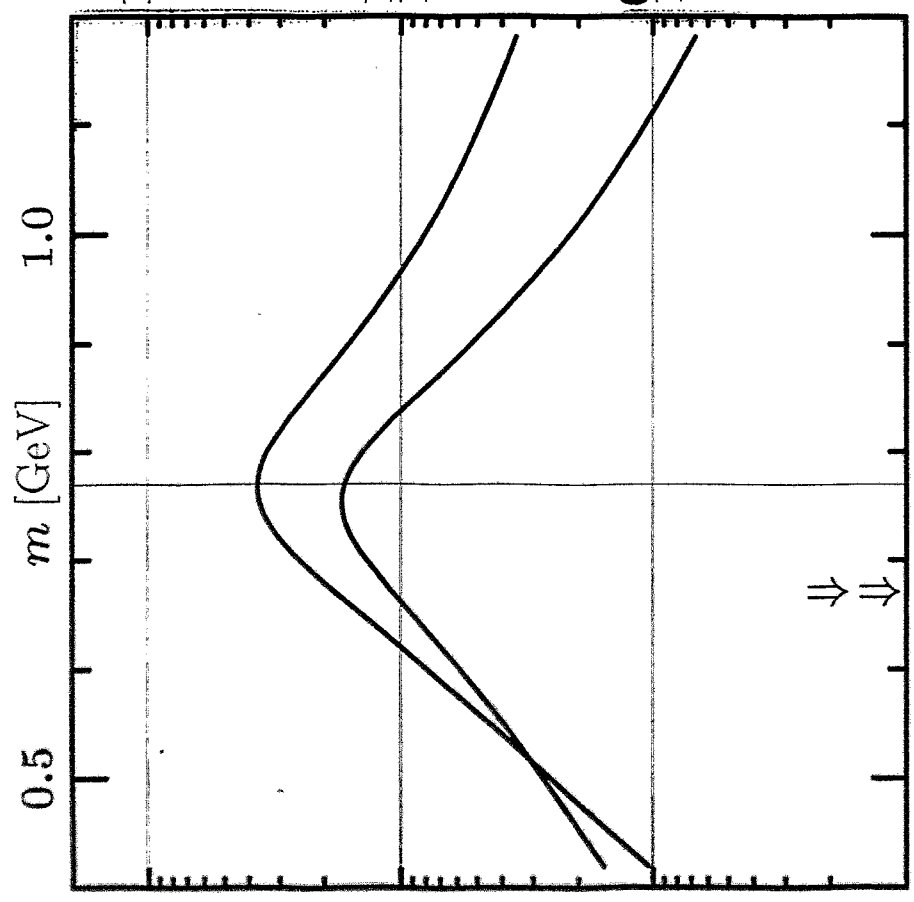
(Dipl. Thesis)

ERICE-98: NUCL-TH/981

Mass Scaling



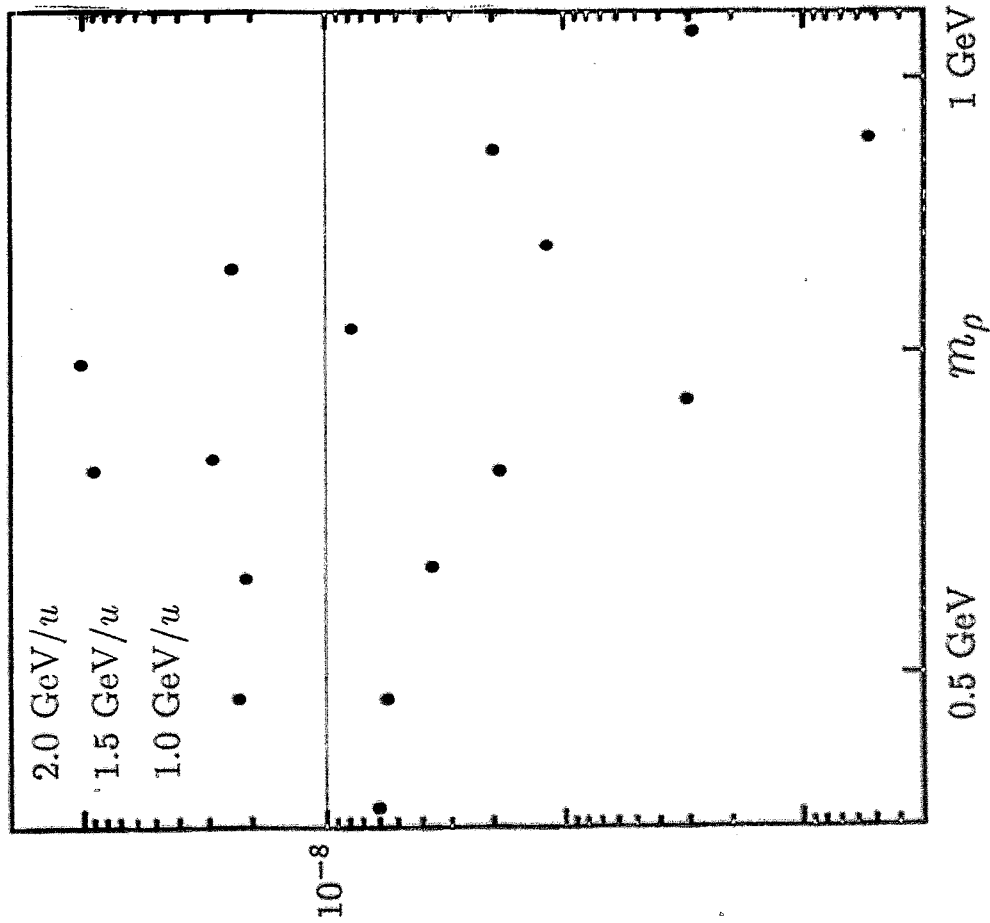
Beam Energy Ruler



- ρ -mesons per 1 GeV
- - - di-electrons per 1 GeV

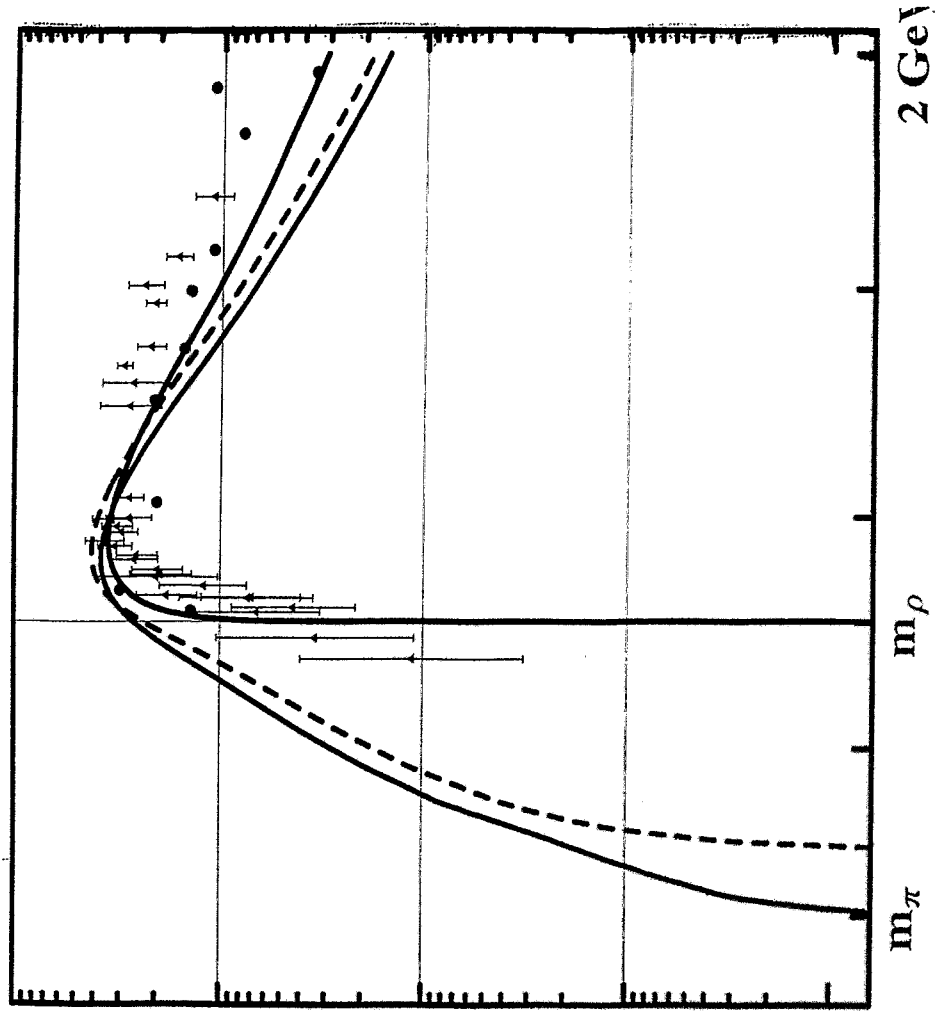
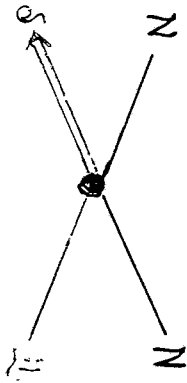
Di-leptons from Mass Scaling

di-leptons per GeV and Participants



$\pi N \rightarrow \rho N$ Cross Section

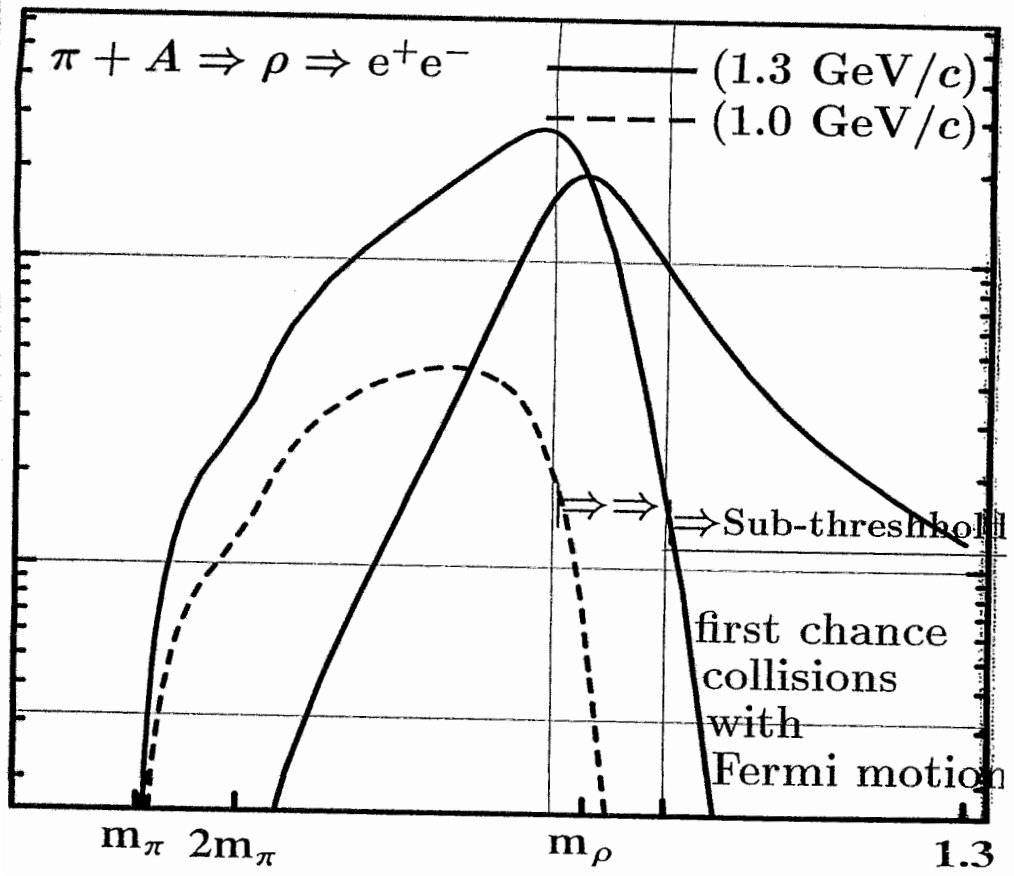
Constant Matrix element & $\Gamma_{tot} = \Gamma_{\rho\pi\pi} + \Gamma_{\rho\pi N}$



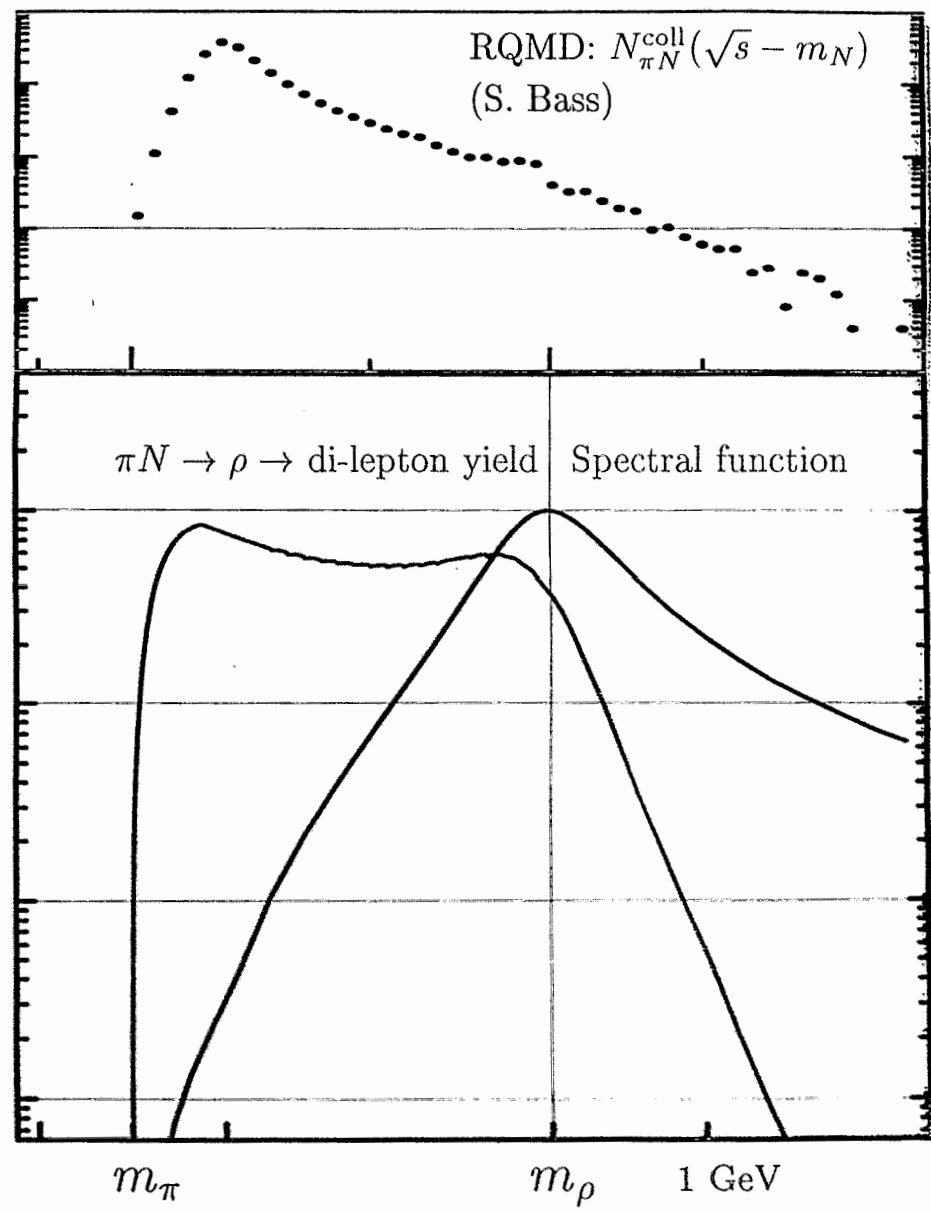
First Chance Collision Kinematics

$$\frac{dn^{e^+e^-}}{dtdm} =$$

$$\underbrace{F_\rho(m, p)}_{\text{Phase-Space}} \frac{\Gamma_{\pi N \rightarrow \rho N}^{in}(m, p)}{(m^2 - m_\rho^2)^2 + \Gamma_{tot}^2/4} \underbrace{\Gamma_{\rho \rightarrow e^+e^-}^{out}(m)}_{\propto 1/m^2 \text{ (VD)}}$$



ρ -mesons from Ni+Ni at 1 GeV/u



e^+e^- from intermediate ρ -mesons

$$\frac{dn^{e^+e^-}}{dtdm} = \text{diagram showing } e^+e^- \text{ annihilation into } \gamma^* \text{ and } \rho \text{ meson exchange, with } \gamma^* \text{ decaying to } e^+e^- \text{ and } \rho \text{ decaying to } e^+e^-.$$

$$= n_\rho(\omega, T) A_\rho(\omega, \vec{p}) \Gamma^\rho e^+e^-(m)$$

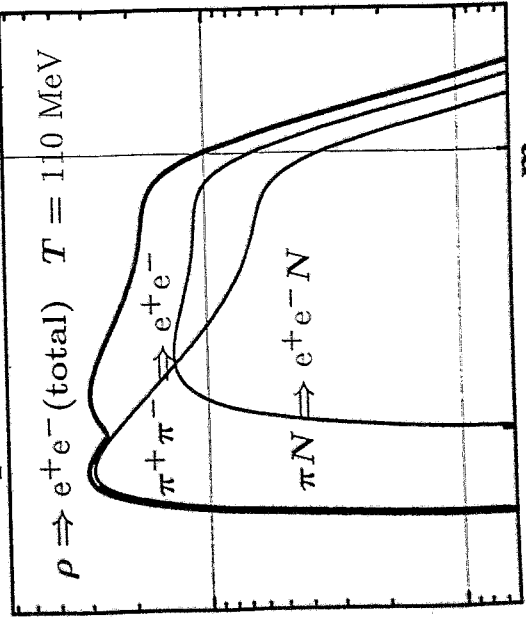
$$A_\rho(\omega, \vec{p}) = \text{diagram with } \pi^+ \text{ and } \pi^- \text{ loop} + \text{diagram with } N \text{ and } \pi \text{ loop}$$

$$= \frac{\Gamma^\rho \pi^+ \pi^-(m) + \Gamma^\rho \pi N N^{-1}(m)}{\dots}$$

$$= \underbrace{(m^2 - m_\rho^2 - \text{Re}\Sigma)^2 + \Gamma_{tot}^2/4}_{\text{interacting } \pi N \text{ System}}$$

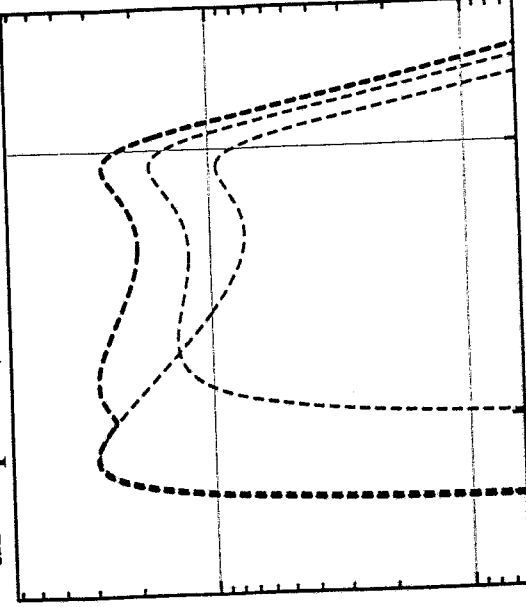
$$\Rightarrow \langle \sigma(\pi\pi \rightarrow e^+e^-) \rangle + \langle \sigma(\pi N \rightarrow \rho N \rightarrow e^+e^- N) \rangle$$

di-leptons via rho-mesons



Klingl et al.;
Friman Pirner

di-leptons via rho-mesons



dashed lines:
free Cross sect.
 $\Gamma_{tot} \leftarrow \Gamma^\rho \pi^+ \pi^-$
 \Downarrow
Peak too large
violates Unitarity

== free

--- Spectral
function

